

**EXPERIMENTAL AND NUMERICAL
INVESTIGATION INTO BEHAVIOUR OF FLY ASH
COMPOSITE MATERIAL IN THE SUBBASE OF
SURFACE COAL MINE HAUL ROAD**

Banita Behera

EXPERIMENTAL AND NUMERICAL INVESTIGATION INTO BEHAVIOUR OF FLY ASH COMPOSITE MATERIAL IN THE SUBBASE OF SURFACE COAL MINE HAUL ROAD

A thesis submitted in partial fulfillment of the requirements
for the degree of

Doctor of Philosophy

in

Engineering

by

Banita Behera

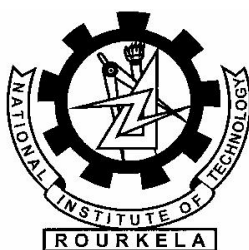


**Department of Mining Engineering
National Institute of Technology
Rourkela - 769 008, India**

January, 2013

Dedicated to

My Parents



**National Institute of Technology
Rourkela**

CERTIFICATE

This is to certify that the thesis entitled “**EXPERIMENTAL AND NUMERICAL INVESTIGATION INTO BEHAVIOUR OF FLY ASH COMPOSITE MATERIAL IN THE SUBBASE OF SURFACE COAL MINE HAUL ROAD**” submitted by **Banita Behera** to National Institute of Technology, Rourkela for the award of the degree of Doctor of Philosophy in Engineering, is a record of bonafide research work under my supervision and guidance. The candidate has fulfilled all prescribed requirements for the thesis, which is based on candidate’s own work and the thesis in my opinion, is worthy of consideration for the award of the degree of Doctor of Philosophy of the Institute.

The results embodied in this thesis have not been submitted to any other University/Institute for the award of any other degree or diploma.

Prof. M. K. Mishra
Dept. of Mining Engineering
National Institute of Technology
Rourkela – 769008

ACKNOWLEDGEMENT

I would first like to express deep sense of respect and gratitude towards my supervisor Prof. M.K. Mishra, for his inspiration, motivation, guidance, and generous support throughout this research. I am greatly indebted for his constant encouragement and valuable advice at every phase of the doctoral programme. The dissertation work would not have been possible without his elaborate guidance and full encouragement. What I learned from him will be an invaluable benefit for the rest of my life.

I would like to express my respect to Prof. N.R. Mohanty, Prof. M.R. Barik, Prof. K. Dey, Prof. S.C. Mishra and Prof. S. Mula for teaching me in research related courses. They have been great sources of inspiration to me and I really thank them from the bottom of my heart.

I would like to extend my special thanks to the Chief General Manager and other staff members of Bharatpur Opencast Mine, Talcher, Odisha for their assistance in collecting the necessary data and overburden materials used for this research and also to the Head, Captive power plant II of Rourkela Steel Plant for providing fly ash used in this research.

My special thanks to Prof. H.K. Naik, Head of Mining Engineering Department, all faculty and staff members of the department for their timely help in completion of this work.

I also express my thanks to HODs and staff members of Civil Engineering, Metallurgical and Materials Engineering and Ceramic Engineering for their help and cooperation in sample testing and instrumental analysis in their department.

I want to extend my sincere gratitude to all the members of my doctoral scrutiny committee, Prof. P. Rath and Prof. S. Jayanthu for their comments and suggestions throughout this work.

I am also thankful to Fly Ash Unit, Department of Science and Technology, Govt. of India which has provided fellowship to work in the project title “Bulk use of fly ash composite material in the subbase of Surface Coal Mine Haul Road to reduce strain” under investigation of my supervisor.

I am also grateful to my friends for their assistance and constant encouragement throughout my dissertation work.

Finally, I would like to express my deepest gratitude to my beloved parents, my brother and two sisters and also my husband who made all of this possible, for their endless encouragement, support, love and patience throughout the research period.

(Banita Behera)

ABSTRACTS

Surface mining will continue to play major role in meeting the demand of fossil fuel. India's power generation will be about 1, 65,000 MW this 11th five year plan out of which the share of coal would be 75%. Majority of the coal demand is met from surface mining due to its speed and ease of operations. The current coal production from surface mines in India is about 390 MT (85%) that will have to be increased substantially to meet the demand. Opencast mine economy depends on the cost of haul road design, construction and its maintenance in addition to other factors. These roads are used by heavy earth moving equipments. With a poorly laid, constructed and maintained haul road, production suffers, accident and breakdown occurs. The haul road has received inadequate attention although production, usage of heavy machineries have increased manifold. The surface of the haul road depends on the behaviour of material beneath it. Strengthening of the base and subbase layers beneath the surface of the surface coal mine haul road are of vital importance to improve upon its performance. The materials that are used in haul road construction, typically sourced locally. It is envisioned that suitable material would address this issue.

Solid wastes from the surface mining as well as combustion of coal pose serious environmental problems of vital concern to the producers and users of coal as well as the general public. Opencast mining involves displacement of large amount of overburden dumps materials as mine waste to excavate coal from the earth. The overburden dumps formed outside the open pits not only occupy huge land area but also alter the surface topography and contribute to the environmental degradation. Fly ash is at present an unavoidable coal combustion byproduct. The major challenge with this production of the fly ash is in its huge

land coverage, adverse impact on environment, etc. The problem with safe disposal of fly ash is a major issue as India is poised to generate huge volume of fly ash due to the high ash (40% to 50%) content of the coal. In most of the surface mines, the material used in the haul road is not adequate to support the wheel loads. Fly ash possesses many attributes to be used as an engineering material in those sections/layers. The prospects of utilizing fly ash that would have been dumped as waste is explored, investigated, experimented and evaluated in the investigation. Different compositions of fly ash, mine overburden and lime have been prepared. The geotechnical properties such as compaction characteristics, California bearing ratio, unconfined compressive strength, Brazilian tensile strength, ultrasonic pulse velocity, morphology, phase characteristics, chemical compositions and leaching behaviour have been determined. The effects of lime content and curing period on the geotechnical characteristics of the fly ash composites are highlighted. Numerical investigation have been carried out to evaluate the behaviour of fly ash composite materials in reducing strain in the haul road of surface coal mine. There were significant improvements in the stress-strain behaviour of developed composites. All the composites resulted in enough strength values to be used as subbase material. Curing periods and lime content have varying influence in the strength development of the composites. The composites with 30% fly ash and 9% lime gave the best performance in reducing the stress-strain values at different section of haul road pavement. There were no traces of toxic elements in the developed composites.

Keywords: Brazilian tensile strength, CBR, Fly ash, Lime, Maximum dry density, Mine overburden material, Pulse velocity, Surface mine haul road, Unconfined compressive strength.

CONTENTS

CERTIFICATES	i
ACKNOWLEDGMENT	ii
ABSTRACTS	iii
LIST OF FIGURES	ix
LIST OF TABLES	xv
 CHAPTER 1: INTRODUCTION	
1.1 Background	1
1.2 Statement of the problem	2
1.3 Research Objectives	4
1.4 Scope and Methodology	5
1.5 Parametric variations	8
1.6 Organization of Thesis	9
 CHAPTER 2: LITERATURE REVIEW	
2.1 Introduction	11
2.2 Mine haul roads and haul trucks	15
2.2.1 Classification of haul roads	16
2.2.2 Design of haul road pavement	17
2.2.2.1 Haul Road Pavement design based on CBR	20
2.2.2.1.1 Design Procedure	21
2.2.2.2 Haul Road Pavement design based on resilient modulus	23
2.2.2.2.1 Design Procedure	24
2.2.2.3 Critical strains and typical mode of failure in a haul road	25
2.2.2.4 Critical strain limit	26
2.2.3 Symptoms and causes of haul road deterioration	27
2.2.4 Characteristics of Base/Subbase course materials of the haul road	28

2.2.5	Haul Trucks	28
2.2.5.1	Haul trucks tires	29
2.2.5.1.1	Tire foot print area and pressure	30
2.3	Geotechnical properties of fly ash	35
2.3.1	Physical Properties	36
2.3.2	Chemical Properties	37
2.3.3	Engineering Properties	41
2.3.3.1	Compaction characteristics	42
2.3.3.2	Permeability characteristics	43
2.3.3.3	Strength characteristics	44
2.3.3.4	California bearing ratio (CBR) behavior	45
2.3.3.5	Ultrasonic velocity	46
2.4	Uses and strength behavior of fly ash	46
2.5	Environmental aspects of fly ash utilization	53
2.6	Fly ash – lime or fly ash – soil – lime interaction	56

CHAPTER 3: METHODOLOGY

3.1	General	60
3.2	Materials and Methods	60
3.2.1	Materials	60
3.2.1.1	Fly ash	60
3.2.1.2	Overburden Materials	61
3.2.1.3	Lime	65
3.2.2	Methods	66
3.2.2.1	Sample preparation	66
3.2.2.1.1	Sample preparation for CBR test	68
3.2.2.1.2	Sample preparation for UCS test	68
3.2.2.1.3	Sample preparation for tensile strength test	69
3.2.2.1.4	Sample preparation for Ultrasonic pulse velocity test	69

3.2.2.1.5	Sample preparation for SEM, EDX and XRD Analyses	70
3.2.2.1.6	Sample preparation for leaching study	70
3.2.2.2	Experimental methods	71
3.2.2.2.1	Specific Gravity	71
3.2.2.2.2	Grain size distribution	71
3.2.2.2.3	Specific surface area	72
3.2.2.2.4	Consistency limits	72
3.2.2.2.5	Free swell index	72
3.2.2.2.6	X-ray diffraction (XRD) analysis	73
3.2.2.2.7	SEM and EDX studies	73
3.2.2.2.8	Loss on ignition (LOI)	74
3.2.2.2.9	pH test	74
3.2.2.2.10	Compaction test	74
3.2.2.2.11	Triaxial compression test	74
3.2.2.2.12	Permeability test	75
3.2.2.2.13	California bearing ratio test	75
3.2.2.2.14	Unconfined Compressive strength test	77
3.2.2.2.15	Brazilian tensile strength test	79
3.2.2.2.16	Ultrasonic Pulse velocity test	80
3.2.2.2.17	Leaching study	83
3.3	Experimental Size	83

CHAPTER 4: RESULTS AND DISCUSSION

4.1	Introduction	87
4.2	Results of Geotechnical properties of ingredients	88
4.2.1	Physical Properties	88
4.2.2	Chemical Properties	91
4.2.3	Engineering Properties	94
4.3	Geotechnical properties of developed composite materials	97

4.3.1	Compaction characteristics	97
4.3.2	California Bearing Ratio behavior	101
4.3.2.1	Effect of curing on the CBR of untreated composites	101
4.3.2.2	CBR behaviour of lime stabilized fly ash composites	102
4.3.3	Unconfined compressive strength characteristics	107
4.3.3.1	Unconfined compressive strength of untreated composites	108
4.3.3.2	Unconfined compressive strength of treated composites	108
4.3.4	Brazilian Tensile strength characteristics	113
4.3.5	Ultrasonic pulse velocity	117
4.3.6	Microscopy analysis	123
4.3.7	Energy dispersive X-ray analysis	125
4.3.8	X-ray diffraction analysis	128
4.3.9	Leachate characteristics	129
4.4	Development of empirical models	131

CHAPTER 5: NUMERICAL INVESTIGATION

5.1	General	138
5.2	Modeling and Boundary condition	139

CHAPTER 6: SUMMARY AND CONCLUSIONS

6.1	Untreated materials	157
6.2	Treated materials	158
6.3	Scope for Further Research	160

REFERENCES	162
-------------------	-----

APPENDIX	185
-----------------	-----

LIST OF PUBLICATIONS

CURRICULUM VITAE

LIST OF FIGURES

Fig. No.	Title	Page No.
1.1	Flowchart of the methodology	7
2.1	A typical permanent haul road	15
2.2	A typical system of haul road classification in an opencast mine	17
2.3	Typical haul road cross-section	19
2.4	CBR design chart (recommended by Indian Roads Congress)	22
2.5	Method to obtain resilient modulus (after Bowles 1984)	23
2.6	Critical strains and failure mode in pavement structures	26
2.7	Bias ply and radial tires (Good Year, 2008)	30
2.8	Deflection factors for ESWL determination (after Foster and Ahlvin, 1954)	34
2.9	Critical points for a fully loaded truck (after Thompson, 1996)	34
2.10	Load distribution beneath a tire	35
3.1	Map of Talcher Coalfield, Odisha	63
3.2	Sketch of Bharatpur Opencast coal mine	64
3.3	Collection of mine overburden	64
3.4	Undulations and potholes are marked in the haul roads	65
3.5	CBR mould	69
3.6	UCS mould, spacer discs and mixed ingredients	69
3.7	Set up for collection of leaching effluent	71
3.8	Prepared CBR samples inside the moulds	76

3.9	Soaking of CBR samples	76
3.10	An experimental setup for CBR test	77
3.11	Sample of UCS specimens prepared (undergoing curing)	78
3.12	An experimental setup for UCS test	79
3.13	Schematic representation of ultrasonic velocity measurement	81
3.14	An experimental setup for Ultrasonic velocity measurement	82
4.1	Grain size distribution curves of fly ash and mine overburden	90
4.2	Scanning electron micrograph of (a) mine overburden material and (b) fly ash	92
4.3	X-ray diffractogram of (a) mine overburden and (b) fly ash	93
4.4	Compaction curves of fly ash and overburden	97
4.5	Compaction curves of untreated composites	98
4.6	Variation of maximum dry density with fly ash content	98
4.7	Variation of optimum moisture content with fly ash content	98
4.8	Compaction curves of the composites containing 15, 20 and 25% fly ash	99
4.9	Compaction curves of the composites containing 30, 35 and 40% fly ash	100
4.10	Compaction curves of the composites containing 45 and 50% fly ash	100
4.11	Variation of CBR with the addition of fly ash to mine overburden	102
4.12	Effect of curing on the CBR of fly ash and mine overburden composites	102
4.13	Effect of lime on CBR behavior of composites in soaked condition	104

4.14	Effect of lime on CBR behavior of composites at 7 days curing	104
4.15	Effect of lime on CBR behavior of composites at 28 days curing	105
4.16	Influence of Lime in CBR Gain for all composites at soaked condition	106
4.17	Influence of Lime in CBR Gain for all composites at 7 days curing	107
4.18	Influence of Lime in CBR Gain for all composites at 28 days curing	107
4.19	Effect of lime on compressive strength of composites at 7 days curing	109
4.20	Effect of lime on compressive strength of composites at 14 days curing	109
4.21	Effect of lime on compressive strength of composites at 28 days	110
4.22	Effect of lime on compressive strength of composites at 56 days	110
4.23	Post failure profiles of a few UCS specimens	111
4.24	Stress- strain behaviour of a sample	112
4.25	Post failure profiles of few Brazilian tensile test specimens	114
4.26	Effect of lime on tensile strength of composites at 28 days curing	115
4.27	Effect of lime on tensile strength of composites at 56 days curing	115
4.28	Effect of curing period on tensile strength as percentage of unconfined compressive strength of the composites containing 15, 20, 25 and 30% fly ash	116
4.29	Effect of curing period on tensile strength as percentage of unconfined compressive strength of the composites containing 35, 40, 45 and 50% fly ash	117

4.30	Effect of lime on pulse wave velocity of fly ash composites at 7 days curing	118
4.31	Effect of lime on pulse wave velocity of fly ash composites at 14 days curing	119
4.32	Effect of lime on pulse wave velocity of fly ash composites at 28 days curing	119
4.33	Effect of lime on pulse wave velocity of fly ash composites at 56 days curing	120
4.34	A typical P wave velocity signal plot of fly ash composite	120
4.35(a)	SEM photograph of (15FA+85O/B) +2L	124
4.35(b)	SEM photograph of (30FA+70O/B) +6L	125
4.35(c)	SEM photograph of (30FA+70O/B) +9L	125
4.36	XRD patterns of (30FA+70O/B) stabilised with 2, 3, 6 and 9% lime at 28 days	129
4.37(a)	Relationship between Brazilian tensile strength and unconfined compressive strength for all samples at 28 days of curing	132
4.37(b)	Relationship between Brazilian tensile strength and unconfined compressive strength for all samples at 56 days of curing	133
4.38(a)	Relationship between bearing ratio and unconfined compressive strength for all samples at 7 days of curing	133
4.38(b)	Relationship between bearing ratio and unconfined compressive strength for all samples at 28 days of curing	134
4.39(a)	Effect CaO content, CaO/SiO ₂ and CaO/(SiO ₂ + Al ₂ O ₃) ratios on CBR and compressive strength values	136
4.39(b)	Effect CaO content, CaO/SiO ₂ and CaO/(SiO ₂ + Al ₂ O ₃) ratios on tensile strength and ultrasonic velocity values	137
4.40	Variation of maximum dry density with lime content (Appendix)	186

4.41	Variation of optimum moisture content with lime content (Appendix)	186
4.42	Load vs penetration curves of untreated composites in unsoaked condition (Appendix)	187
4.43	Load vs penetration curves of untreated composites in soaked condition (Appendix)	187
4.44	SEM photographs of fly ash composites (Appendix)	188-189
4.45	XRD patterns of fly ash composites at 28 days curing (Appendix)	190-193
5.1	A typical haul road pavement under wheel load	140
5.2	Schematic layout of FEM modelling of haul road	141
5.3	Haul road cross-section under axisymmetry loading	143
5.4	Maximum strain of haul road pavement with conventional materials	145
5.5	Haul road pavement model with various positions in layers	145
5.6	Strain values at different depth of the pavement	146
5.7 (a)	Strain values at different depth of the pavement with varying subbase thickness	147
5.7 (b)	Stress values at different depth of the pavement with varying subbase thickness	147
5.8 (a)	Strain values at different depth of the pavement with 1.5subbase thickness with (30PA+70OB)+9L composite.	149
5.8 (b)	Stress values at different depth of the pavement with 1.5subbase thickness with (30FA+70OB)+9L composite.	149
5.9 (a)	Strain at different depth of the pavement using dynamic elastic parameters.	151
5.9 (b)	Stress at different depth of the pavement using dynamic elastic parameters.	151

5.10 (a)	Strain values at different depth of the pavement with composites containing 15 and 20% fly ash as subbase material	153
5.10 (b)	Strain values at different depth of the pavement with composites containing 25 and 30% fly ash as subbase material	153
5.10 (c)	Strain values at different depth of the pavement with composites containing 35 and 40% fly ash as subbase material	154
5.11 (a)	Stress values at different depth of the pavement with composites containing 15 and 20% fly ash as subbase material	154
5.11 (b)	Stress values at different depth of the pavement with composites containing 25 and 30% fly ash as subbase material	155
5.11 (c)	Stress values at different depth of the pavement with composites containing 35 and 40% fly ash as subbase material	155
5.12	Total strain and stress at various layers of haul road pavement with fly ash composites as subbase material (Appendix)	193-200

LIST OF TABLES

Table. No.	Title	Page No.
1.1	Parametric variations considered for the study	8
2.1	Haul road cross-section based on the CBR chart for a wheel load of 80mt	22
2.2	Range of chemical composition of Indian coal ashes and soils	40
3.1	Various proportions of flyash and overburden	66
3.2	Compositions (%) of (FA+O/B)+L	67
3.3	Relationship between CBR and quality of subgrade soil	76
3.4	Relationship between UCS and quality of subgrade soil	78
3.5	Experimental Design Chart	84
4.1	Physical properties of fly ash and mine overburden	90
4.2	Chemical compositions of fly ash, mine overburden and lime (wt. %)	94
4.3	Engineering properties of overburden and fly ash	96
4.4	Young's modulus values of the fly ash composites for 7, 14, 28 and 56 days curing	112
4.5	Poisson's ratios of the fly ash composites for 7, 14, 28 and 56 days curing	121
4.6	Young's (dynamic) modulus values of the fly ash composites at 7, 14, 28 and 56 days	122
4.7	Chemical compositions of the composites, cured for 28 days	127

4.8	Leachate concentration (ppm) at 7 days curing period	130
4.9	Best fit regression models between California bearing ratio values, unconfined compressive strength and tensile strength at different curing period	134
4.10	Best fit of regression models at 28 days curing period	135
5.1	Young's modulus, E (MPa) and Thickness, t (m) of the pavement layers for different cases	144
5.2	Dynamic Elastic parameters and Thickness of the pavement layers	151
5.3	Young's modulus, E (MPa) of fly ash composites	152

CHAPTER 1

INTRODUCTION

1.1 Background

The overall development of a nation primarily depends on the power or energy produced as well as consumed as it is directly related to the industrialization of nation. India needs huge power resources to meet the expectation of its denizen of as well as in its aim to be a developed nation by 2020. Fossil fuel continues to enjoy the dominant statue in meeting the demand for power generation and the trend will continue for next two to three decades. Coal is the world's most abundant and widely distributed fossil fuel. An estimate reflects that 75% of India's total installed power is thermal of which the share of coal is about 90%. Mining of the coal will remain a major activity. With the recent advances in mining technology, majority of the coal demand is met from surface mining due to its speed and ease of operations. The current coal production from surface mines in India is about 390 MT (85%) that will have to be increased substantially to meet the demand for power. Haul roads are the life line of any surface mine. Opencast mine economy depends on the cost of haul road design, construction as well as its maintenance in addition to other factors. These roads are used by heavy earth moving equipments. Production suffers, accident and breakdown occurs if they are not properly laid, constructed and maintained. Traditionally least attention is extended to its design, construction and maintenance. As a result mine economics gets adversely affected in terms of loss of production, dumper breakdown, poor working

conditions etc. The surface of the haul road depends on the behaviour of material beneath it. Strengthening of the base and sub-base layers beneath the surface of the surface coal mine haul road are of vital importance to improve upon mine economics. The materials used in haul road construction are typically sourced locally. It is envisioned that suitable material would address this issue. India produced huge quantity of fly ash due to high ash content in its coal reserves and its disposal is a major challenge to power plant operators. However due to technological advances fly ash has found multiple gainful usages in many applications. But those approaches do not address the huge generation completely.

1.2 Statement of the problem

A stable road base is one of the most important components of road design. Haul road is a multi-layered structure which consists of four layers as surface, base, subbase and subgrade. A typical surface coal mine has about 3 to 5 kms of permanent haul road, larger ones having longer lengths and various other branch roads that are constructed either with overburden material or from locally available material found near to the mine property. Common construction material for haul road as sand, gravels, clay, etc. result only in filling the spaces instead of offering total solution to ground stability. The behaviour of the surface course of haul road depends on the bearing capacity of the materials that are lying beneath it. It has been observed that surface course exhibits excessive rutting, potholes, settlement, sinking and overall deterioration. There has been exponential rise in carrying capacity of dumpers. But the construction of haul road has not been appropriately addressed to accommodate these changes. Typically truck haulage cost is nearly 50% of the total operating cost incurred by a surface mine (Thompson and Visser, 2003). The cost increases as the tonnage increases and large capacity dumpers are employed. Poor construction materials

result in haul road accidents, high maintenance cost of road as well as the machines with reduced profit. Surface mine operators spend a significant amount of money on haul road construction and its maintenance. In the past 30 years the carrying capacity of hauling equipments e.g. dumpers/trucks in India has grown from a 12 tons to 170 tons, 220 to 300 tons being envisioned at places, requiring better haul roads to carry heavy loads. However, there is a need to reduce vehicle operating cost and maintenance cost by well constructed good haul roads. Strengthening of the base and sub-base of the surface coal mine haul road is of vital importance to improve upon mine economics. It is desired that the base and sub-base of the haul road should exhibit reduced strain so as to achieve a strong and smooth road surface course.

Solid wastes from the mining and combustion of coal are serious environmental problems of vital concern to the producers and users of coal as well as the general public. Opencast mining involves displacement of large amount of overburden dump materials as mine waste to excavate coal from the earth. Overburden is the waste material which lies above as well as in between the coal seams. With the rising demand for coal, often surface mine operation go deeper and deeper. It creates dump site with huge excavated wastes. The overburden dumps formed outside the open pits besides occupying the lands alter the surface topography and contribute to the environmental degradation.

Fly ash is a waste by-product from thermal power plants, which use coal as fuel. Typically thermal plants are located near to surface coal mines that produce huge amount of fly ashes. The current annual production of coal ash is estimated around 600 million tons worldwide, with fly ash constituting about 500 million tons at 75-80% of the total ash produced (Ahmaruzzaman, 2010). Thus, the amount of fly ash generated from thermal power

plants has been increasing throughout the world, and the disposal of the large amount of fly ash has become a serious environmental problem as well as ecological imbalance. The problem with safe disposal of fly ash is a major issue as India is poised to burn 1800 million tonnes generating about 600 million tonnes of fly ash by 2031-32 due to the high ash (30% to 40%) content of the coal. Present generation of fly ash in India is 160 MT/year and it is expected to increase upto 300 MT/year by 2016-17 (Ram et al., 2011). Currently there exist about 160 opencast coal mines in India of various capacities. In most of the mines, the material used in the haul road is not adequate for supporting the wheel loads. Fly ash has potential to meet this criterion. The prospects of utilizing about 20 to 25 million ton of fly ash that would have been dumped as waste needs to be investigated, experimented and documented. It is expected to result (in the save) in cost to the nation in terms of reduced extraction of top soil and other materials for road construction purposes. The research undertaken focused on development of fly ash based composite materials using mine overburden and evaluated its performance to support heavy truck loads or dumpers in both dry as well as wet climatic conditions in the haul road.

1.3 Research Objectives

The aim of the investigation was to improve the performance of haul road so as to have smooth and better riding conditions, least maintenance and operator fatigue. It was proposed to be achieved with a strong surface course devoid of potholes, undulations and exhibit sufficient elasticity. The behaviour of surface course depends on that of the subbase course. The goal has been achieved by addressing the following specific objectives.

1. Detail study of the design of haul road particularly the base/subbase course in a typical surface coal mine.
2. Study of the haul road construction materials particularly that used in the subbase layer.
3. Determination of geotechnical properties of other available waste materials, as fly ash and mine overburden.
4. Investigation on available strength enhancing material.
5. Preparation and development of alternate haul road construction materials with fly ash, mine overburden and lime.
6. Determination of different geotechnical properties of the developed composite materials.
7. Leaching studies to determine the presence of heavy metals in the developed composite materials.
8. Numerical modeling to evaluate the performance of the developed material in haul road construction.
9. Prediction of quantum of fly ash usage.

1.4 Scope and Methodology

Coal extraction through opencast coal mines will continue to be a major source of power. Opencast mine economy also depends on the cost of haul road design, construction and its maintenance. Surface mine operators bear significant amount of expense on haul road construction and its maintenance. The subbase material for the haul road is either sourced from far off places or from the local soft clay, overburden material is used. Typically thermal power plants are located near to surface coal mines that produce huge amount of fly ashes. Its disposal is a major problem. Fly ash has many attributes for geotechnical applications. But its effectiveness in the use of haul road has not yet been completely explored and established.

The present research focuses on the use of the fly ash based composite materials for haul road construction and evaluate its performance to support heavy truck loads in both dry as well as wet climatic conditions in the haul road. The outcome of the research would be useful in improving the performance of haul road as well as increasing the prospects of utilization of fly ash by the industry. In addition to improve mine economics, saving due to gainful utilization of fly ash disposal would be enormous.

This investigation was an attempt to utilise coal mine overburden material and fly ash in different compositions along with lime, a popular strength enhancing media to improve the behaviour of haul road. The overall approach adopted to achieve the various objectives to reach the goal is outlined below (Figure 1.1).

- Review of literature on design and construction of haul road, impact of varying capacities of dumpers/ trucks, specifications of larger trucks and their tires, geotechnical properties of fly ash and its potential benefits for haul road construction.
- Development of experimental setup and characterization of ingredients.
- Development of fly ash and mine overburden mixed composite materials stabilized with additives and optimization of parametric variations.
- Determination of geotechnical properties of the developed composites by performing the tests and analyses as moisture density relationship, unconfined compressive strength, California bearing ratio, Brazilian tensile strength, Ultrasonic pulse velocity, morphological behaviour, X-ray diffraction analysis, energy dispersive X-ray analysis etc.
- Evaluation of potential of leaching heavy metals to ground water.
- Simulation of stress-strain behaviour to predict the thickness of the subbase layer as well as potential of fly ash usage.

The following methodology would be adopted to achieve the objectives and goal (Figure 1.1).

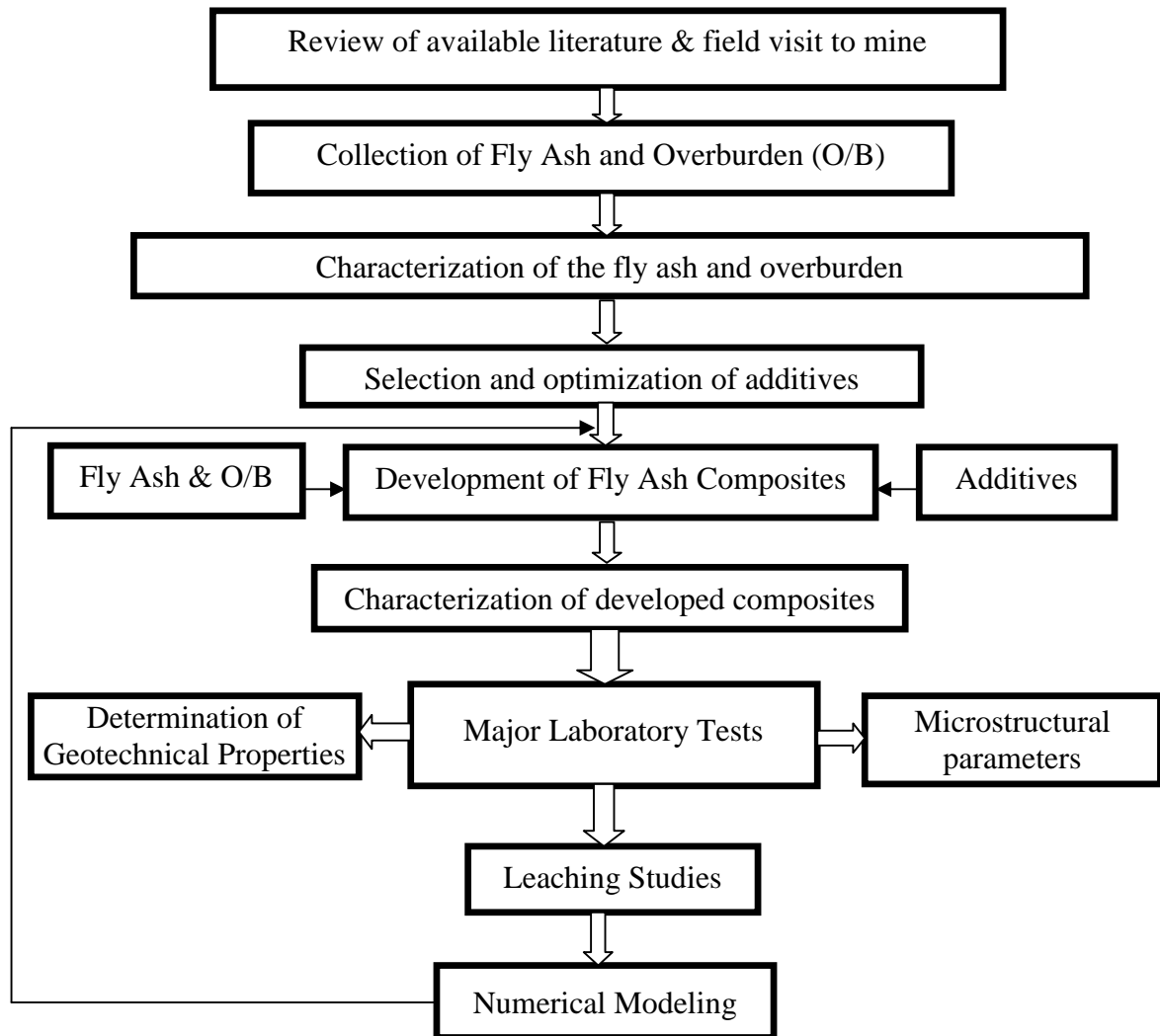


Figure 1.1: Flowchart of the methodology

1.5 Parametric variations

The objectives have been achieved by following a well designed methodology as well as considering the following parametric variations.

Table 1.1: Parametric variations considered for the study

A. Laboratory Investigation	<u>Parameters</u>	<u>Variations</u>
1. Characterisation of constituents	Fly ash and overburden	Physical properties: specific gravity, grain size distribution, consistency limits, plasticity index, free swell index Chemical properties: chemical composition, morphology, mineralogy, pH Engineering properties: compaction characteristics, permeability, shear strength parameters, angle of repose, California Bearing Ratio, Unconfined Compressive Strength
	Lime	Chemical composition
2. Development of composite material	Fly ash (%)	15, 20, 25, 30, 35, 40, 45 and 50
	Overburden (%)	85, 80, 75, 70, 65, 60, 55 and 50
	Lime (%)	2, 3, 6 and 9
	Curing period (days)	7, 14, 28, 56
3. Geotechnical characterization		Compaction characteristics, California Bearing Ratio (CBR), Unconfined Compressive Strength (UCS), Brazilian Tensile Strength, Pulse velocity, Young's modulus, Poisson's ratio
4. Environmental parameters		Leaching study

B. Numerical modeling

1. Finite element analysis software	ANSYS
2. Modeling	2D (Axisymmetry), Quadrilateral 4-noded
3. Model haul road pavement	4 layers: surface, base, subbase and subgrade
4. Layer thickness (s)	Surface (m): 0.2, 0.5 Base (m): 0.3, 1 Subbase (m): 0.8, 1, 1.5 Subgrade: semi-infinite
5. Tire pressure (kPa)*	700(max.)

* Tannant and Regensburg, 2001; Lav et al., 2006; Caterpillar Performance Handbook, 2010 (for new profile heavier dumper tires)

1.6 Organization of Thesis

The thesis is covered in six chapters. The first chapter gives an introduction which includes background of the research, statement of problem, objectives, scope and methodology of research work as well as parametric variations. Second chapter includes a detailed review of literature on mine haul road, haul trucks and geotechnical properties as well as applications of fly ash. Besides these it also covers environmental aspects of fly ash utilization and its interaction with soil, lime as well. The materials and methods of the investigation come under chapter 3 which includes collection of ingredients, sample preparation and testing techniques used for characterisation of materials as well as development of composite materials. Chapter 4 deals with results, discussion and analysis that include the results of geotechnical properties of ingredients and developed composite materials, results of microstructural analyses and leaching studies and finally development of model relationship between geotechnical parameters. It also includes the best fit models among various parameters. Numerical investigation to study the effectiveness of the

developed composite materials on the stress-strain behavior of haul road pavement is described in Chapter 5. Chapter 6 focused on summary and conclusion part of the investigation. At the end the reference and the detail experimental and numerical results are included in Annexure.

CHAPTER 2

LITERATURE REVIEW

2.1 Introduction

Mining provides us with essential resources. Historically, mining has evolved from small and simple operations to large and complex mining and processing systems that employ the latest in engineering technology. The total numbers of working mines at present are 2628 in 2010-11 out of which 574 mines deal in coal and lignite, 608 mines deal in metallic minerals and rest in non-metallic minerals. Presently, India produces around 90 minerals out of which 4 are fuel minerals, 10 are metallic minerals, 50 are non-metallic minerals, 3 are atomic minerals and 23 are minor minerals (Jha, 2011).

Coal is the world's most abundant and widely distributed fossil fuel. India is the third largest producer of coal in the world and has the fourth largest reserves of coal in the world (approx 197 billion tonnes) (Rai et al., 2011). An estimated 55% of India's installed capacity of 124,287 MW of power generation is through coal based thermal power plants. As per XI Plan, coal production would be raised to 680 million tonnes by the end of 2011-12 to meet the energy demand of the country (Ministry of Coal, 2007). Coal is mined by two main methods - surface or opencast mining and underground mining. Though underground mining is the oldest method of excavation, surface mining have been in force in recent years for its manifold advantages to meet the increasing demand of coal. In 1974-75 the share of total coal production from opencast mines was only 11%, whereas in 2009-10 and 2010-11 this has risen to 72.61% and 85% respectively.

In most of surface coal mines, explosives are first used in order to break through the surface or overburden of the mining area. The overburden is then removed either by draglines or by shovel and truck. Once the coal seam is exposed, it is drilled, fractured and thoroughly mined in strips. The coal is then loaded on to large trucks or conveyors for transport to either the coal preparation plant or directly to where it will be used. The overburden originates from the consolidated and unconsolidated materials overlying the minerals and coal seams, and is required to be removed. The average stripping ratio (overburden to coal) during the last three decades in India was $1.97\text{m}^3/\text{t}$ (Chaulya et al., 2000). Though there are attempts to reclaim the mined out area with filling by the waste dumps, the measures do not often accommodate all the displaced overburden. One of the major environmental challenges is to manage the huge volume of overburden generated in these opencast mines which is associated with the problems as aesthetics, visual impacts and landslides, loss of topsoil, soil erosion, water and air pollution, ecological disruption, social problems, safety, risk and health etc. The overburden is highly heterogeneous. These consists of alluvium, laterite, sandstone, carbonaceous shale, coal bands, clays, between coarse to medium grained highly ferruginous sandstone, thymide, turbidite, etc. Gradation results suggest that fines and coarse grains are approximately equally represented in the soil (Ulusay et al., 1995).

A typical surface coal mine has about 3 to 5 kms of permanent haul road, larger ones having longer lengths and various other lumpy roads that are constructed either with overburden material or from locally available material found near to the mine property. Some of those materials are asphaltic concrete, mudstone, sandstone, etc. Crushed gravel is often placed on top surface of the road. Asphaltic concrete needs base layer with CBR value more than 80 and is very costly. Common construction material for haul road as sand, gravels,

clay, etc. result only in filling the spaces instead of offering total solution to ground stability. Often it is observed that the operating and maintenance cost of dumpers are significantly high in addition to haul road maintenance cost. It results in reduced production, frequent breakdown, accidents, death hazards, low worker motivation, etc. These days' opencast mines are planned to significant depths, often beyond industry's current experience, expertise and knowledge base. In the past 30 years the carrying capacity of hauling equipments e.g. dumpers/trucks has grown from a tiny 10 tons to 170 tons, 350 tons being envisioned at places, requiring better haul roads to carry heavy loads. So, better haul road construction material would address the increase loading due to higher capacities.

Typically thermal power plants are located near to surface coal mines that produce huge amount of fly ash as a waste byproduct. The combustion of powdered coal in thermal power plants produces ash, which contains 80% fly ash and 20% bottom ash. The ash collected in electrostatic precipitators is called fly ash. Coal based thermal power plants all over the world face a serious problem of handling and disposal of the fly ash. The current annual production of coal ash is estimated around 600 million tons worldwide, which constitutes about 500 million tons of fly ash at 75-80% of the total ash produced (Ahmaruzzaman, 2010). Hence this huge amount of fly ash generated from thermal power plants and its disposal has become a threat to environment and even creating ecological problem by occupying large tracts of scarce cultivated lands. The high ash content (40-50%) of the coal in India makes this problem more complex. In India, the current level of generation of fly ash is 160 million tonnes per year and is projected to increase about 300 million tonnes by 2017 and 1000 million tonnes per year by 2032 (Kumar, 2010). Safe disposal of the ash without adversely affecting the environment and the large storage area

required are major issues and challenges for safe and sustainable development of the country. Hence efforts are being made continuously by making stringent regulations by the Government to fully utilize the fly ash. At present about 50% of the fly ash is being gainfully utilized in India (Sahay, 2010). But a conservative estimate puts the unutilized fly ash occupying about 65000 acres of land (Das and Yudhbir, 2006) which demands increase in the utilization percentage. The disposal of fly ash would require 1000km^2 which in turn shall necessitate new disposal areas, sites involving displacement and hence rehabilitation problems by 2015 (Kumar, 2010). Thus it is very essential to find new avenues for its effective utilization in bulk. Bulk utilization of fly ash can be accomplished only in geotechnical engineering applications such as construction of embankments, as a base/subbase material in roads, structural fills and dykes etc. Utilization of fly ash in such applications minimizes the disposal problem of fly ash and also reduces the construction cost of the projects. Surface mine haul road construction is one such avenue for fly ash use in bulk.

Fly ash, being very finer, is more reactive and consequently more suitable for haul road construction material as compared to other materials. Potential application of fly ash alone or soil stabilized with fly ash or fly ash and admixtures for road construction has been reported by a number of researchers (Consoli et al., 2001; Kumar, 2005; Mohanty and Chugh, 2006; Mackos et al., 2009). The enhancement of mechanical strength of fly ash with addition of lime has been reported elsewhere (Sivapullaiah, 2000; Beeghly, 2003; Mishra and Rao, 2006; Ghosh and Subbarao, 2007). There have been many successful instances of fly ash being used as road construction material. Yet its effectiveness in the surface coal mine haul road has not been evaluated so as to establish it commercially.

Surface coal mine haul road undergoes more stress/strain due to multiple reasons such as poor surface course, inadequate construction process, poor construction materials, varying load on the surface, improper drainage system, etc. An attempt has been made in this research to evaluate the potential of overburden and fly ash mixes in addressing the same. Literature related to surface coal mine haul road construction and fly ash as construction material is reviewed in this chapter.

2.2 Mine haul roads and haul trucks

In open cast coal mines, haul roads are basically required for the transportation of coal from the various coal faces to the coal receiving pits, overburden materials to the dump yard and also for the movement of vehicles to the workshops or parking places (Figure 2.1). Construction of haul road is a very important part in controlling sediment-laden runoff from a mine site.



Figure 2.1: A typical permanent haul road

2.2.1 Classification of haul roads

Haul roads are classified into following categories depending upon the traffic and the nature of operations on the various haul roads.

Permanent haul roads: These are the initial constructed roads, often include the approach to property and extend to the end of the dumping yard. The characteristics of this type of roads are long life, made of maximum thickness, high quality construction materials, expensive to build, etc. These roads are generally made outside the quarry area which is the first access. They have to be maintained for the whole life of the open cast project. A typical system of haul road classification in an open cast mine is shown in Figure 2.2

Semi-permanent haul roads: The characteristics of these roads are medium life period, engineered to desired thickness, high quality construction materials, relatively expensive to build, used as main haul roads in pits and dumping yards. These types of roads which have a lifespan of 3 to 5 years are often clubbed with permanent haul roads (Vittal and Mathur, 2010). These roads are also made of similar materials used in the permanent haul road with lesser thicknesses.

Temporary haul roads: These roads are characterized as short life period, minimum pavement thickness, low quality construction materials, inexpensive to build and used mainly for shovel or dumping yard access. They change considerably with the advancement of the quarry face. Typical construction materials consist of those found in the mine property in the vicinity.

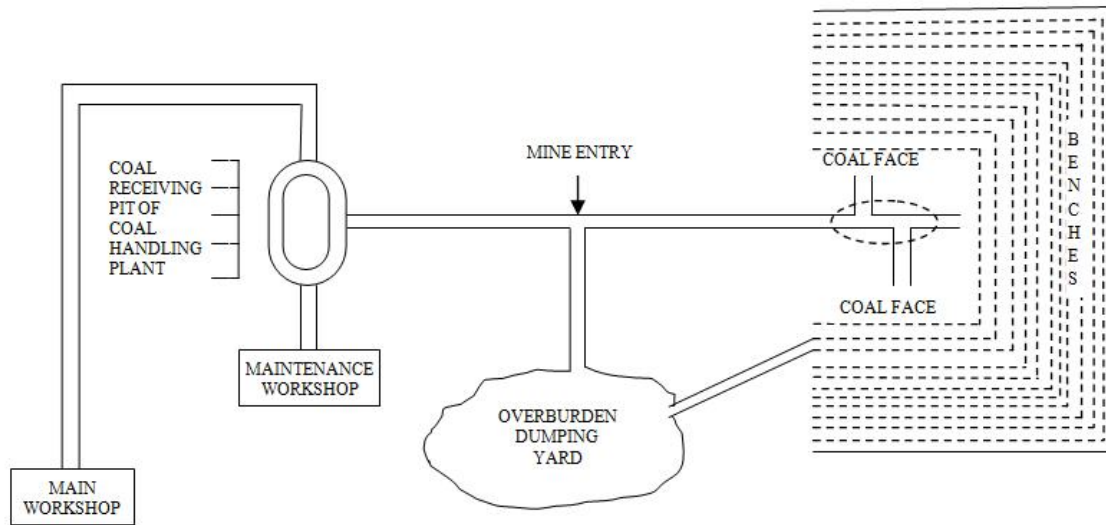


Figure 2.2: A typical system of haul road classification in an opencast mine

2.2.2 Design of haul road pavement

Road surface should not only be stable, non-yielding but also even along the longitudinal profile to enable the vehicles move faster safely and comfortably. The pavement carries the wheel load and transfers the stresses through a wide area on the soil sub grade below. It results in the stress being transferred to the sub grade soil through pavement layers considerably lower than the contact pressure or compressive stresses under the wheel load on the surface. This reduction in wheel stresses depends on factors as thickness of layer as well as characteristics of the pavement layers. So though an effective pavement construction should ensure distribution of wheel load stress to a larger area per unit depth of the layer, yet a small amount of temporary deformation is always associated. Design and construction should ensure to keep this elastic deformation of pavement within limits. Between the two pavement structures- rigid and flexible type, the later is followed in the construction of haul road. Pavement structure deflects or flexes, under loading in flexible pavement. Flexible pavement structure is typically composed of several layers of materials. Each layer receives loads from

the above layer, spreads them out and passes on these loads to the next layer below. Thus the stresses are reduced from top layer to the bottom layer. The layers are usually arranged in the order of descending load bearing capacity with the highest load bearing capacity material (and most expensive) on the top and the lowest load bearing capacity material (and least expensive) on the bottom. It transmits the vertical or compressive stresses to the lower layer by grain to grain transfer through the points of contact in the granular structure. It needs a well compacted granular structures consisting of strong materials to transfer the compressive stresses. The stress or compressive loading is maximum on the pavement surface directly under the wheel load and is equal to the contact pressure under the wheel. These stresses get distributed to a larger area in the shape of truncated cone and hence decrease at lower layers. Hence multilayer construction of road is desirable. Haul road pavement consists of four distinct layers namely, surface course, base course, sub-base and sub-grade as shown in Figure 2.3.

- The surface course is the layer of a haul road with which the wheels of vehicles are in actual contact. The characteristics of the surface course should be of high adhesion, low rolling resistance coefficient, no penetration under load. It is generally made of bitumen, asphalt or compacted gravel to provide a smooth riding surface and will resist pressure exerted by the tires.
- The base course is the layer of material which lies immediately below the surface course. It consists of granular material like stone fragments or slag that can be stabilized with binding materials like cement, natural pozzolans etc. The base course is the main source of the structural strength of the road.

- Subbase is the layer of a haul road pavement, which lies between base course and subgrade. The base course and sub- base courses are primarily used to improve load supporting capacity by distributing the load. It usually consists of same type of materials used in base course like laterite, crushed stone, gravel, moorum, natural sand either cemented or untreated. Apart from providing structural strength to the road, it serves many other purposes such as preventing intrusion of sub-grade soil into the base course, accumulation of water in the road structure, and providing working platform for the construction equipment. The subbase distributes vehicle load over an area large enough that the stresses can be borne by the natural, subgrade material (Khanna and Justo, 2001).
- The sub-grade is the naturally occurring surface on which the haul road pavement is constructed. It may be leveled by excavation or back-filled to provide a suitable surface. The performance of the haul road is affected by the characteristics of the sub-grade. The loads on the pavement are ultimately received by the sub-grade to be transferred to the earth mass. It should not be overstresses at anytime i.e. the pressure on top of it should be within permissible limit.

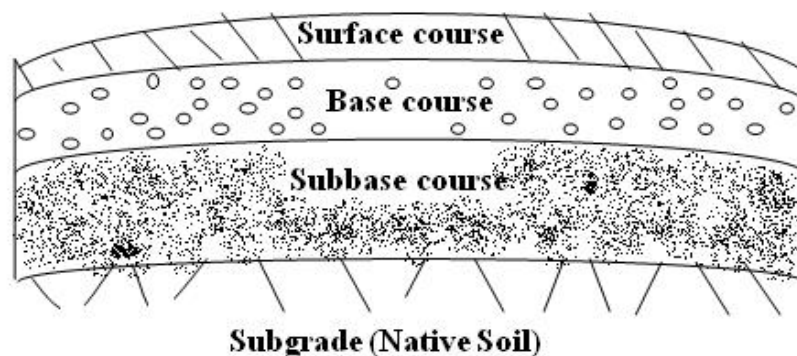


Figure 2.3: Typical haul road cross-section

There exist two road design methods that calculate the appropriate thickness of each layer in the haul road by considering material properties such as CBR (California Bearing Ratio) and resilient modulus (Yoder and Witczak, 1975; Kaufman and Ault, 1977; Thompson and Visser, 1996; Mohammad et al., 1998). One of the most popular method that uses the CBR values of the construction materials as a design criteria. The CBR method was developed by the California Division of Highways, USA during 1928–1929 for design of road pavements. In resilient modulus based method, the road cross-section is designed using predicted stresses, strains and each layer's resilient modulus.

2.2.2.1 Haul Road Pavement design based on CBR

The load bearing capacity of a soil is directly related to its Shear strength defined by Mohr-Coulomb relation. Tire loadings of haul roads often exceed the bearing capacity of most road base materials at their normal insitu moisture content and hence strong material construction is needed for stable design. CBR test is a laboratory penetration test of a soaked sample of pavement construction materials as an inference of its shear strength. CBR value is a relationship between the force necessary to drive a piston into the material and corresponding value to likewise drive the piston into a standard gravel sample upto a known depth and the result are reported as a percentage of standard (gravel) tests. California bearing ratio (CBR) method is one of the most popular and widely used empirical methods for road construction. It was observed that failure or poor pavement performance of road occur due to inadequate compaction of materials forming the road layers and insufficient cover thickness over weak in situ material. Porter (1949) developed the cover thickness requirements over in situ materials of specific CBR (%) values that were applicable for airfield pavement design. The use of CBR method for the design of haul roads in surface mines was first recommended

by Kaufman and Ault (1977). CBR value for a specific material was developed from a laboratory penetration test of a soaked samples of pavement material from which its shear strength could be inferred.

2.2.2.1.1 Design Procedure

The CBR method estimates the bearing capacity of a construction material by measuring the resistance offered by it to the penetration of a standard cylindrical plunger. The detail procedure for conducting the test is described in the Indian Standard (IS): 2720 Part 16. Design charts have been developed that relate pavement, base and sub base thickness to vehicle wheel load and CBR values (Figure 2.4). Cover thickness requirements for various wheel loads corresponding to a wide range of CBR values of the construction materials are also illustrated (Figure 2.4). The CBR method assumes that failure will occur when the cover thickness above a certain material is less than required, according to standard CBR chart. The maximum wheel load is determined by dividing the loaded vehicle weight over each axle by the number of tires on that axle. The highest wheel load of a loaded vehicle is used in the CBR design chart.

A relation between CBR, layer thickness, layer type and total fill cover has been suggested (Table 2.1). The layer thickness can be determined from the cover thickness required by one possible layer from the cover thickness required for the immediate lower layer. The CBR method of haul road design has been very popular and is being followed (Kaufman and Ault, 1977; Atkinson, 1992; Thompson, 1996; CMPDIL, 2000). The method is simple, well understood and gives good design guidelines for haul roads. In India, CBR method is used for haul road construction in surface mines (CMPDIL, 2000).

Table 2.1: Haul road cross-section based on the CBR chart for a wheel load of 80mt (Tannant and Regensburg, 2001)

Layer	Typical material	CBR (%)	Total fill cover (m)	Layer thickness (m)
Surface	Crushed rock	95	-	0.30
Base	Pitrun sand & gravel	60	0.30	0.30
Sub-base	Till, mine spoil	25	0.60	1.60
Sub-grade	Firm clay	4	2.20	-

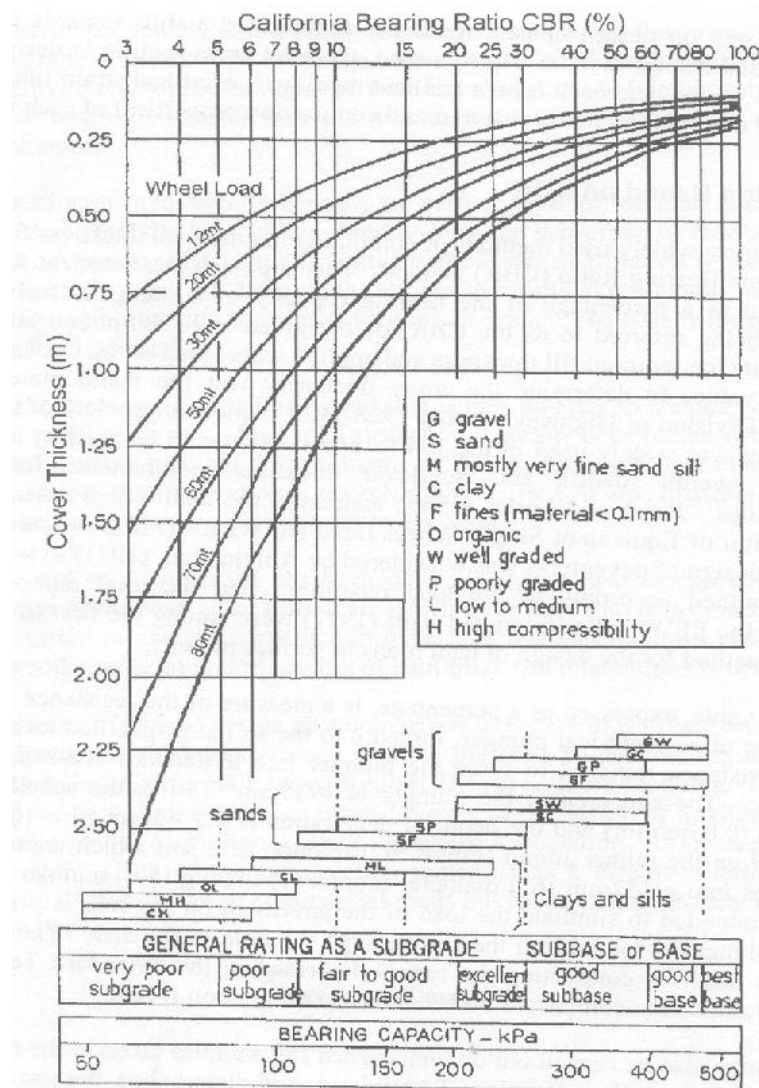


Figure 2.4: CBR design chart (recommended by Indian Roads Congress, 1970)

2.2.2.2 Haul Road Pavement design based on resilient modulus

It is a non-linear approach to measure the pavement roadbed soil strength under dynamic loading. The determination of resilient modulus is a complicated process (Ping, 2001). AASHTO (1993) T294 is the most commonly used laboratory test method to determine the resilient modulus of an unbound soil by repetitive loading of a soil sample in a triaxial chamber. Alternatively, other methods are available to estimate the resilient modulus. Thompson (1996) estimated the resilient modulus by the falling weight deflectometer test. This test is easier to conduct and can provide in-situ layer moduli at a lower cost and with a minimum amount of disturbance, although the values may not always be accurate. A material's resilient modulus is actually an estimate of its modulus of elasticity (E). While the modulus is stress divided by strain for a slowly applied load, resilient modulus is stress divided by strain for rapidly applied loads. The stiffness of a material increases with repetition of loading and thus the initial Young's modulus is lower than the resilient modulus (Figure 2.5). Conventionally, determination of the Young's modulus gives a reasonable estimate of the resilient modulus, even if on the conservative side as there is no confining pressure and stiffening of soil due to repeated loading.

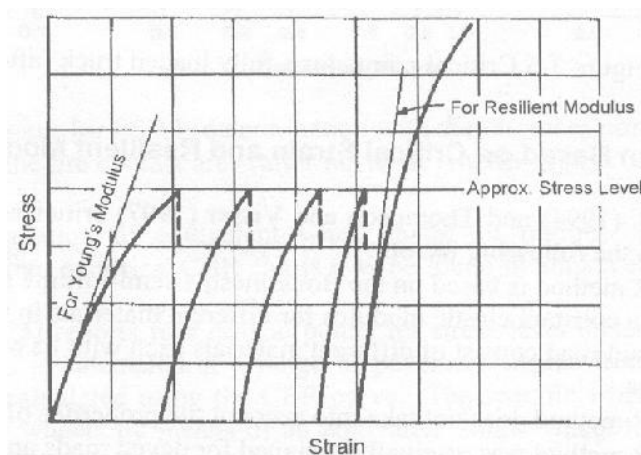


Figure 2.5: Method to obtain resilient modulus (after Bowles, 1984)

Mohammad et al. (1998) and Rahim et al. (2002) described yet another method for calculation of resilient modulus using a cone penetration test with continuous measurement of tip resistance and sleeve friction. Kim et al. (2001) proposed an alternative testing method to determine resilient modulus of soils using a static triaxial compression test. The resilient modulus test provides a relationship between deformation and stresses in pavement materials, including subgrade soils, subjected to moving vehicular wheels. It also provides a means of analyzing different materials and soil conditions, such as moisture and density and stress states that simulate the loading of actual wheels. Determination of the subgrade resilient modulus is important for designing pavement thickness. If the selected design resilient modulus value is much higher than actual field, or in situ resilient modulus, then thickness of the pavement will be insufficient. If the design value is too low, the design will be too conservative and uneconomical (Kasaibati et al., 1995). The magnitude of resilient modulus is greatly affected when low values of specimen deflection or strain, occur because of physical difficulties and limitations in measuring very small deflection values. Generally, values of resilient modulus tend to be more accurate as specimen deflections increase and fall within the accuracy range of equipment used to measure deflections (Hopkins et al., 2001). The resilient modulus method is based on the strain caused in different layers of the haul road provided by Morgan et al. (1994) and Thompson and Visser (1997). The induced strain is a function of the modulus of the material for a given stress in a layer.

2.2.2.2.1 Design Procedure

The resilient modulus method is a mechanistic-empirical based method in which pavement structure and load configuration is assumed. The structure is then simplified to four distinct layers (AASHTO, 1962; Lav et al., 2006). Initially, the thickness of each layer is

estimated based on past experience or designs at mines with similar conditions. After simplifying the structure, the stress induced by specified wheel loading is calculated in order to identify the critical strains in the structure (pavement analysis) by means of purpose developed computer programs or software. These are usually based on linear elastic theory or finite element methods. The layers in the pavement structure are generally considered to be homogenous and isotropic. Fundamental properties of layers are expressed by elastic modulus and poisson's ratio. The layer thickness depends on the resilient (Young's) modulus of the haul road construction material. Strain modeling is performed to ensure that the vertical strain at all points is less than the critical strain limit.

Mines using ultra-large trucks/ dumpers with gross vehicular weight more than 400T use the results of resilient modulus of the construction materials (Tannant and Regensburg, 2001).

2.2.2.3 Critical strains and typical mode of failure in a haul road

The critical strains usually occur under the wheel paths (Lav et al., 2006). These are horizontal tensile strains developed at the bottom of the surface layer and base/sub base layer due to axial load which control fatigue cracking, while the vertical compressive strains at the top of the subgrade layer control the permanent deformation (Figure 2.6).

The failure of a flexible pavement structure supported on a subgrade soil and subjected to repeated traffic loading can occur through two primary mechanisms - collapse of the pavement structure or cracking of the surface of the pavement. A collapse of the pavement structure occurs due to large plastic (permanent) deformations in the subgrade soils. At times, even when the loads on the pavement are not excessive but nominal, the pavement surface crack due to fatigue, caused by the reversal of elastic strains at any location in the pavement

system. As a result of repeated (cyclic) loads such as those caused by moving traffic, cohesive soils in the subgrade incur repeated elastic deformations. When these deformations exceed a threshold value, premature fatigue failure of the flexible pavement through cracking of the pavement surface occurs.

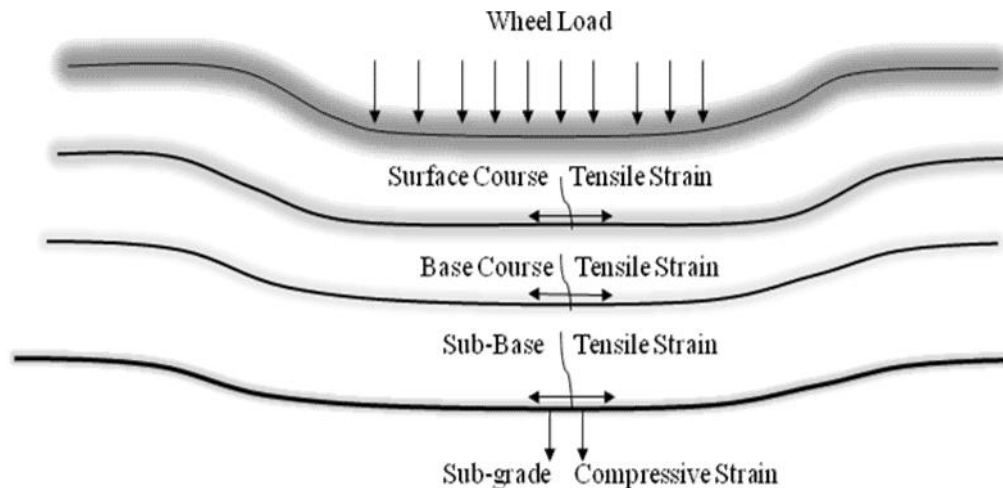


Figure 2.6: Critical strains and failure mode in pavement structures

2.2.2.4 Critical strain limit

The important criterion for haul road design is a critical strain limit for each layer. A road cannot adequately support haul trucks when vertical strain exceeds a critical strain limit (Tannant and Regensburg, 2001). Critical strain limit was about 1500 micro-strains at the top of the subgrade found by Morgan et al. (1994). Thompson and Visser (1997) noted that the critical strain limit was around 2000 micro-strains at the road surface. The critical strain limit is determined for a particular road depending on the number of loaded trucks expected to travel over it during the designed life of the road. The number of loads passing a particular section of a road depends on the designed life of the road as well as the traffic density. The

maximum critical strain limits have been established to be 1500-2000 micro-strains for typical haul roads (Thompson and Visser, 1999; Tannant and Regensburg, 2001).

2.2.3 Symptoms and causes of haul road deterioration

Haul road exhibits excessive rutting, potholes, settlement, sinking and overall deterioration. The precipitation/runoff, heavy traffic volume, spring breakup and vehicle spillage and poor compaction are the major causes of the surface course of haul road deterioration. The base course of the haul road deteriorates due to precipitation/runoff, heavy traffic volume, spring breakup and poor compaction. Poor compaction, high ground water level and precipitation are major causes of deterioration to subbase and existing layer (Mining officials, 2008). Lack of sufficient rigid bearing material beneath the surface course exhibits excessive rutting, potholes, settlement, sinking and overall deterioration of the travel way (Kaufman and Ault, 1977; Wade, 1989; Collins et al., 1986; Thompson and Visser, 1996; Tannant and Kumar, 2000). Potholes are those depressions in the haul road surface that occur in the wheel path mostly due to traffic movement. One of the reasons is local structure failure that arises from poor compaction and/or shear in the subgrade. Excessive roughness on haul roads also causes corrugations. Though it is a surface phenomenon, its origin may be linked to low plasticity materials on the base and subbase courses, especially those with high sand and gravel fraction (Heath and Robinson, 1980).

Rutting is the formation of progressive longitudinal depression in the wheel tracks. It primarily originates on mine haul road either due to deformation of wearing course materials as due to sub-grade materials. Poor construction materials result in haul road accidents, high maintenance cost of road as well as the machines with reduced profit.

2.2.4 Characteristics of Base/Subbase course materials of the haul road

Base and sub-base layers are constructed either with interburden/overburden material or from locally available material found near to the mine property. The stabilization of the above materials is required when the design with current materials yields unacceptable thickness of layers and/or the suitable construction materials are uneconomic to use due to distance or depth limitations or environment restrictions. Generally, pit run gravel is used for the base layer. The sub-base is often constructed from interburden/overburden, sand, silty or sandy till, or other suitable materials. Usually the materials used in base and sub-base layers are not crushed thus a particular particle size distribution is difficult to enforce. Some materials have high plasticity index and cohesive in nature. Common construction materials for haul road base/ subbase result only in filling the spaces instead of offering total solution to ground stability (Chironis, 1978; Fung, 1981; Atkinson, 1992; Thompson and Visser, 1997).

2.2.5 Haul Trucks

In the past 30 years the carrying capacity of hauling equipments e.g. dumpers/trucks has grown from a tiny 10 tons to 170 tons, 350 tons being envisioned at places, requiring better haul roads to carry heavy loads. Larger haul trucks are being designed, produced, and accepted by the industry due to economy of scale. Haul trucks used in surface mines have grown significantly in terms of size and capacity. The larger haul trucks have an impact on road design. The haul road width depends upon the width as well as turning radius of the larger haul trucks. The maximum width of the haul truck has gone up from 9m in 1999 to 15m in 2010. The turning radius of the haul trucks has increased by 12% over that of a generation earlier. Hence, larger turning radius and width of road is required to accommodate the largest trucks.

2.2.5.1 Haul trucks tires

Haul truck tires have grown with the size and capacity of trucks. The major component materials of a tire are: rubber (both synthetic and natural), carbon black, sulphur, steel cable, polyester, nylon, and other chemical agents. A common ratio of rubber to other materials is 50:50 for a radial car tire and about 80:20 for an off-road haul truck tire. For large haul truck tires, about 80% of the rubber comes from natural sources. A higher proportion of natural rubber means a greater capacity to dissipate heat, but lower wear resistance. A higher proportion of carbon black leads to greater wear resistance of tires, but carbon tends to retain heat, thus the tire gets heated more easily. If the haul road has an abrasive surface, a tire with a greater percentage of carbon black would be desired. But, if the haul road is smooth and free of abrasive materials, a tire with higher percentage of natural rubber would give better service in terms of tonne-km/hr (Tannant and Regensburg, 2001).

There are two major types of tire: bias ply and radial (Figure 2.7). Bias ply tires use rubber-cushioned nylon to form the carcass and steel wire bundles for beads. Radial tires consist of a ply of steel cables laid radially about the tire as carcass. The bead of the radial tire is formed by a single bundle of steel cables or steel strip. Radial tires have longer tread life, greater stability, more uniform ground pressure, less rolling resistance and less heat buildup from internal friction when the tire is in motion as compared to bias ply tires (Michelin, 2005). Large haul trucks tend to use radial tires due to these reasons. Werniuk (2000) reported that the 95% of the tires used on large surface haul trucks are radial tires. The information on tires is described in detail in the Tire Maintenance Manual (Good Year, 2008) and Caterpillar Performance Handbook (2010).

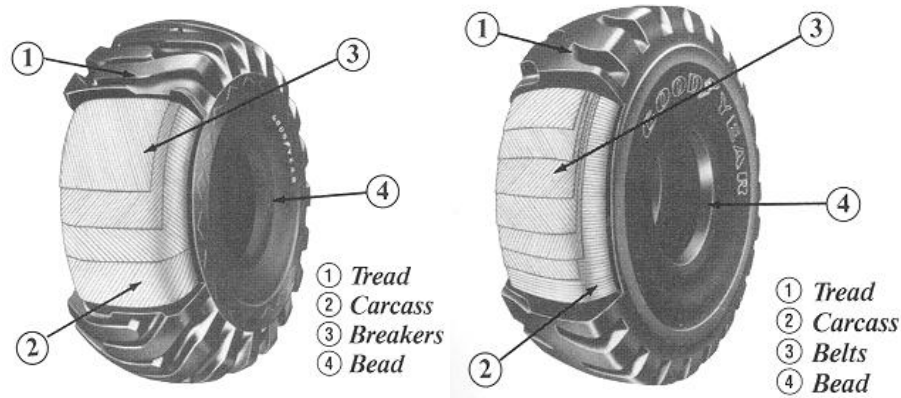


Figure 2.7: Bias ply and radial tires (Good Year, 2008)

2.2.5.1.1 Tire foot print area and pressure

Two important elements of tires that affect haul road design are foot print area and tire pressure. The inflation pressure of new low profile truck tires vary between 586 kPa to 703 kPa (Good Year, 2008; Caterpillar Performance Handbook, 2010). The bearing capacity of the haul road construction materials should be greater than the tire pressure. Thus the bearing capacity of materials should be more than 1MPa (equivalent to compressive strength of soft rock) used for the surface course (Tannant and Regensburg, 2001). A well designed subbase and base layers with sufficient bearing capacities and stiffness is very much important because the stress bulb below a tire can extend quite deep due to the large tire footprint areas. The shape of tire footprint is approximated as either a circular or rounded rectangle. The pressure distribution beneath a tire is non-uniform, especially for bias ply tires. However, an assumption of uniform pressure distribution across the tire foot print area for the purpose of stress analysis in haul road layers is suggested (Kumar, 2000).

The different wheel loading conditions typically considered are based on (i) maximum wheel load, (ii) contact pressure, (iii) multiple wheel loads or its equivalent, and (iv) repetition of loads.

The vertical stresses due to wheel loading on the haul road have strong influence on pavement strain prediction. There are many approaches to predict the stresses at any point in the pavement mass; one among those is elastic theory. According to it there exists constant ratio between stresses and strain even though the material is not elastic. Initially the thickness of the pavement is determined using traffic volume, single wheel load and increased wheel load based on permissible maximum allowable shear stress for specific materials. Now the dual wheel cases have been considered as equivalent single wheel load (ESWL) where a load is determined that generates the same tyre contact area and maximum deflection as would the group of wheels. The concept to consider equivalent single wheel load to multiple wheels give rise to corresponding equivalent deflection. Turnbull and Ahlvin (1957) suggested mathematical approach to determine thickness of pavement using CBR method.

The contact pressure and its distribution between any tire and the pavement depends on tire pressure, wheel load and tire construction. Usually the maximum weight of the haulage machine is considered in designing the road section. Though the true contact area between tire and road surface is elliptical, it is considered circular in shape for case of calculation (Husrulid and Kuchta, 2006). The contact area is usually circular for a low ratio between applied load and maximum rated load (Marshek, 1978). Typically the ratio varies between 0.7 to 0.9 for fully loaded mine trucks (Good Year, 1990) and the contact area is almost rectangle. The governing mathematical relations adopted from Thompson (1996) are given below.

$$\text{Contact Area (m}^2\text{), } A = \frac{\text{Load}}{\text{Tire Pressure}} \dots \dots \dots (1)$$

$$\text{The contact radius (m), } r = \sqrt{\frac{A}{\pi}} \dots \dots \dots (2)$$

The thickness (m), $t = \sqrt{\frac{P}{55.8 \times CBR} - \frac{A}{\pi}} \dots \dots \dots (3)$

The above equation is applicable for CBR less than 12 with multiple wheel groups the corresponding thickness for multiple wheel groups is

$$t = \sqrt{A} \left(-0.0481 - 1.1562 \left(\log \frac{CBR}{P_e} \right) - 0.6414 \left(\log \frac{CBR}{P_e} \right)^2 - 0.4730 \left(\log \frac{CBR}{P_e} \right)^3 \right) \dots \dots (4)$$

where P_e = equivalent tyre pressure at depth t

$$P_e = \frac{ESWL}{A} \dots \dots \dots (5)$$

Incorporating the repetition factor, the equation to calculate CBR is

$$CBR (\%) = \frac{ESWL}{55.8 \left[\left(\frac{t}{a} \right)^2 + \frac{A}{\pi} \right]} \dots \dots \dots (6)$$

where α = repetition factor as determined elsewhere (Ahlvin et al., 1971)

or

$$t = \alpha \sqrt{A} \left(-0.0481 - 1.1562 \left(\log \frac{CBR}{P_e} \right) - 0.6414 \left(\log \frac{CBR}{P_e} \right)^2 - 0.4730 \left(\log \frac{CBR}{P_e} \right)^3 \right) \dots \dots (7)$$

The deflection under a single wheel load (W_s) is given by

$$W_s = \frac{r_s}{E} b_s F_s \dots \dots \dots (8)$$

and deflection for a group of wheels (W_d) is

$$W_d = \frac{r_d}{E} b_d F_d \dots \dots \dots (9)$$

where, r_e = contact radius for single wheel (m)

E = Elastic modulus of pavement (MPa)

b_s = tyre pressure for single wheel (MPa)

F_s = deflection factor for single wheel.

r_d = contact radius for multiple wheels (m)

b_d = tyre pressure for multiple wheel (MPa)

F_d = deflection factor for group of wheels

Rearranging eq. (6) with input from eq. (1) and eq. (2)

We have $P_s = r_s^2 b_s$ and $P_d = r_d^2 b_d$ (10)

where, $P_{s,d}$ represent tyre pressure for single wheel load and multiple wheel loads respectively.

Equating $W_s = W_d$ and $r_s = r_d$ we have

$$\frac{F_s}{F_d} = \frac{b_d}{b_s} \text{ or } \frac{P_s}{P_d} = \frac{F_d}{F_s} \dots\dots\dots (11)$$

The equation (11) shows the relationship between tire load and the deflection factor, which can be obtained from the established curve (Figure 2.8). It was reported that four critical points for stress level exists under a haul truck (Yoder and Witczak, 1975). The ESWL represents dual assembly and the critical points occur either under the center of one rear load (D) or at the center of the rear axle (C) (Figure 2.9). Two additional critical points (A and B) are also analyzed considering the front axle interaction in proportion to the fully laden axle weight distribution. The influence of the each wheel at depth increment is calculated and the maximum ESWL at that depth is determined using equation (7 and 11). The load distribution beneath a tire in the road pavement is shown in Figure 2.10.

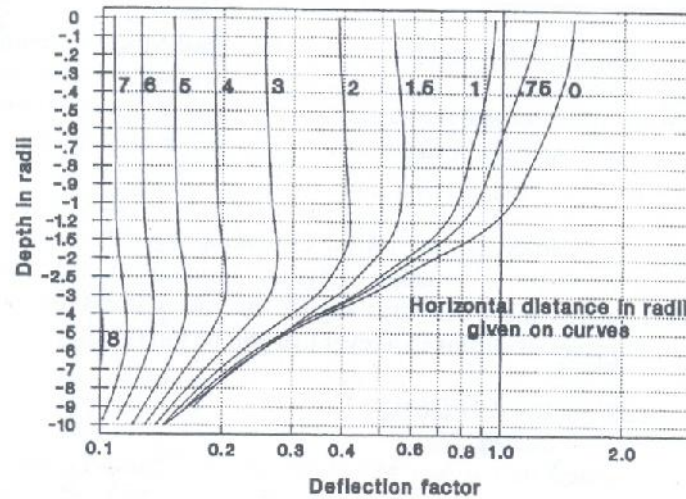


Figure 2.8: Deflection factors for ESWL determination (after Foster and Ahlvin, 1954)

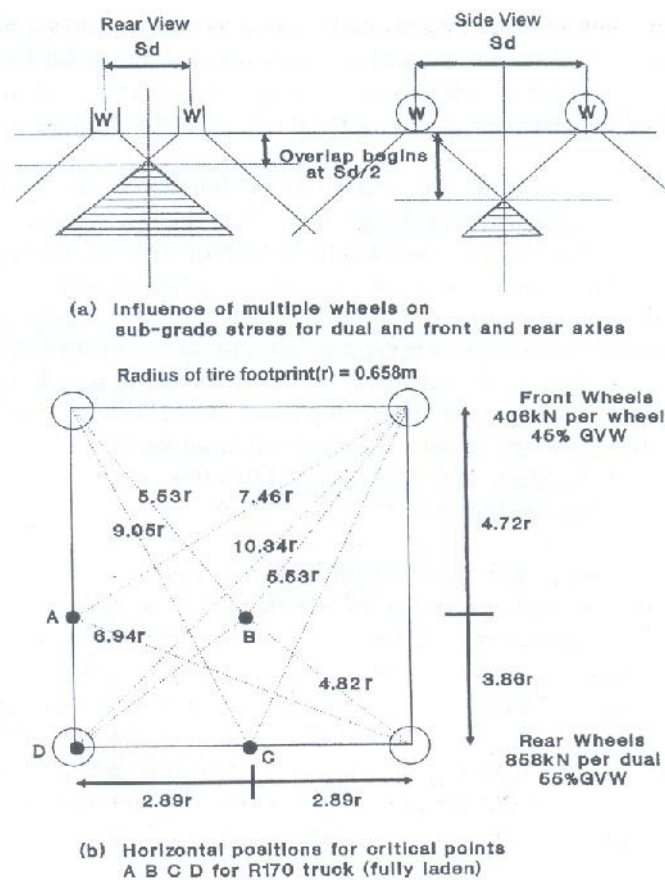


Figure 2.9: Critical points for a fully loaded truck (after Thompson, 1996)

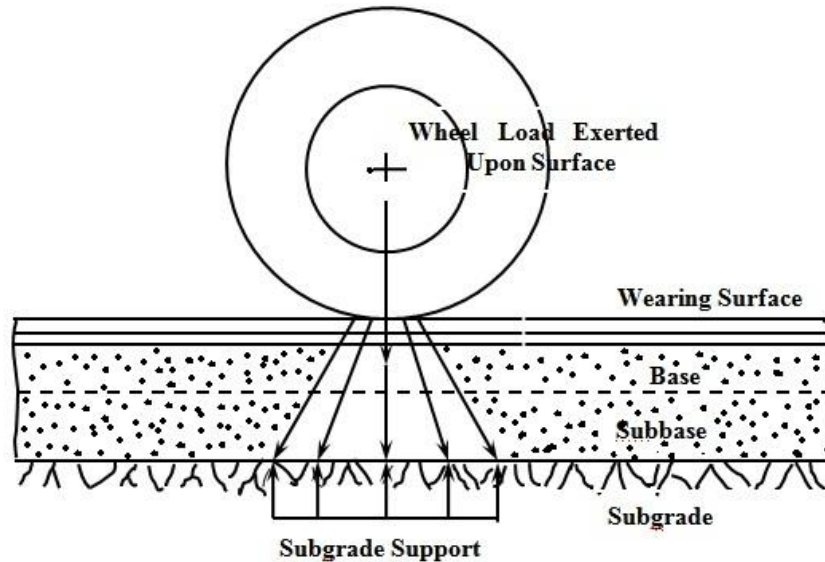


Figure 2.10: Load distribution beneath a tire

2.3 Geotechnical properties of fly ash

Fly ash is a byproduct of burning of pulverized coal in thermal power plants. The pulverized coal is burnt at 1300° to 1500°C . Typically the fine residue composed of unburned particles that solidified while suspended in exhaust gases is called fly ash. It is carried off in stack gases from boiler and is collected either by mechanical methods or by electrostatic precipitator. Typically it constitutes 80% of ash and rest being termed as bottom ash. The physical and chemical properties of ash vary depending on origin of coal, type of plant, burning process, inorganic chemical composition of coal, degree of pulverization, types of emission control systems, handling and collection systems etc. Typically two types class C and class F exists. Class F is a non-self cementing type and is produced from burning of anthracite and bituminous coal. It contains very small amount of lime (CaO) unlike class C which possess higher quantity to produce cementitious product. Class F fly ash (pozzolans) has silicon and aluminum material that itself possess little or no cementitious value level. It reacts chemically with lime and cement at room temperature to form cementitious compounds

(Chu et al., 1993). The following features of various properties of fly ash as well as reports the many application of it elsewhere.

2.3.1 Physical Properties

Physical properties of fly ash help in classifying the fly ashes for engineering purposes. Rehsi and Garg (1988) have made a critical assessment of the different physical properties of Indian fly ashes. The particles of the fly ashes were angular as well as irregular. The shape of the particles were affected the different physical properties of fly ash. The specific gravity of fly ash is generally low compared to that of soil (Ghosh, 1996; Sridharan and Prakash, 2007). Pandian et al. (1998) reported that the range of specific gravity varies from 1.46 to 2.66 for Indian fly ashes. Specific gravity of Indian fly ashes varies in the range of 1.66 to 2.55 reported by Sridharan and Prakash (2007). Gray and Lin (1972) reported that the variation of specific gravity of the fly ash is the result of a combination of many factors such as gradation, particle shape and chemical composition. The low specific gravity of the fly ash is mainly attributed due to the presence of large number of hollow cenospheres from which the entrapped air cannot be removed, or the variation in the chemical composition, in particular iron content, or both (Ghosh, 1996; Pandian et al., 1998; Pandian, 2004; Sridharan and Prakash, 2007).

Grain size distribution indicates if a material is well graded, poorly graded, fine or coarse, etc. Pandian et al. (1998) carried out experimental investigation on Indian coal ashes and reported the fly ashes are fine grained substances consisting of mainly silt-size particles with some clay-size particles of uniform gradation. Consistency limits namely liquid limit, plastic limit and shrinkage limit are extensively used in the field of geotechnical engineering. Pandian (2004) reported that fly ashes have liquid limit ranging from 26 to 51%. He observed

from the experimental study that fly ashes are non-plastic and hence plastic limit could not be determined. It was also not possible to carry out shrinkage limit tests since the ash pats crumbled upon drying. Free swell index has been developed in the field of geotechnical engineering to differentiate between the swelling and non-swelling soils (Sridharan and Prakash, 2007). Nearly 70% of Indian coal ashes exhibit negative free swell index which is due to flocculation low specific gravity and less quantity of clay size particles (Pandian, 2004; Sridharan and Prakash, 2007).

The classification of coal ashes from geotechnical engineering point of view is important for an effective and efficient use in geotechnical engineering practice (Pandian, 2004). The fly ashes are classified as fined grained ashes as they comprise of predominantly silt sized particles. They can belong to one of the five subgroups, namely MLN, MLN-MIN, MIN, MIN-MHN and MHN reported by Sridharan and Prakash (2007). If more than 50% of fines belongs to either the coarse silt size ($20\ \mu\text{m} < \text{particle size} \leq 75\ \mu\text{m}$) category, or the medium silt size ($7.5\ \mu\text{m} < \text{particle size} \leq 20\ \mu\text{m}$) category or fine silt plus clay size (particle size $\leq 7.5\ \mu\text{m}$) category, then the ash is accordingly represented as MLN, MIN and MHN. The coarse and medium silt size fractions comprise more than 50% fines and more than the percentage of combined medium silt and fine silt plus clay size fractions, then the ash is designated as MLN-MIN group. If the medium and fine silt plus clay silt size fractions comprise more than 50% fines and also more than the percentage of combined coarse silt and medium silt size fractions, then the ash is designated as MIN-MHN group.

2.3.2 Chemical Properties

Sridharan and Prakash (2007) stated that the chemical properties of fly ash depends upon many factors such as geological factors related with coal deposits deciding its quality,

the composition of the parent coal, the combustion conditions like the method of burning and control of combustion process, the additives used for flame stabilization, corrosion control additives used, hopper position, flow dynamics of the precipitators and the removal efficiency of pollution control devices. In particular, fly ashes that are produced from the same source with similar chemical composition can have significantly different mineralogy depending upon the coal combustion technology used, which in turn affect the ash hydration properties. The mineral groups present in coal such as hydrated silicates, carbonates, silicates, sulphates, sulphides, phosphates and their varying proportions normally play a dominant role in deciding the chemical composition of the ash. When the pulverized coal is subjected to combustion, the clay minerals undergo complex thermo-chemical transformations. During this process, sillimanite and Mullite are crystallized as slender needles along with glass formation. Pyrites and other iron bearing minerals form iron oxides and calcite gets transformed into CaO. The glassy phase formed renders pozzolanicity to the fly ash. In almost all geotechnical engineering applications, the pozzolanic property of fly ash plays an important role (Krishna, 2001). He stated that the term pozzolana is employed to designate a siliceous or a siliceous and aluminous material which by itself, possesses no cementitious value but in the presence of water, chemically reacts with calcium hydroxide to form the compounds possessing cementitious properties. Based on pozzolanic property, fly ashes can be classified as self pozzolanic, pozzolanic and non-pozzolanic. Fly ashes can also be classified as reactive and non reactive fly ashes. Reactive fly ashes are those, which react with lime to give sufficient amount of strength. Non-reactive fly ashes are those, which do not give sufficient even on addition of lime. Self pozzolanic and pozzolanic fly ashes are reactive fly ashes whereas non-pozzolanic fly ashes are nothing but non reactive fly ashes.

According to the American Society for Testing Materials (ASTM C618 – 08a) the ash containing more than 70 wt% $\text{SiO}_2 + \text{Al}_2\text{O}_3 + \text{Fe}_2\text{O}_3$ and being low in lime are defined as class F, while those with a $\text{SiO}_2 + \text{Al}_2\text{O}_3 + \text{Fe}_2\text{O}_3$ content between 50 and 70 wt% and high in lime are defined as class C. The low-calcium Class F fly ash is commonly produced from the burning of higher-rank coals (bituminous coals or anthracites) that are pozzolanic in nature. The high-calcium Class C fly ash is normally produced from the burning of low-rank coals (lignites or sub-bituminous coals) and is self pozzolanic in nature. Ahmaruzzaman (2010) stated that the chief difference between Class F and Class C fly ash is in the amount of calcium and the silica, alumina, and iron content in the ash. In Class F fly ash, total calcium typically ranges from 1 to 12%, mostly in the form of calcium hydroxide, calcium sulphate, and glassy components, in combination with silica and alumina. In contrast, Class C fly ash may have reported calcium oxide contents as high as 30 - 40%. Another difference between Class F and Class C is that the amount of alkalis (combined sodium and potassium), and sulphates (SO_4), are generally higher in the Class C fly ash than in the Class F fly ash. The range of chemical composition of Indian coal ashes together with that for soil (for comparison purposes) is reported in Table 2.2.

Roode (1987) reported that loss on ignition is generally equal to the carbon content. Throne and Watt (1965) observed that the amount of SiO_2 or $\text{SiO}_2 + \text{Al}_2\text{O}_3$ present in fly ash influences the pozzolonic activity for a longer period of time. Minnick (1959) has reported that a relatively high percentage of carbon decreases the pozzolonic activity. Torrey (1978) reports that fly ash collected by electrostatic precipitators (ESP) has 38% more CaO and 58% less carbon than ash collected by mechanical collectors. Moreover the former is finer than the latter. Davis (1949) has stated that finer the fly ash, higher is the pozzolanic reactivity.

Tannant and Kumar (2000) reported that the fly ash collected by ESP is more reactive and consequentially, more suitable as haul road construction material than fly ash collected by mechanical collectors.

Table 2.2: Range of chemical composition (%) of Indian coal ashes and soils (Pandian, 2004)

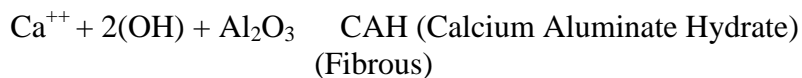
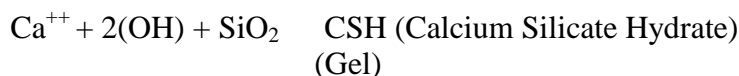
Compounds	Fly ash	Soils
SiO ₂	38–63	43–61
Al ₂ O ₃	27–44	12–39
TiO ₂	0.4–1.8	0.2–2
Fe ₂ O ₃	3.3–6.4	1–14
MnO	0–0.5	0–0.1
MgO	0.01–0.5	0.2–3.0
CaO	0.2–8	0–7
K ₂ O	0.04–0.9	0.3–2
Na ₂ O	0.07–0.43	0.2–3
LOI	0.2–3.4	5–16

The investigations carried out on Indian fly ashes show that all the fly ashes contain silica, alumina, iron oxide and calcium oxide (Pandian and Balasubramonian, 2000). The mineralogical composition of fly ash, which depends on the geological factors related to the formation and deposition of coal, its combustion conditions, can be established by X-ray diffraction (XRD) analysis. Quartz and mullite are the major crystalline constituents of low-calcium fly ash (CaO < 5%), whereas high-calcium fly ash (CaO > 15%) consists of quartz, C₃A, CS and C₄AS (Sen Gupta, 1991; Erol et al., 2000; Singh and Kolay, 2002; Pandian, 2004; Sridharan and Prakash, 2007; Ahmaruzzaman, 2010). The morphological studies through Scanning Electron Microscope (SEM) indicate that the coal ash contains glassy solid spheres (plerospheres), hollow spheres called cenospheres, sub rounded porous grains,

irregular agglomerates and irregular porous grains of unburned carbon (Erol et al., 2000; Sridharan and Prakash, 2007).

When water or any aqueous medium comes in contact with fly ash, iron, aluminum and manganese oxides sink determine the release of the trace elements associated with them into the aqueous medium. The degree of solubility of these oxides in turn depends upon the pH of the aqueous medium (Sridharan and Prakash, 2007). The fly ash with higher free lime and alkaline oxides exhibits higher pH values (Pandian, 2004; Sridharan and Prakash, 2007). Sridharan and Prakash (2007) reported that about 50% of Indian fly ashes are alkaline in nature.

Formation of cementitious materials by the reaction of lime with the pozzolans in presence of water is called hydration. The hydrated calcium silicate or calcium aluminate, join the inert materials together. The pozzolanic reactions for stabilisation are given by the following equation.



Class C type fly ash does not need addition of lime where class F does (Senol et al., 2002).

2.3.3 Engineering Properties

A thorough understanding of the engineering behaviour of fly ash is very much essential for the bulk use of fly ash in geotechnical applications. The density of fly ash is an important parameter since it controls the strength, compressibility and permeability.

Densification of ash improves the engineering properties. The compacted unit weight of the material depends on the amount and method of energy application, grain size distribution, plasticity characteristics and moisture content at compaction (Krishna, 2001; Pandian, 2004). Compaction is a process of densification of the material by packing the particles closer together with reduction in the volume of air voids.

2.3.3.1 Compaction characteristics

Moulton (1978) as well as Sridharan et al. (2000) observed the variation of dry density with moisture content for fly ashes is less compared to that for a well-graded soil, both having the same median grain size. The tendency for fly ash to be less sensitive to variation in moisture content than for soils could be explained by the higher air void content of fly ash. Soils normally have air void content ranging between 1 and 5% at maximum dry density, whereas fly ash contains 5 to 15%. The higher void content could tend to limit the buildup of pore pressures during compaction, thus allowing the fly ash to be compacted over a larger range of water content reported by Toth et al. (1988). Gatti and Tripiciano (1981) carried out compaction tests on coal ashes collected from Vado Ligure Power Plant, Italy and obtained maximum dry density varied between 11.4 kN/m^3 and 45 kN/m^3 with the corresponding optimum moisture contents ranging between 28% and 36%. DiGioia et al. (1986) provided typical standard Proctor compaction curves for Western Pennsylvania Class F fly ash. They found that the maximum dry density ranged from 11.9 to 18.7 kN/m^3 and optimum water content ranged from 13 to 32%. Das and Prakash (1990) reported optimum moisture content (OMC) of 40% and maximum dry density (MDD) of 10.1 kN/m^3 for Titagarh fly ash by performing standard Proctor compaction test. There is a very little difference between the results obtained from standard Proctor's (light) and modified Proctor's (heavy) compaction

tests on fly ashes (McLaren and Digioia, 1987). Indian fly ashes have been observed to have maximum dry density in the range 8.9 to 13.8 kN/m³ and optimum moisture content in the range 17.9 to 62.3% from standard Proctor compaction test (Sridharan et al., 2001b; Das and Yudhbir, 2006; Sridharan and Prakash, 2007). Fly ash has low MDD and high OMC due to presence of cenospheres and plerospheres compared to soil with organic content reported by Das and Yudhbir (2006). Fly ashes originating from different sources themselves show large variations in OMC and MDD due to their specific gravity depends on iron content and carbon contents (Singh, 1996; Krishna, 2001).

2.3.3.2 Permeability characteristics

Shenbaga and Gayathri (2004) reported that the values of coefficient of permeability were in the same range as those of non-plastic silts. They reported the permeability of fly ashes produced from bituminous coals is in the range of 1×10^{-5} to 3×10^{-6} cm/s. The compacted fly ash deposits, therefore, would be moderately permeable. The permeability of ash depends on its grain size distribution, degree of compaction and pozzolanic activity reported elsewhere (Pandian and Vesperman et al., 1985; Balasubramonian, 1999; Sridharan and Prakash, 2007). Porbaha et al. (2000) carried out permeability tests on two class F Japanese fly ashes and reported the permeability values are in the range of 10^{-4} – 10^{-5} cm/s. Glogowski et al. (1992) reported the average value of coefficient of permeability of eastern U.S. fly ashes as 1.9×10^{-5} cm/s, with standard deviation and coefficient of variation as 2.8×10^{-5} cm/s and 147%, respectively. The corresponding values for the western U.S. fly ashes are 3.1×10^{-5} cm/s, 6×10^{-5} cm/s and 194%, respectively. The permeability of Indian fly ashes is in the range of 8×10^{-6} cm/s to 1.87×10^{-4} cm/s (Pandian, 2004).

2.3.3.3 Strength characteristics

An important engineering property that is necessary for using fly ash in many geotechnical applications is its strength. The unconfined compressive strengths for fine ash are higher than those for the coarser ash specimens reported by Leonards and Bailey (1982). Gray and Lin (1972) observed that the unconfined compressive strength (UCS) increased from 390 to 900 kPa at 7 days curing and 400 to 1200 kPa at 90 days curing of British fly ashes compacted at Proctor's maximum dry densities. Sherwood and Ryley (1966) reported that the fraction of lime, present as free lime in the form of calcium oxide or calcium hydroxide, controls self-hardening characteristics of fly ashes. Singh (1996) studied the unconfined compressive strength of fly ashes as a function of free lime present in them. Yudhbir and Honjo (1991) reported that the UCS of fly ash increased exponentially with the free lime content. They also reported the carbon content in fly ashes reduced the strength. This could be attributed to the lower frictional resistance of carbon particles at the inter particle level. The class-F fly ash achieved unconfined compressive strength of 126 kPa at 7 days, 137 kPa at 28 days and 172 at 90 days curing investigated by Ghosh and Subbarao (2006).

The major advantage of fly ashes with regard to shear strength in the compacted and saturated condition is that the variation of effective friction angle is negligibly small, irrespective of whether it is obtained from consolidated drained test or consolidated undrained test (Sridharan and Prakash, 2007). McLaren and Digioia (1987) reported that the shear strength of class F fly ash is primarily depend on cohesion component when it is in partially saturated (compacted with OMC) state. When the sample is fully saturated or dried, it loses its cohesive part of the strength. Its frictional component depends on the density of the

sample. When density increases its friction also increases (Capco, 1990). Indraratna et al. (1991) compared cohesion intercept and angle of shearing resistance of saturated and unsaturated fresh fly ash specimens and reported complete loss of cohesion owing to full saturation and no change in the angle of shearing resistance. The shear strength parameters of typical Indian fly ashes obtained by drained test under compacted condition were in the range of 33° to 43° (frictional angle) and 16 to 93 kPa (cohesion) and by undrained test under compacted condition were in the range of 27° to 39° (frictional angle) and 16 to 96 kPa (cohesion) reported by elsewhere (Sridharan et al., 2001a; Pandian, 2004; Sridharan and Prakash, 2007).

A simple time-saving experimental procedure has been developed to determine the angle of repose which can be used in the field to determine the angle of internal friction under loose and dry conditions (Pandian et al., 2000; Pandian, 2004). As the fly ash exhibits pseudo-cohesion, even in its dry state by virtue of its fineness, it is difficult to determine the angle of repose for fly ashes (Sridharan and Prakash, 2007).

2.3.3.4 California bearing ratio (CBR) behavior

A major application area for fly ash utilization is its use as a sub-base material in the construction of pavements. The CBR value of fly ashes varies between 6.8 and 13.5% in soaked condition and 10.8 and 15.4% in unsoaked condition reported by Toth et al. (1988). Das and Prakash (1990) reported a CBR value of 11% for fly ash under compacted unsoaked condition and this increased to 19% when soaked for 15 days. Indraratna et al. (1991) conducted investigation on the engineering behavior of low carbon, pozzolanic fly ash and reported that CBR values at soaked condition are less than those at unsoaked condition and also concluded that properly compacted and cured fly ash samples give excellent CBR values.

The CBR values of typical Indian fly ashes vary from 11.3 to 20.6% for unsoaked condition and 0.2 in soaked condition as reported in literature (Sridharan et al., 2001c; Pandian, 2004; Sridharan and Prakash 2007).

2.3.3.5 Ultrasonic velocity

Ultrasonic nondestructive testing is a versatile technique which is applied to a wide variety of material analysis applications. Leslie and Cheesman (1949) in Canada and Jones (1949) in England developed this method at the same time. The ultrasonic method has been applied to evaluate the properties of concrete mixes (Malhotra, 1976; Kewalramani and Gupta, 2006; Solis-Carcano and Moren, 2007). Mishra et al. (2003) reported that the ultrasonic velocity of fly ash – cement composites increased over time. The ultrasonic velocity increased with increase in curing period of the masonry composite material made of limestone powder and fly ash (Turgut, 2010). He reported that the ultrasonic pulse velocity increased from 1150 to 1800 m/s in the composite containing 10% fly ash at 7 days curing. Dimter et al. (2011) reported that the increase in fly ash percentage (from 0% to 75%) causes a decrease in ultrasonic velocity. The ultrasonic velocity of the mix containing 25% fly ash was 2.06 km/s and 75% fly ash was 1.36 km/s. He also reported that the ultrasonic velocity increases with increase in density of the material.

2.4 Uses and strength behaviour of fly ash

Research work and studies have been carried out for utilizing fly ash for various purposes to minimize the environmental and disposal problems. Fly ash has been proposed for various applications, including soil stabilization, wastewater treatment, land reclamation, recovery of metals, cement replacement, fill material, manufacture of brick, road and embankment construction etc. It has been found that fly ash can be used for various

applications due to its beneficial properties. There are many reports on potential use of fly ash in road constructions (Laguros and Zenieris, 1987; Moulder, 1996; Marsh, 1996; Barstis and Crawley, 2000; Vittal and Mathur, 2005; Mohanty and Chugh, 2006; Jackson et al., 2009). The addition of fly ash reduced the volume change characteristics and improved the subgrade strength. Fly ash provides silica and alumina needed for cementitious reaction with lime to increase the strength, stiffness, and durability of the stabilized base layer (Butalia, 2007; Mackos et al., 2009).

Gray and Lin (1972) have reported the engineering properties of compacted fly ash and opined that properly compacted and stabilized fly ash had the requisite properties for use in load-bearing fills or highway sub-bases. Joshi et al. (1975) observed that the plasticity index of clay was decreased with the addition of lime and fly ash.

The use of fly ash to stabilize soils should have multiple benefits to their use in haul roads improving mining productivity (Hobeda, 1984). There exist a couple of road projects, more specifically in rural sectors where cementitious fly ash has been used as a sub-base material (Laguros and Zenieris, 1987). The suitability of fly ash as construction material in road base and subbase construction on stabilizing the ash with 5 and 10% lime or cement was investigated by Poran and Ahtchi-Ali (1989). The addition of fly ash to clay-based building materials improves the quality of products (Temimi et al., 1995). But the effectiveness of fly ash for surface coal mine haul road is still in its infancy (Mulder, 1996; Tannant and Kumar, 2000).

Incorporation of fly ash in the clay material improves the mechanical properties of the clay (Queralt et al., 1997; Temimi et al., 1998). The gain in strength and modulus is dependent on the fly ash and cement contents in the fly-soil mixture (Kaniraj and Havanagi,

1999). In India, a regulation issued by the Ministry of Environment and Forests (MOEF) in 1999 stipulated that all new coal thermal power plants should be able to use 100% of the fly ash they produce within the first nine years of operation. For existing power plants, MOEF has set a time period of 15 years for 100% fly ash utilisation from the date of issue of the regulation (MOEF, 1999).

Tannant and Kumar (2000) mixed fly ash, kiln dust and mine spoil at 25:5:70 ratios and found the composite suitable for use in constructing coal mine haul road base and subbase layers. They observed that the unconfined compressive strength increased from 0.4 to 0.6 MPa after 7 days curing and 0.6 to 1.1 MPa at 28 days curing with elastic modulus ranged between 150 and 350 after 14 to 28 days. The composite showed Young's moduli high enough to meet the strain requirement for haul road construction. The reclaimed fly ash fill was inexpensive compared to typical pavement base material and it gained strength over time (Bergeson and Mahrt, 2000). Bulk utilization of fly ash is possible only through geotechnical applications (Sridharan, 2000).

In more recent years, for economic and environmental reasons, renewed attention has been given to the use of 'waste' materials in lieu of conventional aggregates in pavements (Brennan and O'Flaherty, 2001). Sahu (2001) confirmed that higher amount of fly ash is needed for effective pozzolanic activity in case of poorly graded material. Consoli et al. (2001) reported unconfined compressive strength and Brazilian tensile strength characteristics of fly ash mixed with varying percentages of soil and carbide lime. Unconfined compressive strengths and Brazilian tensile strengths were obtained from 410 to 1924kPa and 17 to 200kPa at 7 to 90 days of curing for the mixes containing soil and 25% fly ash stabilized with 4%, 7%

and 10% of lime. They also reported that the compressive strength of fly ash-lime-soil were 410 - 634 KPa in 7 days, 822 - 1,243 KPa at 28 days and 6.9 - 9.4 MPa in 180 days.

Edil et al. (2002) reported that the use of fly ash in the subgrade stabilization achieved higher stiffness (10-18 MN/m) than other construction materials like excavated rock (9-12 MN/m) from the soil stiffness gage (SSG) test in the field. They also reported the CBR value and unconfined compressive strength of fly ash (10%) stabilized subbase to be 32% and 540kPa. Sobhan and Mashnad (2002) reported that recycled plastic strip mixed with soil-cement-fly ash can develop a sufficient bond which delay the propagation of tensile cracks in the base course of the road structure that can be suitable for haul road construction. Mingkai et al. (2002) reported strength of fly ash mixed with varying percentage of phosphogypsum (20% to 80%) and 8% of lime. Unconfined compressive strengths increased from 3.04MPa to 3.13MPa at 7 days curing for the fly ash contents from 12% to 52% in the mixes and then increase in fly ash content from 62% to 72%, the strength value decreased from 2.76 to 2.56MPa.

Acosta et al. (2003) reported that the soil - fly ash mixtures prepared with 18% fly ash content and compacted at 7% wet of optimum water content showed significant improvement compared to the untreated soils, with CBR ranging from 15% to 31%. The resilient modulus was approximately 30% higher as compared to the resilient modulus of untreated soil. The resilient modulus also increased from 20% to 50% with increasing curing time from 7 days to 28 days and unconfined compressive strength of the soil-fly ash mixture was 4 times higher than that of untreated soil. It was found out that a reduction of 33% in base layer thickness obtained using developed soil – fly ash mixtures.

Siswosoebrotho et al. (2003) reported an investigation on examining the use of pulverized fuel ash (PFA) mixed with granite as a suitable material for constructing access roads into the oil field explorations taking place in Riau Province, Sumatera, Indonesia. According to their investigation, percentages of PFA in the PFA and Granite mixes were 5, 10, 15, 15 and 50% by weight of the total mixtures used. The strongest mix, in term of CBR strength, was obtained when the PFA content was 15% with a minimum curing period of 14 days and the weakest when the mixture contained a 50% PFA content. The maximum CBR attained was about 235% in the mix containing 15% PFA after 14 days curing.

According to Pandian (2004), fly ash has good potential use in geotechnical applications. Its low specific gravity, freely draining nature, ease of compaction, insensitiveness to changes in moisture content, good frictional properties etc. can be gainfully exploited in the construction of roads, embankments etc. Prabakar et al. (2004) studied fly ash plus soil mixes and concluded that the addition of fly ash reduces the dry density of the soil due to low specific gravity and unit weight. They also concluded that the CBR values of pure soils are 4.7%, 2.03% and 3.53%; by adding fly ash up to 46%, the CBR value is increased up to 11.41%. Thus, fly ash effectively utilized in the soil to get improvement in shear strength, cohesion and the bearing capacity. Fly ash addition in soil can also be effectively used as the base materials for the roads, back filling, and improvement of the soil bearing capacity of any structure.

Arora and Aydilek (2005) evaluated the engineering properties of Class F fly ash amended soils as highway base materials. They mixed fly ash (40%) with sandy soils with plastic fines contents and activated the mix with 7% cement and obtained California bearing ratio (CBR) and unconfined compressive strength of 140% and 3.2 MPa respectively. Similar

observations were made by Vishwanathan et al. (1997) when silty and sandy soils were stabilized with lime-activated Class F fly ash for highway bases.

Sahu (2005) reported that the plasticity index and linear shrinkage of all types of soil decreased from 15% to 1% and 7% to 1% respectively. The CBR value increased from 36% to 162% which enhanced the suitability of the soils for construction of base and subbase in road works by conducting a study on four types of soil samples as clayey sand, gneiss with calcrete, quartz and schist and friable calcrete, each mixed with 4%, 8%, 16% and 20% fly ash. There are many attempts to use fly ash in raw stage in road construction, particularly in rural road construction (Vittal and Mathur, 2005; Singh and Kumar, 2005). Chugh and Mohanty (2005) reported successful use of 60,000 m³ of unstabilised fly ash in the construction of a 3.4 km long and 7.3 m wide road.

In one specific study fly ash utilization resulted in maximum savings in the sub-base course limited to about 60 to 90 km of lead for rigid and flexible pavements (Kumar and Patil, 2006). This is important as most of our power plants are situated within this range of most coal mines. One conservative estimate puts the unutilized fly ash occupying about 65000 acres of land (Das and Yudhbir, 2006) which demands increase the utilization percentage.

Unconfined compressive strength (UCS) and California bearing ratio (CBR) values increased due to increase in fly ash contents (10% - 20%) in the soil - fly ash mixtures as observed by Senol et al. (2006). They opined stabilized fly ash-soil mixtures offer an alternative for soft sub-grade improvement of highway construction. The class-F fly ash after stabilizing with only lime (10%) and lime (10%) with gypsum (1%) achieved compressive strength of 552 kPa and 5902 kPa at 28 days curing and 4046 kPa and 6308 kPa at 90 days curing reported by Ghosh and Subbarao (2006). They also reported that the CBR value of the

specimens stabilized with only lime (10%) and lime (10%) with gypsum (1%) result 77% and 172% at 28 days curing period compared to 34% at 28 days for unstabilised fly ash.

Fly ash provides silica and alumina needed for cementitious reaction with lime to increase strength, stiffness, and durability of the stabilized base layer (Butalia, 2007). He reported that fly ash acted as a mineral filler to fill the voids in the granular pulverized pavement mix, reducing the permeability of the Full Depth Reclamation (FDR) stabilized base layer. Shen et al. (2007) experimented with lime, phosphogypsum and fly ash in ratio of 8:46:46 and observed continued increase in strength value of 2.4 MPa at 7 days to more than 16 MPa at 365 days. They concluded that the fly ash mixture was a better material for semi-rigid road base material.

Full-Depth Cold In-Place Recycling (CPR) with self-cementing fly ash was observed to be an effective method of converting conglomerate pavement sections into durable roads (Misra, 2008). CPR demonstration projects have been performed in several states, where it has been shown to produce longer life at a major saving. This technology provides several economic and environmental benefits. In addition to providing environmental benefits and longer lasting pavements, it has been reported that this technology could result in saving of upto 33% over conventional techniques.

Shen et al. (2009) reported that the fly ash and steel slag mixed with 2.5% of phosphogypsum dosage results in highest strength. They studied the solidified material by comparing with some typical road base materials and observed increase in strength value of 8 MPa at 28 days to 12 MPa at 360 days respectively has higher strength than lime-fly ash and lime-soil road base material and opined the material as a road base application.

Jackson et al. (2009) successfully used bottom ash and fly ash for pavement construction. With increase in height of compacted fly ash layer over soft soil layer, the bearing ratio value of compacted fly ash increases as reported by Ghosh and Dey (2009). The silica and alumina in the fly ash reacts with lime to form hydration products which increase the strength, stiffness and durability of the stabilized base layer (Mackos et al., 2009).

Cetin et al. (2010) reported that the CBR value of the soil stabilized with fly ash (10% and 20%) and lime kiln dust (2.5% and 5%) were found to be 69 to 142 after 7 days curing and greater than 164 after 28 days curing.

2.5 Environmental aspects of fly ash utilization

It becomes increasingly important to assess the environmental risk involved in the storage and utilization of waste materials. The toxic elements contained in the fly ash may slowly and gradually get released from the ash and cause contamination of surface and groundwater as well as soil degradation, there by posing health hazards to the neighboring habitat. The physico-chemical properties of fly ashes combined with operational parameters of power plants and disposal environments, in which ashes are placed, control the leaching susceptibility of trace elements from ashes. The utilization of fly ash can be accepted only when it meets the regulations for environmental safety. Stabilization of fly ash with proper additives is one of the promising methods to mitigate the problems of leaching and dusting (Canter and Knox, 1985). Gidley and Sack (1984) presented a general survey on waste utilization in construction from environmental point of view and reported different solidification techniques for waste disposal, among which stabilization with lime was one of the most suitable methods.

Huang and Lovell (1990) conducted leaching tests through extraction procedure (EP) toxicity test and studied the leaching behavior of bottom ash and its effect on ground water quality. They reported bottom ashes were characterized as nonhazardous wastes and were recommended for use in different civil engineering applications as construction material.

Edit et al. (1992) studied the feasibility of using compacted fly ash or fly ash mixed with sand as a construction material for waste containment liners or impermeable covers. Compacted specimens of fly ash and sand mixture of different permeabilities were subjected to long term permeability tests. It was observed from their study that the permeability can be reduced to below 10^{-7} cm/sec. A synthetic inorganic solution simulating a fly ash landfill leachate did not have any adverse effect on the permeability of the compacted fly ash. Permeability affected the concentrations of certain elements leaching or desorbing out of, or adsorbing into the fly ash. Calcium (Ca), sulphur (S) and boron (B) concentrations were lower in low permeability specimens while cadmium (Cd) and zinc (Zn) concentrations were higher. The high pH of the fly ash leachate helped in keeping the cadmium, zinc and boron in the fly ash matrix.

Goh and Tay (1993) reported large scale leachate tests on municipal solid waste incinerator fly ash stabilized with lime as well as cement to simulate field recycling conditions as closely as possible. Sridharan et al. (1994) reported the use of fly ash as a pre-filter media for clay liner used in the construction of landfill. They examined the feasibility of fly ash as pre-filter media for Zn. It was observed that fly ash with more lime retained more Zn. Pandian et al. (1995) observed that fly ash having more lime content was very effective to retain lead (Pb) ions compared to low lime fly ash.

The quantity of a metal in the leachate is predominantly influenced by the hydraulic conductivity of the stabilized material and the concentration of a metal in the leachate (Ghosh, 1996; Ghosh and Subbarao, 1998). Ghosh and Subbarao (1998) reported the concentration of heavy metals in the leachate effluent emanating from the hydraulic conductivity specimens of stabilized fly ash with higher proportions of lime or lime with gypsum were below threshold limits acceptable for contaminants flowing into ground water. Wang et al. (1999) carried out comparative leaching experiments for trace elements in raw coal, fly ash and bottom ash and identified lead (Pb) and Arsenic (As) as the potential toxic elements. The pH of the solution and leaching time were also found to strongly influence the leaching behavior. They observed that the leaching intensity of strontium (Sr), zinc (Zn), lead (Pb), nickel (Ni) and arsenic (As) was found to increase with decreasing pH of the solution. The stronger the acidity of solution, then larger is the leaching intensity of these elements.

Pandian and Balasubramonian (2000) conducted leaching studies on fly ashes by Oedometer method using two types of fly ashes, one with low and other with higher free lime content. In the, Oedometer method a known amount of fly ash was statically compacted and a solution of known pH was allowed to pass through the compacted sample in the upflow mode. The outflow was collected periodically and analyzed. They observed that the leaching of trace elements from fly ash mainly depends upon pH of the leaching solution and duration of reaction time. If the pH value is higher, the complete leaching of metal ions from fly ash is possible.

Kim and Batchelor (2001) listed three major factors affecting leaching based on their studies on dynamic leaching of metal contaminants from wastes subjected to solidification/stabilization (s/s) process as acid/base reactions that determine the pH within the waste, pH

dependent reactions that determine whether the contaminants are in mobile or immobile forms and diffusion that transports mobile contaminants from the waste.

Pozzolanic-based stabilization/solidification (S/S) is an effective, yet economic remediation technology to immobilize heavy metals in contaminated soils and sludges (Dermatas and Meng, 2003). They reported that addition of quicklime and fly ash to the contaminated soils effectively reduced heavy metal leachability well below the nonhazardous regulatory limits. Overall, fly ash addition increases the immobilization pH region for all heavy metals and significantly improves the stress-strain properties of the treated solids, thus allowing their reuse as readily available construction materials.

Goswami and Mahanta (2007) found out that on the use of fly ash and lime for stabilization of lateritic soil did not have significant impact on the environment, as most of the toxic metals present in the fly ash were within the threshold limits. Most of the metals were kept within the stabilised soil matrix by the high pH induced by lime treatment of the mixes. Recent experiments showed that residual lateritic soils not only responded well to fly ash and lime stabilisation, but also provided a tremendous opportunity for the bulk utilisation of fly ash through geotechnical applications such as construction of embankments, roads and various fill applications.

2.6 Fly ash – lime or fly ash – soil – lime interaction

The enhancement of mechanical strength and microstructural development of fly ash with addition of lime has been reported elsewhere (Das and Prakash 1990; Sivapullaiah et al., 1995; Lav and Lav, 2000; Ghosh and Subbarao, 2001; Beeghly, 2003; Antiohos, 2004; Mishra and Rao, 2006; Cicek and Tanriverdi, 2007; Cetin et al., 2010). The lime stabilization of soils or soil-fly ash mixtures have been extensively described in the literature which

involves the physico-chemical mechanisms of both short- and long-term reactions (Consoli et al. 2001; Faluyi and Amu, 2005; Goswami and Mahanta, 2007; Mackos et al., 2009). The permeability of fly ash or soil–fly ash mixes stabilized with lime gradually decreased due to the formation of hydration products, reduced the interconnectivity between the pores (Ghosh and Subbarao, 2001; Sridharan and Prakash, 2007).

Chu et al. (1955) observed lime-fly ash interaction while studying stabilization of soil with lime and fly ash mixture. They stated that the improvement in the properties of soil-lime-fly ash mixes was due to the formation of cementitious compounds such as calcium silicate hydrate (CSH) which is formed as a result of the reaction between lime and fly ash in the presence of water.

The interaction between fly ash and lime was complex and pozzolanic reaction was very slow reported by Croft (1964). He observed from his investigation on lime-stabilized fly ash that the appearance of new crystalline phases were considered as gel like varieties of calcium silicate hydrate in the X-ray diffraction patterns after a curing period of 4 weeks and also the presence of hydrated calcium aluminate (C_4AH_{13}) after a curing period of 8 week.

Luxa'n et al. (1989) identified the formation of calcium aluminum hydrate (C_4AH_{13}), carboaluminate (C_4ACH_{11}), monosulfoaluminate (C_4ASH_{12}), and calcium silicate hydrate (CSH) as pozzolanic reaction products of fly ash and calcium hydroxide (hydrated lime). Soliman (1990) observed that the lime-fly ash reaction (pozzolanic) was a slow process that took place without any heat generation. When water and fly ash are mixed with lime, the silica and alumina reacts with lime and the resulting product is tricalcium silicate and tricalcium aluminate.

Goh and Tay (1993) observed from long-duration leaching experiments on municipal solid waste incineration fly ash (MSWIF) that the concentration of all the elements in the leachate of MSWIF samples stabilized with lime were significantly lower than that of the unstabilized MSWIF samples. Malhotra (1994) observed that class F fly ashes hydrate with the addition of lime. The reactive silica in the fly ash reacts with the calcium hydroxide producing calcium silicate hydrate (CSH). The alumina in the fly ash also takes part in the reaction and the reaction products formed include calcium aluminate hydrate (CAH), ettringite, gehlenite and calcium monosulfoaluminate hydrate.

Sivapullaiah et al. (1995) reported that for every fly ash, there is an optimum lime content for its maximum reactivity. They conducted a simple physico-chemical test to assess the optimum lime content and compare it with the results obtained from strength test and showed that a good relationship exists between the optimum lime content determined by pH, liquid limit or free swell index with that obtained by an unconfined compressive strength test.

Ghosh and Subbarao (1998) observed that hydraulic conductivity of lime stabilized fly ash reduced with increase in lime content, moulding water content, flow period and curing period. They also reported that the concentration of metals in the leachate effluents emanating from stabilized fly ash show positive effects of lime stabilization and concluded that the stabilized material has the potential for use in a broad spectrum of applications such as structural fills, road subbase construction, covers, liners and cutoff trench walls, minimize the potential for groundwater contamination.

Lav and Lav (2000) conducted microstructural, chemical, mineralogical and thermal analysis as well as unconfined compressive strength tests on cement and lime stabilized fly ash for use as pavement base material. They observed that the strength development is

dependent on the amount of hydration products as well as their interlocking mechanisms. Ghosh and Subbarao (2001) studied the physico-chemical and microstructural developments of low calcium fly ash modified with 6 and 10% and 1% gypsum through X-ray diffraction, differential thermal analysis, SEM and EDAX. They observed that the compact matrix was formed due to the new cementitious compounds, developed within the pore spaces result in a reduction of the radius of pore spaces that confirms the reduction of permeability and increase in strength without any adverse effect on ground water quality.

Lav et al. (2006) observed from SEM analysis that when cement or lime and fly ash mixed with water, the self-hardening mechanism of fly ash occurred due to reaction with calcium ion in solution to form CSH (pozzolanic reaction) and due to presence of either cement or lime produces hydration products resulting higher strength in the material. They also observed that ultrasonic pulse velocity of the cement stabilized fly ash increased with increasing curing period.

When lime kiln dust (LKD) is mixed with moist soil and fly ash, the hydration of calcium oxide (CaO) causes the formation of Ca(OH)_2 and dissociation of Ca(OH)_2 favors dissolution of silica and alumina in fly ash. This phenomenon gives rise to formation of CSH and CASH around soil and fly ash particles (Cetin et al., 2010).

CHAPTER 3

METHODOLOGY

3.1 General

The aim of the investigation is to improve upon the condition of surface coal mine haul road as well as evaluate the potential of fly ash to achieve this. This chapter reflects methodology adopted and materials used to achieve the objectives. The main inputs are overburden material, fly ash and lime. Fly ash collected from local power plant used in this investigation. Sample preparation and testing techniques used for characterisation of materials as well as development of composite materials are also reported.

3.2 Materials and Methods

3.2.1 Materials

The details of ingredients used in this study are given below.

3.2.1.1 Fly ash

Fly ash, a by-product of thermal power units was collected from nearby places, namely Rourkela Steel Plant (RSP), SAIL. The reasons for selecting the units are:

1. It is situated near the two main coalfields i.e. Talcher & IB Valley areas.
2. It uses coal from Talcher coalfields.
3. It produces huge quantities of fly ash and dumping is a problem. There are many adverse environmental issues associated with the ash ponds

4. The ash sample if found suitable would help in addressing the utilization issue as well as in improving the haul road economics.

Rourkela Steel Plant is an integrated steel plant of Steel Authority of India Limited located in Rourkela set up in 1958. It has a captive power plant (CPP) consumes 2230 tonne of coal a year generates 120 MW and produces about 600 tonne of ash. The ash so generated is typically dumped in a nearby pond area but of late it has reached its capacity and hence alternate methods are being actively explored.

- Collection method

The fly ash used in the present study was collected in dry state from electrostatic precipitators of CPP-II of RSP. During the combustion of pulverized coal in suspension-fired furnaces of thermal power unit, the volatile matter is vaporized and the majority of the carbon is burned off. The mineral matter associated with the coal, such as clay, quartz and feldspar disintegrate or slag to varying degree. The finer particles that escape with flue gases are collected as fly ash using electrostatic precipitators in hoppers and stored. The hoppers have small outlets. Gunny bags made of strong poly-coated cotton with 50kg capacity each were used to collect the dry fly ash. The chute of hoppers was slowly opened and the bags were filled. The mouth of each bag was sealed immediately after collection and the same was again inserted in another polypack to prevent atmospheric influences. The bags were transported with utmost care from the plant to laboratory and kept in a secure and controlled environment. Samples of fly ash were taken out as per requirement of test.

3.2.1.2 Overburden Materials

Overburden from a surface coal mine is an important material for the investigation. It was sourced from an active mine Bharatpur opencast coal mine, Talcher, Odisha. It is

situated at about 300 km from Rourkela (Figure 3.1). The coal belongs to Gondwana sequence. Major part of the area is covered by Barakar / Karharbari / Talcher exposure with east west strike of beds. The typical overburden material consists of alluvium, laterite, fine to medium grained sandstone, carbonaceous shale, pink clays, etc. The mine produces coal of about 9 MT annually. The layout of the mine permanent haul roads and branch haul roads which are connected with the coal transportation roads is shown (Figure 3.2). The length of main haul road is 5.760km and branch haul roads are 930m, 1.150km, and 1.335km at different locations of the mine. Haul roads are basically flexible pavement type which are designed by California Bearing Ratio (CBR) method. The mine follows drilling, blasting, loading and dumping operations. Shovel and dumper combinations are used to handle overburden materials. 50ton and 85ton dumpers (make: BEML and Hindustan) are used to haul overburden material.

- Collection method of overburden material (Figure 3.3)

The overburden dump area is about 2 to 2.5 kms from the active benches. The overburden area spreads about 300m long and 400m wide. Dozers/spreaders are used to spread the material once dumpers dump those. Samples for testing were selected and collected that those represent the average materials found in the mine. Sample collections were carried out from all parts of the dump area. Gunny bags were used to collect the loose soils sample leaving the gravels, boulders etc aside. The process followed for fly ash collection was also repeated to collect overburden material. The material was explored in the laboratory sieved to discard gravels, pebbles etc. The materials were thoroughly mixed, covered for 2 hours for homogenization and then stored in poly pack for experimentations.

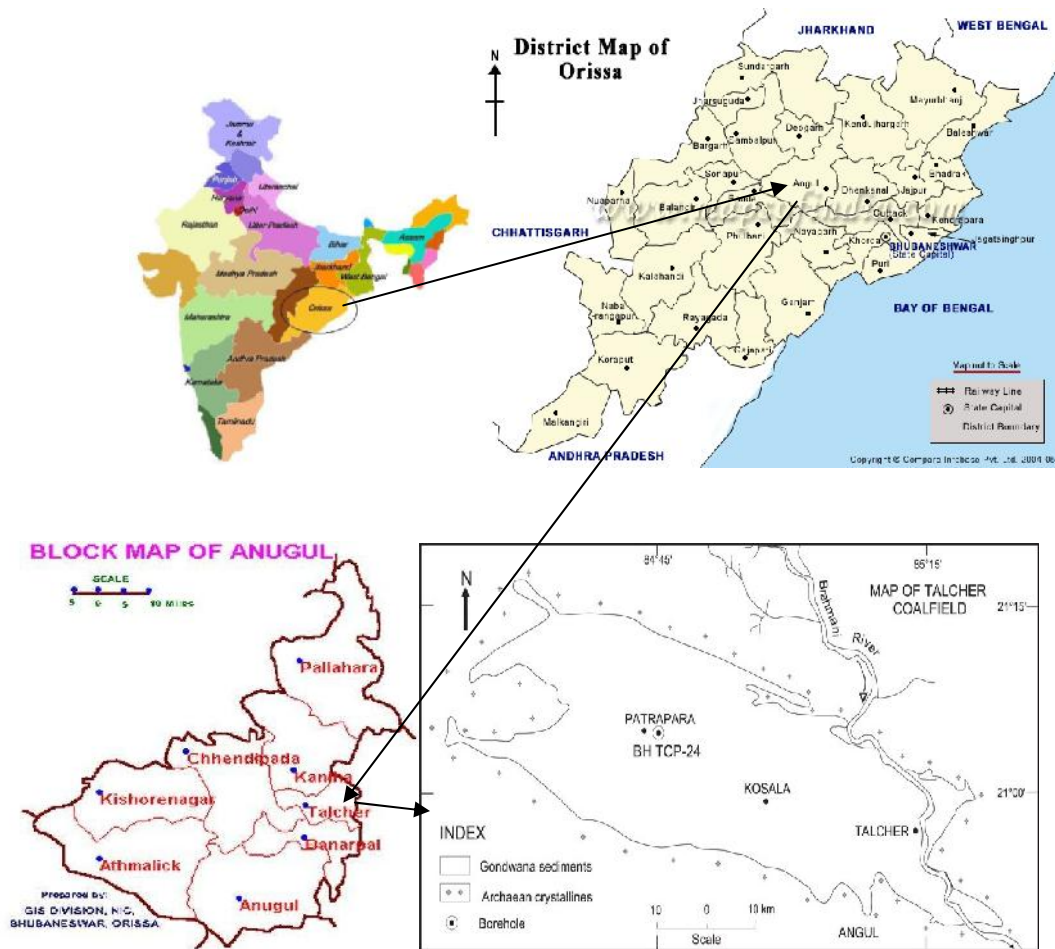


Figure 3.1: Map of Talcher Coalfield, Odisha

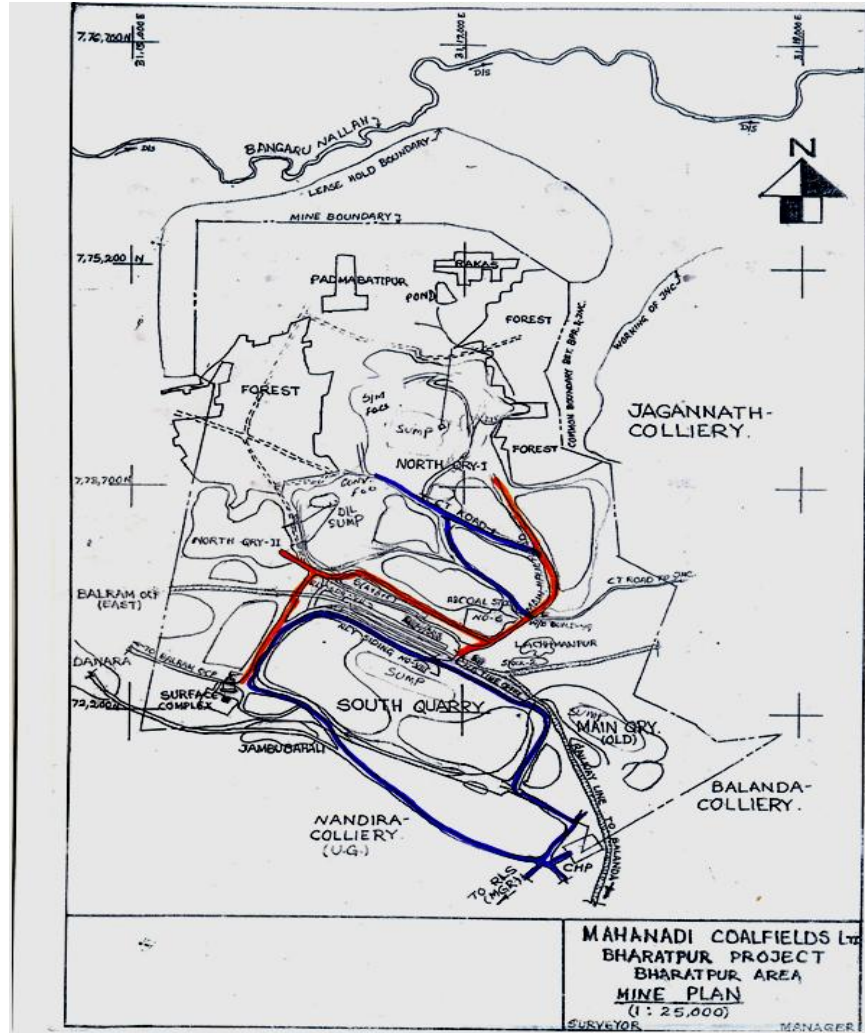


Figure 3.2: Sketch of Bharatpur Opencast coal mine



Figure 3.3: Collection of mine overburden

- Observation from mine visit (Figure 3.4)

Frequent mine visits were made to Bharatpur opencast mine, Talcher not only to collect overburden samples but also to obtain mine operation data, to inspect the haul road condition and study the haul road construction process, to hold discussion with mine officials as well as with dumper operators, to critically observe the various problems associated with haul road, etc. A sample photograph (Figure 3.4) depicts the observation.

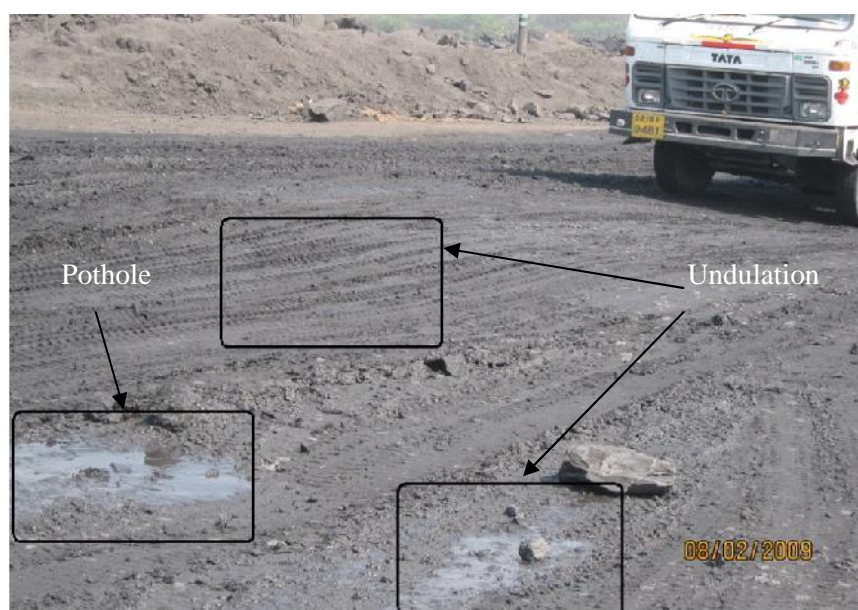


Figure 3.4: Undulations and potholes are marked in the haul roads

3.2.1.3 Lime

The additive selected was commercially available superior grade quick lime (make: Rajasthan Lime, India). Quicklime is manufactured by chemically transforming calcium carbonate (limestone – CaCO_3) into calcium oxide (CaO).

3.2.2 Methods

3.2.2.1 Sample preparation

These are many published reports of evaluating the performance of soil stabilized with fly ash (Kaniraj and Havanagi, 1999; Tannant and Kumar, 2000; Consoli et al., 2001; Prabakar et al., 2004; Lav et al., 2006; Goktepe et al., 2008; Jackson et al., 2009; Cetin et al., 2010). The soil chosen in those studies represent more or less uniform material. Overburden is a highly heterogeneous formation. The over burden material disposal is not only a challenge to the mine operator but also has many drawbacks in its use as construction materials of haul road and branch roads. At the same time all avenues are being explored to increase the usage of fly ash. The aim of the study was to improve the behaviour of haul road with fly ash replacing a part of the conventional subbase material i.e. the overburden. Its aim was to develop and evaluate the performance of composite material with fly ash and mine waste i.e. overburden materials. Hence experiments were carried out to maximum of 50% fly ash addition in the overburden (Table 3.1).

Table 3.1: Various proportions of flyash and overburden

Fly ash (%)	Overburden (%)
15	85
20	80
25	75
30	70
35	65
40	60
45	55
50	50

Availability of free lime enhances the pozzolanic activity of materials. In this investigation a varying percentage of lime 2%, 3%, 6% and 9% were used in preparing the fly ash-overburden composites (Table 3.2).

Table 3.2: Compositions (%) of (FA+O/B)+L

Sample ID	Compositions (%)	Sample ID	Compositions (%)
1(a)	(15FA+85O/B)+2L	5(a)	(35FA+65O/B)+2L
1(b)	(15FA+85O/B)+3L	5(b)	(35FA+65O/B)+3L
1(c)	(15FA+85O/B)+6L	5(c)	(35FA+65O/B)+6L
1(d)	(15FA+85O/B)+9L	5(d)	(35FA+65O/B)+9L
2(a)	(20FA+80O/B)+2L	6(a)	(40FA+60O/B)+2L
2(b)	(20FA+80O/B)+3L	6(b)	(40FA+60O/B)+3L
2(c)	(20FA+80O/B)+6L	6(c)	(40FA+60O/B)+6L
2(d)	(20FA+80O/B)+9L	6(d)	(40FA+60O/B)+9L
3(a)	(25FA+75O/B)+2L	7(a)	(45FA+55O/B)+2L
3(b)	(25FA+75O/B)+3L	7(b)	(45FA+55O/B)+3L
3(c)	(25FA+75O/B)+6L	7(c)	(45FA+55O/B)+6L
3(d)	(25FA+75O/B)+9L	7(d)	(45FA+55O/B)+9L
4(a)	(30FA+70O/B)+2L	8(a)	(50FA+50O/B)+2L
4(b)	(30FA+70O/B)+3L	8(b)	(50FA+50O/B)+3L
4(c)	(30FA+70O/B)+6L	8(c)	(50FA+50O/B)+6L
4(d)	(30FA+70O/B)+9L	8(d)	(50FA+50O/B)+9L

Note: FA= fly ash, O/B = Overburden, L = Lime

Heavy compaction (modified Proctor compaction) tests were performed as per IS: 2720-Part (1983) to determine the maximum dry density and optimum moisture content of all

the mixes for preparation of sample. The samples were prepared at their respective optimum moisture content and maximum dry density. The raw materials such as fly ash, mine overburden and lime were blended in the required proportion in dry condition. The dry mixed ingredients were put in a poly pack, covered and left for about an hour for homogenization. Then the required amount of water was added to the mixture and mixed thoroughly. Then the mixture was left in a closed container for uniform mixing and to prevent loss of moisture to atmosphere. The wet mixture of amount corresponding to the required dry density was compacted in the mould.

3.2.2.1.1 Sample preparation for CBR test

The California bearing ratio (CBR) test samples were prepared using standard CBR mould of 150mm diameter and 175mm height (Figure 3.5) as per IS: 2720-Part 16 (1987). The sample was statically compacted in the mould, such that the height was maintained at 127mm. A circular metal spacer disc of 148 mm diameter and 47.7mm height was used to compact the sample.

3.2.2.1.2 Sample preparation for UCS test

Split mould of 38mm diameter and 86mm length was used for preparation of the unconfined compressive strength (UCS) test samples as per IS: 2720-Part 10 (1991). Samples were prepared with uniform tamping. Two circular metal spacer discs of height 5mm and diameter 37.5mm each with base (7mm height, 50mm diameter) were used at top and bottom ends of the mould to compact the sample such that the length of the specimen was maintained at 76mm. Then the discs were removed and an another spacer disc of height 100mm and diameter 37.5mm with a base (height 7mm, 50mm diameter) was used to remove the sample

from mould. The final prepared specimen has its length to diameter ratio of 2. Figure 3.6 shows the mould, spacer discs and prepared ingredients.



Figure 3.5: CBR mould



Figure 3.6: UCS mould, spacer discs and mixed ingredients

3.2.2.1.3 Sample preparation for tensile strength test

The sample for Brazilian tensile strength test was prepared using the same mould of UCS test samples. For this purpose, two circular metal spacer discs of 5mm and 62mm heights and 37.5mm diameters with base (height 7mm, 50mm diameter) were used. The final prepared specimen has its length to diameter ratio of 0.5.

3.2.2.1.4 Sample preparation for Ultrasonic Pulse velocity test

Split mould of 38mm diameter and 86mm length was used for preparation of the Ultrasonic test. The procedure for the sample preparation of the above test is same as unconfined compressive strength (UCS) test samples. The final prepared specimen has its length to diameter ratio of 2.

3.2.2.1.5 Sample preparation for SEM, EDX and XRD analyses

The raw materials after oven dried were taken for scanning electron microscopy (SEM), energy dispersive X-ray (EDX) and X-ray diffraction studies. Fractured pieces of composites samples retrieved from CBR moulds after CBR tests at 28 days curing periods were taken for the above analyses. For SEM and EDX analyses, fragments of the specimens were collected and oven dried to constant mass. For, XRD analyses, fractures pieces of the samples after oven dried were crushed and sieved the powders passing through 75 μ m sieve.

3.2.2.1.6 Sample preparation for leaching study

Leaching study was conducted by permeability method as per IS: 2720 (Part 17) for the collection of leaching effluents. Samples for permeability test were prepared following the same process as per CBR test. The wet mixtures of the samples were compacted in the permeameter mould of 100mm internal diameter and 127mm height. The moulds were fitted properly and kept for 7 days curing of the samples after compaction. Permeability tests were carried out at the end of 7 days curing period. The moulds were connected through the top inlet to the constant head water reservoirs after curing of the specimens. Air vents were kept open for sufficient time till air bubbles were removed from the specimens to make the samples fully saturated. It took one to two days for saturation. The permeability was measured by falling head method according to IS: 2720-Part 17. Water was allowed to flow through the specimens continuously for seven days and readings were recorded daily. The leaching effluent coming out from specimen through the outlet of the permeability mould was collected in a measuring cylinder. The measuring cylinder was washed with dilute HCL acid and distilled water to clean any impurities before collecting the effluent for leachate analysis. The set up for collection of leaching effluent is shown in Figure 3.7. The leachate sample

obtained from the experiment was filtrate using Gelman filter paper and acidified with concentrated nitric (HNO_3) acid to maintain pH value between 2 to 2.5 (US EPA, 1985; Dermatas and Meng, 2003). Then the leachate sample was stored in a sampling bottle and kept at $\sim 10^\circ\text{C}$ before use to prevent it from evaporation and volume change.



Figure 3.7: Set up for collection of leaching effluent

3.2.2.2 Experimental methods

3.2.2.2.1 Specific Gravity

The specific gravity of the mine overburden and fly ash were determined using volumetric flask method as per IS: 2720-Part 3 (1980).

3.2.2.2.2 Grain size distribution

Grain size distribution was carried out through a standard set of sieves as per IS: 2720-Part 4 (1985) by wet sieving using a sieve of $75\mu\text{m}$ size. The material retained on the $75\mu\text{m}$ sieve was oven dried and sieved using IS standard sieves of 4.75, 2, 1, 0.6, 0.425, 0.212, 0.15,

0.075 mm sizes. The material passing through the 75 μ m size was collected carefully and grain size distribution analysis was performed by using Hydrometer method. The overburden and fly ash have been classified based on particle size (IS: 1498, 1970).

3.2.2.2.3 Specific surface area

The specific surface area of the mine overburden and fly ash were determined using Blain's air permeability method as per IS: 1727 (1967).

3.2.2.2.4 Consistency limits

The consistency limits of the mine overburden were determined as per IS: 2720-Part 5 (1985) and Part 6 (1972). The liquid limit is the minimum moisture content at which the soil type material can flow under a specified small disturbing force, the disturbing force being defined by the method of testing. The liquid limit of overburden was determined using Casagrande liquid limit device. The liquid limit of fly ash was determined by the cone penetration method as per BS: 1377-Part 2 (1990) due to difficulty in cutting a groove using Casagrande device. The plastic limit is the minimum water content at which soil ceases to behave as a plastic material. It was determined by rolling about 5 gm of wet soil pat into a thread on the glass plate with tips of the fingers of one hand to 3-4 mm diameter. The shrinkage limit is the maximum water content below which the soil ceases to decrease in volume on further drying. It was determined using shrinkage limit dish.

3.2.2.2.5 Free swell index

Free swell index of the overburden and fly ash was determined as per IS: 2720-Part 40 (1977).

3.2.2.2.6 X-ray diffraction (XRD) analysis

X-ray diffraction provides a powerful tool to study the structure of the materials which is a key requirement for understanding materials properties. X-ray diffraction is based on constructive interference of monochromatic X-rays and a crystalline sample. X-ray powder diffraction is most widely used for the identification of unknown crystalline materials (e.g. minerals, inorganic compounds). It is a technique for analyzing structures unknown solids which is critical to studies in geology, environmental science, material science, engineering and biology. X-ray beam hits a crystal, scattering the beam in a manner characterized by the atomic structure. Even complex structures can be analyzed by x-ray diffraction, such as DNA and proteins. In the present investigation, XRD analysis was performed on a Philips diffractometer (PANalytical X-ray B.V., UK) employing Cu K α radiation in the range $2\theta = 0^\circ$ to 90° at a goniometer rate of $2\theta = 2^\circ/\text{min}$ to detect the mineral phases.

3.2.2.2.7 SEM and EDX studies

Scanning Electron Microscopy (SEM) is a powerful analytical technique for the evaluation of particulate matter. Scanning electron microscope uses a beam of energetic electrons to examine objects on a very fine scale. It is capable of performing analyses of selected point locations on the sample and is especially useful for determining chemical compositions. The SEM analyses were conducted in a JEOL JSM 6480 LV, (Japan) model operated at 15 kV and linked with an energy dispersive X-ray (EDX) attachment. Microstructure and chemical composition of the samples were examined by SEM and EDX techniques.

3.2.2.2.8 Loss on ignition (LOI)

Loss on ignition of overburden and fly ash were determined as per IS: 1760-Part 1 (1991).

3.2.2.2.9 pH test

The pH value was determined as per IS: 2720-Part 26 (1987) to identify the acidic or alkaline characteristic of overburden and fly ash. The measurement of pH was carried out using pH meter (make: Systronics, India) with accuracy up to ± 0.02 units. The instrument was standardized with three standard buffer solutions of pH 7.00, 4.00 and 10.00 at 25°C. The suspension was stirred well and allowed to come to room temperature ($25 \pm 1^\circ\text{C}$) before taking the pH measurement.

3.2.2.2.10 Compaction test

Higher compaction is needed to meet the bearing capacity for heavy vehicle transportation and typically the machineries operating in surface coal mines weigh about 80 tonne. Modified Proctor compaction test is typically used to give a higher standard of compaction. It was performed to determine the maximum dry density and optimum moisture content of the material as per IS: 2720-Part 8 (1983). The sample was compacted in the mould in five layers using a rammer of 4.9kg mass with a fall of 450mm by giving 25 blows per layer. The compacted energy value given was 2674 KJ/m³.

3.2.2.2.11 Triaxial compression test

The undrained, compression triaxial test was carried out as per IS: 2720-Part 11 (1993) to determine the shear strength parameters of the mine overburden and fly ash. Three identical samples of 38mm diameter and 76mm length were prepared at optimum moisture

content and maximum dry density of the materials obtained from the modified Proctor compaction test. The samples were tested by giving confining pressures 1 kg/cm², 2 kg/cm² and 3 kg/cm² respectively. Average values of three tests for each type were considered for analysis. Mohr-Coulomb relation between two normal stresses ($\sigma = C + \sigma_n \tan \phi$) has been used to determine Cohesion and angle of internal friction of the materials.

3.2.2.2.12 Permeability test

The permeability was measured by falling head permeability test as per IS: 2720-Part 17 (1986). Sample was compacted in the permeability mould by taking maximum dry density and optimum moisture content values of the mine overburden, fly ash and mixes obtained from the modified Proctor compaction tests.

3.2.2.2.13 California bearing ratio test

California bearing ratio (CBR) tests were performed in accordance with IS: 2720-Part 16 (1987). The samples were statically compacted to 95% of maximum dry density in the mould for CBR test. The samples were soaked for four days in water and were allowed to drain for 15 min before test to obtain soaked condition results. The curing periods adopted were immediate, 7 days (3 days moist curing + 4 days soaking) and 28 days (24 days moist curing + 4 days soaking) (Krishna, 2001; Leelavathamma et al., 2005; Cetin et al., 2010). CBR tests were carried out at the end of respective curing period. Two surcharge disks, each weighing 2.5 kg, were placed over the sample and a plunger, 50 mm in diameter, was used to penetrate the sample at a rate of 1.25 mm/min during CBR test. Figure 3.8, 3.9 and 3.10 show the prepared CBR samples in the moulds, soaking of CBR samples in the water tank and an experimental set up for CBR test.

The general relationship between CBR and quality of sub-grade soil suggested for pavement construction has been referred to in the analysis (Table 3.3).

Table 3.3: Relationship between CBR and quality of subgrade soil (Bowels, 1992)

CBR	Quality of sub-grade
0-3%	Very poor sub-grade
3-7%	Poor to fair sub-grade
7-20%	Fair sub-grade
20-50%	Good sub-grade
75%	Excellent sub-grade



Figure 3.8: Prepared CBR samples inside the moulds



Figure 3.9: Soaking of CBR samples



Figure 3.10: An experimental setup for CBR test

3.2.2.2.14 Unconfined Compressive strength test

Unconfined compressive strength is a common criterion to determine its resistance to any external loading. The specimens prepared for compressive strength test were of 38 mm diameter and 76 mm long. The availability of free lime and reactive silica and aluminum etc. are vital to strength gain. Moisture content of the composite has performed effect on the reactivity. Hence it is preserved by curing the specimen in a controlled chamber with $>95\%$ humidity at $30 \pm 2^{\circ}\text{C}$ for the required days (Figure 3.11). The unconfined compressive strength tests were conducted as per IS: 2720-Part 10 (1991) at a strain rate of 1.2 mm/min. Load and deformation data was recorded till failure of the specimen. The experimental set up for unconfined compression test of the specimens is shown in Figure 3.12.

The general relationship between UCS and quality of sub-grade soil suggested for pavement construction is also referred (Table 3.4).

Table 3.4: Relationship between UCS and quality of subgrade soil (Das, 1994)

UCS (kPa)	Quality of Sub-grade
25-50	Soft sub-grade
50-100	Medium sub-grade
100-200	Stiff sub-grade
200-380	Very stiff sub-grade
> 380	Hard sub-grade



Figure 3.11: Sample of UCS specimens prepared (undergoing curing)



Figure 3.12: An experimental setup for UCS test

3.2.2.2.15 Brazilian tensile strength test

The determination of direct tensile strength of soil or rock material is difficult. So, indirect way (Brazilian tensile strength) of its determination is practiced. The Brazilian tensile test make the sample fail under tension though the loading pattern is compressive in nature. The tensile strength is determined as per ASTM D3967. In this test, the length (thickness) to diameter ratio is 0.5. The specimens prepared for tensile strength test were of 38 mm diameter and 19 mm thick. The specimens were placed diametrically during test. The sample fails diametrically in tension by application of load. The indirect tensile strength is calculated as follows:

$$\sigma_t = \frac{2P}{\pi DL}$$

where, σ_t = Brazilian Tensile Strength; P = Failure Load, D = Diameter of the specimen; L = length of the specimen.

3.2.2.2.16 Ultrasonic Pulse velocity test

Ultrasonic pulse velocity test is a nondestructive testing technique which is used to determine the dynamic properties of materials. This method is valid for wave velocity measurement in both anisotropic and isotropic materials though velocities obtained in anisotropic materials may be influenced by factors as direction, material composition, dampness, weakness present, travel distance and diameter of transducer.

The ultrasonic pulse velocity test is a measurement of the transit time of a longitudinal vibration pulse through a sample which has a known path length. It is carried out by applying two transducers (transmitting and receiving) to the opposite end surfaces of the samples. The schematic representation of Ultrasonic velocity measurement system is shown in Figure 3.13. The electrical impulses of a specified frequency are generated by pulse generator. These impulses are converted into elastic waves which propagate through a sample by transmitter. The mechanical energy of the propagating waves that propagate through the sample are received by the second transducer called receiver placed on the opposite side of the specimen and then turns into electrical energy of the same frequency. The signal travel time is measured electronically through the specimen and is registered in the oscilloscope.

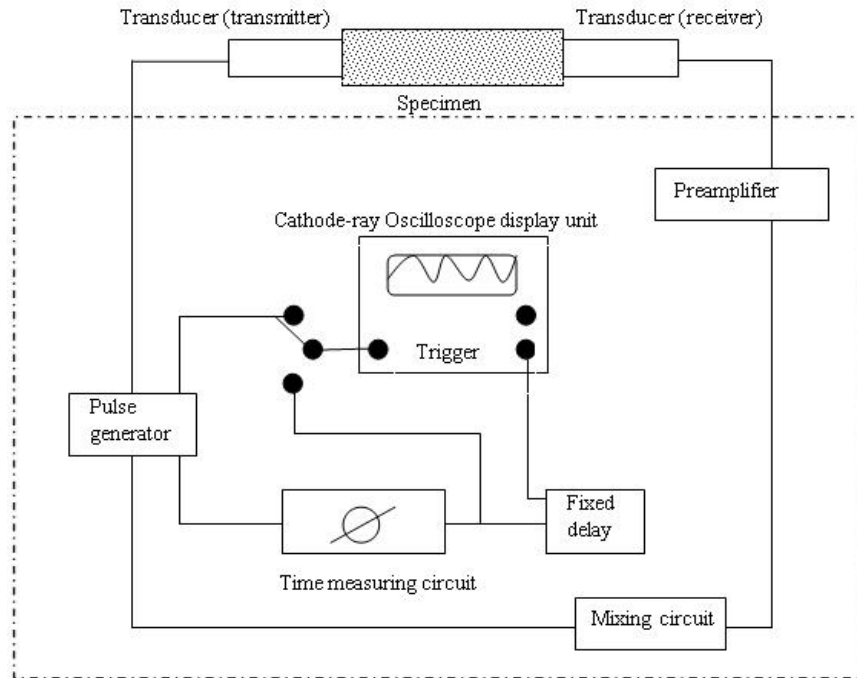


Figure 3.13: Schematic representation of ultrasonic velocity measurement

All pulse velocity measurements were determined using an Ultrasonic Velocity Measurement System (make: GCTS, USA) (Figure 3.14). This system includes 10 MHz bandwidth receiver pulse raise time less than 5 nano-seconds, 20MHz acquisition rate with 12bit resolution digitizing board, transducer platens with 200 KHz compression mode and 200KHz shears mode. The GCTS pulse velocity device operates in a through transmission mode of testing, that is, a signal is produced at one end of the specimen and received at the other end. The two, 54-mm diameter test platens are wired to a data acquisition and processing unit. The equipment provides pulse and shear wave velocity to determine elastic constants. The measurement was carried out according to ASTM D 2845-05.

The relationship between various parameters on pulse velocity, density, elastic constants, modulus values are given by the following equations.

$$\nu = \frac{V_p^2 - 2V_s^2}{2(V_p^2 - V_s^2)} \dots\dots\dots (1)$$

$$E = \frac{\rho V_s^2 (V_p^2 - 4V_s^2)}{V_p^2 - V_s^2} \dots\dots\dots (2)$$

$$K = \frac{\rho (V_p^2 - 4V_s^2)}{3} \dots\dots\dots (3)$$

$$G = \rho V_s^2 \dots\dots\dots (4)$$

where,

V_p = compression P wave velocity, m/s

V_s = shear S wave velocity, m/s

ρ = density, kg/m³

ν = Poisson's ratio

E= Young's Modulus, Pa

K= Bulk Modulus, Pa

G= Shear (Rigidity) Modulus, Pa



Figure 3.14: An experimental setup for Ultrasonic velocity measurement

3.2.2.2.17 Leaching study

Leaching analysis was carried out by using an Atomic Absorption Spectrophotometer (AA 200, Perkin Elmer). Atomic absorption spectroscopy (AAS) is a spectroanalytical procedure for the qualitative and quantitative determination of chemical elements employing the absorption of optical radiation (light) by free atoms in the gaseous state. The technique is used to determine the concentration of a particular element (the analyte) in a sample. It analyzes the concentration of elements in a liquid sample based on energy absorbed from certain wavelengths of light (usually 190 to 900 nm). Atomic absorption spectrophotometer typically includes a flame burner to atomize the sample (most commonly a hollow cathode lamp), a monochromator and a photon detector.

3.3 Experimental Size

The investigation included many characterization studies including major laboratory tests as compaction, California bearing ratio (CBR), unconfined compressive strength (UCS), Brazilian tensile strength (BTS), Ultrasonic tests in addition to other index tests. The reported results represent average values of three to four samples for each test type except that for compaction to determine MDD and OMC. The best results that were not within 5% to 10% of each other were discarded and fresh samples were prepared for retesting. A total of about 2000 samples were prepared and tested for various parameters. The details of the test size are given below (Table 3.5).

Table 3.5: Experimental Design Chart

Sl No.	Compositions(%): (FA+O/B)+L (L= Lime)	Major laboratory tests of composites (curing period)													
		Compaction for MDD & OMC	CBR			UCS			UTS			Ultrasonic			
			Soaking	7	28	7	14	28	56	28	56	7	14	28	56
				days	days	days	days	days	days	days	days	days	days	days	days
1	15FA + 85O/B		*	*	*	+	+	+	+	×	×	+	+	+	+
2	20FA + 80O/B		*	*	*	+	+	+	+	×	×	+	+	+	+
3	25FA + 75O/B		*	*	*	+	+	+	+	×	×	+	+	+	+
4	30FA + 70O/B		*	*	*	+	+	+	+	×	×	+	+	+	+
5	35FA + 65O/B		*	*	*	+	+	+	+	×	×	+	+	+	+
6	40FA + 60O/B		*	*	*	+	+	+	+	×	×	+	+	+	+
7	45FA + 55O/B		*	*	*	+	+	+	+	×	×	+	+	+	+
8	50FA + 50O/B		*	*	*	+	+	+	+	×	×	+	+	+	+
9	(15FA+85O/B)+2L		*	*	*	+	+	+	+	×	×	+	+	+	+
10	(15FA+85O/B)+3L		*	*	*	+	+	+	+	×	×	+	+	+	+
11	(15FA+85O/B)+6L		*	*	*	+	+	+	+	×	×	+	+	+	+
12	(15FA+85O/B)+9L		*	*	*	+	+	+	+	×	×	+	+	+	+
13	(20FA+80O/B)+2L		*	*	*	+	+	+	+	×	×	+	+	+	+
14	(20FA+80O/B)+3L		*	*	*	+	+	+	+	×	×	+	+	+	+
15	(20FA+80O/B)+6L		*	*	*	+	+	+	+	×	×	+	+	+	+
16	(20FA+80O/B)+9L		*	*	*	+	+	+	+	×	×	+	+	+	+
17	(25FA+75O/B)+2L		*	*	*	+	+	+	+	×	×	+	+	+	+
18	(25FA+75O/B)+3L		*	*	*	+	+	+	+	×	×	+	+	+	+
19	(25FA+75O/B)+6L		*	*	*	+	+	+	+	×	×	+	+	+	+
20	(25FA+75O/B)+9L		*	*	*	+	+	+	+	×	×	+	+	+	+

21	(30FA+70O/B)+2L	*	*	*	+	+	+	+	×	×	+	+	+	+
22	(30FA+70O/B)+3L	*	*	*	+	+	+	+	×	×	+	+	+	+
23	(30FA+70O/B)+6L	*	*	*	+	+	+	+	×	×	+	+	+	+
24	(30FA+70O/B)+9L	*	*	*	+	+	+	+	×	×	+	+	+	+
25	(35FA+65O/B)+2L	*	*	*	+	+	+	+	×	×	+	+	+	+
26	(35FA+65O/B)+3L	*	*	*	+	+	+	+	×	×	+	+	+	+
27	(35FA+65O/B)+6L	*	*	*	+	+	+	+	×	×	+	+	+	+
28	(35FA+65O/B)+9L	*	*	*	+	+	+	+	×	×	+	+	+	+
29	(40FA+60O/B)+2L	*	*	*	+	+	+	+	×	×	+	+	+	+
30	(40FA+60O/B)+3L	*	*	*	+	+	+	+	×	×	+	+	+	+
31	(40FA+60O/B)+6L	*	*	*	+	+	+	+	×	×	+	+	+	+
32	(40FA+60O/B)+9L	*	*	*	+	+	+	+	×	×	+	+	+	+
33	(45FA+55O/B)+2L	*	*	*	+	+	+	+	×	×	+	+	+	+
34	(45FA+55O/B)+3L	*	*	*	+	+	+	+	×	×	+	+	+	+
35	(45FA+55O/B)+6L	*	*	*	+	+	+	+	×	×	+	+	+	+
36	(45FA+55O/B)+9L	*	*	*	+	+	+	+	×	×	+	+	+	+
37	(50FA+50O/B)+2L	*	*	*	+	+	+	+	×	×	+	+	+	+
38	(50FA+50O/B)+3L	*	*	*	+	+	+	+	×	×	+	+	+	+
39	(50FA+50O/B)+6L	*	*	*	+	+	+	+	×	×	+	+	+	+
40	(50FA+50O/B)+9L	*	*	*	+	+	+	+	×	×	+	+	+	+

No. of tests with curing period:

Compaction	CBR	UCS	UTS	Ultrasonic
40	$3 \times 40 = 120$	$4 \times 40 = 160$	$2 \times 40 = 80$	$3 \times 40 = 120$
Total = $40 + 120 + 160 + 80 + 120 = 520$				

Total No. of samples (@ 1 to 4 for each type of test)

Compaction	CBR	UCS	UTS	Ultrasonic
40	$3 \times 120 = 360$	$4 \times 160 = 640$	$3 \times 80 = 240$	$3 \times 160 = 480$
Total = $40 + 360 + 640 + 240 + 480 = 1760$				

CHAPTER 4

RESULTS AND DISCUSSION

4.1 Introduction

A typical surface coal mine in India has about 5km of permanent haul road with a life span of 25 to 30 years. The carrying capacity of transportation trucks as well as other heavy machineries undergoes many upward revisions in the life of an operating coal mine as the demand for fuel continues to increase. However the design of haul road and its construction do not undergo corresponding improvement. It is often observed that mine operators simply cut or fill haul roads with the materials existing at the location to save capital cost. In case of acute adverse condition, only the surface course of the haul road is repaired without, any change to other courses, specifically to subbase course. So, it is most important to design and build the haul road sub-base with material of sufficient bearing capacity. The engineering properties of a material are dependent on the composition of material to a great extent. There exists wide variation in the composition of fly ash depending on coal type, type of furnace, temperature, collection mechanism, etc (Mishra, 2003). The overburden material over coal strata in the Gondwana basin also exhibit similar heterogeneous attributes. The pertinent geotechnical properties of the develop materials were determined as per established mechanism. All the results of the above investigation and their corresponding analyses have been presented in different section as mentioned below:

- I. Results of geotechnical properties of ingredients.
- II. Results of geotechnical properties of developed composite materials.

- III. Results of microstructural analyses.
- IV. Results of leaching studies.
- V. Development of model relationship between geotechnical parameters.

4.2 Results of geotechnical properties of ingredients

The aim was to develop suitable engineering material for the subbase course with fly ash and overburden. So a detail analysis of the constituent materials as well as the developed composites was carried out.

4.2.1 Physical Properties

The fly ash was collected in dry state and was in loose stage. Its average water content was less than 1%. The fly ash used had a powdery structure with medium to dark grey colour indicating low lime (Meyers et al., 1976).

The physical properties of fly ash and mine overburden are reported in Table 4.1. The specific gravity of fly ash and mine overburden obtained are 2.16 and 2.6. The specific gravity of fly ash is found to be less than that of mine overburden, due to the presence of cenospheres and less iron content. The materials with higher iron content have relatively high specific gravity (Sridharan and Prakash, 2007).

The grain size distribution of the construction material has a strong influence on the density that can be achieved. The grain size distribution curves for the fly ash and overburden are shown in Figure 4.1. The overburden contains sand size fraction with appreciable amount of non-plastic fines or fines with low plasticity. It is typically described as poorly graded sand-silt mixtures and belongs to SM group. It contains 32.91% of sand, 43.73% of silt and 13.65% of clay particles.

The United States classification systems (USCS) of soils do not classify the coal ashes satisfactorily because of its non-plastic nature. Hence geotechnical classification system developed for the purpose has been followed in this investigation (Sridharan and Prakash, 2007). The fly ash belongs to non-plastic inorganic coarse silt sized fractions (MLN) group as it contains more than 50% of fines is in the range 20 μm to 75 μm . The particle sizes corresponding to the 10% finer are 6.4 μm and that to 60% finer is 68 μm . The coefficient of uniformity ($C_u = D_{60}/D_{10}$) as calculated is 10.62. The fly ash used is of medium graded soil.

Specific surface area is a measure of the fineness of the material which influences the reactivity with other ingredients. The specific surface areas of fly ash particles and over burden materials are measured by Blaine's Air permeability method. The respective surface area of fly ash is 458 m^2/kg and that of over burden material is 943 m^2/kg . The low value of fly ash is due to more percent of silt particle as compared to that in overburden material (Sridharan and Prakash, 2007).

Consistency limits as liquid limit (LL), plastic limit (PL), plasticity index (PI) and shrinkage limit are important factors in material identification and classification. These parameters reflect a few geotechnical problems as swelling potential and workability. The respective values of LL for fly ash and overburden are 30.7% and 25.7% respectively. Though both values are close overburden material is less workable than that for fly ash. Lime in general is suitable for soils with plasticity index (PI) 20 % (Anon, 1985). The overburden material has PI of about 15% and hence is not suitable to be modified by lime addition for stabilization. However stabilization can be achieved by addition of fly ash that are pozzolanic. The tests also confirm that fly ash is non-cohesive and has negligible shrinkage index thus better suited to geotechnical application. Free swell index of the fly ash

is found to be negligible due to flocculation which confirms to that reported elsewhere (Pandian, 2004).

Table 4.1: Physical properties of fly ash and mine overburden

Property	Fly ash	Overburden
Specific gravity	2.16	2.6
Particle size analysis (%)		
Gravel (>4.75 mm)	----	9.71
Sand (4.75 mm – 0.075 mm)	22.17	32.91
Silt (0.075 mm – 0.002 mm)	75.04	43.73
Clay (<0.002 mm)	2.79	13.65
Specific Surface Area (m ² /kg)	458	943
Consistency limits		
Liquid limit (%)	30.75	25.7
Plastic limit (%)	Non-plastic	15.04
Shrinkage limit (%)	----	13.44
Plasticity index (%)	----	10.66
Free swell index (%)	Negligible	20

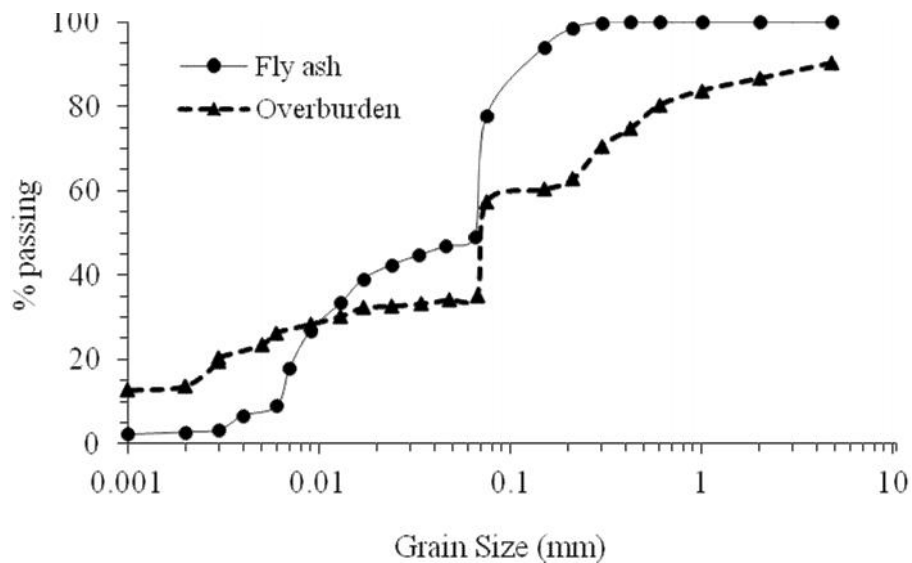


Figure 4.1: Grain size distribution curves of fly ash and mine overburden

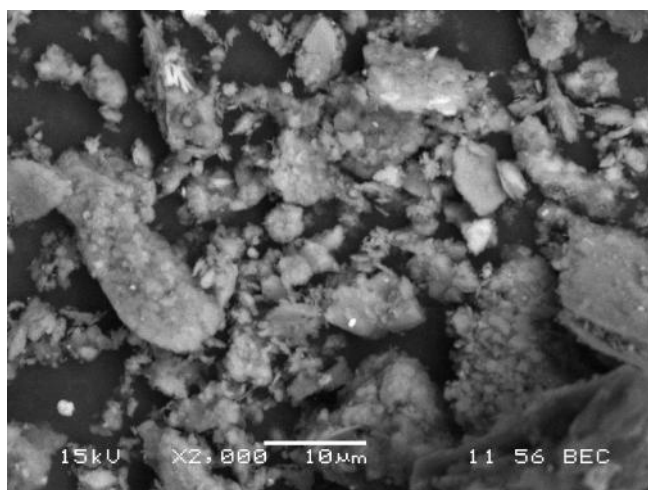
4.2.2 Chemical Properties

The chemical composition of fly ash, overburden and lime are important indicators of suitability of a material for geotechnical applications. The chemical compositions of mine overburden and fly ash are presented in Table 4.2. The chemical composition of fly ash indicates that it has not only less calcium content but also the quantity of $\text{SiO}_2 + \text{Al}_2\text{O}_3 + \text{Fe}_2\text{O}_3$ exceed 70%. Thus, it is classified as “Class F” fly ash as per ASTM 618 specifications. The fly ash and mine overburden consist mostly of silica (SiO_2), alumina (Al_2O_3) and iron oxide (Fe_2O_3). Oxides of calcium, magnesium, potassium, titanium, sodium are also present in small quantities. The major constituent of lime is calcium oxide (75.82%).

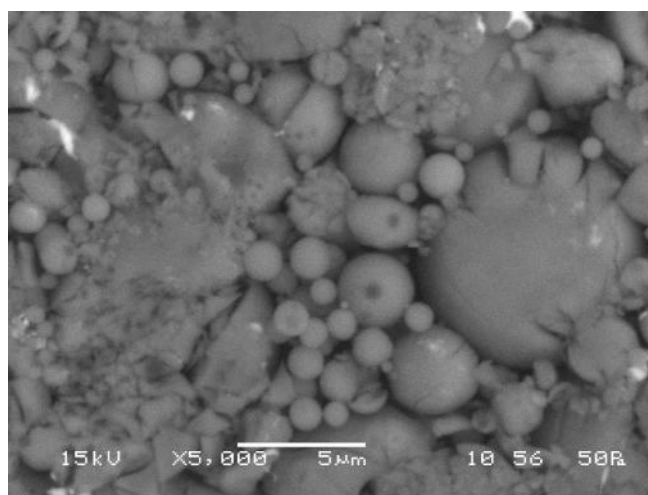
The morphology of fly ash indicates the presence of glassy solid spheres, hollow spheres (cenospheres), rounded and smooth porous grains as well as irregular agglomerates ((Figure 4.2 (a)). These particles affect the compaction behaviour (Leonards and Bailey, 1982; De Santayana and Mazo, 1994). The micrograph is without any formation of cementitious compound. It confirms that the fly ash used in the investigation has low calcium content. It compares favourably to those observed elsewhere (Baker and Lagurous, 1985; Krishna, 2001).

The morphology of overburden indicates the presence of irregular shape solid particles (Figure 4.2 (b)). The X-ray diffraction profiles of the overburden and fly ash indicate the presence of crystalline phases (Figure 4.3 (a and b)). It is noticed from the XRD analysis that Kaolinite and Quartz are the major mineral constituents of the overburden. The major mineral constituents of fly ash are Quartz, Silliminate and Mullite. Quartz is the most prominent mineral present in both overburden and fly ash materials. It peaks at 950 counts/s near $2\theta = 26.66^\circ$ for fly ash samples and at 450 counts/s near $2\theta = 26.66^\circ$ for overburden samples.

The pH of overburden and fly ash are found to be 4.85 and 7.2. The pH values indicate that fly ash is alkaline and overburden is acidic depending on alkaline oxide content and free lime content. The silica lime reaction is pH dependent. The higher the pH, the better is the solubility of silica and lime-silica reaction in producing pozzolanic products. The pH of the solution increases if presence of lime is in excess of the amount required for the silica to react. But addition of lime in excess than that required for the reactions makes pH constant as the solution becomes saturated (Sivapullaiah et al., 1995).



(a)



(b)

Figure 4.2: Scanning electron micrograph of (a) mine overburden material and (b) fly ash

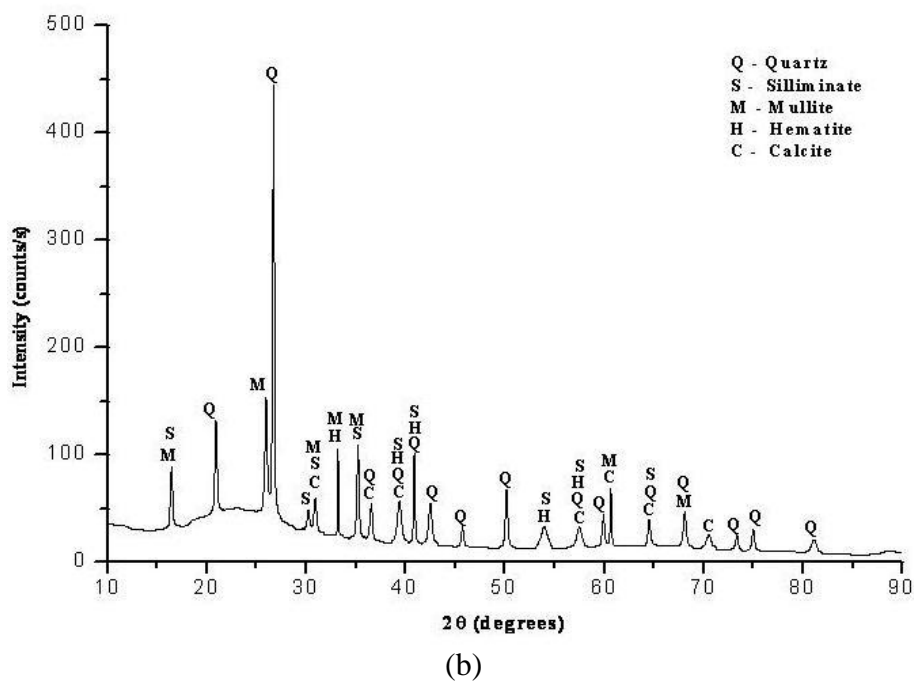
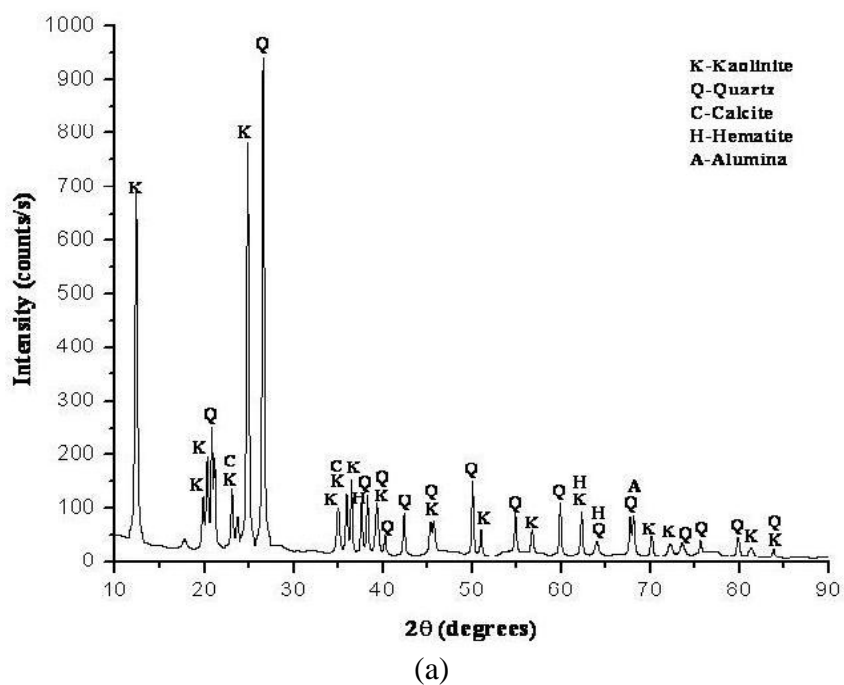


Figure 4.3: X-ray diffractogram of (a) mine overburden and (b) fly ash

Table 4.2: Chemical compositions of fly ash, mine overburden and lime (wt. %)

Constituents	Fly ash	Mine overburden	Lime
SiO ₂	50.88	49.8	0.92
Al ₂ O ₃	34.78	28.49	0.29
Fe ₂ O ₃	6.31	8.32	0.45
CaO	0.52	1.09	75.82
K ₂ O	1.42	0.39	--
MgO	0.51	1.23	3.94
TiO ₂	2.95	0.69	--
Na ₂ O	0.2	--	--
P ₂ O ₅	--	--	0.04
SO ₃	--	--	0.55
LOI	2.4	10	17.99

4.2.3 Engineering Properties

The engineering properties of a material such as compressive strength, tensile strength, CBR, permeability etc. is dependent on the moisture content and density at which the composite is prepared. Typically the higher the compaction the better is its geotechnical characteristics. Hence it is necessary to achieve the desired degree of compaction which is necessary to meet the expected properties (Nicholson et al., 1994).

Compaction is the process of increasing the density of material by the application of mechanical energy such as tamping, rolling and vibration. It is achieved by forcing the particles closer with a reduction in air voids. Optimum moisture content (OMC) is the moisture content at which compacted material reaches the maximum dry density of solid particles. The compaction characteristics of ingredients as fly ash and mine overburden were carried out to determine the optimum moisture content and maximum dry density (Figure

4.4). The maximum dry density of fly ash was lower than that obtained for mine overburden due to low specific gravity and non-cohesive in nature. Fly ash has higher optimum moisture content due to the fact that particles themselves are hollow or cenospheres and holds a considerable quantity of water internally. The compaction curve of fly ash is almost flat and indicates it's insensitive to moisture variation. It confirms to similar observations reported elsewhere (Sridharan et al., 2000; Das and Yudhbir, 2006; Sridharan and Prakash, 2007). The maximum dry density of fly ash is less than that of overburden due to less iron content and specific gravity of the fly ash. The MDD of overburden and fly ash were 2040 kg/m^3 and 1396 kg/m^3 respectively (Table 4.3). Corresponding values for OMC were 8.15% and 20.06% respectively. The low density value of fly ash was due to the high moisture content, unlike the overburden which has less water content.

The permeability of overburden and fly ash are $3.06 \times 10^{-6} \text{ cm/s}$ and $1.01 \times 10^{-5} \text{ cm/s}$ respectively (Table 4.3). Both represent low permeability though fly ash exhibit more value than that of overburden. This phenomenon is because of uniform particle sizes in fly ash where as overburden grains are heterogeneous.

The shear strength parameters of compacted overburden and fly ash are represented in Table 4.3. As the sand and clay contents of overburden are more than that of fly ash, the cohesion and angle of internal friction of overburden are relatively higher than that of fly ash. Angle of repose is the maximum inclination of the sloping surface of a material exhibiting the limiting stability. The angle of repose of over burden material is close to its angle of internal friction value. It is very low for fly ash as fly ash exhibits pseudo-cohesion, even in its dry state by virtue of its fineness.

Unconfined compressive strength (UCS) of a material is its resistance to any externally applied load. It reflects inter granular cohesion as well as strength of cementing material holding those grains. The UCS values of fly ash and overburden material are 142 KPa and 313 KPa respectively (Table 4.3). The value of overburden is more than twice to that of fly ash due to presence of high quantity binding material (CaO) as compared to fly ash.

The California Bearing Ratio values for overburden and fly ash materials are almost same in unsoaked condition at around 22%. But the values reduce drastically at soaked condition. Over burden exhibited value at 2.95% and fly ash at 0.72%. Both these values are less than 3 % that make the materials unsuitable for sub-base application (Bowels, 1992).

Table 4.3: Engineering properties of overburden and fly ash

Property	Overburden	Fly ash
1. Compaction characteristics (from Heavy compaction or Modified Proctor test)		
(a) Maximum dry density (kg/m^3)	2040	1396
(b) Optimum moisture content (%)	8.15	20.06
2. Permeability (cm/sec)	3.06E-06	1.01E-05
3. Shear strength parameters		
(a) Cohesion (kPa)	58.09	39.35
(b) Angle of internal friction	36.23 ⁰	28.45 ⁰
4. Angle of repose	33.77 ⁰	12 ⁰
5. Unconfined compressive strength (kPa)	313.91	142.76
6. CBR value (%)		
(a) Unsoaked condition	23.65	22.42
(b) Soaked condition	2.95	0.72

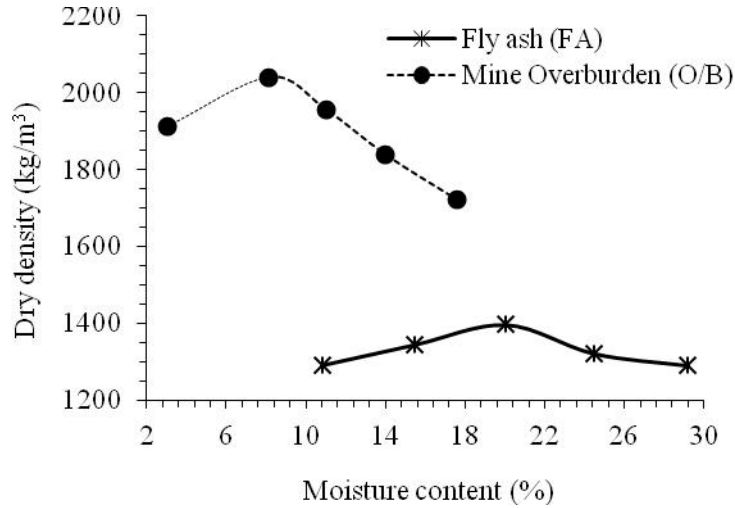


Figure 4.4: Compaction curves of fly ash and overburden

4.3 Geotechnical properties of developed composite materials

The developed composite materials were subjected to various engineering tests as compaction behaviour, UCS, CBR, Brazilian tensile strength, ultrasonic pulse velocity and micro- structural analyses.

4.3.1 Compaction characteristics

The compaction characteristics of untreated composites varied between 1965 kg/m^3 to 1686 kg/m^3 (Figure 4.5). It reduced as the quality of fly ash percentage increased in the composites (Figure 4.6). But the trend is reverse for the optimum level of moisture holding capacity of the composites. As the fly ash percentage was increased the values for OMC also increased (Figure 4.7).

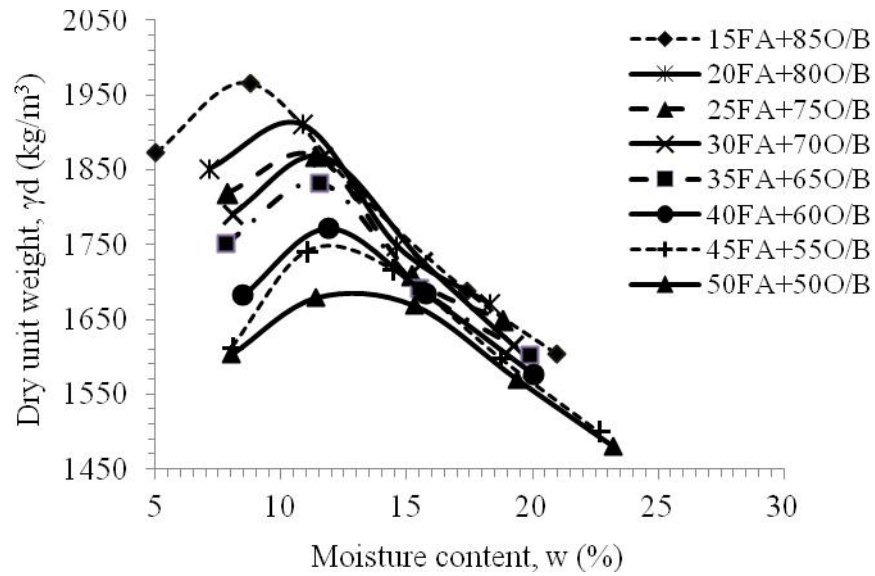


Figure 4.5: Compaction curves of untreated composites

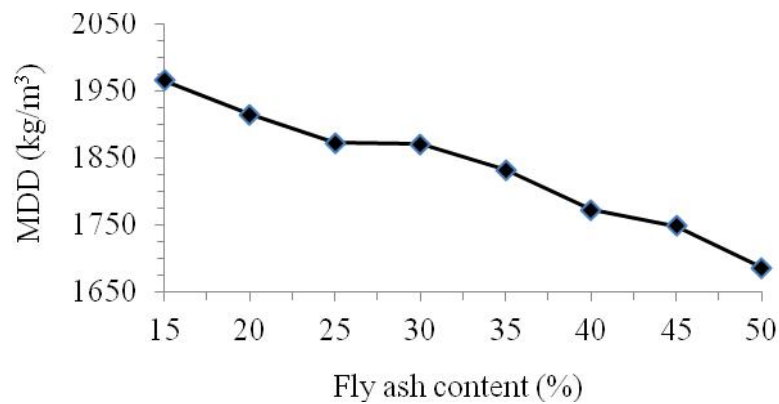


Figure 4.6: Variation of maximum dry density with fly ash content

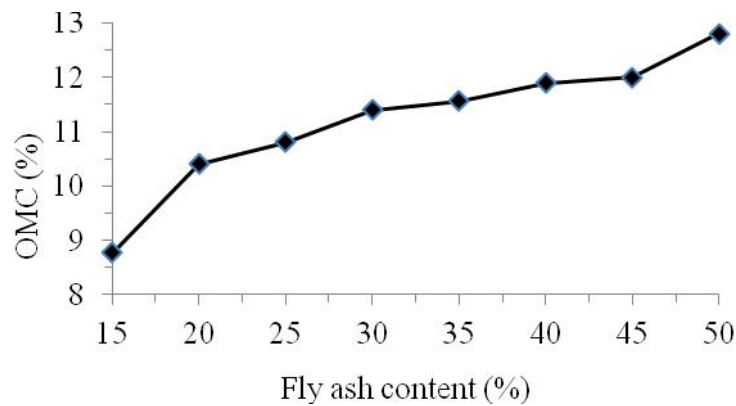


Figure 4.7: Variation of optimum moisture content with fly ash content

The aim of the investigation was to develop an engineering material with mine overburden and fly ash stabilized with lime. Accordingly samples were prepared (Table 3.2). The specimen behaviour changed when lime added in various proportions. The maximum dry density values of all composite materials decreased and optimum moisture content increased with increase in lime content (Figures 4.8, 4.9 and 4.10). It confirms to similar observations for fly ash-soil-lime mixtures (Consoli et al., 2001; Arora and Aydilek, 2005; Kaniraj and Havanagi, 1999; Krishna, 2001; Sahu, 2005; Das and Yudhbir, 2006; Jadhao and Nagarnaik, 2008). The variation of MDD and OMC values with lime content are given in Appendix.

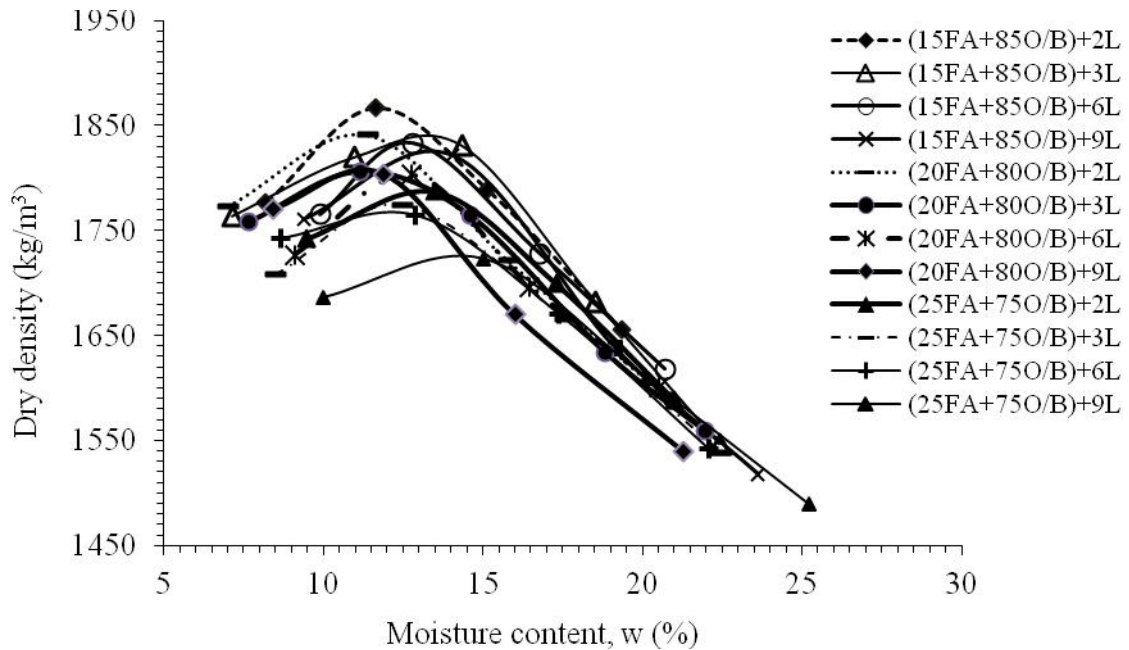


Figure 4.8: Compaction curves of the composites containing 15, 20 and 25% fly ash

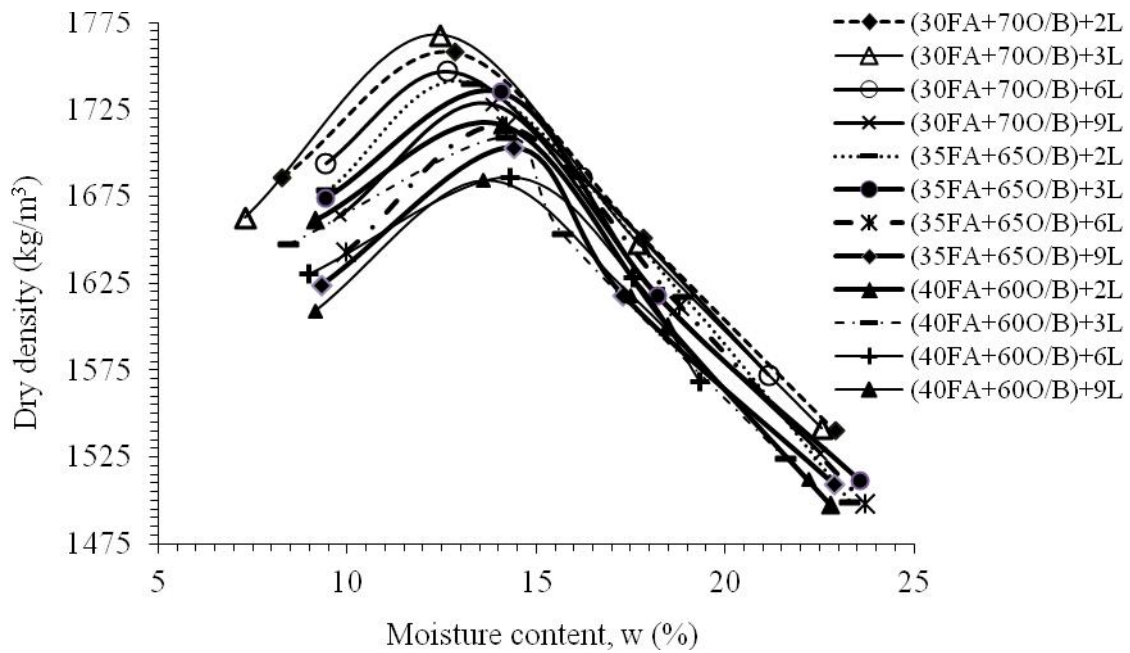


Figure 4.9: Compaction curves of the composites containing 30, 35 and 40% fly ash

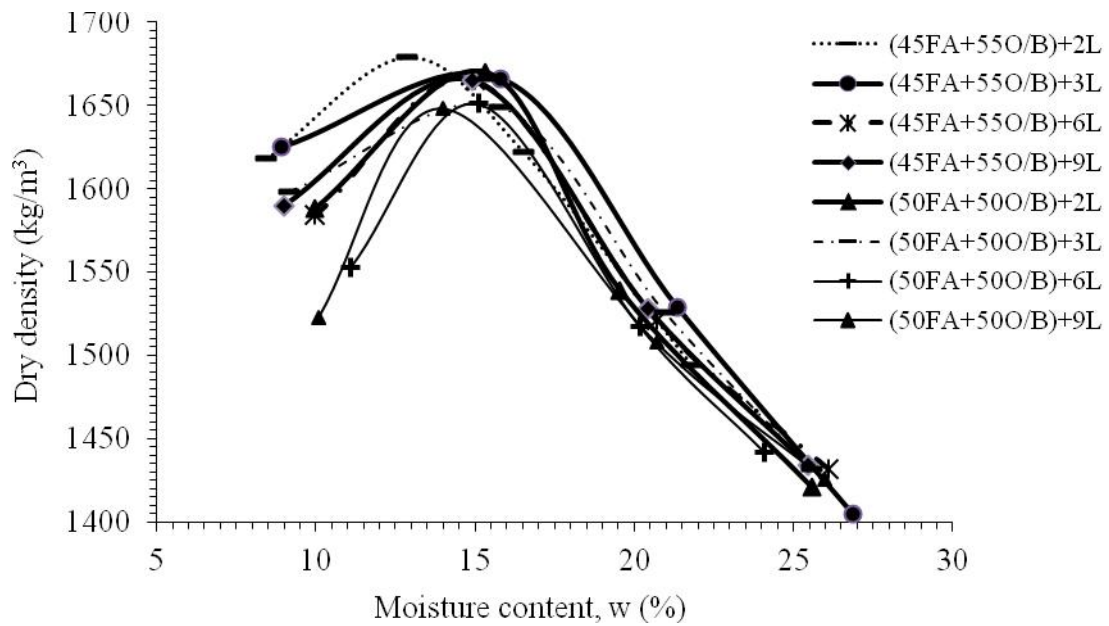


Figure 4.10: Compaction curves of the composites containing 45 and 50% fly ash

4.3.2 California Bearing Ratio behavior

CBR value is used as an index of material strength and its bearing capacity. This method is well established and popular for design of the base and subbase material for pavement. In this investigation CBR tests were carried out to characterize the strength and the bearing capacity of the untreated fly ash-overburden composite as well as lime treated fly ash-overburden composite materials.

4.3.2.1 Effect of curing on the CBR of untreated composites

The variation of CBR with the addition of fly ash to mine overburden for both unsoaked and soaked conditions were reported (Figure 4.11). The results of penetration test (CBR test) carried out for different composites exhibit the weakening in soaked conditions as compared to that of unsoaked conditions (Appendix). The CBR values of untreated fly ash-overburden composite materials ranged from 26% to 45% in unsoaked conditions (Figure 4.12). Similar values in soaked condition are less than 3%. The higher CBR value in unsoaked condition is due to the capillary forces created at optimum moisture content and maximum dry density condition in addition to the friction resisting the penetration of the plunger. However when the samples were tested after 96 hour soaking in water, the CBR values exhibited very low due to the destruction of the capillary forces (Figure 4.11). Soaked condition though a conservative estimate, yet considered for worst case scenario. The obtained CBR value less than 3% is unsuitable for subgrade material (Bowels, 1992) and hence need to be stabilized with additives for pavement applications.

The CBR values of composites when tested at different curing periods exhibited little change over uncured results. The CBR values of 28 days cured samples almost doubled to

that at soaked conditions. However in all cases, the CBR values were less than 5% and hence unsuitable for subbase material (Figure 4.12). Hence it was decided to improve the CBR of fly ash and mine overburden mixes by using additive.

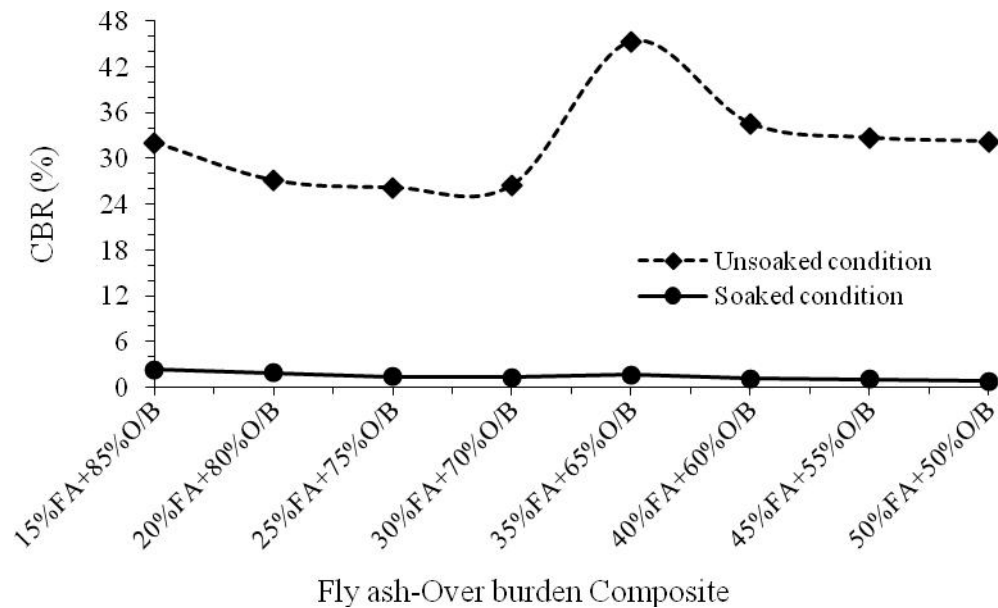


Figure 4.11: Variation of CBR with the addition of fly ash to mine overburden

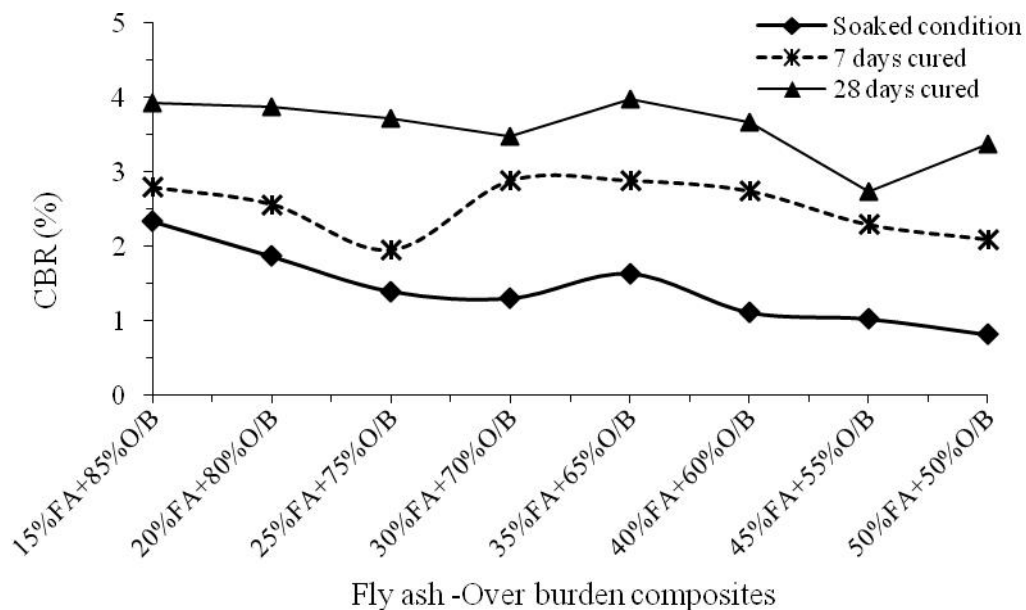


Figure 4.12: Effect of curing on the CBR of fly ash and mine overburden composites

4.3.2.2 CBR behaviour of lime stabilized fly ash composites

Generally additives like cement or lime improve the strength of the soil or fly ash (Consoli et al., 2001; Ghosh and Subbarao, 2006; Mackos et al., 2009). CBR values were determined for fly ash-overburden material stabilized with lime. Lime was added between 2% to 9% to observe the effect of lime. As the lime was added, each composition showed significant improvement in CBR values. The results represented are for the soaked and cured conditions. In soaked condition the composite with 15% fly ash exhibited maximum CBR value 77.08 at 9% lime content (Figure 4.13). However as the lime content increased the composites with higher fly ash content showed more CBR values (Figure 4.14) thus confining that availability of silica, alumina added to strength gain over time. The maximum CBR value obtained was for composite with 40%FA+60%O/B with 3% lime at 28 days curing at 140 MPa (Figure 4.15). The corresponding values for composites with 45% and 50% fly ash content were almost same. It shows that there exists a maximum limit for fly ash content to add to the increased CBR value. But the results show curing and fly ash content has strong effect on the bearing capacity of the composite. It confirms to the observation found elsewhere for soil with class C fly ash (Ismail, 2006).

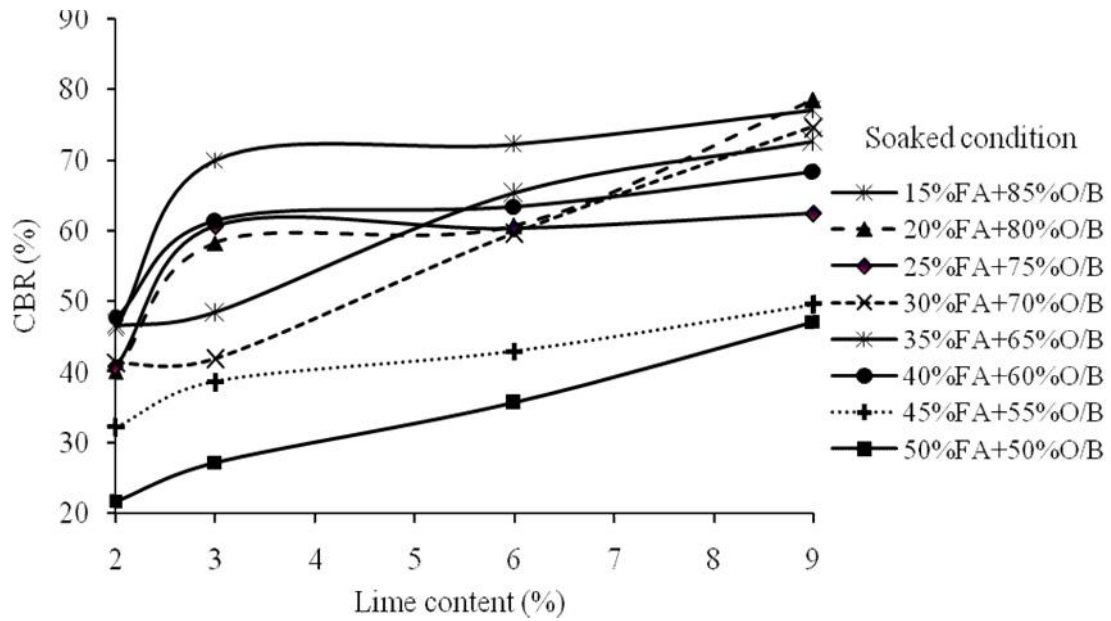


Figure 4.13: Effect of lime on CBR behavior of composites in soaked condition

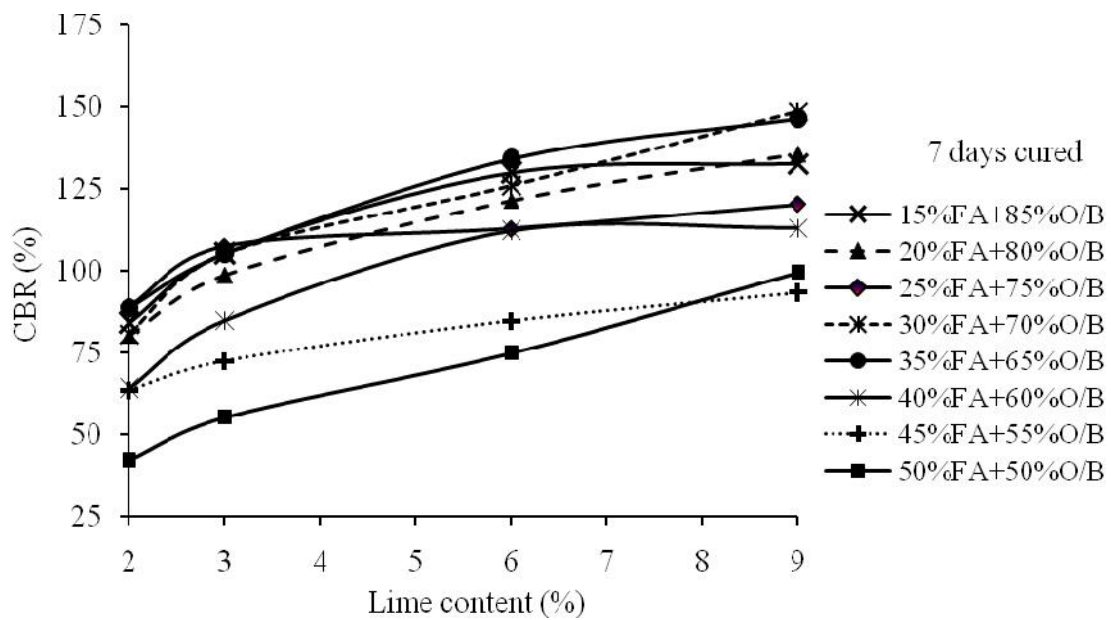


Figure 4.14: Effect of lime on CBR behavior of composites at 7 days curing

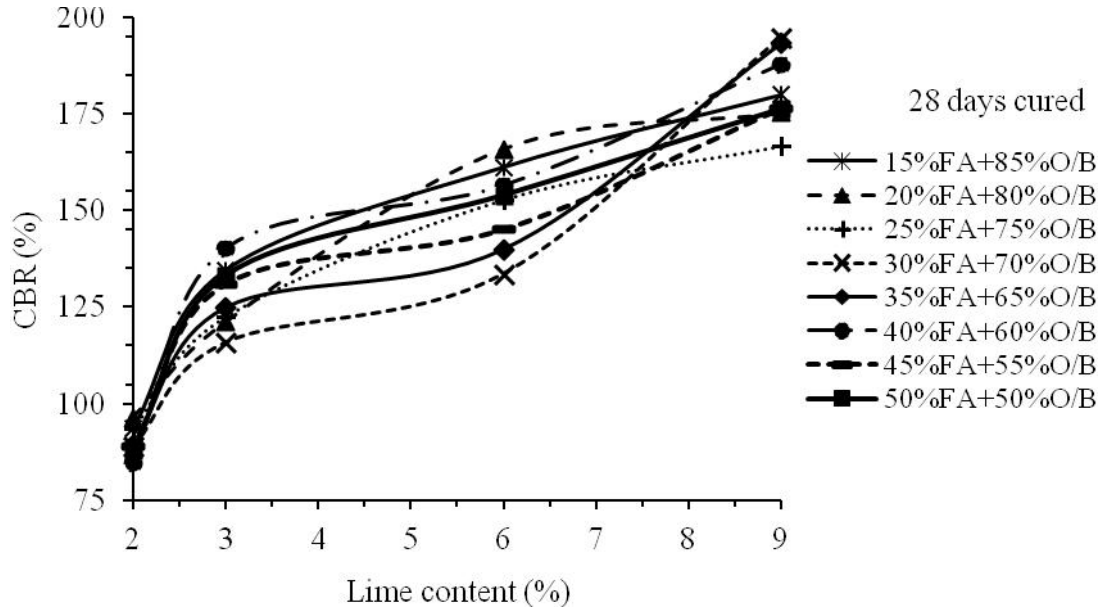


Figure 4.15: Effect of lime on CBR behavior of composites at 28 days curing

It is observed from the results that the CBR values increased from 42% to 149% and 85% to 195% at 7 and 28 days of curing respectively. Thus, increasing in curing period revealed that increase in percentage of lime increases the CBR value. This is because hydration of lime forms calcium silicate hydrate gel and with addition of more and more lime, more amount of this gets formed. Hence there is a continuous increase in the CBR values with different curing period. The mine overburden mixed with 30% fly ash and 9% lime resulted in maximum bearing ratio as compared to that of other mixes at 7 and 28 days curing respectively. There is a strong binding between the fly ash and mine overburden particles by the cementitious products and hence higher CBR in the composite. The value compares favourably with the CBR result of the soil stabilized with fly ash (10% and 20%) and lime kiln dust (2.5% and 5%) to be 69 to 142 at 7 days curing and greater than 164 at 28 days curing (Cetin et al., 2010).

CBR gain factor is the strength enhancement due to addition of lime in the treated composites with respect to that of untreated composites. The maximum gain factor was obtained for composite (40%FA+60%O/B)+9%L at 61.1 and the minimum factor was for the composite (15%FA+85%O/B)+2%L at soaked condition (Figure 4.16). The composite (30%FA+70%O/B)+9%L gained by 19.76 times. The maximum and minimum gain factors at 7 days curing were for (25%FA+75%O/B)+6%L and (50%FA+50%O/B)+2%L composites with values 56 and 20 respectively (Figure 4.17). The corresponding gain factor for the composite (30%FA+70%O/B)+9%L was 51.4. At 28 days curing minimum gain was with the composite (35%FA+65%O/B)+2%L at 22 and maximum at 64.5 was for (45%FA+55%O/B)+9%L (Figure 4.18). The gain factor for the composite (30%FA+70%O/B)+9%L at 28 days was 56. The maximum gain factor values were 42.5, 55, 56.7 and 61 at 2, 3, 6 and 9% lime respectively in soaked condition (Figure 4.16). Similarly, the maximum gain factors were 45.5, 56, 56.3 and 55 at 7 days curing and 32.5, 48, 53.1 and 64.5 at 28 days curing with varying percentage of lime respectively (Figures 4.17 and 4.18).

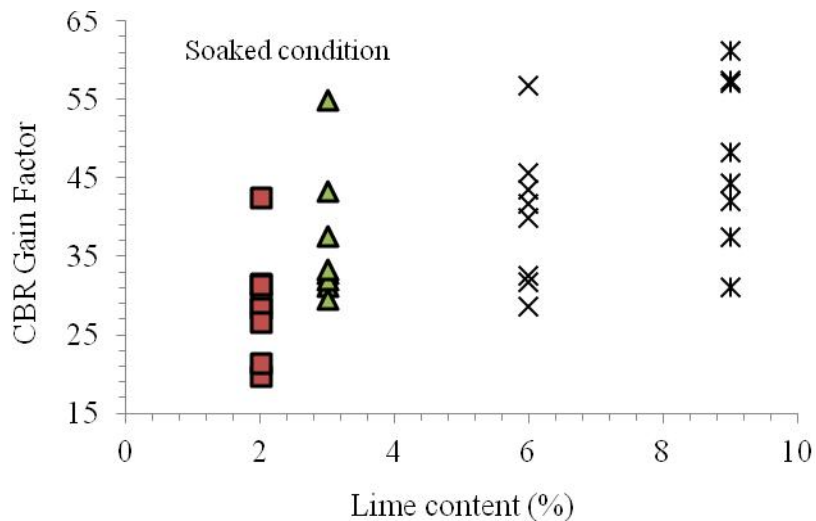


Figure 4.16: Influence of Lime in CBR Gain for all composites at soaked condition

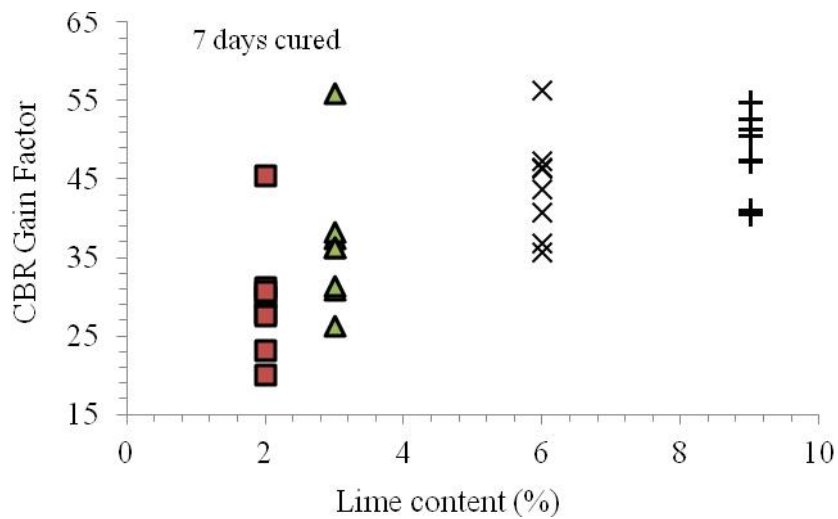


Figure 4.17: Influence of Lime in CBR Gain for all composites at 7 days curing

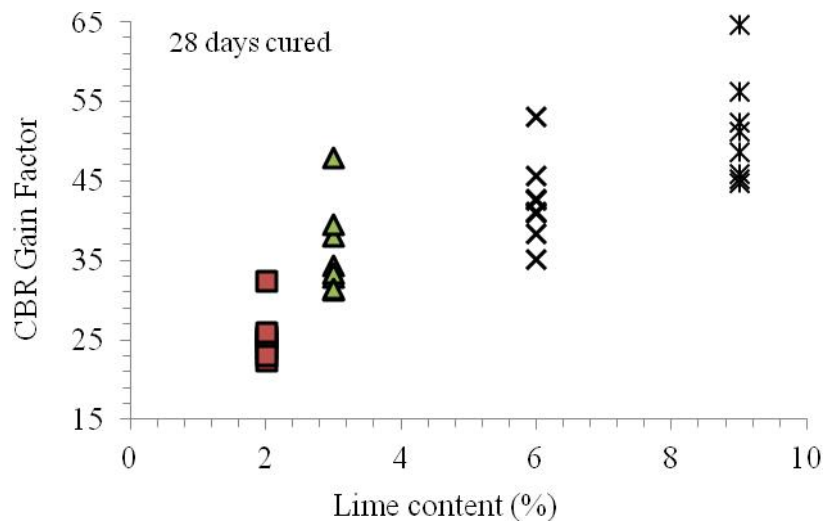


Figure 4.18: Influence of Lime in CBR Gain for all composites at 28 days curing

4.3.3 Unconfined compressive strength characteristics

The unconfined compression test is one of the widely used laboratory tests in pavement and soil stabilization applications. It is often used as an index to quantify the improvement of materials due to treatment. The results of UCS tests for both untreated and treated composites are reported and discussed here.

4.3.3.1 Unconfined compressive strength of untreated composites

The UCS values of all untreated fly ash and overburden compositions immediately after preparation could not be obtained due to weak development of bonds. The strength values were less than 0.04 MPa. Marginal increase in corresponding values was observed at different curing periods and hence those were also not reported here.

4.3.3.2 Unconfined compressive strength of treated composites

The compressive strength values changed dramatically with addition of lime and curing period. At 7 days curing all composites showed more than 0.7MPa strength values with maximum values at 3% lime exhibited by 15% fly ash and 85% overburden (Figure 4.19). The composite containing 30% fly ash and 70% overburden with 3, 6 and 9% lime resulted in higher strength (1.58 to 2.04 MPa) as compared to others in 14 days curing period. The sample with 30% fly ash and 70% overburden exhibited 3.14MPa with 9% lime at 56 days curing (Figure 4.22). It showed availability of additional lime has produced additional bonding between reactive elements. Each composition exhibited higher strength values with an increase in lime content and curing periods. These values are above the minimum suggested for subgrade quality (Das, 1994).

The composite containing 30% fly ash and 70% mine overburden with 9% lime exhibited maximum compressive strength as compared to that for other composites at 7, 14, 28 and 56 days of curing (Figures 4.19 – 4.22). Addition of lime improved the strength of fly ash – overburden composites. Typically the stress values at the base/subbase layers of mine haul road for 35-170T dumpers are 300 to 650 kPa respectively (Tannant and Kumar, 2000). The strength achieved in all the mixes in this study is above these values after a period of curing and hence useful for mine haul road construction.

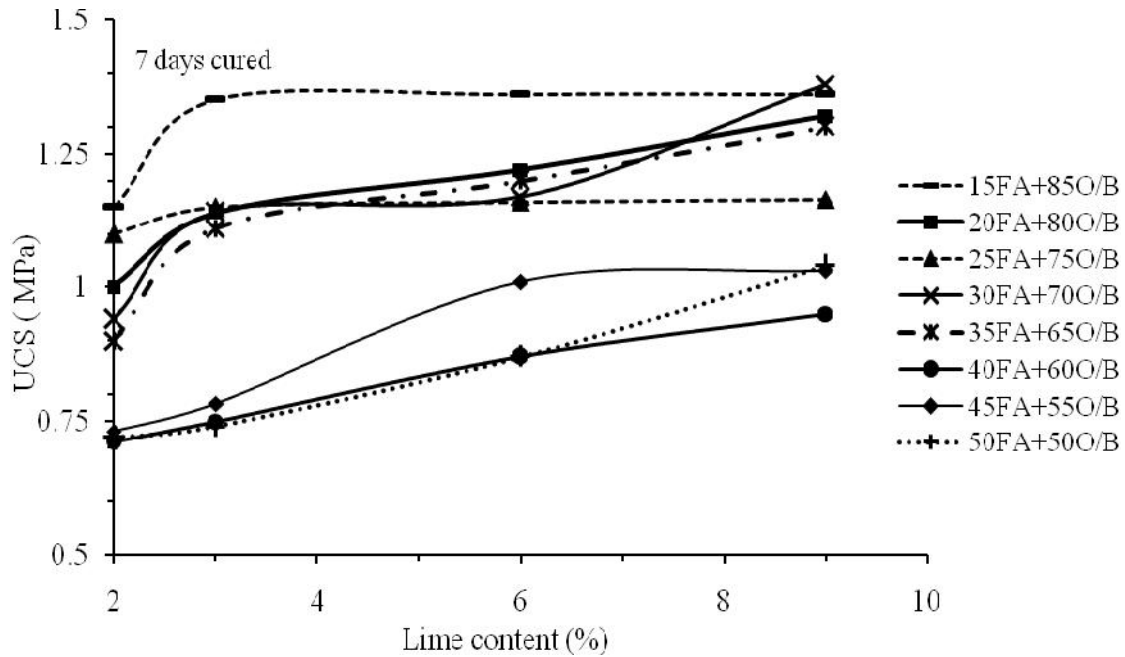


Figure 4.19: Effect of lime on compressive strength of composites at 7 days curing

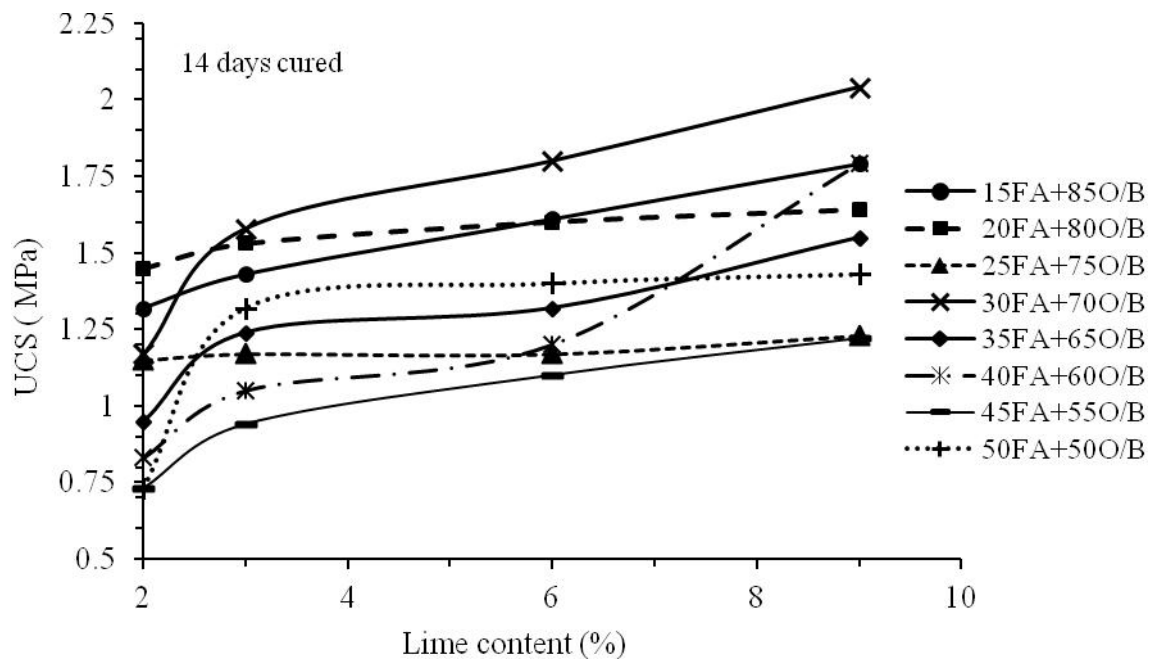


Figure 4.20: Effect of lime on compressive strength of composites at 14 days curing

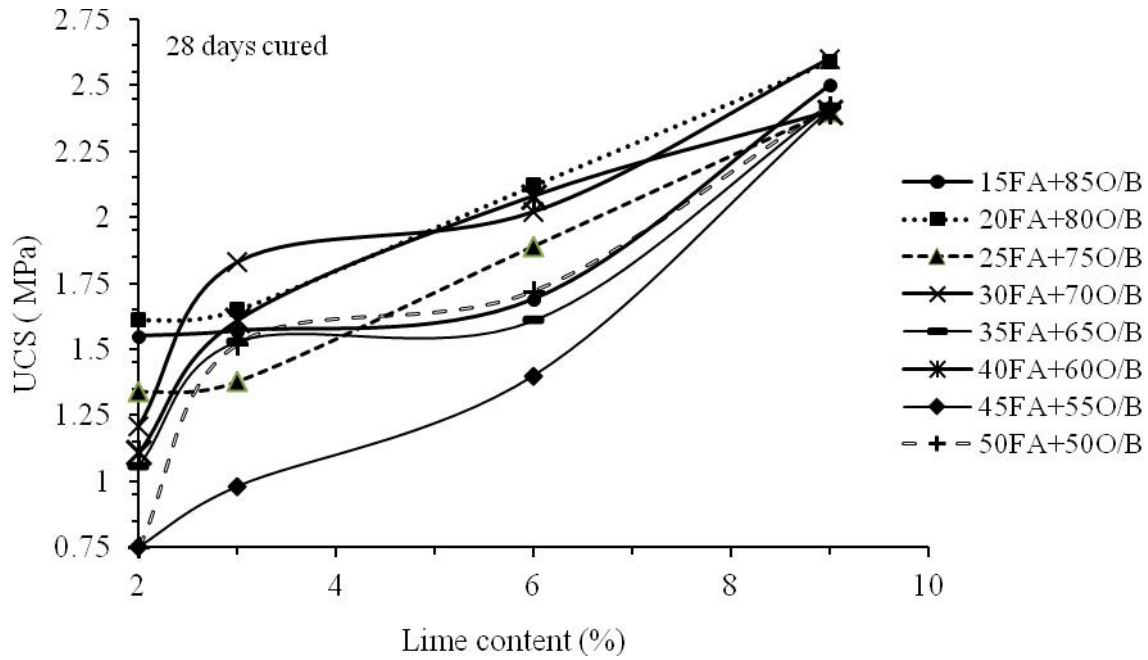


Figure 4.21: Effect of lime on compressive strength of composites at 28 days

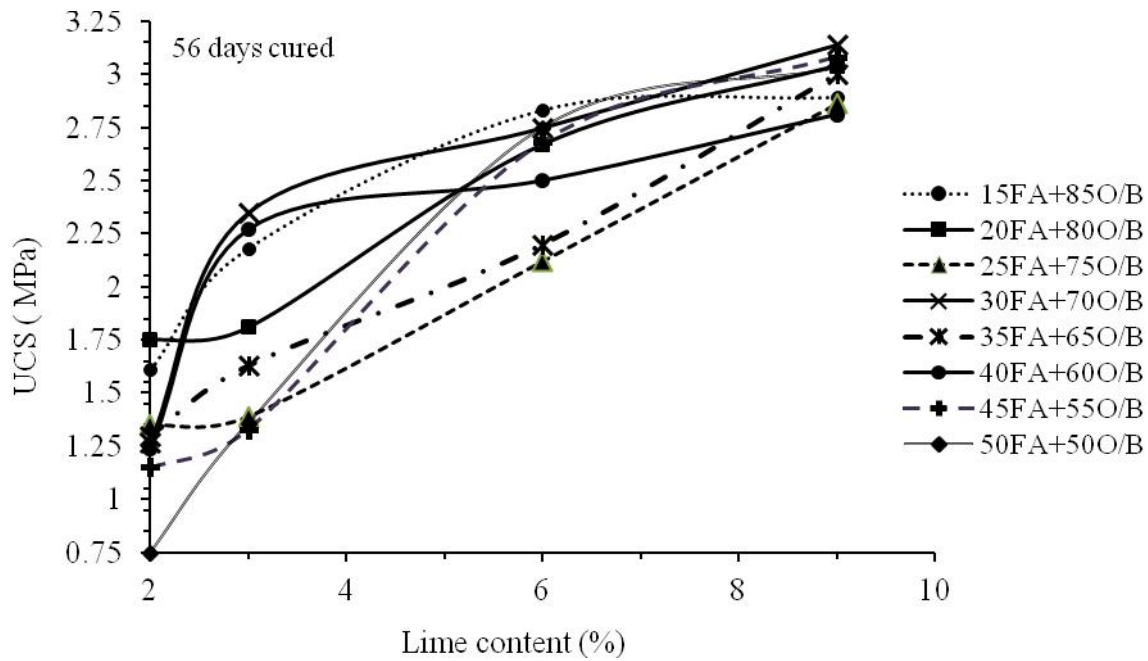


Figure 4.22: Effect of lime on compressive strength of composites at 56 days

All the samples in unconfined compressive loading conditions exhibited shear type failure (Figure 4.23). Except a few samples all samples failed by shear which reflect the influence of

sample and machine characteristics (Singh and Ghosh, 2006). Load bearing capacity and longitudinal displacement recording were made till failure i.e. peak strength of all the specimen. The axial strain values could not be recorded for post failure investigation as the weakened specimen got disintegrated soon after its peak strength. Typical axial stress- strain behaviour of a sample is shown in Figure 4.24. The Young's modulus values were computed for each specimen (Table 4.4).



Figure 4.23: Post failure profiles of a few UCS specimens

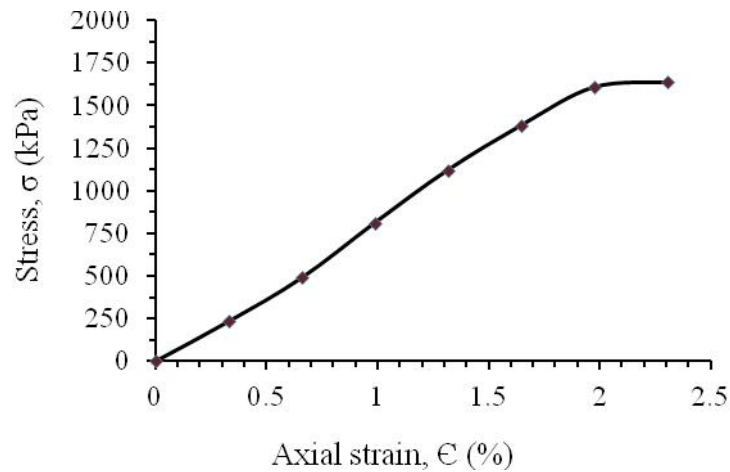


Figure 4.24: Stress- strain behaviour of a sample

Table 4.4: Young's modulus values of the fly ash composites for 7, 14, 28 and 56 days curing

Curing Period	7 days curing	14 days curing	28 days curing	56 days curing
Composites	Young's modulus (MPa)			
(15FA+85O/B)+2L	62	98	102.3	123
(15FA+85O/B)+3L	68	67.1	115.1	136
(15FA+85O/B)+6L	55	65.8	130.8	157
(15FA+85O/B)+9L	54.2	137.5	139	166
(20FA+80O/B)+2L	57	87.32	115.6	114
(20FA+80O/B)+3L	59	101.43	108.8	113.4
(20FA+80O/B)+6L	55.24	99.1	136	148
(20FA+80O/B)+9L	62	105	138.8	201
(25FA+75O/B)+2L	60	87.4	98	87.5
(25FA+75O/B)+3L	57.52	84	87.6	141
(25FA+75O/B)+6L	62	97	115.2	131
(25FA+75O/B)+9L	55	87.23	138.3	192
(30FA+70O/B)+2L	48.24	100	108.5	127
(30FA+70O/B)+3L	60	112	122	186
(30FA+70O/B)+6L	57.1	122.3	140.5	164

(30FA+70O/B)+9L	69.3	140	142	183
(35FA+65O/B)+2L	49	50.3	51.5	112
(35FA+65O/B)+3L	48.7	76.8	95.8	114
(35FA+65O/B)+6L	62	105	133.4	127
(35FA+65O/B)+9L	57.4	123	141	166
(40FA+60O/B)+2L	39.5	59.16	83.5	100
(40FA+60O/B)+3L	43.8	87.3	90.8	116
(40FA+60O/B)+6L	43.42	107	120	143
(40FA+60O/B)+9L	51.22	111	121.2	174
(45FA+55O/B)+2L	41.33	45.2	49.2	75
(45FA+55O/B)+3L	48.22	52	69.8	105
(45FA+55O/B)+6L	57	84	89	136
(45FA+55O/B)+9L	53	105	145	156
(50FA+50O/B)+2L	43.52	45.4	52.5	52.2
(50FA+50O/B)+3L	46.2	103	106.3	122.2
(50FA+50O/B)+6L	57.45	104	106	165
(50FA+50O/B)+9L	62	119	157	192

4.3.4 Brazilian Tensile strength characteristics

The tensile strength is a vital parameter to evaluate the suitability of the stabilized soil or fly ash as road base material. Tensile strength is an important property to predict the cracking behaviour of pavement, structures using stabilized soils (Baghdadi et al., 1995). In the present study split tensile test was conducted on specimen to characterize the tensile strength and the cracking behaviour of lime treated fly ash–overburden material as described in section 2.3. The tensile strength of untreated fly ash, untreated overburden as well as untreated fly ash–overburden composite materials was very low and hence not reported here. However the behavior of composites changed dramatically and values could be recorded as

lime was added. The treated fly ash–overburden composite materials at 7 and 14 days exhibited marginal values due to low strength and hence not reported here. All the specimens failed more or less at the middle through an induced force which is tensile in nature (Figure 4.25). The failure occurred within 60 to 100 seconds.

At 28 days curing all composites showed more than 50kPa strength values with maximum values at 9% lime with 30% fly ash and 70% overburden. The sample exhibited 291kPa at 28 days curing (Figure 4.26). Brazilian tensile strength of all the composites was between 73 to 357 kPa at 56 days of curing (Figure 4.27). The mine overburden mixed with 30% fly ash and 9% lime exhibited maximum tensile strength as compared to that of other composites at 28 and 56 days of curing respectively. The strength achieved in all the composites in this investigation is above these values after a period of curing and hence useful for mine haul road construction.

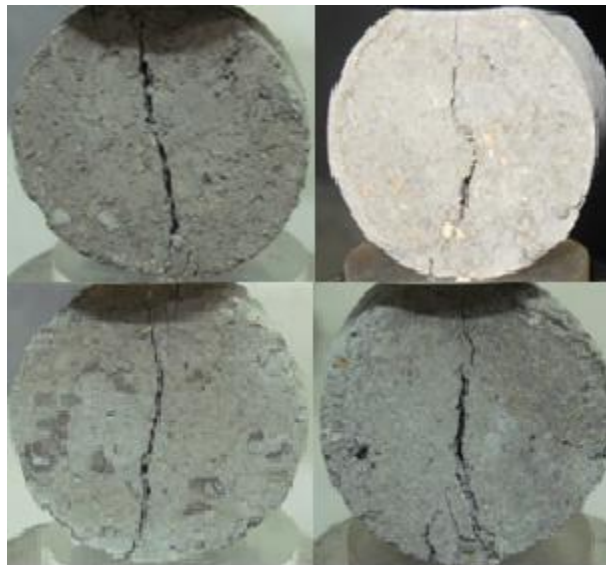


Figure 4.25: Post failure profiles of a few Brazilian tensile test specimens

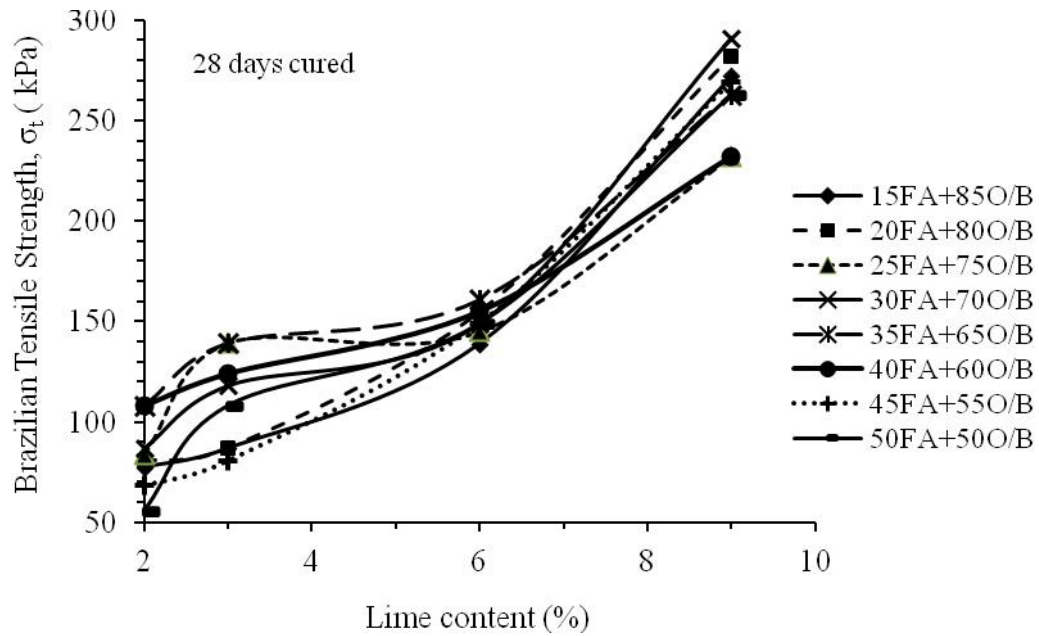


Figure 4.26: Effect of lime on tensile strength of composites at 28 days curing

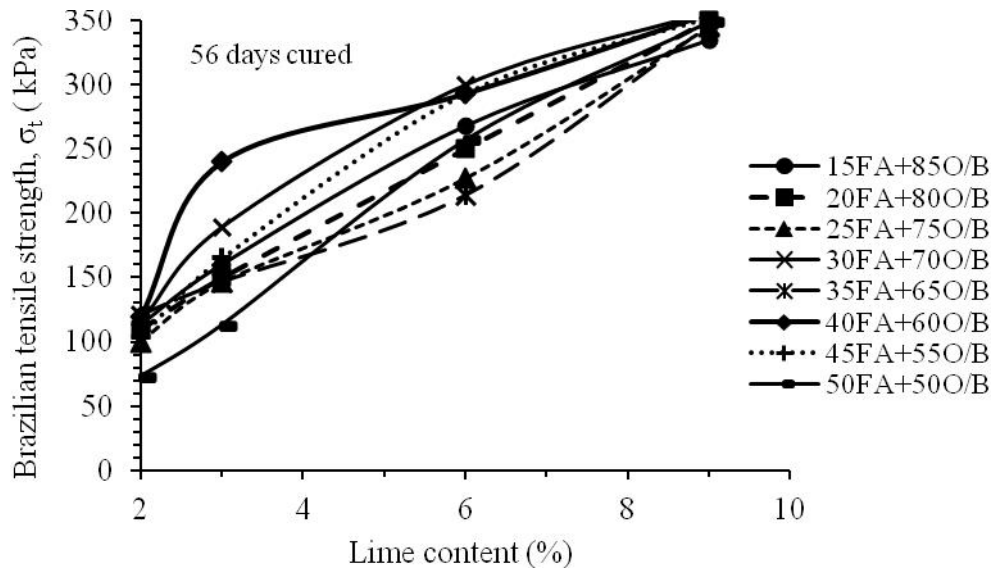


Figure 4.27: Effect of lime on tensile strength of composites at 56 days curing

The Brazilian tensile strength as a percentage of unconfined compressive strength against curing period is plotted (Figures 4.28 and 4.29). The average value of Brazilian tensile strength as a percentage of unconfined compressive strength was 8.4% at 28 days and 10% at 56 days. The percentage increased from 5% to 11% at 28 days curing and 6.3% to

13% in 56 days curing. The tensile strength was a function of the amount of cementitious compounds formed, which increased with increase in curing period. It compares favourably with that observed for the fly ash stabilized with 10% lime only (Ghosh and Subbarao, 2006). Consoli et al. (2001) observed that the average ratio of Brazilian tensile strength and unconfined compressive strength increased from 4% at 7 days to about 15% at 180 days for the mixes containing soil and 25% fly ash stabilized with 4%, 7% and 10% of lime. The current investigation confirms these observations.

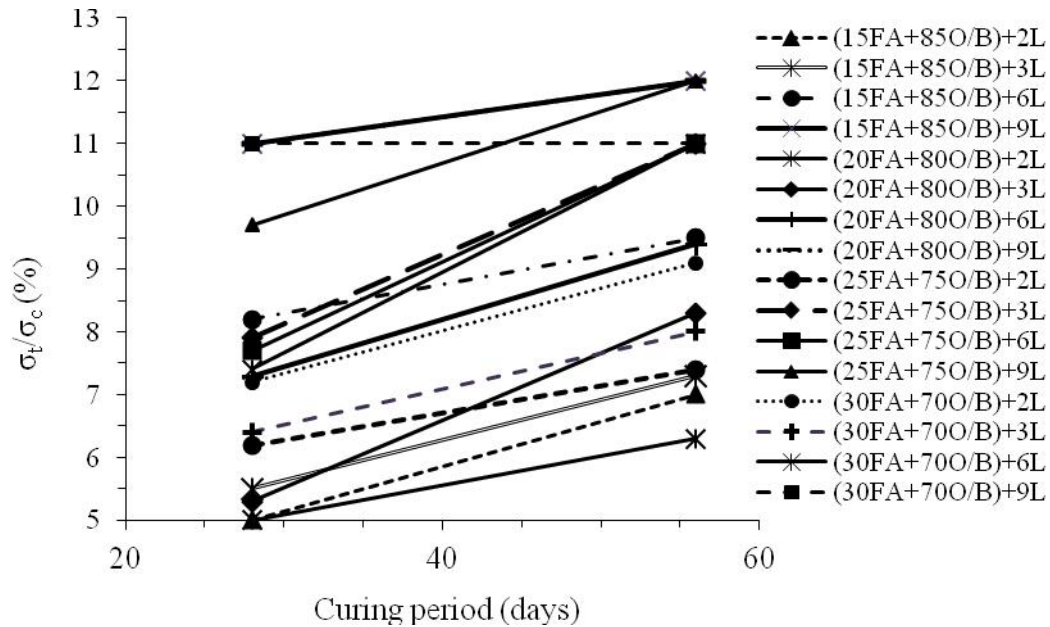


Figure 4.28: Effect of curing period on tensile strength as percentage of unconfined compressive strength of the composites containing 15, 20, 25 and 30% fly ash

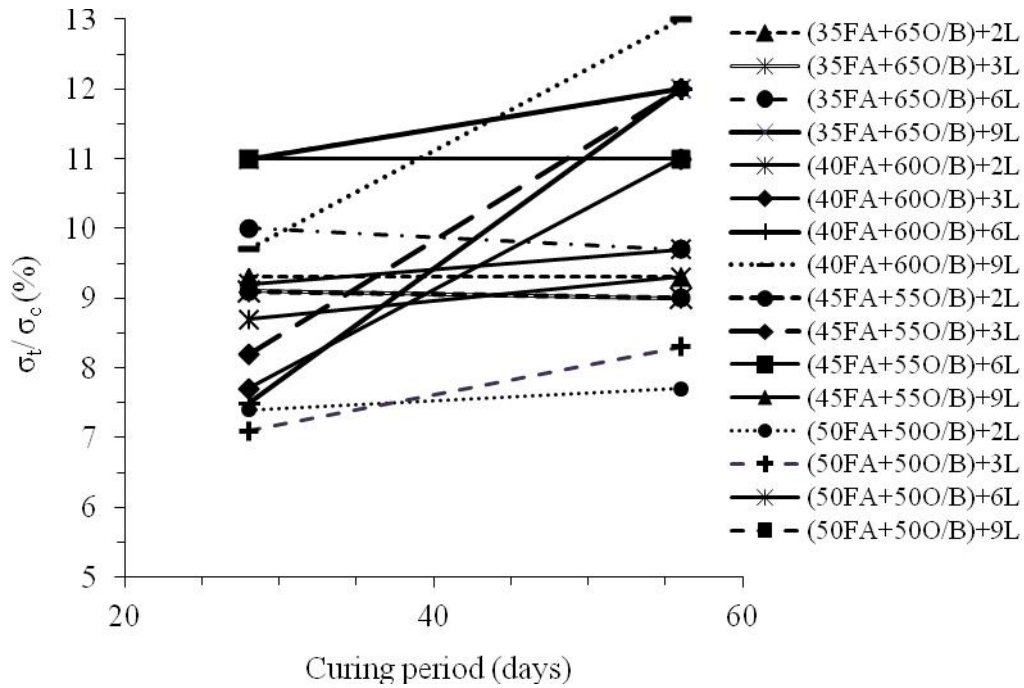


Figure 4.29: Effect of curing period on tensile strength as percentage of unconfined compressive strength of the composites containing 35, 40, 45 and 50% fly ash

4.3.5 Ultrasonic pulse velocity

The velocity of Ultrasonic P (pulse) wave is measured over a distance and it depends on the quality of transmission, cohesiveness of constituent materials, dampness, presence of weaknesses as crack, voids, etc. Its accuracy also depends on the homogeneity of the sample. The P wave tests conducted in all the samples confirm it. The P wave velocities of untreated fly ash, overburden and composites were not conducted as those did not exhibit any significant strength values.

The P wave values of treated samples are reported here and analyzed. The ultrasonic pulse velocities varied in the range of 797 m/s to 1699 m/s for varying curing periods. Maximum velocity values were obtained at 56 days curing, thus confirming the increased conductivity in the samples. The conductivity is a result of enhanced pozzolanic activities

due to enhanced reactivity of calcium, aluminium, silicon which is a time dependent behaviour. The increase in P wave velocity was steep between 2 to 3% lime content at 7 days, 14 days and 28 days curing period (Figures 4.30, 4.31 and 4.32). The rise is marginal at 56 days curing, though the values are much higher (Figure 4.33). The maximum P wave velocity values were obtained for composite with 30% fly ash+70% overburden and 9% lime which is similar to the results obtained for UCS, UTS and CBR tests. P wave velocities obtained at 7, 14, 28 and 56 days curing ranged from 797 to 1170 m/s, 1012 to 1350 m/s, 1057 to 1553 m/s and 1187 to 1699 m/s respectively. There was a continuous increase in the UPV with time for all the composites. Addition of lime improved the pulse velocity of fly ash composites. The P wave velocity signal plot of fly ash composite is shown in Figure 4.34.

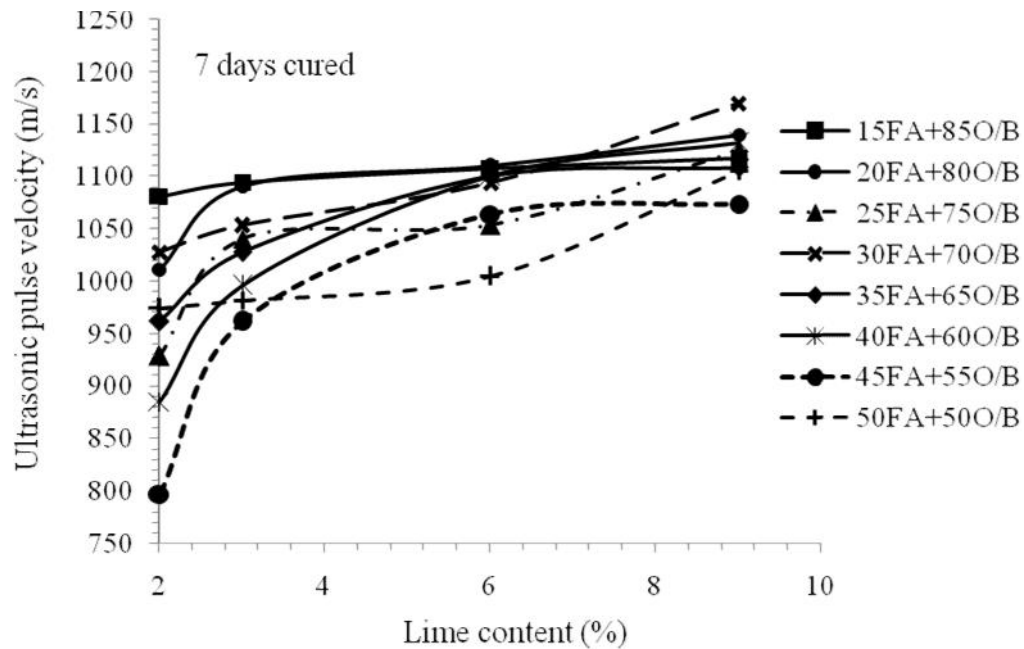


Figure 4.30: Effect of lime on pulse wave velocity of fly ash composites at 7 days curing

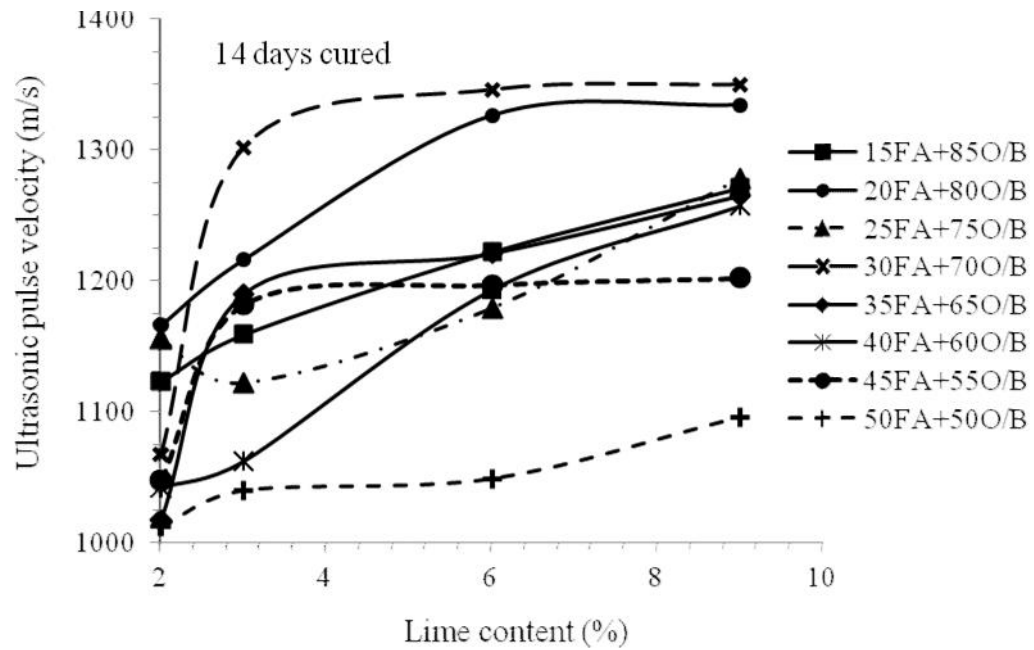


Figure 4.31: Effect of lime on pulse wave velocity of fly ash composites at 14 days curing

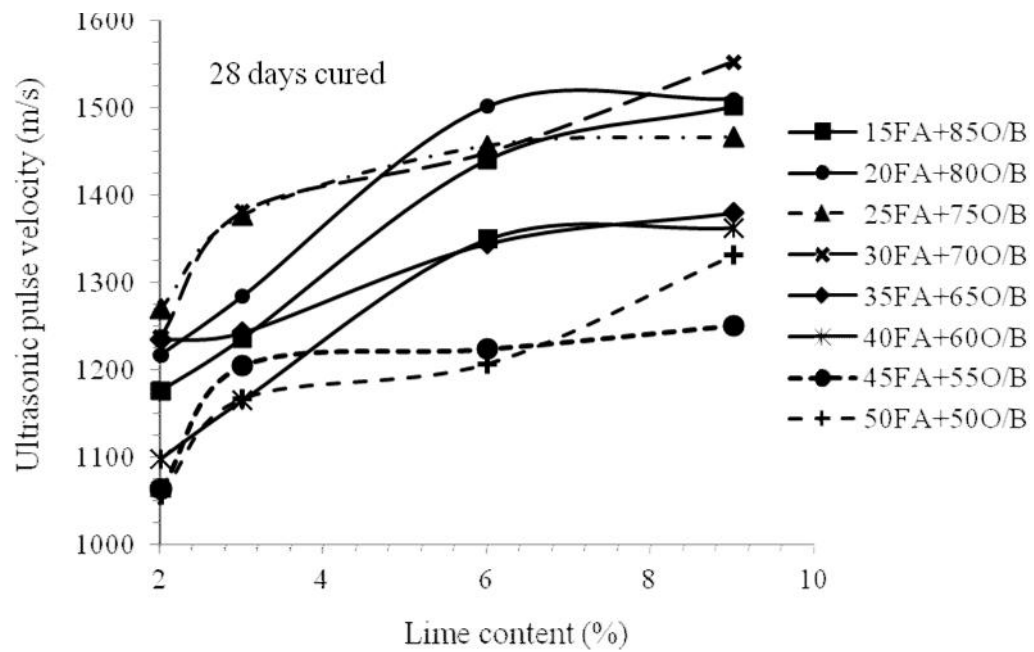


Figure 4.32: Effect of lime on pulse wave velocity of fly ash composites at 28 days curing

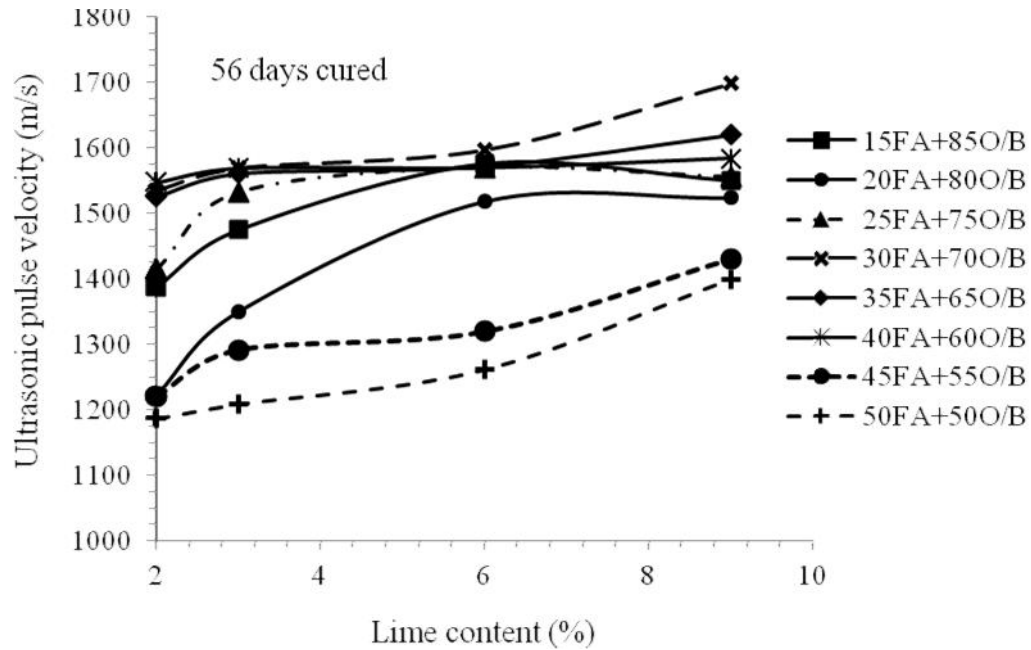


Figure 4.33: Effect of lime on pulse wave velocity of fly ash composites at 56 days curing

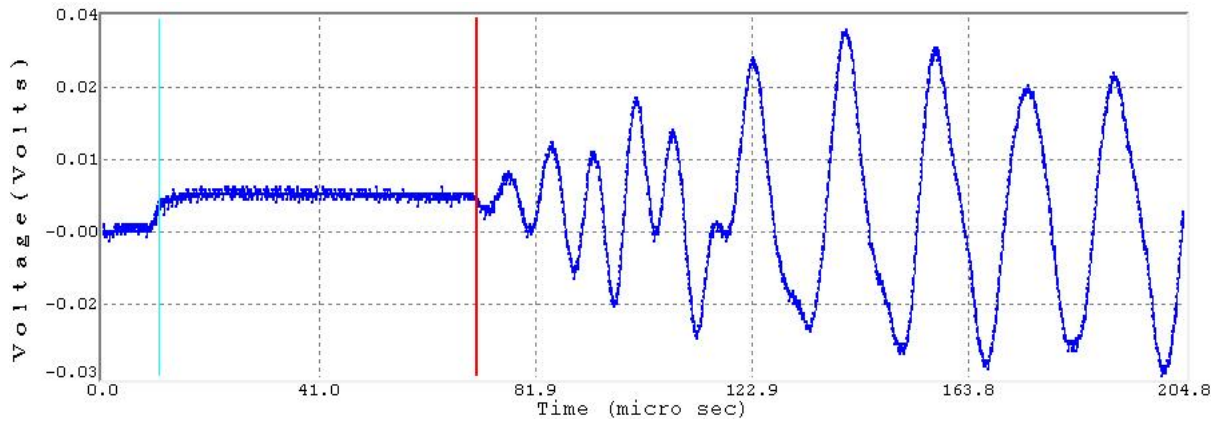


Figure 4.34: A typical P wave velocity signal plot of fly ash composite

The Poisson's ratio is a measure of the behaviour of material under loading. The ultrasonic tests produced the Poisson's ratio between 0.30 and 0.41 (Table 4.5) except a few composites with 0.24 to 0.29. The Poisson's ratio values of each composite did not change significantly either with higher lime content or longer curing periods which are the typical characteristics of any material.

Young's modulus (E) values were also obtained from nondestructive testing. Its values ranged between 776 to 3107 MPa (Table 4.6). These values are very high compared to that obtained from static tests. Nondestructive tests do not cause either generation or extension of flaws unlike static tests. The Young's modulus (E) values increased with lime content as well as curing periods confirming to enhance pozzolanic activities resulting in higher stiffness of the composites. The velocity of propagation increases with increased stiffness of the material (Yesiller et al., 2000).

Tables 4.5: Poisson's ratios of the composites for 7, 14, 28 and 56 days

Sample		Curing period (days)	Lime content (% weight)			
Fly ash (% weight)	Overburden (% weight)		2	3	6	9
			Poisson's ratios			
15	85	7	0.35	0.33	0.34	0.33
		14	0.35	0.32	0.35	0.35
		28	0.34	0.34	0.36	0.35
		56	0.31	0.39	0.35	0.29
20	80	7	0.33	0.33	0.29	0.27
		14	0.37	0.37	0.36	0.36
		28	0.37	0.35	0.37	0.39
		56	0.37	0.38	0.38	0.33
25	75	7	0.35	0.34	0.24	0.3
		14	0.36	0.29	0.41	0.38
		28	0.37	0.36	0.36	0.35
		56	0.39	0.35	0.38	0.35
30	70	7	0.33	0.36	0.37	0.28
		14	0.31	0.36	0.36	0.26
		28	0.34	0.37	0.37	0.35
		56	0.39	0.3	0.35	0.35
35	65	7	0.35	0.34	0.32	0.34

40	60	14	0.37	0.3	0.37	0.33
		28	0.34	0.29	0.36	0.32
		56	0.31	0.4	0.34	0.36
		7	0.3	0.33	0.32	0.32
		14	0.3	0.32	0.35	0.35
		28	0.29	0.32	0.34	0.36
		56	0.4	0.36	0.38	0.34
		7	0.31	0.37	0.37	0.37
		14	0.35	0.38	0.36	0.34
		28	0.31	0.35	0.34	0.33
		56	0.32	0.31	0.3	0.3
		7	0.36	0.36	0.35	0.37
45	55	14	0.31	0.32	0.39	0.36
		28	0.33	0.33	0.38	0.33
		56	0.31	0.27	0.31	0.34

Tables 4.6: Young's (dynamic) modulus values of the composites at 7, 14, 28 and 56 days

Sample		Curing period (days)	Lime content (% weight)			
Fly ash (% weight)	Overburden (% weight)		2	3	6	9
			Young's moduli (MPa)			
15	85	7	1501	1644	1679	1740
		14	1528	1855	1794	1893
		28	1755	1866	2291	2536
		56	1904	2358	2992	3190
20	80	7	1353	1512	1786	1893
		14	1240	1435	1908	1931
		28	1605	1909	2111	2298
		56	1617	1810	2354	2727
25	75	7	1212	1328	1691	1676
		14	1098	1793	1501	1574

		28	1740	2081	2306	2395
		56	1784	2354	2455	2927
		7	1066	1230	1215	1732
30	70	14	1539	1857	2085	2633
		28	1803	1879	2102	2822
		56	1921	2645	2974	3107
		7	1084	1287	1532	1440
35	65	14	1108	1755	1427	1686
		28	1759	2075	1895	2200
		56	2713	2146	2454	2573
		7	1092	1173	1413	1512
40	60	14	1426	1438	1514	1766
		28	1528	1634	1876	1999
		56	2036	2331	2733	2829
		7	776.6	915.1	1111	1061
45	55	14	1187	1300	1436	1693
		28	1296	1439	1532	1731
		56	1628	1987	2116	2781
		7	954.8	974.3	1037	1114
50	50	14	1257	1302	1320	1354
		28	1532	1237	1507	1985
		56	1550	1801	1910	2269

4.3.6 Microscopy analysis

It is observed that the glassy portions of the micro-particles of the composite are potentially attacked by lime. The micrographs show the development of hardened paste at different stages of pozzolanic activity. Particles exhibit evidence of corrosion and etching on surface. There was evidence of formation of ettringite rods (Appendix). It confirms to the observation that during early stages, the reactive particles in the fly ash-overburden-lime

composite served as nucleation sites for hydration and pozzolanic reaction products (C-S-H, CH and Ettringite) (Lav and Lav, 2000).

The cementitious compounds formed around the fly ash and overburden particles are shown in Figure 4.35(a), (b) and (c). The composite ((30%FA + 70%O/B)+9%L) at 28 days exhibited dense gel - like mass covering all reactive particles completely and filling up the inter-particle spaces with blurred grain boundaries (Figure 4.35(c)). It appears like a massive unit compared to the other composites. The dense gel acted as a binding substance and appears to be evenly distributed to form compact structure, thus creating more contact and higher cohesion that in turn reflects in greater strength values. It was observed from static laboratory tests that all samples exhibited maximum strength values at 28 days. So its SEM analysis was carried out to understand the microstructural aspects. Cetin et al. (2010) reported that the CBR of lime kiln dust amended soil-fly ash mixtures increase with increasing curing time due to the formation of calcium silicate hydrate (CSH) and calcium aluminate silicate hydrate gels (CASH) around soil and fly ash particles.

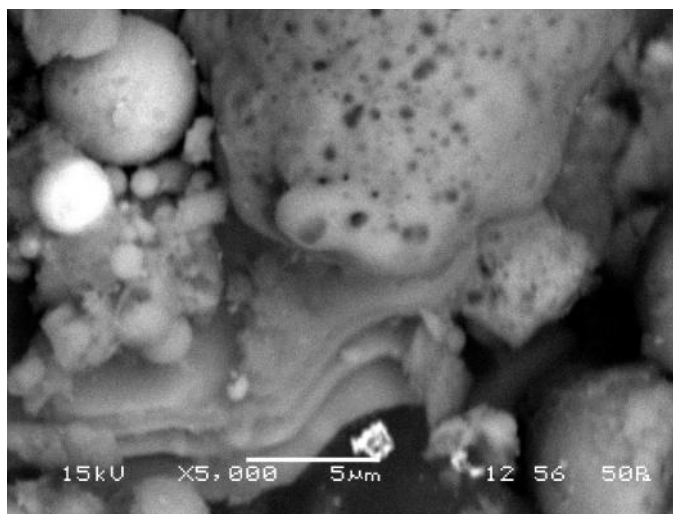


Figure 4.35 (a): SEM photograph of (15FA+85O/B) +2L

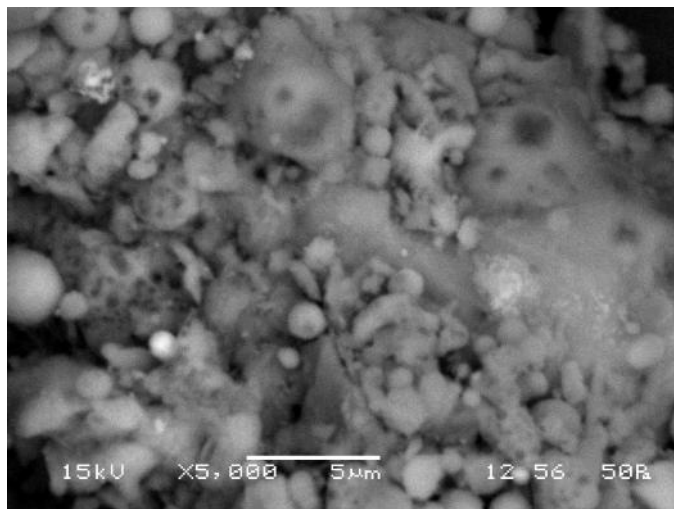


Figure 4.35 (b): SEM photograph of (30FA+70O/B) +6L

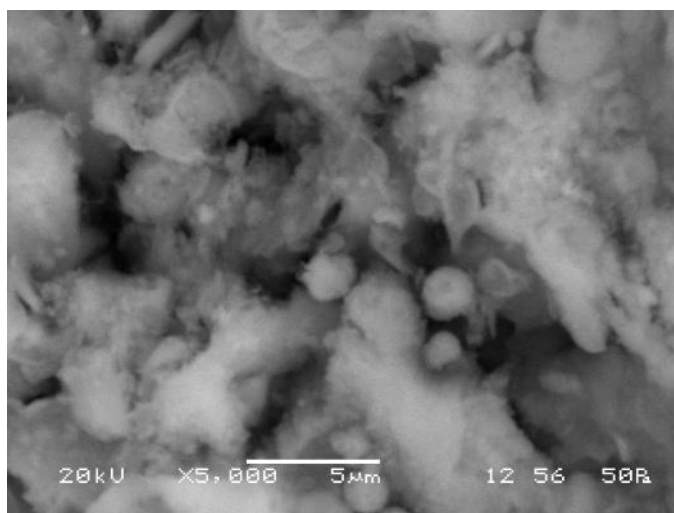


Figure 4.35 (c): SEM photograph of (30FA+70O/B) +9L

4.3.7 Energy dispersive X-ray analysis

EDX is an analytical technique for elemental analysis or chemical characterization. The EDX analyses of all the mixes were carried out to observe the effect of hydration at 28 days of curing. There were variations in elemental composition in various mixes (Table 4.7). In all mixes calcium content increased due to increase in lime content. Alumina content also increased with increase in fly ash content in the mixes. But, increase in lime content reduces the alumina percentage in all mixes. The silica content decreased with increase in fly ash

content at 3 and 6% of lime in the mixes. But, the silica content was more in 20% of fly ash with 2 and 9% of lime. These results confirm to similar observation reported elsewhere (Cetin et al., 2010). All the mixes contain very small or negligible percentages of Na, Mg, P, S, Mn, Cu, Ba and Mo elements. The chemical composition of all the mixes indicates that they contain high percentages of silica (SiO_2), alumina, iron and calcium oxides as well as small percentages of other elements. Among all these oxides, calcium oxide (CaO) is very reactive. In the presence of aqueous solution, calcium oxide undergoes hydration. The formation of calcium silicate hydrate (CSH) gel and calcium aluminate hydrate (CAH) gel leads to increase in calcium content. The effectiveness of the lime treatment depends on the quality and quantity of lime as well as the chemical composition of the soil/fly ash. The strength developed is obviously influenced by the quantity of cementitious gel produced and consequently by the amount of lime consumed (Abdelmadjid and Muzahim, 2008).

CaO/SiO_2 is a good indicator of pozzolanic reactions which yields higher strength values (Janz and Johansson, 2002). The CaO/SiO_2 and $\text{CaO}/(\text{SiO}_2 + \text{Al}_2\text{O}_3)$ ratios ranged from 0.03 to 1.06 and 0.02 to 0.59 respectively in the composites. The composite containing 30% fly ash and 70% overburden treated with 9% lime gave CaO/SiO_2 and $\text{CaO}/(\text{SiO}_2 + \text{Al}_2\text{O}_3)$ ratios of 1.06 and 0.59 which exhibited maximum strength value. The CaO content is more (i.e 27%) in the composite containing 30% fly ash and 70% overburden treated with 9% lime as compared to other composites. The strength values increased with increase in CaO content, CaO/SiO_2 and $\text{CaO}/(\text{SiO}_2 + \text{Al}_2\text{O}_3)$ ratios reported elsewhere (Cetin et al., 2010).

Table 4.7: Chemical compositions of the composites, cured for 28 days

Elements in oxide form	(15FA+ 85O/B)	(15FA+ 85O/B)	(15FA+ 85O/B)	(15FA+ 85O/B)	(20FA+ 80O/B)	(20FA+ 80O/B)	(20FA+ 80O/B)	(20FA+ 80O/B)	(25FA+ 75O/B)	(25FA+ 75O/B)	(25FA+ 75O/B)	(25FA+ 75O/B)	(30FA+ 70O/B)	(30FA+ 70O/B)	(30FA+ 70O/B)	(30FA+ 70O/B)
	+2L	+3L	+6L	+9L	+2L	+3L	+6L	+9L	+2L	+3L	+6L	+9L	+2L	+3L	+6L	+9L
Na	1.71	0	0.28	0.97	0.11	0	0.7	0.01	0.05	0	0.04	0	0	0.4	0.5	0.15
Mg	1.66	0.09	0.43	0.79	0.96	1.23	0.93	0.46	0.92	0	1.41	0	1.01	1.3	1.68	0.59
Al	26.3	21.5	20	13.2	26.7	24	22.5	18.3	30	27.7	19	23.4	30.2	25	22.8	20.4
Si	38.8	50.3	37.8	36.5	43	42.7	36.7	38.2	41.3	34	32.7	22.8	42.6	41	34.2	25.5
P	0.35	0	0.03	0	0.5	0.33	0	0	0.18	0.33	0	0	0	0.8	0.17	0.34
S	0.08	0.55	0.33	0	0.48	0	1.08	0.95	0	0.71	0.06	0	0.41	1.2	0.26	0.5
K	0.07	2.97	3.82	1.26	2.24	1.34	2.28	0.65	2.24	2.34	1.25	1.82	2.05	2.3	1.99	1.21
Ca	3.29	4.36	6.59	16.2	3.44	6.28	14.4	19.7	3.46	13	19.5	22.6	4.31	8.5	15.6	27
Ti	1.98	0	1.27	1.74	3.05	1.08	0.89	0.2	3.2	7.4	2.7	3.74	2.22	0.5	0.51	0.97
Mn	0	0	0.5	0.29	0	0	0	0.12	0	0.35	0	1.76	0	0	0.91	0.48
Fe	10.1	5.03	10.7	1.85	4.5	6.25	4.2	3.9	4.57	2.03	7.68	8.1	8.39	6.9	2.15	4.93
Cu	2.06	0	2.79	6.49	1.51	0	1.58	1.08	0.67	0.47	1.37	0	0	0	3.65	1.61
Zn	1.96	2.23	1.05	1.11	1.32	2.07	1.75	0.93	0.63	1.87	0.58	2.75	0.88	2.6	3.76	3.86
Ba	0.75	1.67	0	1.9	2.02	2.64	0.35	1.8	3.23	0	2.19	0	0	1.4	2.14	2.28
Mo	0	0	0.73	2.98	0	1.63	0	0	0	0	0.04	0	0	0	0	0
LOI	10.9	11.3	13.6	14.8	9.9	10.4	12.7	13.9	9.6	9.69	11.3	13	7.89	7.8	9.6	10.2
CaO/SiO ₂	0.08	0.09	0.17	0.44	0.08	0.15	0.39	0.52	0.08	0.38	0.6	0.99	0.1	0.21	0.46	1.06
CaO/(SiO ₂ + Al ₂ O ₃)	0.05	0.06	0.11	0.33	0.05	0.09	0.24	0.35	0.05	0.21	0.49	0.38	0.06	0.13	0.27	0.59

4.3.8 X-ray diffraction analysis

The mineralogical analyses of the composites are very important to determine the changes in the mineralogical phases due to pozzolanic reactions. The formation of reaction products such as calcium silicate hydrate (CSH), calcium aluminate hydrate (CAH) and calcium aluminate silicate hydrates (CASH) confirmed from X-ray diffraction analysis (Figures 4.36). These new cementitious compounds induce aggregation effect in fly ash and overburden particles, bind the particles together to form crumbs of fly ash-overburden clusters and result in the overall improved behaviour of the composites. The X-ray diffraction analysis of the selected composite ((30%FA+70%O/B) +9%L) show the influence of lime content on the hydration products (CAH, CSH, CASH). The intensity increased with increase in lime content, maximum being at 9% lime. The peaks for the composite vary with the lime contents, minimum at 2% and maximum observed at 9% (Figure 4.36). Quartz, the primary mineral present in fly ash is indicated by sharp peaks.

Cementing compounds such as CSH, CAH and CASH were identified in 3% cement stabilized fly ash only and fly ash – black cotton soil mixes after 28 days curing by XRD analysis (Krishna, 2001). The strength development is also dependent on the amount of hydration products as well as their interlocking mechanisms (Lav and Lav, 2000). X-ray diffraction patterns of all composites are given in Appendix.

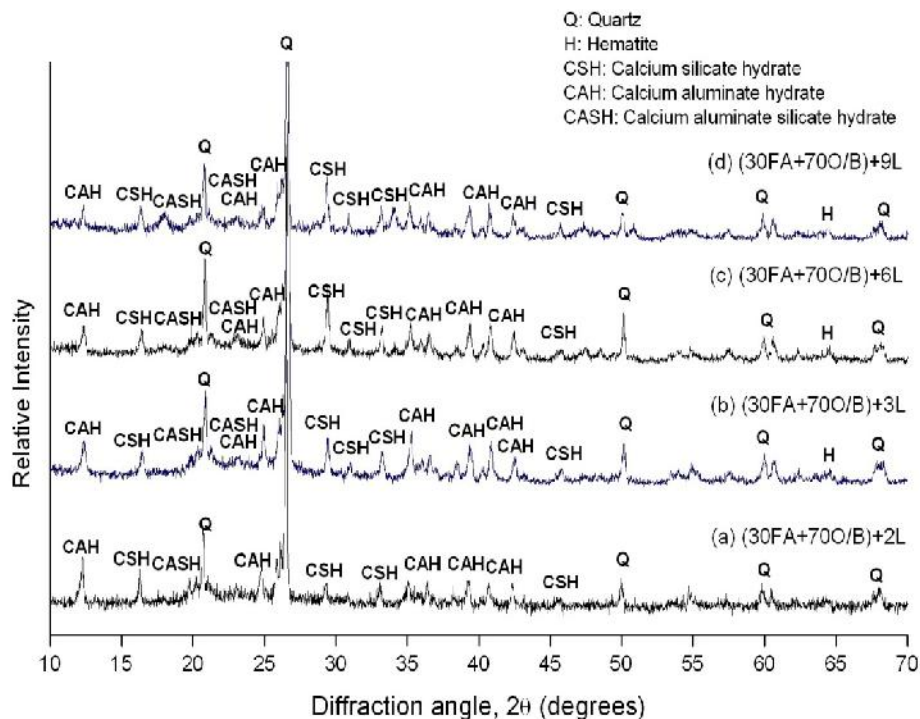


Figure 4.36: XRD patterns of (30FA+70O/B) stabilised with 2, 3, 6 and 9% lime at 28 days

4.3.9 Leachate characteristics

The concentration of metals in leachate of all the treated samples were analyzed for Ni, Cr, Pb, Cu, Zn, As, Hg, Cd and Se on 7th day of flow. The presence of metals As and Hg were below the detection level (Table 4.8). Threshold value for maximum contaminant level is considered as 100 times the allowable limit reported elsewhere (IS 10500; Gidley and Sack, 1984; Ghosh and Subbarao, 1998). It is observed that the leachate effluents contain Ni, Cr, Pb, Cu and Zn between 0.002 to 1.1 ppm. Concentrations of Ni and Pb were above the allowable limits of drinking water quality for some of the composites. Concentration of Cr was above the allowable limits for the composites. The concentrations of Cu and Zn in the leachate were below the allowable limit for drinking water quality. It is observed from the leachate effluents that concentration of Cadmium is in between 0.001 to 0.009 ppm. The concentration of Selenium was below the detection level. However, the concentrations of all

the metals were below the threshold limits. These results compare favourably with those obtained elsewhere (Ghosh and Subbarao, 1998) for high (4 % to 10 %) lime and gypsum (0.5 % to 1 %) to content with only fly ash.

Table 4.8: Leachate concentration (ppm) at 7 days curing period

Mix	Leachate concentration (ppm)				
	Ni	Cr	Pb	Cu	Zn
Allowable limits	0.02	0.05	0.05	1	5
Threshold limits	2	5	5	100	500
(15FA+85O/B)+2L	0.025	0.312	0.116	0.05	0.108
(15FA+85O/B)+3L	0.028	0.415	0.208	0.078	0.245
(15FA+85O/B)+6L	0.204	0.64	0.681	0.245	0.160
(15FA+85O/B)+9L	0.21	0.642	0.684	0.248	0.191
(20FA+80O/B)+2L	0.004	0.081	0.002	0.033	0.08
(20FA+80O/B)+3L	0.006	0.1	ND	0.068	0.162
(20FA+80O/B)+6L	0.011	0.72	0.704	0.156	0.355
(20FA+80O/B)+9L	0.015	0.728	0.706	0.159	0.36
(25FA+75O/B)+2L	0.01	0.61	0.006	0.023	0.155
(25FA+75O/B)+3L	0.231	0.656	ND	0.058	0.237
(25FA+75O/B)+6L	0.116	0.735	0.385	0.214	0.535
(25FA+75O/B)+9L	0.121	0.731	0.388	0.218	0.539
(30FA+70O/B)+2L	0.102	0.501	0.064	0.129	0.26
(30FA+70O/B)+3L	0.107	0.542	0.075	0.278	0.490
(30FA+70O/B)+6L	0.137	0.529	0.194	0.085	0.053
(30FA+70O/B)+9L	0.14	0.545	0.211	0.112	0.1
(35FA+65O/B)+2L	0.05	0.009	0.071	0.056	0.351
(35FA+65O/B)+3L	0.071	0.125	0.095	0.134	0.538
(35FA+65O/B)+6L	0.014	0.416	0.3	0.046	0.109
(35FA+65O/B)+9L	0.035	0.424	0.315	0.1	0.46
(40FA+60O/B)+2L	0.024	0.445	0.072	0.083	0.45

(40FA+60O/B)+3L	0.078	0.491	0.077	0.189	0.504
(40FA+60O/B)+6L	0.164	0.619	0.147	0.097	1.031
(40FA+60O/B)+9L	0.142	0.625	0.154	0.182	1.1
(45FA+55O/B)+2L	0.13	0.634	0.24	0.053	0.4
(45FA+55O/B)+3L	0.152	0.669	0.705	0.065	0.435
(45FA+55O/B)+6L	0.180	0.823	0.693	0.122	0.578
(45FA+55O/B)+9L	0.184	0.825	0.711	0.13	0.583
(50FA+50O/B)+2L	0.147	0.803	0.15	0.048	0.65
(50FA+50O/B)+3L	0.258	0.845	0.345	0.066	0.842
(50FA+50O/B)+6L	0.346	0.855	0.562	0.071	0.640
(50FA+50O/B)+9L	0.348	0.858	0.567	0.081	0.8

ND: Not detected

4.4 Development of empirical models

A part of the objectives is to develop model equations for the investigation with the parameters like unconfined compressive strength, tensile strength, CBR, CaO/SiO_2 , $\text{CaO}/(\text{SiO}_2 + \text{Al}_2\text{O}_3)$ and P-wave velocity. Those are reported for the best fit correlations as below.

4.4.1 Relation between Tensile Strength, CBR and UCS

The investigation involved 1760 specimens for various parametric determinations. Each parameter has been discussed separately earlier. A few empirical models have been developed to establish mutual relationships between UCS and Brazilian tensile strength and CBR and UCS.

The variation of tensile strength and California bearing ratio with unconfined compressive strength are shown in Figures 4.37 and 4.38. The data are analyzed using linear regression model by the method of least squares. There exists relation between compressive

strength of fly ash/lime and fly ash/lime and gypsum mixes with chemical composition, loss on ignition, CBR and tensile strength using power model (Das and Yudhbir, 2006; Ghosh and Subbarao, 2006). It is observed that linear regression model suits for the fly ash and overburden mixes stabilized with lime. It is observed from the relationship between tensile strength and compressive strength that R^2 value is more at 56 days than that at 28 days curing (Figure 4.37(b)). It confirms that the relationship between tensile strength and compressive strength become stronger with increasing curing period. Similar results were also observed between CBR and unconfined compressive strength (Figure 4.38(b)). The results of linear regression model between California bearing ratio values, unconfined compressive strength and tensile strength at different curing period are reported (Table 4.9).

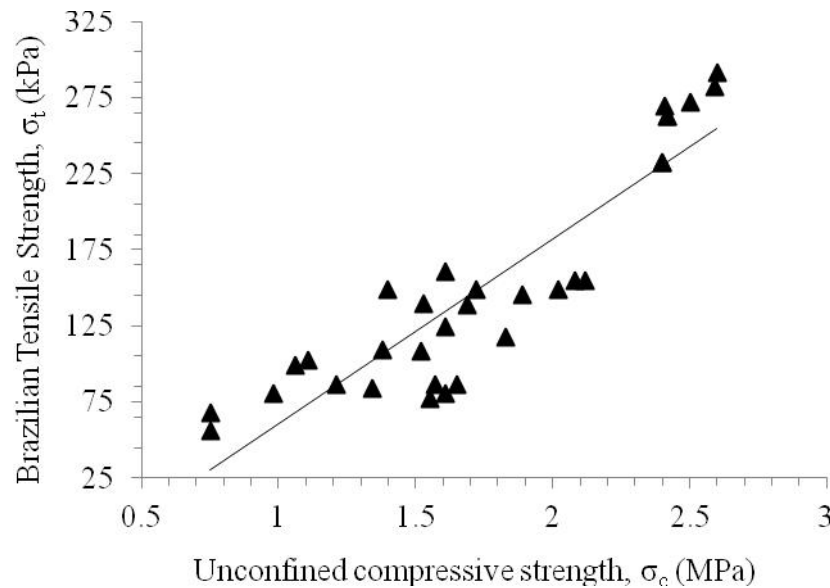


Figure 4.37 (a): Relationship between Brazilian tensile strength and unconfined compressive strength for all samples at 28 days of curing

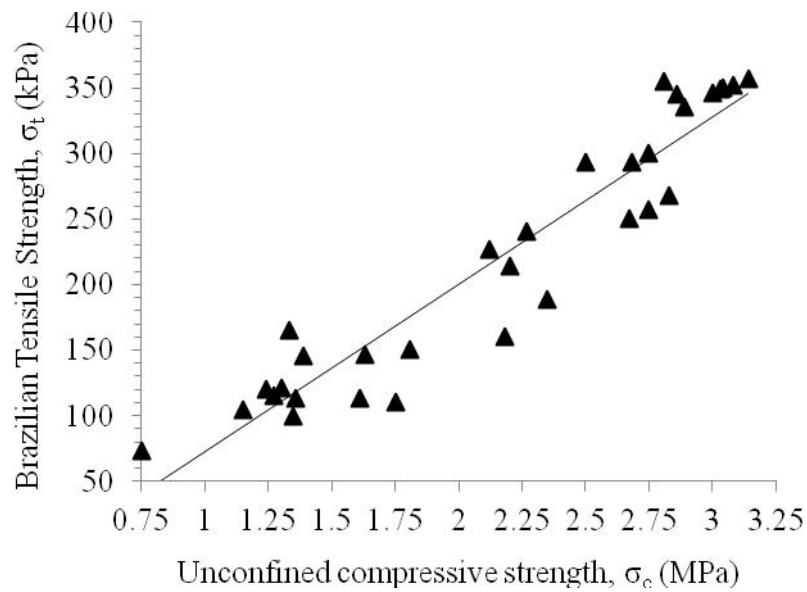


Figure 4.37 (b): Relationship between Brazilian tensile strength and unconfined compressive strength for all samples at 56 days of curing

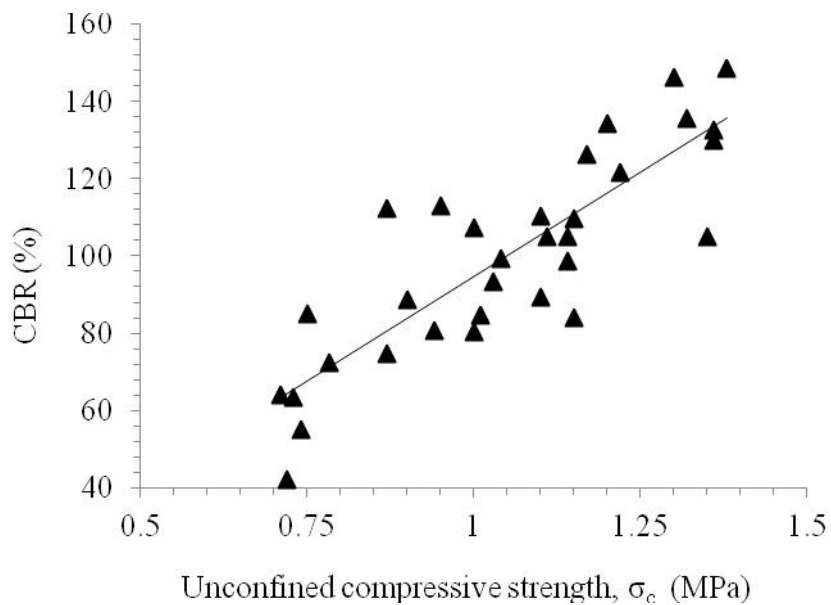


Figure 4.38 (a): Relationship between bearing ratio and unconfined compressive strength for all samples at 7 days of curing

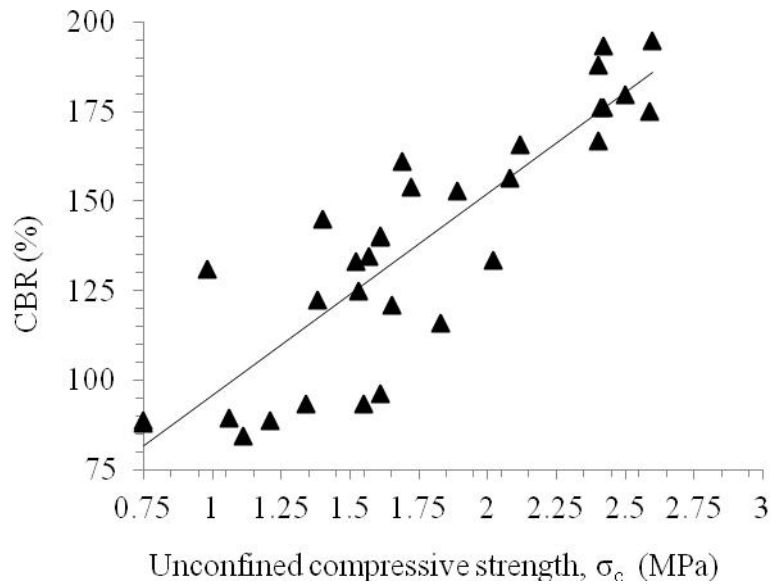


Figure 4.38 (b): Relationship between bearing ratio and unconfined compressive strength for all samples at 28 days of curing

Table 4.9: Best fit regression models between California bearing ratio values, unconfined compressive strength and tensile strength at different curing period

Dependent	Best fit Equation	R ² value	R value	No. of Observation	Curing period (days)
Brazilian tensile strength, σ_t	$\sigma_t = 121.5 \sigma_c - 61.211$	0.8122	0.9012	32	28
Brazilian tensile strength, σ_t	$\sigma_t = 127.96 \sigma_c - 55.752$	0.9022	0.9498	32	56
California bearing ratio (CBR)	$\text{CBR} = 108.38 \sigma_c - 13.818$	0.7202	0.8486	32	7
California bearing ratio (CBR)	$\text{CBR} = 56.369 \sigma_c + 39.447$	0.7603	0.8719	32	28

4.4.2 Effect of chemical composition on CBR, UCS, tensile strength and Ultrasonic velocity results

In order to evaluate the effect of chemical composition of the mixtures on observed CBR, compressive strength, tensile strength and ultrasonic velocity values, the best suit regression model at 28 days curing were plotted against CaO content, CaO/SiO₂ and CaO/(SiO₂ + Al₂O₃) ratios of the mixes (Figure 4.39) and results were reported in Table 4.10.

The best fit curves to the data produced high and modest correlation coefficients (R) for CBR, UCS, tensile strength and ultrasonic velocity values. It confirms from the linear regression model that the CaO content, CaO/SiO₂ and CaO/(SiO₂ + Al₂O₃) ratios exhibited good correlation with CBR, UCS, tensile strength and ultrasonic velocity values. Cetin et al. (2010) observed that the CBR value increased with increasing CaO content as well as with CaO/SiO₂ and CaO/(SiO₂ + Al₂O₃) ratios.

Table 4.10: Best fit regression models at 28 days curing period

Dependent	Best fit Equation	R ² value	R value	No. of Obs.
CBR	CBR = 3.6743x + 94.234	0.6941	0.8331	16
CBR	CBR = 84.359y + 106.64	0.5828	0.7634	16
CBR	CBR = 162.43z + 102.1	0.6516	0.8072	16
UCS	UCS = 0.049x + 1.2989	0.7091	0.842	16
UCS	UCS = 1.1443y + 1.457	0.6166	0.7852	16
UCS	UCS = 2.1146z + 1.4146	0.635	0.7968	16
Tensile strength (UTS)	UTS = 8.4767x + 50.41	0.7489	0.8653	16
Tensile strength (UTS)	UTS = 198.75y + 77.539	0.6558	0.8098	16
Tensile strength (UTS)	UTS = 368.57z + 69.885	0.6801	0.8246	16
Ultrasonic velocity (UV)	UV = 13.927x + 1215.8	0.7797	0.8830	16
Ultrasonic velocity (UV)	UV = 309.17y + 1266.7	0.6121	0.7823	16
Ultrasonic velocity (UV)	UV = 604.77z + 1248	0.7063	0.8404	16

Note: x: CaO; y: CaO/SiO₂; z: CaO/ (SiO₂ + Al₂O₃)

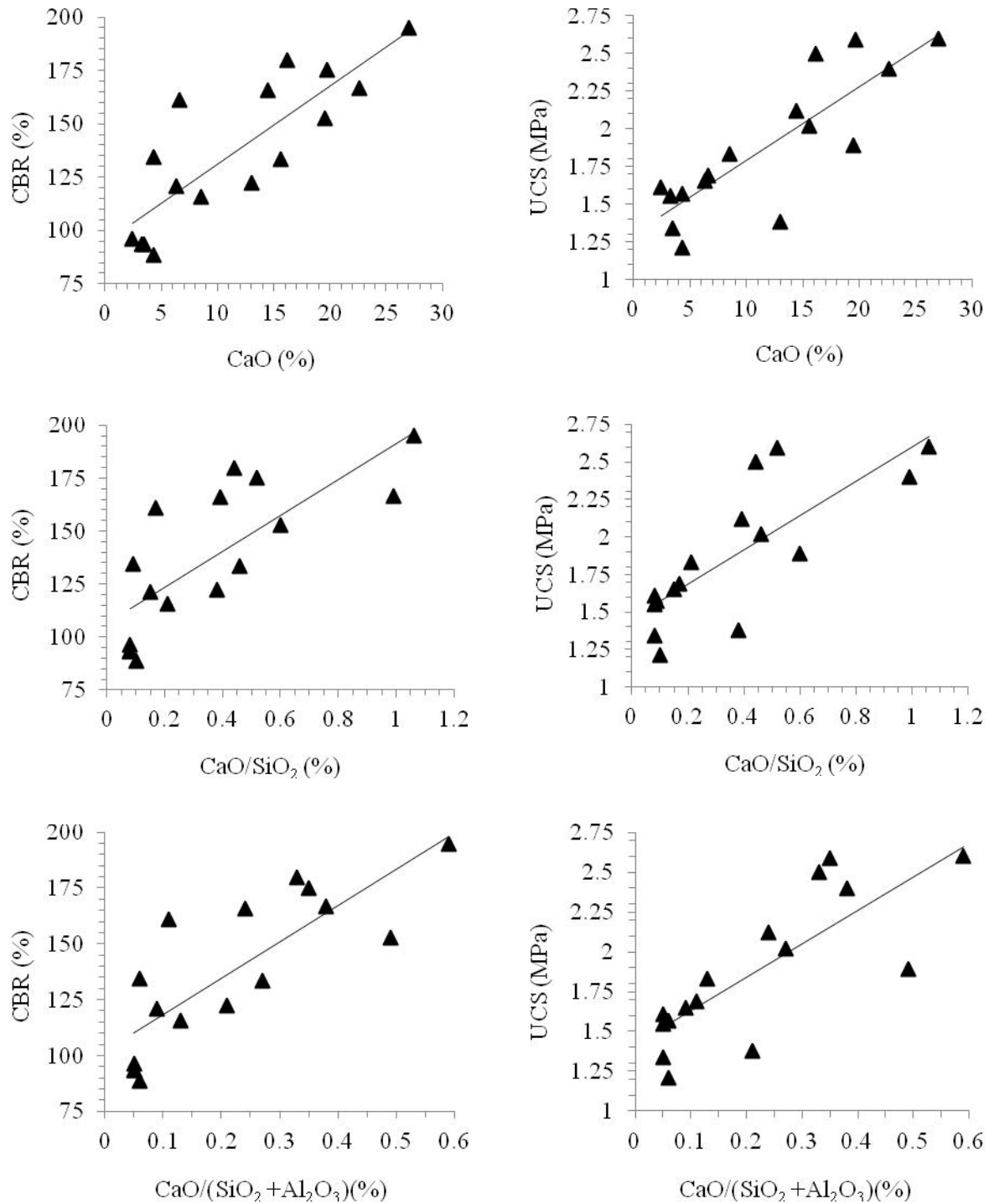


Figure 4.39 (a): Effect CaO content, CaO/SiO₂ and CaO/(SiO₂ + Al₂O₃) ratios on CBR and compressive strength values

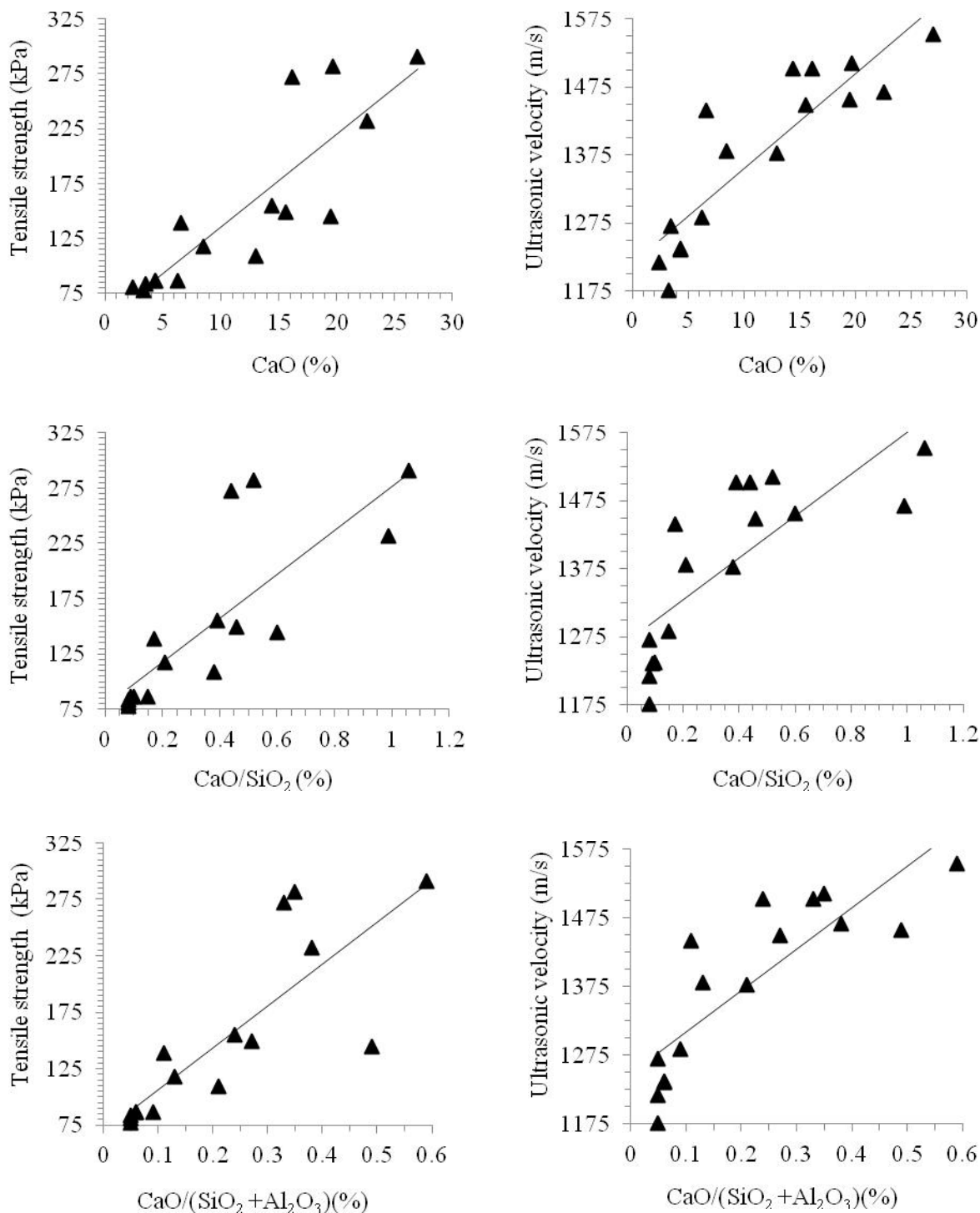


Figure 4.39 (b): Effect CaO content, CaO/SiO₂ and CaO/(SiO₂ + Al₂O₃) ratios on tensile strength and ultrasonic velocity value

CHAPTER 5

NUMERICAL INVESTIGATION

5.1 General

Availability of high speed computer has facilitated and enhanced the simulation of different conditions and situations. There exist many approaches as Finite element method (FEM), Finite boundary method (FBM), Finite difference method (FDM) for designs of structural elements in all field of engineering. FEM is very popular because of its flexibility to adapt variables as irregular geometric shapes and form, unusual loading conditions, varying material characteristics, different field conditions, etc. It is now gaining wide acceptance in other disciplines like thermal analysis, fluid mechanics, electromagnetic etc. It is a numerical analysis technique to obtain the stress, strain and deflection of haul road pavement layers. It is a mathematical method of converting governing differential equations into a system of linear algebraic equations which is solved by using matrix techniques. Finite element method handles irregular and complex geometries, linear and nonlinear problems, non homogenous and anisotropic, structural interactions, various boundary conditions and multiple loading conditions. Analytical method usually uses elastic modulus and Poisson's ratio of the pavement materials as design parameters.

This method involves identification of the problem, its geometric and material characteristics and development of model with the Finite Element Software. The problem geometry is created using a CAD system or Geometric Modeler and then the material

properties, boundary conditions either on FE Model or Geometric Model and loads on the model are assigned. Meshing is done to discretize the model elements. Then the solution is carried out and evaluated in terms of stress, strain and temperature etc.

The first FEM analysis of a pavement structure was reported with an axisymmetric formulation and specified the stiffness of each element in the granular layer as a function of the stresses in the element (Duncan et al., 1968). The use of a FEM model allows the model to accommodate the load dependant stiffness of the base/subbase and subgrade materials, although most models still use linear elastic theory as the constitutive relationship. The FEM analysis involves two approaches as force based and displacement based. In mining and allied areas the displacement (or strain) approach is popular (Mishra, 2003).

Numerical simulation of cement of varying percentage stabilized fly ash uses in road pavement has been observed to exhibit lower strain values (Lav et al., 2006). These exists numerous reports on both linear and non linear numerical analysis of pavement design using different materials (Witczak et al., 2004; Kim and Tutumluer, 2007; Kettil et al., 2007; Park, 2008; Kaliske et al., 2008; Nahi et al., 2011).

5.2 Modeling and Boundary condition

FEM divides the structures into a large of pieces of similar behaviour. It finds solutions for each piece and then combines the individual to find the result of whole. The assumption behind the analysis is that structure represents a continuous mass of physical body. All the analyses were carried out using the code ANSYS 10. It is an event simulation programme. It is capable of carrying out static and dynamic analysis in both linear and non-linear criteria. The program has been validated and used extensively for solutions (Stankus and Gou, 2001; Mishra, 2003).

A haul road represents structural mass experiencing wheel load which is modeled as a semi-infinite circular loading (Desai and Abel, 1987). The three dimensional loading conditions has been simplified as two dimensional modeling and the stress-strain behaviour is axisymmetric about the axial loading. In this analysis an axisymmetric pavement model under wheel load and a road profile width of 10m and depth of 5m had been considered to represent the actual field condition. A typical of pavement and load on it has been shown in Figure 5.1. Haul road pavement is a multilayer structure consists of four layers surface, base, subbase and subgrade. One of the main objectives of the investigation is to evaluate the performance of haul road by replacing its subbase with the developed fly ash based composites.

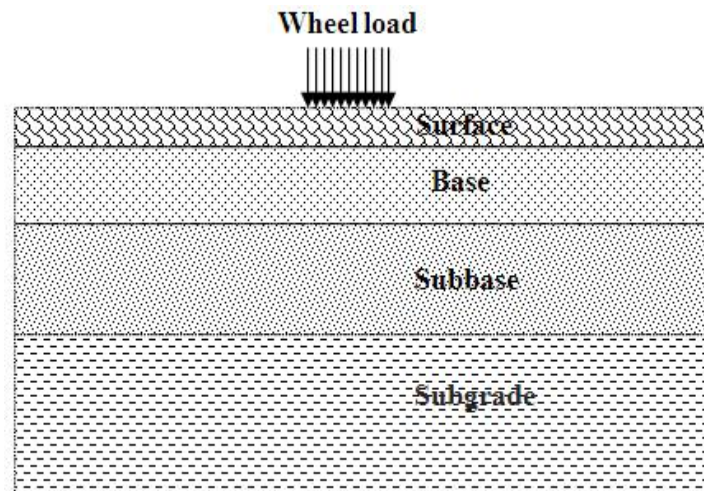


Figure 5.1: A typical haul road pavement under wheel load

The boundary condition of the model of the haul road has been adopted to simulate field behaviour (Figure 5.2). It is assumed that the floor of the pavement is strong enough not to undergo any settlement under loading. There is no movement of the bottom surface and hence all degrees of freedom are constrained in both horizontal and vertical direction. The tire load is applied on the top of the haul road and hence it is allowed to move freely along the

vertical directions. It is also expected that sides of the haul road is laterally constrained as the objective was to evaluate the behaviour of subbase in vertical direction as well as the sides of the pavement would not be excavated.

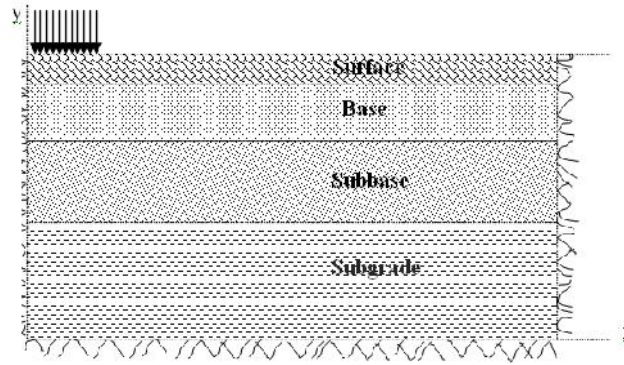


Figure 5.2: Schematic layout of FEM modelling of haul road

Many engineering problems involve axisymmetric solids subjected to axially symmetric loading. A circular footing on a soil mass is a semi-infinite half space loaded by a circular area. Vehicle loading on the pavement represents an axisymmetric problem as shown in Figure 5.3. Though the pavement layers are horizontally layered, the stiffness characteristics of these layers vary in lateral as well as in the vertical direction because of the stress-dependent nature of the materials. The finite element method is best suited for such circumstances (Siddharthan et al., 1991). According to the symmetry, both geometrical and mechanical, around a vertical axis which passes through the loading centre, it is advantageous to use cylindrical coordinates, z , r and h for analysis. The radial symmetry makes the problem independent of the coordinate h . Thus, the strains and stresses at any point are only functions of its vertical and radial coordinates, z and r , respectively. The displacements is described in terms of the components in the vertical and radial directions v and u . The corresponding vectors have the following form:

$$\{\sigma\} = \begin{Bmatrix} \sigma_{zz} \\ \sigma_{rr} \\ \sigma_{\theta\theta} \\ \tau_{zr} \end{Bmatrix} \quad \{\varepsilon\} = \begin{Bmatrix} \varepsilon_{zz} \\ \varepsilon_{rr} \\ \varepsilon_{\theta\theta} \\ \gamma_{zr} \end{Bmatrix} \quad (1)$$

where, σ_{zz} , σ_{rr} , and τ_{zr} are the stress components.

ε_{zz} , ε_{rr} , and γ_{zr} are the strain components.

According to the hypothesis of small displacements, strains are expressed in terms of the first derivations of the displacements:

$$\{\varepsilon\} = \begin{Bmatrix} \varepsilon_{zz} \\ \varepsilon_{rr} \\ \varepsilon_{\theta\theta} \\ \gamma_{zr} \end{Bmatrix} = \begin{Bmatrix} \frac{\partial v}{\partial z} \\ \frac{\partial u}{\partial r} \\ \frac{u}{r} \\ \frac{\partial v}{\partial r} + \frac{\partial u}{\partial z} \end{Bmatrix} \quad (2)$$

The constitutive relation between stresses and strains is:

$$\{\sigma\} = [D]\{\varepsilon\} \quad (3)$$

where, $[D]$ = matrix of elastic constants.

$$[D] = \frac{E}{(1+\mu)(1-2\mu)} \begin{bmatrix} 1-\mu & \mu & \mu & 0 \\ & 1-\mu & \mu & 0 \\ & & 1-\mu & 0 \\ \text{Symmetrical} & & & \frac{1-2\mu}{2} \end{bmatrix}$$

where, E = Young's modulus, μ = Poisson's ratio.

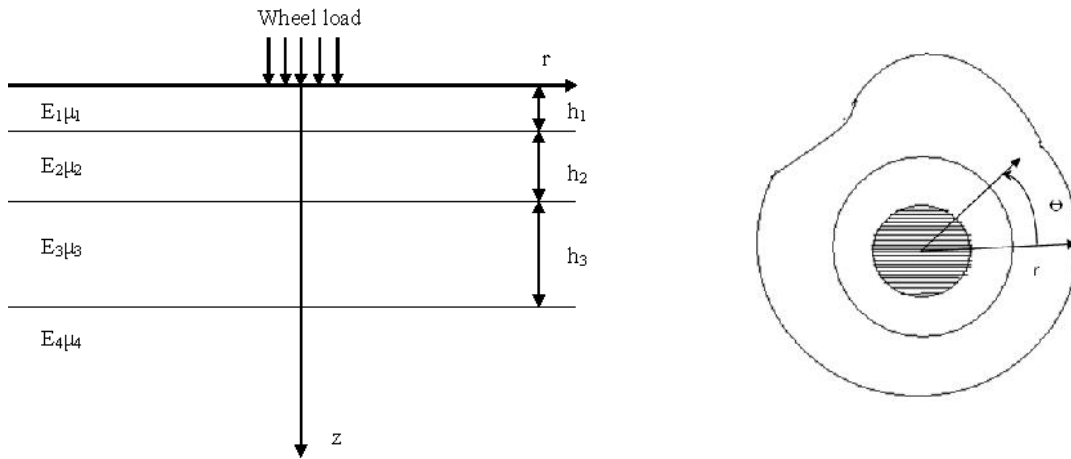


Figure 5.3: Haul road cross-section under axisymmetry loading

Numerical modeling to determine the stress-strain behaviour of pavement was carried out using both conventional materials and the developed composite materials. Typically the construction materials used in haul road are dense sand, gravel, silty sand, sandy clay, clay shale, medium clay, soft clay, silty clay, etc. The elastic constants of these vary over a wide range. In this study the higher values (elastic modulus and Poisson's ratio) of these materials have been considered for analysis. The Young's modulus values for conventional material in respective layers of haul road pavement considered are 200, 100, 50 and 50 MPa (McCarthy, 2007).

The conventional material for subbase was replaced with the composite material ((30%FA+70%O/B) +9%L) exhibiting high strength values among all composites and analyzed for corresponding strain in the pavement. The respective value for the composite (Case I) is 142 MPa as determined from laboratory test (Table 5.1). The Poisson's ratio considered for analysis is 0.4 (Tannant and Regensburg, 2001; McCarthy, 2007; Lav et al., 2006). The thickness of various layers of the haul road pavement was considered as per CMPDI (2000) guidelines.

Table 5.1: Young's modulus, E (MPa) and Thickness, t (m) of the pavement layers for different cases

Construction Materials	Layer							
	Surface		Base		Subbase		Subgrade	
	E	t	E	t	E	t	E	t
Conventional Material (CM)	200	0.22	100	0.3	50	0.83	50	Semi-infinite
Case I	200	0.22	100	0.3	142	0.83	50	Do
Case II	500	0.5	350	1	142	0.83	50	Do
Case III	500	0.5	350	1	142	1	50	Do
Case IV	500	0.5	350	1	142	1.5	50	Do

The maximum strain at the surface course just below the wheel loading point was 4775 microstrain with the conventional materials (CM) (Figure 5.4). The maximum strain was 4498 microstrain after replacement of subbase material with the developed fly ash composite (Case I) thus exhibiting a 6% reduction. The strain at various positions of the pavement had been determined using both conventional and fly ash composite materials. The locations were the interface between each layer (below the wheel loading). These are A, B, C and D representing the position between surface course and base course, base course and subbase course, subbase course and subgrade and bottom of the subgrade respectively (Figure 5.5). Those positions are 0.5m, 1.5m, 3m and 5m from the top of the surface course. All the discussion has been made based on the results of those locations. All other location experienced stress-strain of lesser magnitude.

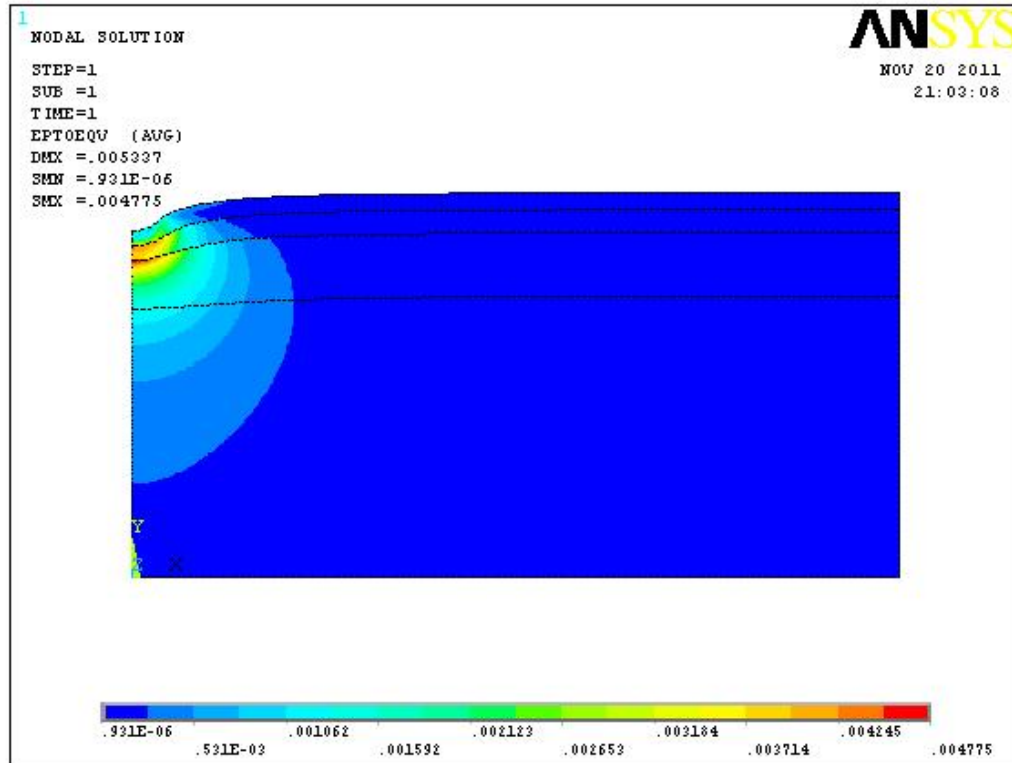


Figure 5.4: Maximum strain of haul road pavement with conventional materials

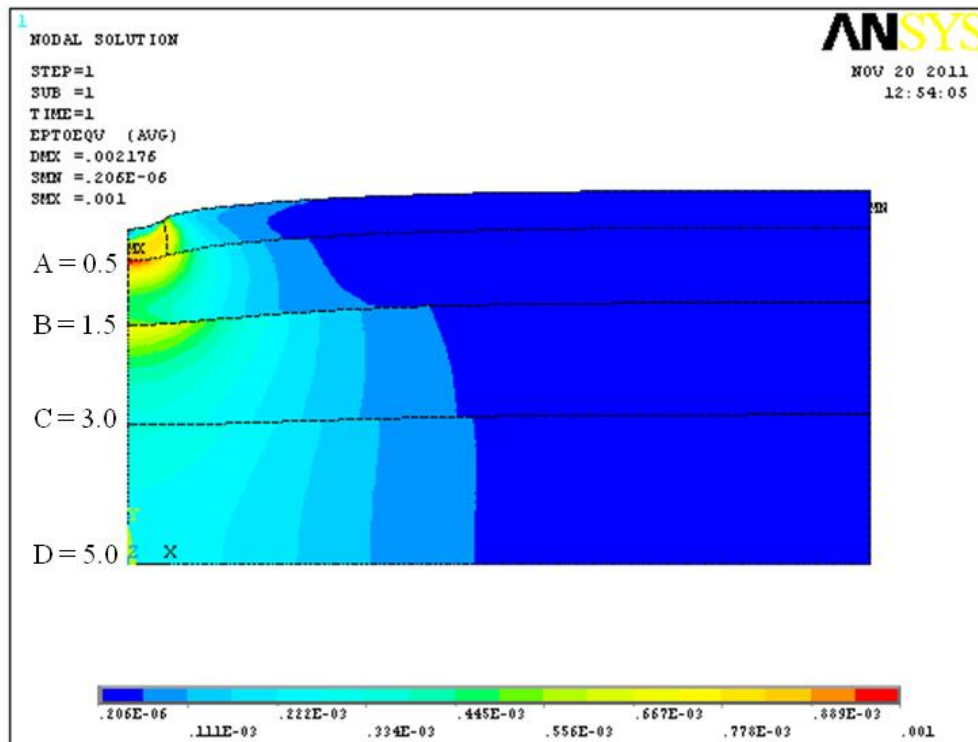


Figure 5.5: Haul road pavement model with various positions in layers

The strain values at different depths from top of haul road pavement model are shown in Figure 5.6. There is not much reduction in strain values after replacement of developed fly ash composite. The maximum strain limit at surface course immediately under the wheel load is 1500-2000 microstrains (Thompson and Visser, 1997; Tannant and Regensburg, 2001). So, a haul road cannot adequately support haul trucks if strain values exceed the maximum strain limit.

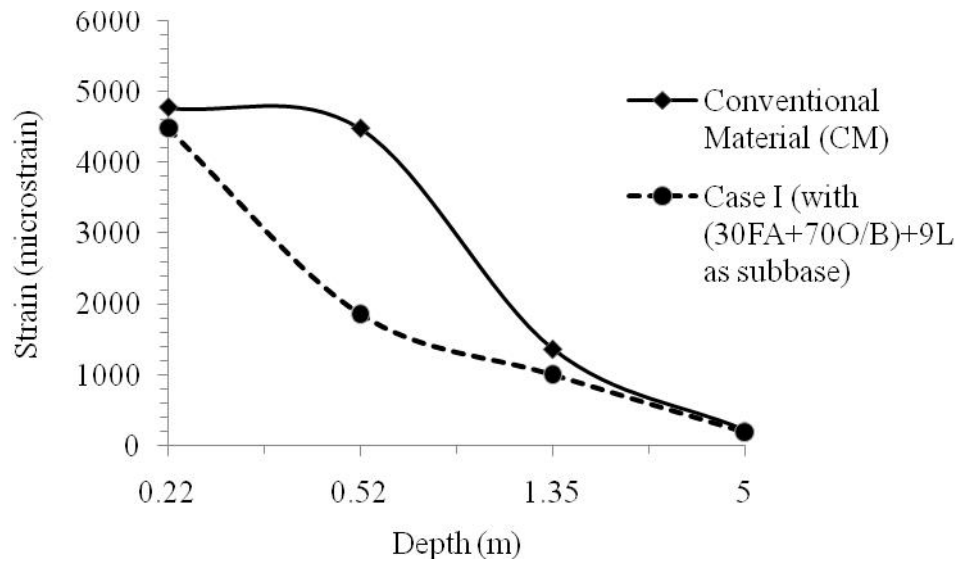


Figure 5.6: Strain values at different depth of the pavement

Further analysis by varying the thickness of layers (Table 5.1) has been conducted to evaluate the performance of developed fly ash composite material. The thickness of subbase layer was varied between 0.83 and 1.5 m for the use of more quantity of fly ash (Table 5.1). The stress and strain values obtained for 0.83m, 1m and 1.5m thickness of subbase layer were 452.5, 453.5 and 456 kPa and 1008, 1010 and 1016 microstrains respectively. It confirmed from the simulation that with varying thickness of the subbase layer, there was not much variation in stress and strain values. Figure 5.7 shows strain values at different depth from top of haul road pavement model and also stress values at different depth.

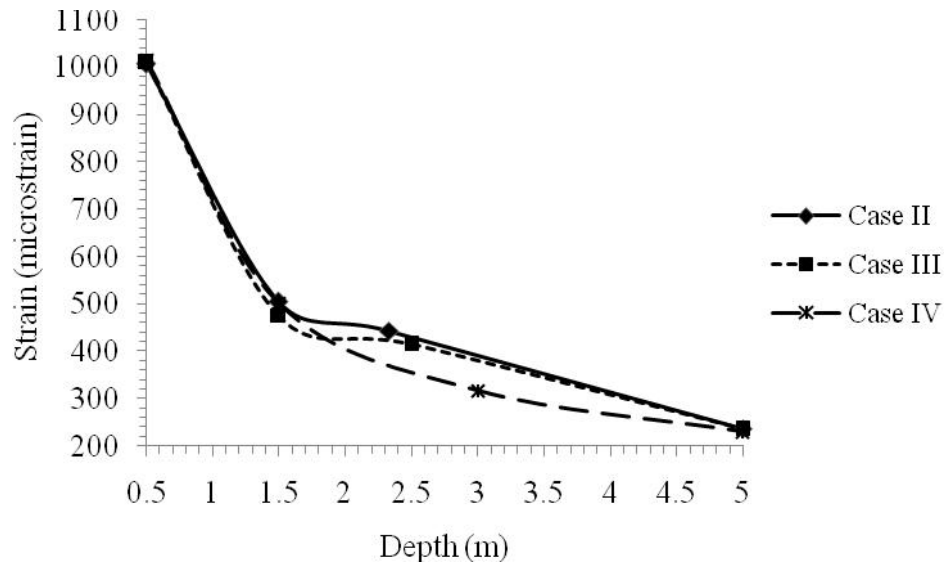


Figure 5.7 (a): Strain values at different depth of the pavement with varying subbase thickness

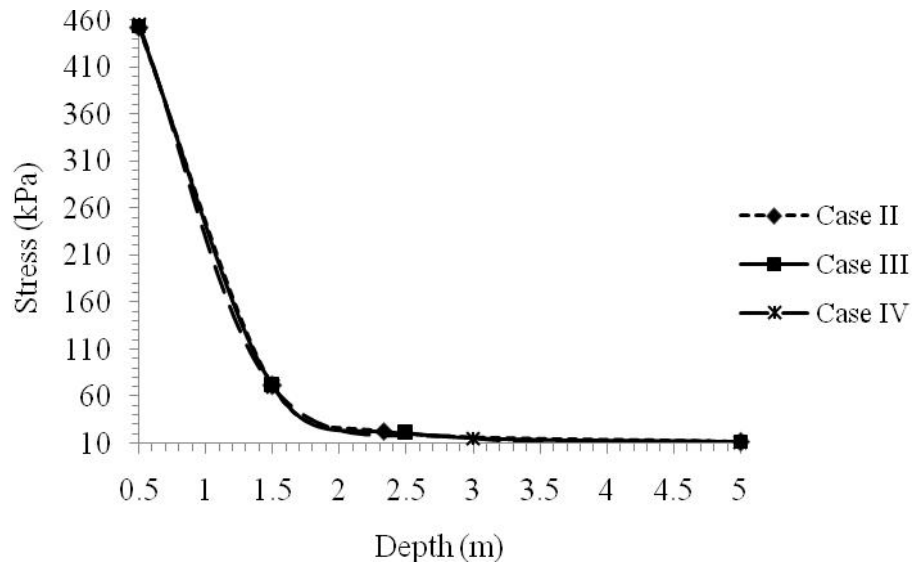


Figure 5.7 (b): Stress values at different depth of the pavement with varying subbase thickness

However the layer with 1.5m thickness offers maximum fly ash consumption possibilities. Numerical modeling for various fly ash composites were carried out to observe the stress-strain behaviour of haul road pavement with 1.5m thickness.

It was determined from the laboratory tests that the composite with 30% fly ash and 9% lime produced maximum strength values. So this composition was selected for its performance evaluation in replacing the conventional subbase material. Accordingly numerical analysis was carried out with the elastic parameters obtained for this composite at 7, 14 and 28 days curing. All the three types of materials exhibited almost equal maximum strain values (Figure 5.8(a)) at immediately below the tire load (at 0.5m). However at a depth of 1.5m the strain values using 7 days cured sample was higher than that of using 14 and 28 days cured samples. Respective values are 709 and 502 microstrain. The strain values at 3m and 5m were almost same for the three specimens. The values were 351 and 317 microstrain. Similar trend was also observed for the stress vs. depth analysis using the three different composites (Figure 5.8(b)).

The stress and strain values for the composite at 7days cured condition were less than the maximum values due to wheel loading (Kumar, 2000).

Further numerical analysis were carried out using the elastic parameters to evaluate the performance of the composite materials cured at 28 days only as those are comparable to 7 days and 14 days cured behaviour of the best developed composite.

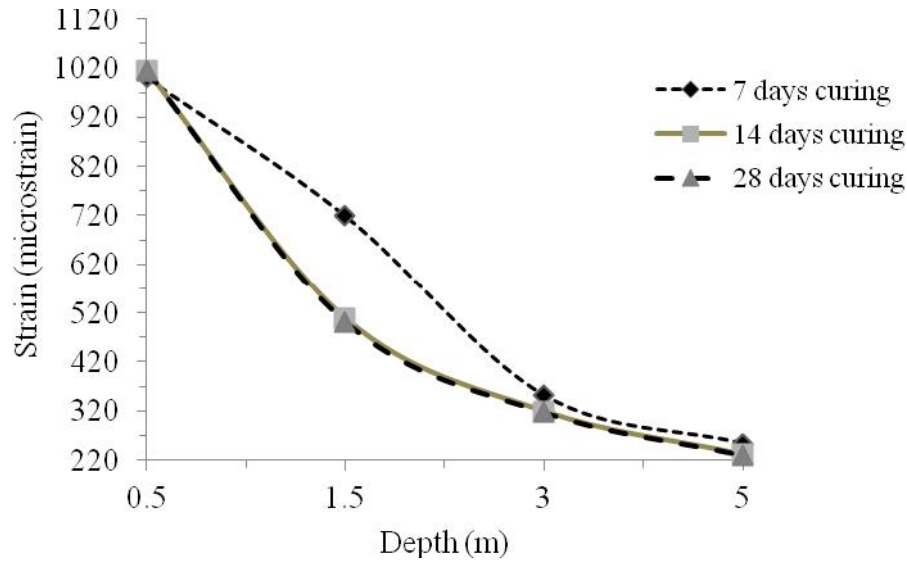


Figure 5.8 (a): Strain values at different depth of the pavement with 1.5 subbase thickness with (30PA+70OB)+9L composite

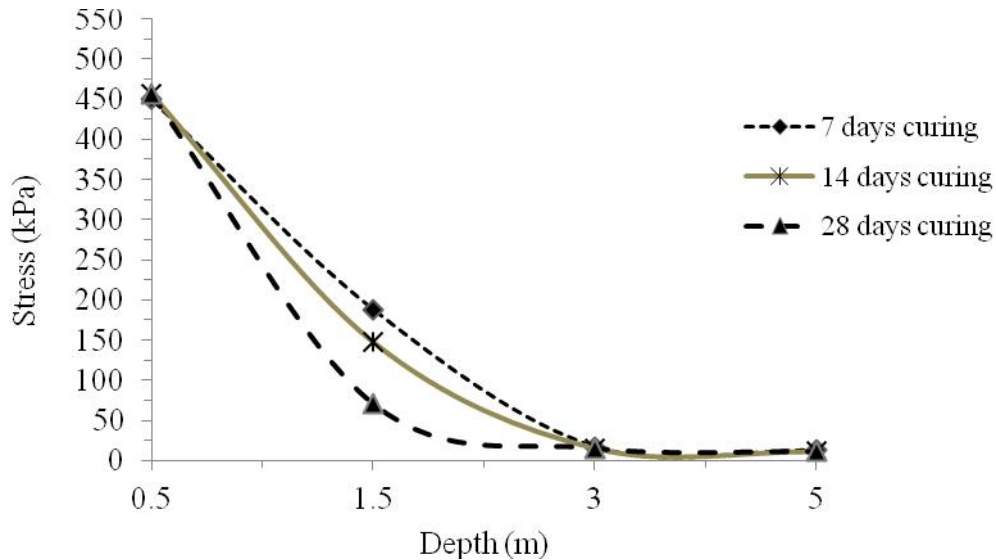


Figure 5.8 (b): Stress values at different depth of the pavement with 1.5 subbase thickness with (30FA+70OB)+9L composite

The dynamic Young's modulus values and Poisson's ratios of the developed composite material containing 30% fly ash and 70% mine overburden stabilized with 9% lime determined from Ultrasonic pulse velocity test were used in subbase layer for numerical modeling (Table 5.2). The dynamic properties of other layers of the haul road pavement

were adopted from published literature (Lav et al., 2006) (Table 5.2). The static tests involve destructive approaches where load is applied at an incremental step. During testing flaws, cracks develop and close till hydrostatic conditions exist beyond which cracks/ flaws keep on extending till failure occurs. But in dynamic loading condition, often carried by non-destructive testing there is little scope for flaws/cracks to change their position and hence the modulus values obtained are high.

The stress and strain values obtained were very low (Figure 5.9). The maximum strain observed at the top of the surface course was 228 microstrains at 0.5m below the tire loading. The minimum strain values 28 microstrains was determined at 3m and beyond. Corresponding stress values at 0.5m and 3m depth were 512kPa and 12kPa respectively. These values are very low as compared to that obtained by considering static loading parameters. Hence the stress/strains related to static loading are only reported here. The elastic modulus values for respective composites considered are given Table 5.3. The Poisson's value has been kept constant at 0.4.

The stress and strain at different depth vary between 460 to 10 kPa and 1020 to 220 microstrains respectively for all the composites (Figures 5.10 and 5.11). These values are less than the corresponding values for conventional materials as well as less than the maximum strain limits experienced (Thompson and Visser, 1997; Tannant and Regensburg, 2001). Relevant analysis for each material type is given in Annexure.

Table 5.2: Dynamic Elastic parameters and Thickness of the pavement layers

Layer	Thickness, t (m)	Dynamic Elastic parameters of materials	
		Young's modulus, E (MPa)	Poisson's ratio
Surface	0.5	2500	0.4
Base	1	1500	0.4
Subbase	1.5	2822	0.35
Subgrade	Semi-infinite	500	0.45

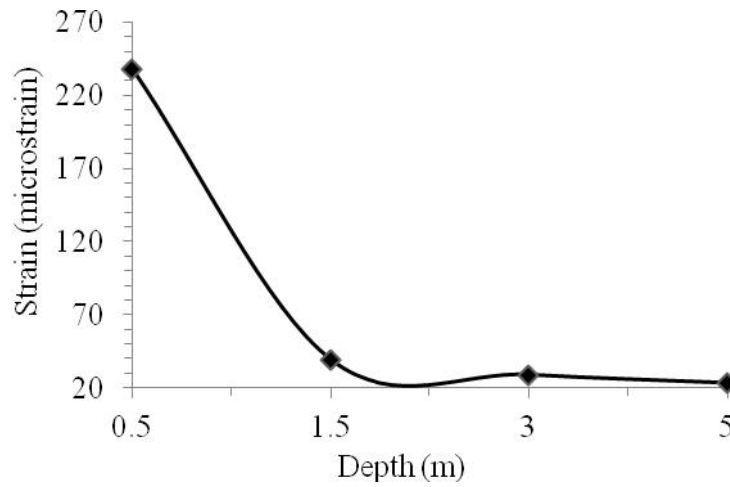


Figure 5.9 (a): Strain at different depth of the pavement using dynamic elastic parameters

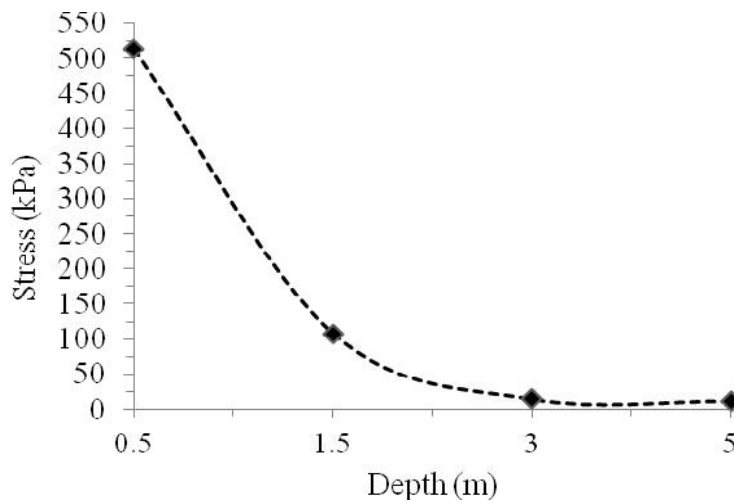


Figure 5.9 (b): Stress at different depth of the pavement using dynamic elastic parameters

Table 5.3: Young's modulus, E (MPa) of fly ash composites

Composite (s)	Young's modulus, E (MPa)
(15%FA+85%O/B) +2%L	102.3
(15%FA+85%O/B) +3%L	115.1
(15%FA+85%O/B) +6%L	130.8
(15%FA+85%O/B) +9%L	139
(20%FA+80%O/B) +2%L	115.6
(20%FA+80%O/B) +3%L	108.8
(20%FA+80%O/B) +6%L	136
(20%FA+80%O/B) +9%L	138.8
(25%FA+75%O/B) +2%L	98
(25%FA+75%O/B) +3%L	87.6
(25%FA+75%O/B) +6%L	115.2
(25%FA+75%O/B) +9%L	138.3
(30%FA+70%O/B) +2%L	108.5
(30%FA+70%O/B) +3%L	122
(30%FA+70%O/B) +6%L	140.5
(30%FA+70%O/B) +9%L	142
(35%FA+65%O/B) +2%L	51.5
(35%FA+65%O/B) +3%L	95.8
(35%FA+65%O/B) +6%L	133.4
(35%FA+65%O/B) +9%L	141
(40%FA+60%O/B) +2%L	83.5
(40%FA+60%O/B) +3%L	90.8
(40%FA+60%O/B) +6%L	120
(40%FA+60%O/B) +9%L	121.2

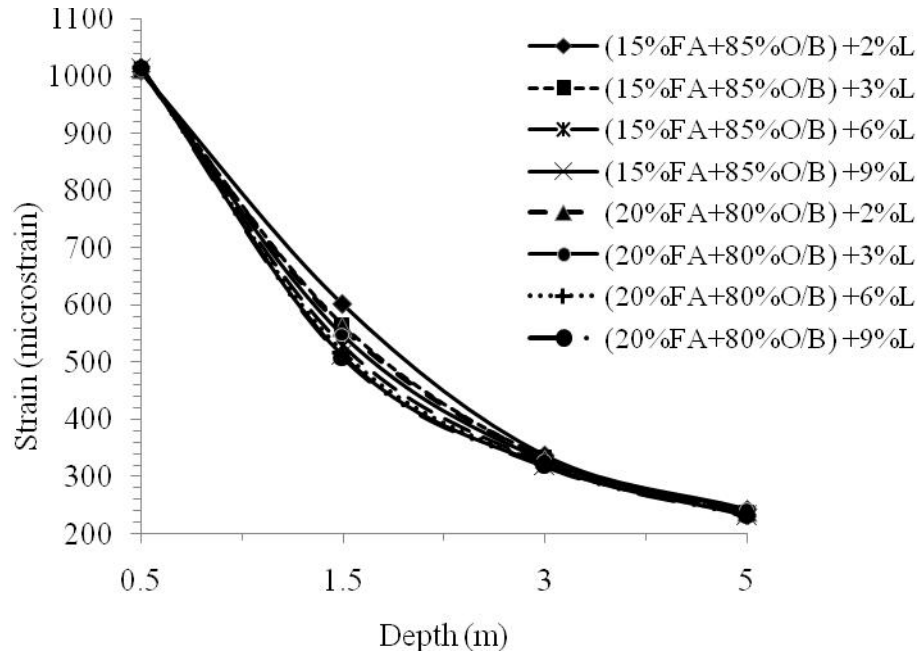


Figure 5.10 (a): Strain values at different depth of the pavement with composites containing 15 and 20% fly ash as subbase material

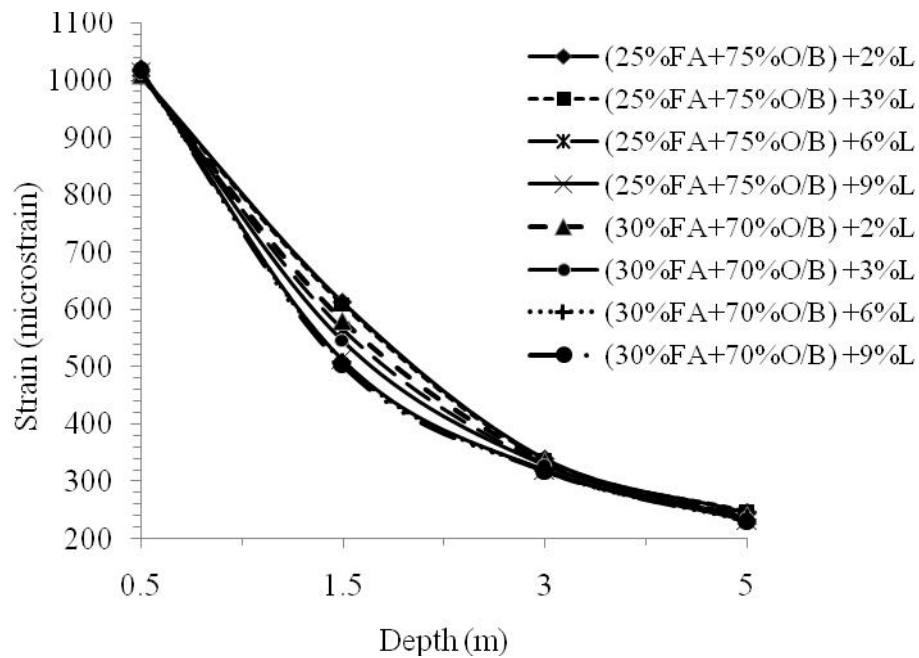


Figure 5.10 (b): Strain values at different depth of the pavement with composites containing 25 and 30% fly ash as subbase material

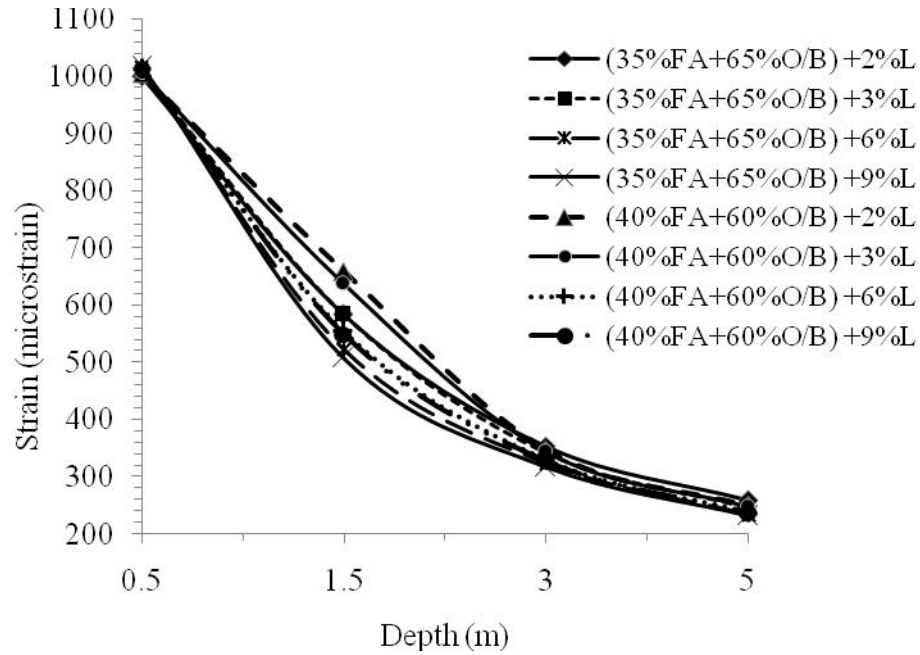


Figure 5.10 (c): Strain values at different depth of the pavement with composites containing 35 and 40% fly ash as subbase material

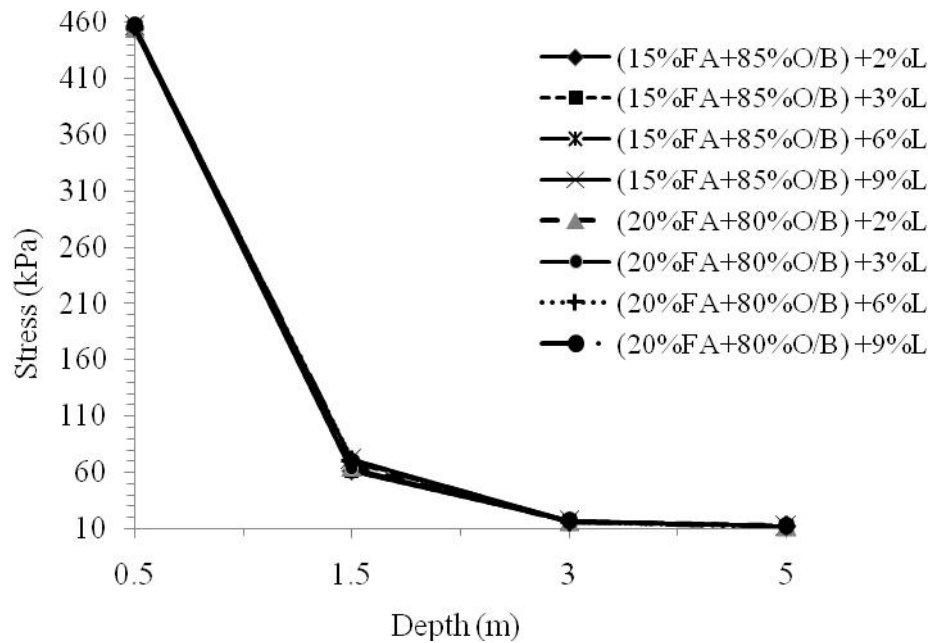


Figure 5.11 (a): Stress values at different depth of the pavement with composites containing 15 and 20% fly ash as subbase material

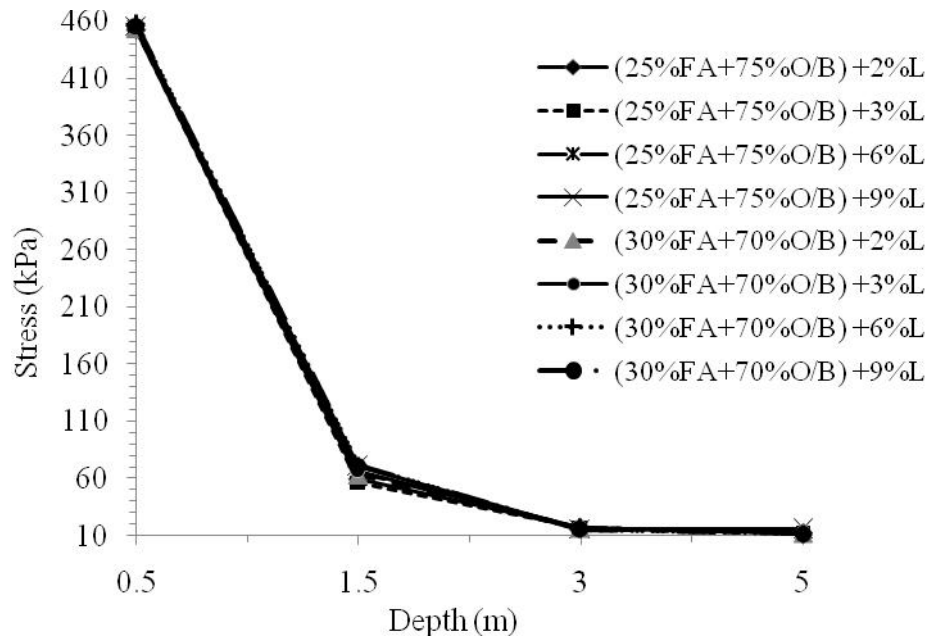


Figure 5.11 (b): Stress values at different depth of the pavement with composites containing 25 and 30% fly ash as subbase material

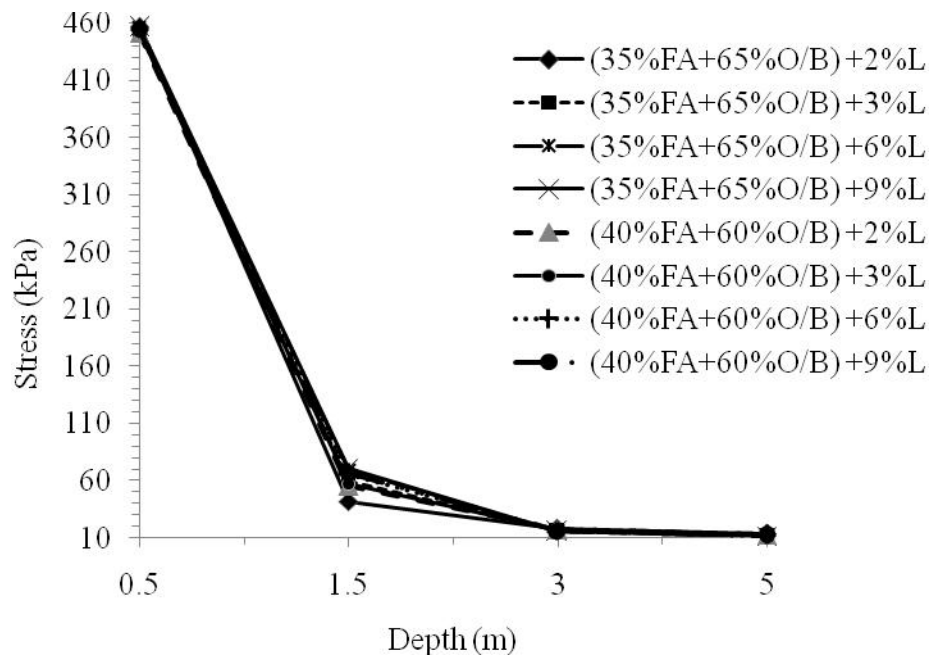


Figure 5.11 (c): Stress values at different depth of the pavement with composites containing 35 and 40% fly ash as subbase material

CHAPTER 6

SUMMARY AND CONCLUSIONS

In this investigation, potential of lime stabilized fly ash and mine overburden was evaluated for haul road construction and improved the road condition by reducing strain in the road pavement through experimental and numerical study. Lime stabilization is widely used to improve the strength of road building materials. The characterisation of fly ash and its interaction behaviour with mine overburden and lime is likely to provide viable solutions for its large scale disposal and utilisation in geotechnical applications as mine haul road construction. Strength characteristics of any construction material are vital parameters to judge its suitability. Strength characteristics of the fly ash composites are studied through different conventional test methods such as CBR, unconfined compressive strength, Brazilian tensile strength and ultrasonic velocity which cover a broad area of design parameters, useful for mine haul road application and to understand the engineering behaviour of composite materials. Microstructural analyses carried out to gain better understanding of the mechanism of lime, fly ash and overburden interaction. The change in surface morphology and variation in chemical composition due to formation of hydration products were analyzed through scanning electron micrographs and energy dispersive X-ray results. X-ray diffraction analyses were carried out to identify the hydration production phases. Leaching studies were carried out to analyze heavy metal concentration in the composites. The numerical studies (2-dimensional finite element modeling) were carried out to study the effectiveness of the developed composite materials on the stress-strain behaviour of haul road pavement.

The experimental and numerical investigation results and discussions presented in previous chapters, following conclusions have been drawn by dividing into two categories:

6.1 Untreated materials

1. Mine overburden has major chemical constituents of silica, alumina and iron oxide and mineral constituents of Kaolinite and Quartz and acidic in nature.
2. The overburden material is poorly graded sand-silt mixtures.
3. Mine overburden has high maximum dry density and low optimum moisture content as compared to fly ash. It exhibits minimum CBR value at soaked condition.
4. It is not amenable to be used as road material with additive alone. It possesses low compressive strength.
5. The fly ash used for the investigation was class F type. The major chemical constituents of fly ash are silica, alumina and iron oxide with major mineral constituents as Quartz, Sillimanite and Mullite.
6. Fly ash has high optimum moisture content and low maximum dry density due to the fact that particles themselves are hollow or cenospheres and hold a considerable quantity of water internally. It exhibits minimum CBR value at soaked condition.
7. The maximum dry density decreased and optimum moisture content increased with increase in fly ash content in the untreated composites.
8. The UCS values were not significant.
9. The CBR values of untreated fly ash-overburden composite materials were low and hence those are unsuitable for road construction.
10. There was not much strength gain in the untreated composites with varying curing periods.

6.2 Treated materials

1. The maximum dry density values of all the treated composite materials decreased and optimum moisture content increased with increase in lime content.
2. The CBR values increased with increase in lime content. It increased from 22 to 77.08% in soaked condition. Similar trend exist for increasing curing period.
3. Unconfined compressive strengths increased from 0.71 to 3.14 MPa with curing period. The composition with 30%FA, 70% O/B and 9% lime exhibited maximum compressive strength 3.14 MPa at 56 days curing as compared to that of other mixes.
4. The unconfined compressive strength increased with increase in lime content and curing period.
5. Brazilian tensile strengths increased from 55.7 to 357 kPa with curing period. Similar trend like CBR and unconfined compressive strength was also observed for the Brazilian tensile strength.
6. The mine overburden mixed with 30% fly ash and 9% lime produced highest compressive strength, tensile strength and bearing ratio value as compared to that of other composites with curing period.
7. The ultrasonic pulse velocities varied in the range of 797 m/s to 1699 m/s for varying curing periods, maximum at 56 days.
8. The composite containing 30% fly ash and 70% overburden treated with 9% lime produced highest ultrasonic velocities as compared to that of other composites at 7, 14, 28 and 56 days of curing respectively.
9. The pulse wave velocity increased with an increase in lime content though the rate of increase varies.

10. The pulse velocity changed marginally with varying fly ash content. Young's modulus values and Poisson's ratios also followed the same trend as the pulse wave velocity.
11. The morphology of all the mixes showed the formation of hydrated gel at 28 days curing. The voids between the particles were filled by growing hydrates with curing time.
12. Microanalysis and compositional analysis confirmed the formation of new cementitious compounds such as calcium silicate hydrate (CSH), calcium aluminate hydrate (CAH) and calcium aluminate silicate hydrate (CASH) which leads to increase in strength of the material over time.
13. The major chemical constituents are alumina, silica iron oxide, calcium oxide in the composites. Very small or negligible percentages of Na, Mg, P, S, Mn, Cu, Ba and Mo elements are found in the mixes.
14. The CaO content, CaO/SiO_2 and $\text{CaO}/(\text{SiO}_2 + \text{Al}_2\text{O}_3)$ ratios are highest (27%, 1.06 and 0.59) in composite the containing 30% fly ash and 70% overburden treated with 9% lime as compared to other mixes which exhibited maximum strength value.
15. XRD patterns indicate CAH is the most dominant formation followed by CSH and CASH.
16. Lime content showed a significant effect on the strength development and pozzolanic reaction rate of natural pozzolans.
17. The concentration of heavy metals (Ni, Cr, Pb, Cu and Zn) in the leachate effluent was below the threshold limits acceptable for contaminants flowing into ground water.

18. The model equations governing the relationship between Brazilian tensile strength and unconfined compressive strength and CBR and unconfined compressive strength and CBR, compressive strength, tensile strength and ultrasonic velocity values against CaO content, CaO/SiO₂ and CaO/(SiO₂ + Al₂O₃) ratios.
19. All the model equations developed have correlation coefficient (R) values are about 80% to 90%.
20. The strain at the surface course with conventional material is above the critical limit with fixed subbase thickness (0.83m). Replacement with fly ash composite material did not show any significant improvement.
21. The maximum strain reduced drastically when subbase thickness changed from 0.83 to 1.5m. The strain value was less than the critical strain limit with dynamic constants of the best developed composite ((30%FA+70%O/B)+9%L).
22. The maximum stress and strain values were very low with dynamic elastic parameters.
23. All the composites exhibited less than the critical strain and stress values for 1.5m thick subbase.
24. About 16MT of fly ash can be used in 5 km long, 20m wide and 5m thick haul road for 200 opencast mines.
25. The developed fly ash composite material ((30%FA+70%O/B)+9%L) has strong potential to be used as subbase material.

6.3 Scope for Further Research

The investigation has certain limitation and hence all the factors that contribute to the haul road performance could not be addressed in time. So the future research should incorporate the following aspects in detail.

- i. Performance of developed composites was evaluated numerically. Same should be carried out in field conditions.
- ii. The CBR value is considered for the road design. The resilient modulus values should be considered and evaluated.

REFERENCES

- AASHTO, Guide for Design of Pavement Structures. American Association of State Highway and Transportation Officials, Washington D.C. USA, 1986.
- AASHTO, Standard Specifications for Transportation Materials and Methods of Sampling and Testing. Part II – Tests, Sixteenth ed., American Association of State Highway and Transportation Officials, Washington D.C. USA, 1993.
- AASHTO, The AASHTO Road Test Report 5: Pavement Research, Special Report 61E, National Academy of Science, National Research Council, Publication 945, Washington, D.C.,USA, 1962.
- Acosta H.A., Edil T.B and Benson C.H., Soil stabilization and drying using fly ash, Geo Engineering Report No. 03-03, Geo Engineering Program, University of Wisconsin, Madison, USA, 2003.
- Ahlvin R.G., Ulery H.H., Hutchinson R.L. and Rice J.L., Multiple wheel heavy gear load pavement tests, Vol 1 Basic Report, USA Waterways Exp. Stn. Report, AFWL-TR-70-113, 1971.
- Ahmaruzzaman M., *A review on the utilization of fly ash*, Journal of Progress in Energy Combust. Sci., 36 (2010): pp. 327-363.
- Anon, Lime Stabilization Construction Manual, 8th ed., National Lime Association, Arlington, Va, US, 1985.

-
- Antiohos S. and Tsimas S., *Activation of fly ash cementitious systems in the presence of quicklime Part I. Compressive strength and pozzolanic reaction rate*, Journal of Cement and Concrete Research, 34 (2004): pp. 769-779.
 - Arora S. and Aydilek A.H., *Class F fly-ash-amended soils as highway base materials*, Journal of Materials in Civil Engg. ASCE 17 (2005): pp. 640-649.
 - ASTM, Specification for coal fly ash and raw or calcined natural pozzolan for use in concrete. in: Annual book of ASTM standards, concrete and aggregates, American Society for Testing Materials, Philadelphia, vol. 04.02. C618-08, 2008.
 - Atkinson T., Design and layout of haul roads. SME Mining Engineering Handbook, 2nd ed., Society of Mining, Metallurgy, and Exploration, Inc. Littleton, Colorado, 1992.
 - Baghdadi Z.A., Fatani M.N. and Sabban N.A., *Soil modification by Cement kiln dust*, Journal of Materials in Civil Engineering, 7 (1995): pp. 218-222.
 - Baker M.D. and Laguros J.G., Reaction products in fly ash concrete, Fly ash and coal conversion by-products: characterisation, utilisation and disposal, G.J. McCarthy, F.P. Glasser and D.M. Roy eds, Materials Research Society, Pittsburgh, 43 (1985): pp. 73-83.
 - Barstis W.F. and Crawley A.B., The use of fly ash in highway construction U.S. 84/98 Adams County. FHWA Demonstration Project 59, Report No. 84-DP59-MS-05, Mississippi Department of Transportation Research Division, P O Box 1850, Jackson MS 39215-1850, 2000.
 - Bowels J., Engineering Properties of soil and their measurements, 4th ed., Mc Graw-Hill, Boston, 1992.

-
- Beeghly J.H., *Recent Experiences with lime - fly ash stabilization of pavement subgrade soils, base and recycled asphalt*, in: proc. of Int. Ash Utilization Symposium'03, Centre for Applied Energy Research, Univ. of Kentucky, 2003 Paper # 46, pp. 1-18.
 - BEML, Construction and mining equipment, Bharat Earth Movers Limited, India, 2011
 - Bergeson K.L. and Mahrt D., *Reclaimed fly ash as selected fills under PCC pavement*, in: Proc. of Mid-content transportation symposium, Iowa State University, Ames, Iowa, 2000, pp. 147-150.
 - Bowles J.E., Physical and Geotechnical Properties of Soils, 2nd ed., McGraw-Hill Book Company, New York, USA, 1984.
 - Brennan M.J. and O'Flaherty C.A., Highways the location, design, construction and maintenance of road pavements, 4th ed., Elsevier publication, 2001.
 - Butalia S.T., Rehabilitating asphalt highways: coal fly ash used on Ohio full depth reclamation projects, Case Study-18, Coal Combustion Product Partnership, Environmental Protection Agency, USA, 2007, pp. 1-4.
 - Canter, L.W. and Knox, R.C., Ground water pollution control, Lewis Publishers, Inc., Chelsea, Mich., 1985.
 - Capco, Pulverized fuel ash as reclamation fill, Report of the China Light and Power Co. Ltd., Hong Kong, 1990, pp.1-34.
 - Caterpillar, Caterpillar Performance Handbook. 40th ed., Caterpillar Inc., Peoria, Illinois, USA, 2010.

- Cetin B., Aydilek A.H. and Guney Y., *Stabilization of recycled base materials with high carbon fly ash*, Journal of Resources, Conser. Recycl., 54 (2010): pp. 878-892.
- Chaulya S.K., Singh R.S., Chakraborty M.K. and Tewary B.K., *Bioreclamation of coal mine overburden dumps in India*, Journal of Land Contamination & Reclamation, 8 (2000): pp. 189-199.
- Chironis N.P., *How to build better haul roads*, Journal of Coal Age, 11 (1978): pp. 122-128.
- Chu T.Y., Davidson D.T., Goecker W.L. and Moh Z.C., *Soil stabilization with lime-fly ash mixtures: preliminary studies with silty and clayey soils*, Highway Research Board Bulletin, 108 (1955): pp. 102 – 112.
- Chugh Y.P. and Mohanty S., *A field demonstration of an unstabilised F-Fly ash-based road subbase*, in Proc. of Fly ash India 2005, Fly ash Utilisation Programme, TIFAC, DST, New Delhi, 2005, pp. VIII 3.1-3.16.
- Cicek T. and Tanriverdi M., *Lime based steam autoclaved fly ash bricks*. Journal of Constr. and Building Mater, 21(2007): pp. 1295-1300.
- CMPDIL HQ, *Technical manual on Guidelines for planning, design and construction of haul road*, Central Mine Planning & Design Institute Limited, Ranchi, India. 2000.
- Collins J.L., Fytas K. and Singhal R., *Design, construction and maintenance of surface mine haul roads*, in: Proc. of the Symposium on Geotechnical stability in Surface Mines, Calgary, Canada, 1986, pp. 39-49.

-
- Consoli N.C., Prietto P.D.M., Carraro J.A.H. and Heineck K.S., *Behavior of compacted soil-fly ash-carbide lime mixtures*, Journal of Geotechnical and Geoenvironmental Engineering, 127, (2001): pp. 774-782.
 - Croft J.B., The pozzolanic reactivities of some New South Wales fly ashes and their application to soil stabilization, Australian Road Research Board, Vermont South, Victoria, 2 (1964): pp. 1144-1168.
 - Das B., Principles of Geotechnical Engineering, 3rd ed., PWS- Kent Publishing Company, Boston, 1994.
 - Das S.C. and Prakash S., *Behaviour of lime stabilized Titagarh PFA through laboratory tests*, IE (I). Journal of civil, 70 (1990): pp. 181-186.
 - Das S.K. and Yudhbir, *Geotechnical properties of low calcium and high calcium fly ash*, Journal of Geotechnical and Geological Engineering, 24 (2006): pp. 249-263.
 - Davis R.E., *A review of pozzolanic materials and their use in cement concrete*, Special Technical Publication, ASTM, 99 (1949): pp. 3-15.
 - Dermatas D. and Meng X., *Utilization of fly ash for stabilization/solidification of heavy metal contaminated soils*, Journal of Engineering Geology, 70 (2003): pp. 377-394.
 - De Santayana F.P. and Mazo C.O., *Behaviour of fly ash in experimental embankments*, in: Proc. of Thirteenth Int. Conference on Soil Mechanics and Foundation Engineering, New Delhi, 1994, pp. 1603-1606.
 - Desai C.S. and Abel J.F., Introduction to the Finite Element Method, A numerical method for Engineering Analysis, 1st India ed., S.K. Jain for CBS publisher, 1987.

-
- DiGioia A.M., McLaren R.J., Burns D.L. and Miller D.E., Fly ash design manual for road and site application, vol. 1: Dry or conditioned placement, Manual prepared for EPRI, CS-4419, Research project 2422-2, Interim report, Electric Power Research Institute, Palo Alto, California, 1986.
 - Dimter S., Rukavina T. And Barisic I., *Application of the ultrasonic method in evaluation of properties of stabilized mixes*, The Baltic Journal of Road and Bridge Engg., 6 (2011): pp. 177-184.
 - Duncan J.M., Monismith C.L. and Wilson E.C., *Finite element analysis of pavements*, Highway Research Board, Highway Research Record 228 (1968): pp. 18-33.
 - Edil T.B., Benson C.H., Bin-Shafique Md S., Tanyu B.F., Kim W.H. and Senol A., Field evaluation of construction alternatives for roadway over soft subgrade, Transportation Research Board, 81th Annual Meeting, Washington, D.C., 02-3808, 2002.
 - Edil, T.B., Sandstrom L. K. and Berthouex, P.M., (1990). *Interaction of inorganic leachate with compacted pozzolanic fly ash*, Journal of Geotechnical Engg., ASCE, 118 (1992):pp.1410-1430.
 - Erol M., Genc A., Ovecoglu M.L., Yucelen E., Kucukbayrak S. and Taptik Y., *Characterization of a glass-ceramic produced from thermal power plant fly ashes*, Journal of European Ceramic Society, 20 (2000): pp. 2209- 2214.
 - Faluyi S.O. and Amu O.O., *Effects of Lime Stabilization on the pH Values of Lateritic Soils in Ado-Ekiti, Nigeria*, Journal of Applied Sci., 5 (2005): pp. 192-194.
 - Foster C.R. and Ahlvin R.G., Stress and deflections induced by a uniform non-circular load, in: Proc. of Highway Research Board, Vol. 33, Washington, DC, USA, 1954.

-
- Fung R., Surface mine haul road design. Surface mine engineering technology; engineering and environment aspects, Noyes Data Corp., USA, 1981.
 - Gatti G. and Tripiciano L., *Mechanical behaviour of coal fly ashes*, in: Proc. of 10th Int. conference on Soil mechanics and foundation engineering, Stockholm, 2 (1981): pp. 317-322.
 - Ghosh A. and Dey U., *Bearing ratio of reinforced fly ash overlying soft soil and deformation modulus of fly ash*, Journal of Geotextiles and Geomembranes, 27 (2009): pp. 313-320.
 - Ghosh A. and Subbarao C., *Strength characteristics of class F fly ash modified with lime and gypsum*, Journal of Geotech and Geoenviron Engg., ASCE, 133 (2007): pp.757-766.
 - Ghosh A. and Subbarao C., *Tensile Strength Bearing Ratio and Slake Durability of Class F Fly Ash Stabilized with Lime and Gypsum*, Journal of Materials in Civil Engg., ASCE, 18 (2006): pp. 18-27.
 - Ghosh A. and Subbarao C., *Microstructural development in fly ash modified with lime and gypsum*, Journal of Materials in Civil Engg., ASCE, 13 (2001): pp. 65-70.
 - Ghosh A. and Subbarao C., *Hydraulic conductivity and leachate characteristics of stabilized fly ash*, Journal of Environmental Engg., ASCE, 124 (1998): pp. 812-820.
 - Ghosh A., Environmental and engineering characteristics of stabilized low lime fly ash, Unpublished Ph.D thesis, Indian Institute of Technology, Kharagpur, India, 1996.

-
- Gidley J.S. and Sack W.A., *Environmental aspects of waste utilization in construction*, Journal of Environmental Engg., ASCE, 110 (1984): pp. 1117-1133.
 - Goh A.T.C. and Tay J. H., *Municipal solid-waste incinerator fly ash for geotechnical applications*, Journal of Geotechnical Engg., ASCE, 199 (1993): pp.811-825
 - Goktepe A.B., Sezer A., Sezer G.I. and Ramyar K., *Classification of time-dependent unconfined strength of fly ash treated clay*, Journal of Construction and Building Materials, 22 (2008): pp. 675-683.
 - Good Year, Good Year (PTY) Ltd., Kriel Colliery tyre load analysis, Kriel Colliery internal report, Kriel, USA, 1990.
 - Good Year, Tire Maintenance Manual, 2008.
 - Goswami R.K. and Mahanta C., *Leaching characteristics of residual lateritic soils stabilised with fly ash and lime for geotechnical applications*, Journal of Waste Management, 27 (2007): pp. 466-481.
 - Gray D.H. and Lin Y.K., *Engineering properties of compacted fly ash*, Journal of Soil Mech. Foundation Engng., ASCE, 98 (1972): pp. 361-380.
 - Heath W. and Robinson R., Review of published research into the formation of corrugations on unpaved roads. Transport and road research laboratory (TRRL) Supp report 620, Department of the Environment, Dept of Transport, Crowthorne, UK, 1980.
 - Hobeda P., Use of Waste Material from Coal Combustion in Road Construction, NTIS, 1984, Temimi M., Camps J.P. and Laquerbe M., *Valorization of fly ash in the*

-
- cold stabilization of clay materials*, Journal of Resources, Conservation and Recycling, 15 (1995): pp. 219-234.
- Hopkins T.C., Beckham T.L., Sun C. and Ni B., Resilient Modulus of Kentucky Soils. Research Report, Kentucky Transportation Centre, University of Kentucky, 2001.
 - Huang, W.H. and Lovell C.W., *Bottom ash as embankment material*, Geotechnics of waste fills – theory and practice, ASTM STP1070, A. Landva and G. D. Knowles, eds. American Society for Testing and Materials, Philadelphia, pp. 71-85.
 - Husrulid W. and Kuchta M., Openpit mine planning and design: Vol-I Fundamentals, 2nd ed., Taylor and Francis Plc., London, UK, 2006.
 - Indraratna B., Notalaya P., Koo K.S. and Kuganenthira N., *Engineering behaviour of a low carbon, pozzolanic fly ash and its potential as a construction fill*, Journal of Can. Geotech., 28 (1991): pp. 542-555.
 - Ismaiel H.A.H., Treatment and improvement of the geotechnical properties of different soft fine-grained soils using chemical stabilization, Unpublished Ph.D thesis, Martin Luther University Halle, Wittenberg, 2006.
 - Jackson N.M. Schultz S. Sander P. and Schopp L., *Beneficial use of CFB ash in pavement construction applications*, Journal of Fuel 88 (2009): pp. 1210-1215.
 - Jadhao P.D. and Nagarnaik P.B., *Strength Characteristics of Soil Fly Ash Mixtures Reinforced with Randomly Oriented Polypropylene Fibers*, in: proc. of First Int. Conference on Emerging Trends in Engineering and Technology, IEEE, DOI 10.1109/ICETET.2008.208, 2008, pp. 1044-1049.
 - Jha N.C., *Mining Industry and the people around*, Transactions of the mining geological and metallurgical institute of India, ISSN: 0371-9538, 107 (2011): pp. 1-11.

- Jones R., *The Nondestructive Testing of Concrete*, Magazine of Concrete Research 1(2), 1949.
- Joshi R.C., Duncan D.M. and Master Mc H.M., *New and conventional engineering uses of fly ash*, Journal of Transportation Engg., ASCE, 101 (1975): pp. 791-806.
- Kaliske M., Freitag S. and Oeser M., *Tire-Pavement Contact Modeling*, in: Proc. of the Symposium of Advances in Contact Mechanics (Prof. J.J. Kalker), Delft, Netherlands, 2008: pp. 22- 24.
- Kaniraj S.R. and Havanagi V.G., *Compressive strength of cement stabilized fly ash-soil mixtures*, Journal of Cement & Concrete Composites, 29 (1999): pp. 673-677.
- Kasaibati K., Burczyk J.M. and Whelan M.N., Effects of selecting subgrade resilient modulus on asphalt overlay design thicknesses, Transportation Research Record TRB No. 1473, Transportation Research Board National Research Council, Washington D.C., 1995.
- Kaufman W.W. and Ault J.C., Design of surface mine haulage roads – A manual. Information circular 8758, U.S. Department of Interior, Bureau of Mines, 1977.
- Kettil P., Lenhof B., Runesson K. and Wiberg N.E., *Simulation of inelastic deformation in road structures due to cyclic mechanical and thermal loads*, Journal of Computers and Structures, 85 (2007): pp. 59-70.
- Kewalramani M.A. and Gupta R., *Concrete compressive strength prediction using ultrasonic pulse velocity through artificial neural networks*, Journal of Automation in Construction, 15 (2006): pp. 374-379.

-
- Khanna K. and Justo C.E.G., Highway Engineering, 8th ed., Khanna Publishers, Roorkee, 2001.
 - Kim D.S., Kweon G.C and Rhee S., *Alternative method of determining resilient modulus of subbase soils using a static triaxial test*, Canadian Geotechnical Journal, 38 (2001): pp. 117-124.
 - Kim I. and Batchelor B., *Empirical partitioning leach model for solidified/ stabilized wastes*, Journal of Environmental Engg., ASCE, 127 (2001): pp. 188-195.
 - Krishna K.C., CBR behaviour of fly ash-soil-cement mixes, Unpublished Ph.D thesis, Indian Institute of Science, Bangalore, India, 2001.
 - Kumar M.A. and Raju G.V.R.P., *Use of lime cement stabilized pavement construction*, Indian Journal of Engineering & Materials Sc., 16 (2009): pp. 269-276.
 - Kumar S. and Patil C.B., *Estimation of resource savings due to fly ash utilization in road construction*, Journal of Resources, Conservation and Recycling, 48 (2006): pp. 125-140.
 - Kumar V., Design and construction of haul roads using fly ash, Unpublished M.S thesis, University of Alberta, Canada, 2000.
 - Kumar V., *A comprehensive model for fly ash handling and transportation for mining sector*, in: Proc. of Fly ash an opportunity for Mining Sector, New Delhi, India, 2010, pp. 186-189.
 - Laguros J.G. and Zenieris P., Feasibility of using Fly ash as a binder in coarse and fine aggregate for bases. University of Oklahoma, Norman, Oklahoma. *Report No. ORA*, 1987, pp. 155- 404.

- Lav A.H. and Lav M.A., *Microstructural development of stabilized fly ash pavement base material*. Journal of Mater. in Civil Engg., 12 (2000): pp. 157-163.
- Lav A.H., Lav M.A. and Goktpe A.B., *Analysis and design of a stabilized fly ash as pavement base material*, Journal of Fuel, 85 (2006): pp. 2359-2370.
- Leonards G.A. and Bailey B., *Pulverized coal ash as structural fill*, Journal of Geotech. Engg. Div., ASCE, 108 (1982): pp. 517-531.
- Leslie R. and Cheesmam W., *An Ultrasonic Method of studying Deterioration and Cracking in Concrete Structures*, Journal of American Concrete Institute (1949).
- Mackos R., Butalia T., Wolfe W. and Walker H.W., *Use of lime-activated class F fly ash in the full depth reclamation of asphalt pavements: environmental aspects*, in: Proc. of World of Coal Ash Conference '09, Lexington, Kentucky, USA, 2009, paper no 121.
- Malhotra V.M., *Fly ash in concrete*. 2nd ed., Ottawa, Canada, CANMET Publication on Concrete, 1994.
- Malhotra V., *Testing Hardened Concrete: Nondestructive Methods*, 1st ed., Iowa State University Press, 1976, pp. 188.
- Marshek D.B., *The selection of gravels for use on unsealed access roads*, in: Proc. of Australian IMM conference on off- highway truck haulage, Mt Newman, Australia, 1982: pp. 23-31.

-
- McLaren R.J. and DiGioia A.M., *The typical engineering properties of fly ash*, in: Proc. of conf. on geotechnical practice for waste disposal: Geotechnical special publication No. 13, ASCE, Wood. R.D. (ed.), New York, 1978, pp. 683-697.
 - Meyers J.F., Pichumani R. and Kapples B.S., Fly ash as a construction material for Highways, Report No. FHWA-FP-76-16, US Department of Transportation, Washington D.C. USA, 1976.
 - Michelin, Michelin Truck Tire Service Manual, Michelin North America, Inc., Greenville, South Carolina, USA, 2005.
 - Mingkai Z., Weiguo S., Shaopeng W. and Qinglin Z., Study on phosphogypsum fly ash lime solidified material, Journal of advances in building technology, 1 (2002): pp. 929-934.
 - Mining officials, Personal Communication, Bharatpur opencast project, Mahanadi Coalfields Limited, 2008.
 - Ministry of Coal, The Export Committee Report part II on Road Map for Coal Sector Reforms, Govt. of India, New Delhi, 2007.
 - Minnick L.J., *Fundamental characteristics of pulverized coal fly ashes*, in: Proc. of ASTM, 59 (1959): pp. 1155-1177.
 - Mishra M.K., Experimental and Numerical analysis of behaviour of model pillars trapped with reinforced fly ash composites, Unpublished Ph.D thesis, Indian Institute of Technology, Kharagpur, India, 2003.

-
- Mishra S.R., Kumar S., Park A., Rho J., Losby J. and Hoffmeister B.K., *Ultrasonic characterization of the curing process of PCC fly ash*, Journal of Materials Characterization, 50 (2003): pp. 317-323.
 - Mishra M.K. and Rao K.U.M., *Geotechnical Characterisation of Fly ash Composites for Backfilling Mine Voids*. Journal of Geotech and Geol Engg., 24 (2006): pp. 1749-1765.
 - Misra A., Cold-in-place recycling of asphalt pavements using self-cementing fly ash: analysis of pavement performance and structure number, Final Report for Combustion By-products recycling Consortium, West Virginia University, Virginia, 2008.
 - MOEF, Gazette notification for Ministry of Environment and Forests. no. 563, Ministry of Environment and Forests, New Delhi, India 1999.
 - Mohammad L.N., Titi H.H. and Herath A., Intrusion technology: An innovative approach to evaluate resilient modulus of subgrade soils Application of Geotechnical Principles in Pavement engineering, American Society of Civil Engineers, Geotechnical Special Publication Number, 85 (1998): pp. 39-58.
 - Mohanty S. and Chugh Y.P., *Structural Performance Monitoring of an unstabilised Fly ash based road subbase*, Journal of Transportation Engineering, 132 (2006): pp. 964-969.
 - Morgan J.R., Tucker J.S. and McInnes D.B., A mechanistic design approach for unsealed mine haul roads, Pavement Design and Performance in Road Construction 1412 (1994): pp. 69-81.
 - Moulder E., *A mixture of fly ashes as road base construction material*, Journal of Waste Management, 16 (1996): pp. 15-20.

-
- Moulton K.L., *Technology and utilization of power plant ash in structural fills and embankments*, West Virginia University, Morgantown W.V., 1978.
 - Nahi M.H., Ismail A. and Ariffin A.K., *Analysis of Asphalt Pavement under nonuniform Tire-pavement Contact Stress using Finite Element Method*, Journal of Applied Sciences, 11 (2011): pp. 2562-2569.
 - Nicholson P., Kashyap V. and Fugi C., Lime and fly ash admixture improvement of tropical Hawaiian soils, Transportation Research Record, Washington, DC, Report No 1440, 1994.
 - Pandian N. S., Rajasekhar C. and Sridharan A.,(1995). *Fly ash-lime systems for the retention of lead ions*, in: Proc. of Indian Geotechnical conference, Bangalore, 1 (1995): pp.219-222.
 - Pandian N.S., *Fly ash characterization with reference to geotechnical applications*, Journal of Indian Inst. of Sc., 84 (2004): pp. 189-216.
 - Pandian N.S. and Balasubramonian S., *Leaching studies on ASTM type F fly ashes by an accelerated process method*, Journal of Testing Evaluation, ASTM, 28 (2000): pp. 44-51.
 - Pandian N.S., Rajasekhar C. and Sridharan A., Studies on the specific gravity of some Indian coal ashes, Journal of Testing and Evaluation, ASTM, 26 (1998): pp. 177-186.
 - Pandian N.S. and Balasubramonian S., *Permeability and consolidation behaviour of fly ashes*, Journal of Testing and Evaluation, ASTM, 27 (1999): pp. 337-342.
 - Pandian N.S., Sridharan A. and Srinivas S., *Angle of internal friction for pond ashes*, Journal of Testing and Evaluation, ASTM, 28 (2000): pp. 443-454.

- Pandian N.S. and Balasubramonian S., *Leaching behaviour of Indian fly ashes by Oedometer method*, Journal of Testing Evaluation, ASTM, 28 (2000): pp. 403-408.
- Ping V.W., Implementation of the Resilient Modulus in the State of Florida Flexible Pavement Design Procedure, 2001.
- Poran C. J. and Ahtchi-Ali, F. *Properties of solid waste incineration fly ash*, Journal of Geotech. Engg., ASCE, 115 (1998): pp. 1119-1133.
- Porter O.J., The preparation of sub-grades. in: Proc. of the Highway Research Board, Washington, 18 (1938): pp. 324-331.
- Porter O.J. Development of the original method for highway design, in: Proc. of the American Society of Civil Engineers, 75 (1949): pp. 11-17.
- Prabakar J., Dendorkar N. and Morchhale R.K., *Influence of fly ash on strength behavior of typical soils*, Journal of Construction and Building Materials, 18 (2004): pp.263-267.
- Queralt I., Querol X., Lopez-Soler A. and Plana F., *Use of coal fly ash for ceramics: a case study for a large Spanish power station*, Journal of Fuel, 76 (1997): pp. 787-791.
- Rahim A.M. and George K.P., Automated Dynamic Cone Penetrometer for Subgrade Resilient Modulus Characterization. Transportation Research Record No 1806, Transportation Research Board, National Research Council, 2002, pp. 70-77.
- Rai A.K., Paul B. and Singh G., *A study on physico chemical properties of overburden dump materials from selected coal mining areas of Jharia coalfields, Jharkhand, India*, Int. Journal of Environmental Sc., 1 (2011): pp. 1350-1360.

- Rehsi S.S. and Garg S.K., *Characteristics of Indian fly ashes*, in: Proc. of National workshop on utilization of fly ash, Roorkee, 1988: pp. 131-135.
- Roode M.V., *X-ray diffraction measurement of glass content in fly ashes and slag*, Journal of Concr. Res., 17 (1987): pp. 183-197.
- Sahay A.N., *R&D initiatives in utilization of fly ash in coal sector*, in: Proc. of Fly ash an opportunity for Mining Sector, New Delhi, India, 2010, pp. 26-35.
- Sahu B.K., *Improvement in California Bearing Ratio of Various Soils in Botswana by Fly Ash*, in: Proc. of Int. Ash Utilization Symposium, Centre for Applied Energy Research, University of Kentucky, Paper No. 90, 2001.
- Sahu B.K., *Use of fly ash for stabilizing sub-standard road construction materials in Botswana*, in: Proc. of Fly ash India 2005, Fly ash Utilisation Programme, TIFAC, DST, New Delhi, 2005, pp. VIII 10.1-10.9.
- Sen Gupta J., *Characterization of Indian coal ash and its utilization as building material*, in: Proc. Int. Conf. on Environmental Impact of Coal Utilization from Raw Materials to Waste Resources (K. C. Sahu, ed.), Indian Institute of Technology, Bombay, 1991: pp.165-184.
- Senol A., Edil T.B, Bin-Shafique M.S., Acosta H.A and Benson C.H., *Soft Subgrades' stabilization by using various fly ashes*, Journal of Resources, Conservation and Recycling, 46 (2006): pp. 365-376.
- Shen W., Zhou M. and Zhao Q., *Study on lime-fly ash-phosphogypsum binder*, Journal of Construction and Building Materials, 21 (2007): pp. 1480-1485.

-
- Shen W., Zhou M., Ma W., Hu J. and Cai Zhi., *Investigation on the application of steel slag-fly ash-phosphogypsum solidified material as road base material*, Journal of Hazardous Materials, 164 (2009): pp. 99-104.
 - Shenbaga R.K. and Gayathri V., *Permeability and consolidation characteristics of compacted fly ash*, Journal of Energy Engineering, 130 (2004): pp. 18-43.
 - Sherwood P.T. and Ryley M.D., *Use of stabilized pulverized fuel ash in road construction*, Road Research Laboratory Report, Ministry of Transport, UK, 49 (1966): pp. 1-44.
 - Siddharthan R., Norris G.M. and Epps J.A., *Use of FWD data for pavement material characterization and performance*, Journal of Transport Engg., ASCE, 117 (1991): pp.660-678.
 - Singh D.N., *Influence of chemical constituents of fly ash characteristics*, in: Proc. of Indian Geotechnical Conference, Madras, 1996, pp. 227-230.
 - Singh R.N. and Ghosh A.K., *Engineering Rock Structure in Mining and Civil Construction*, ISBN 0415 400139, Taylor & Francis Group Plc., London, UK, 2006.
 - Singh D.N. and Kolay P.K., *Simulation of ash-water interaction and its influence on ash characteristics*, Progress in Energy and Combustion Science, 28 (2002): pp. 267-299.
 - Singh S.P and Kumar P., *Utilisation of fibre reinforced fly ash in road sub-bases*, in: Proc. on Fly ash India 2005, Fly ash Utilisation Programme, TIFAC, DST, New Delhi, 2005, pp. VIII 17.1-17.8.

-
- Siswosoebrotho B.I., Younger J.S. and Erwanto T., *Compaction and CBR strength characteristics of Karimun Island granite mixed with Suralaya pulverized fuel ash*, in: Proc. of the Eastern Asia Society for Transportation Studies, 4 (2003): pp. 302-312.
 - Sivapullaiah P.V., Prashanth J.P. and Sridharan A., *Optimization of lime content for fly ash*, Journal of Testing and Evalu., 23 (1995): pp. 222-227.
 - Sobhan K. and Mashnad M., *Tensile Strength and Toughness of Soil-Cement-Fly-Ash Composite Reinforced with Recycled High-Density Polyethylene Strips*, Journal of Materials in Civil Engineering, ASCE, 14 (2002): pp. 177-184.
 - Soliman N.N., Laboratory testing of lime fixed fly ash and FGD sludge. Geotechnics of Waste Fills – Theory and Practices, ASTM STP 1070, Philadelphia, American Society for Testing and Materials, 1990.
 - Solis-Carcano R. and Moreno E. I., *Evaluation of concrete made with crushed limestone Aggregate Based on Ultrasonic Velocity*, Journal of Construction and Building Materials 22 (2008): pp. 1225-1231.
 - Sridharan A. and Prakash K., *Geotechnical Engineering Characterization of Coal Ashes*, 1st ed., S.K. Jain for CBS Publishers, New Delhi, 2007.
 - Sridharan A., Pandian N.S. and Chitti Babu G., Strength behaviour of Indian coal ashes, Technical report of task force on Characterisation of fly ash submitted to Technology Mission-Fly ash disposal and utilization, Dept. of Science and Technology, Govt. of India, vol. 4, 2001a.
 - Sridharan A., Pandian N.S. and Srinivas S., Compaction behaviour of Indian coal ashes, Technical report of task force on Characterisation of fly ash submitted to Technology Mission-Fly ash disposal and utilization, Dept. of Science and Technology, Govt. of India, vol.3, 2001b.

-
- Sridharan A., Pandian N.S. and Srinivas S., *CBR behaviour of Indian coal ashes*, Technical report of task force on Characterisation of fly ash submitted to Technology Mission-Fly ash disposal and utilization, Dept. of Science and Technology, Govt. of India, Vol. 5, 2001c.
 - Sridharan A., Pandian N.S. and Srinivas S., *Compaction behaviour of Indian coal ashes*, Ground Improvement, London, 4 (2000): pp. 1-10.
 - Sridharan A., Rajasekhar C. and Pandian N.S., *Fly ash as pre-filter material for zinc ions*, in: Proc. of Indian Geotechnical conference, Warangal 1994, pp.79- 82.
 - Sridharan A., Pandian N.S. and Prasad P.S., *Liquid Limit Determination of Class F Coal Ash*, Journal of Testing and Evaluation, ASTM, 28 (2000): pp. 455-461.
 - Stankus J.C. and Gou S., Computer Automated Finite Element Analysis – A powerful tool for Fast Mine Design and Ground Control Problem Diagnosis and Solving, www.jennmar.com, 2001, pp.1-12
 - Tannant D.D. and Regensburg B., Guidelines for mine haul road design. 1st ed., University of Alberta, Canada, 2001.
 - Tannant D.D. and Kumar V., *Properties of fly ash stabilized haul road construction Materials*, Int. Journal of Surface. Mining, Reclamation Environ., 14 (2000): pp. 121-135.
 - Temimi M., Rahal M.A., Yahiaoui M. and Jauberthie R., *Recycling of fly ash in the consolidation of clay soils*, Journal of Resources, Conservation and Recycling, 24 (1998): pp. 1-6.

-
- Thompson R.J. and Visser A.T., Mine haul road maintenance management systems, Journal of The South African Institute of Mining and Metallurgy, ISSN 0038-223X/3.00 + 0.00, 2003, pp. 303-312.
 - Thompson R.J. and Visser A.T., An overview of the structural design of mine haul roads, Journal of the South African Institute of Mining and Metallurgy, SA ISSN 0038-223X/3.00+0.00, 1996, pp. 29-37.
 - Thompson R.J., The Design and Management of Surface Mine Haul Roads, Unpublished Ph.D. thesis, Faculty of Engineering, University of Pretoria, 1996.
 - Thompson R.J. and Visser A.T., A mechanistic structural design procedure for surface mine haul roads. International Journal of Surface Mining, Reclamation and Environment 11 (1997): pp.121-128.
 - Throne D.J. and Watt J.D., Composition and pozzolanic properties of pulverized fuel ashes, II. *Pozzolanic properties of fly ashes as determined by crushing strength tests on lime mortars*, Journal of Appl. Chem., 15 (1965): pp. 595-604.
 - Toth P.S., Chan H.T. and Cragg C.B., *Coal ash as structural fill with special reference to Ontario experience*, Can. Geotech. Journal, 25 (1988): pp. 694-704
 - Toth P.S., Chan, H.T. and Cragg C.B., *Coal ash as structural fill with special reference to Ontario experience*, Canadian Geotechnical Journal, 25 (1988): pp. 694-704.
 - Turgut P., *Masonry composite material made of limestone powder and fly ash*, Journal of Powder Technology, 204 (2010): pp. 42-47.

-
- Turnbull W.J. and Ahlvin R.G., *Mathematical expression of the CBR relationships*, in: Proc. of 4th Int. Conf. on Soil Mech. and Foundation Engg., London, UK, 2 (1957): pp. 178.
 - Ulusay R., Arlkan F., Yoleri M.F. and Caglan D., *Engineering geological characterization of coal mine waste material and an evaluation in the context of back-analysis of spoil pile instabilities in a strip mine, SW Turkey*, Journal of Engineering Geology, 40 (1995): pp. 77-101.
 - US EPA, Solid Waste Leaching Procedure Manual. Cincinnati, OH. SW-924, US Environmental Protection Agency, 1985.
 - Vasquez E. and Alonso E.E., *Fly ash stabilization of decomposed granite*, X ICSMFE. 2 (1981): pp. 391-395.
 - Vesperman K.D., Edil T.B. and Berthouex P.M., *Permeability of Fly Ash and Fly Ash-Sand Mixtures*, Hydraulic Barriers in Soil and Rock, ASTM STP 874, American Society for Testing and Materials, Philadelphia, 1985, pp. 289-298.
 - Vishwanathan R., Saylak D. and Estakhri C., *Stabilization of subgrade soils using fly ash*, in: Proc. of the Int. Ash Utilization Symposium, Lexington, Kentucky, 1997, pp. 204-211.
 - Vittal U.K.G. and Mathur S. Enhancement of haul road serviceability by using fly ash, in: Proc. of the Fly ash an opportunity for Mining Sector, New Delhi, India, 2010, pp. 136-143.
 - Vittal U.K.G. and Mathur S., *Construction of rural roads using fly ash-some case studies*, in: Proc. of the Fly ash India 2005, Fly ash Utilisation Programme, TIFAC, DST, New Delhi, 2005, pp. VIII 2.1-2.8.

- Wade N.H., Design Manual for Surface Mine Haul Roads, Monenco Consultant Limited, Calgary, Alberta, 1989.
- Wang Y., Ren D. and Zhao F., *Comparative leaching experiments for trace elements in raw coal, laboratory ash, fly ash and bottom ash*, International Journal of Coal Geolog, 40 (1999): pp. 103-108.
- Yesiller N., Hanson J.L. and Usmen M.A., *Ultrasonic Assessment of Stabilized Soils*, in: Proc. Of the ASCE Geo Institute Soft Ground Technology (GSP 112): pp. 170-181.
- Yoder E.J. and Witczak M.W., Principles of Pavement Design, 2nd ed., Wiley, New York, 1975.
- Yudhbir and Honjo Y., *Applications of geotechnical engineering to environmental control*, in: Proc. of 9th Asian Reg. Conf. on S. M. & F. E., Bangkok, Thailand, 2 (1991): pp.431-469.

APPENDIX

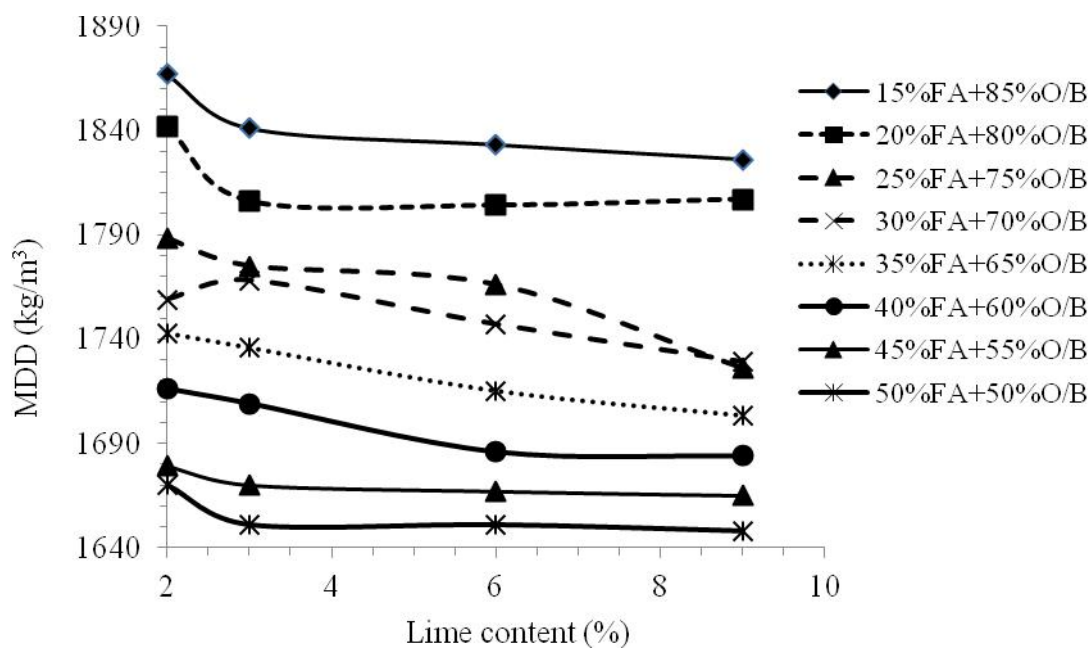


Figure 4.40: Variation of maximum dry density with lime content

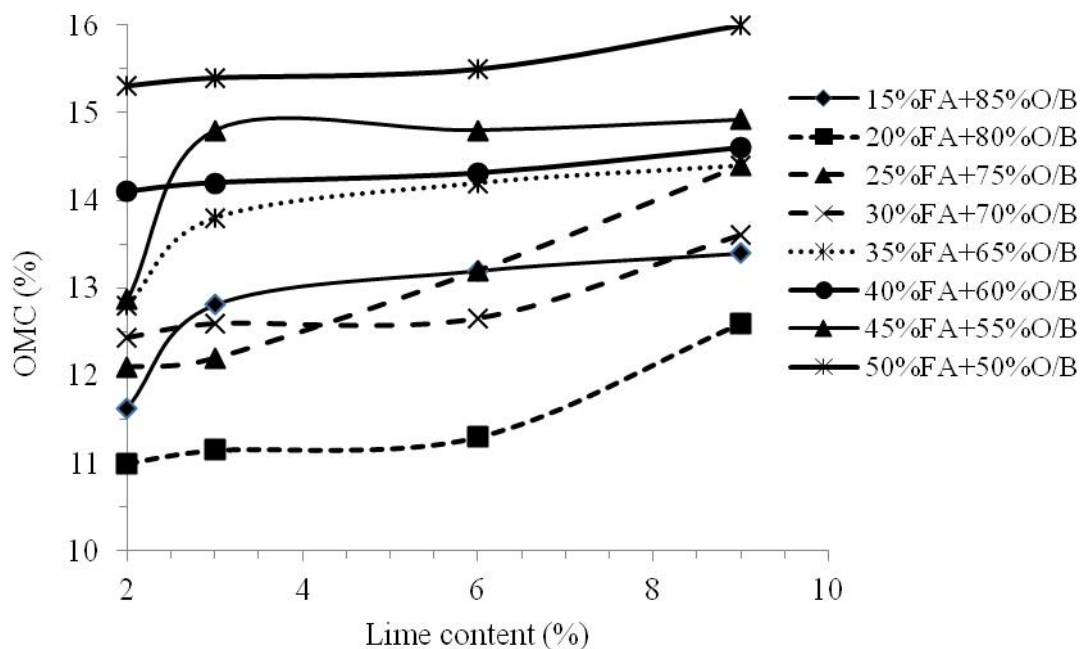


Figure 4.41: Variation of optimum moisture content with lime content

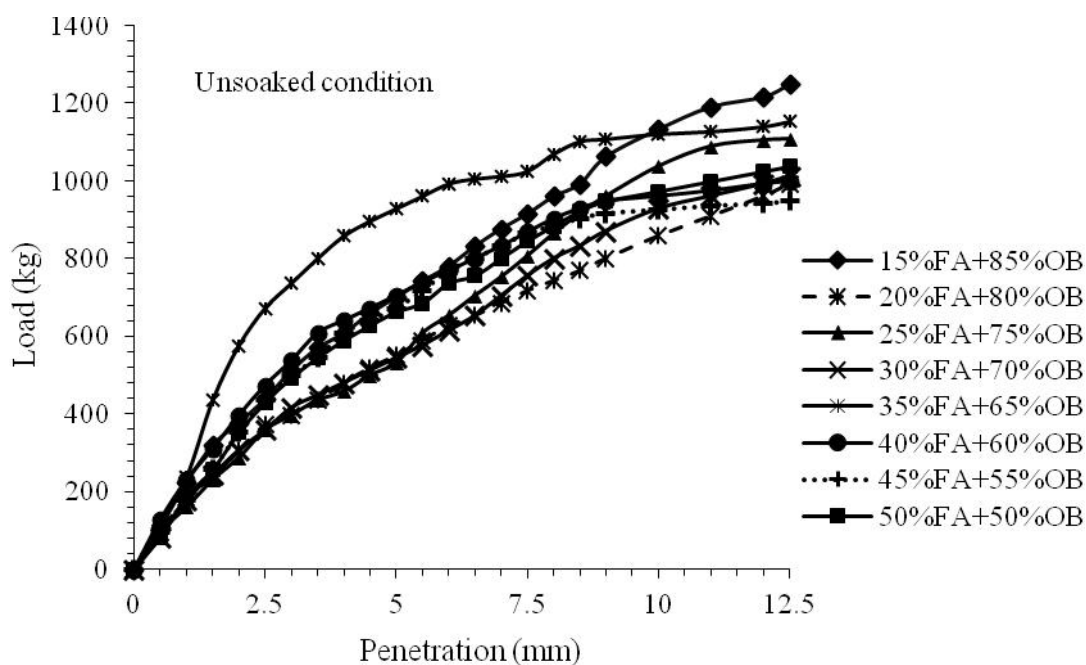


Figure 4.42: Load vs penetration curves of untreated composites in unsoaked condition

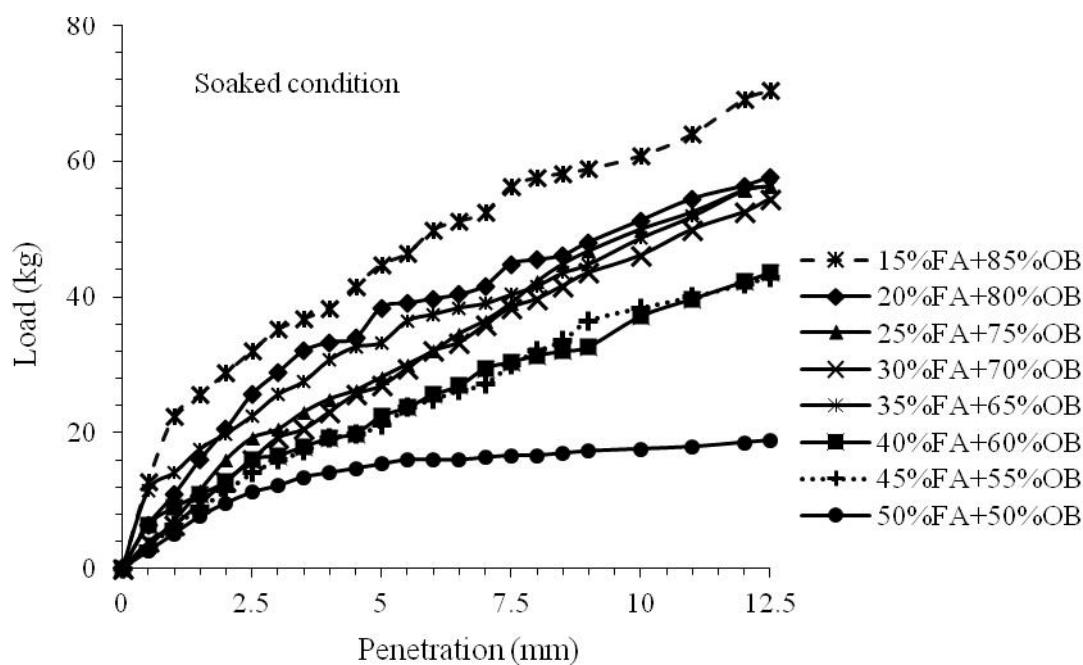


Figure 4.43: Load vs penetration curves of untreated composites in soaked condition

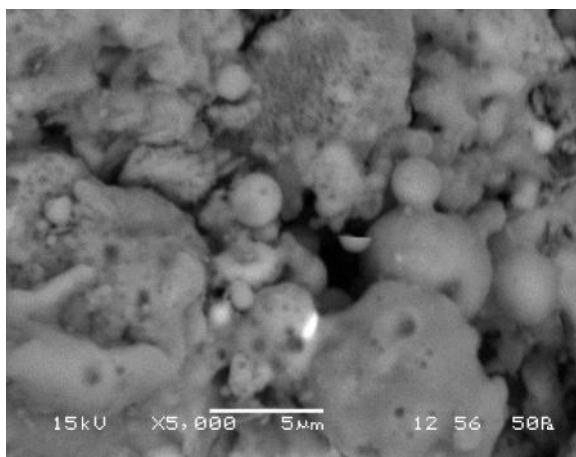


Figure 4.44 (a): SEM photograph of (15FA+85O/B) +3L

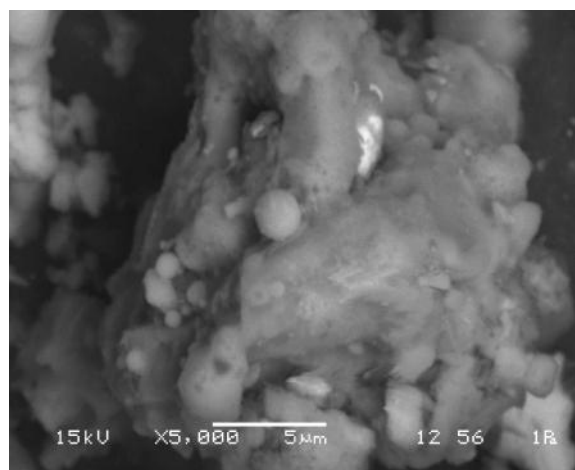


Figure 4.44 (d): SEM photograph of (20FA+80O/B) +9L

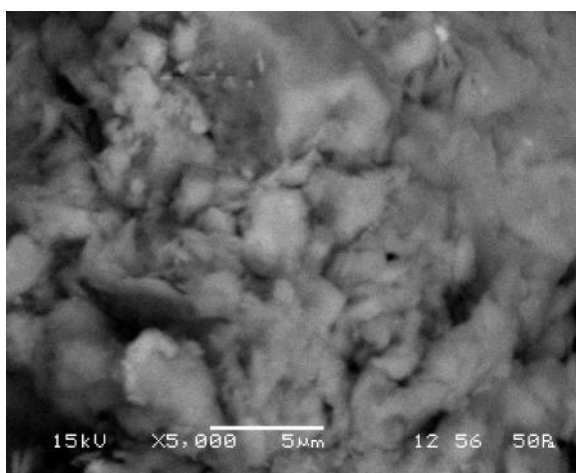


Figure 4.44 (b): SEM photograph of (15FA+85O/B) +6L

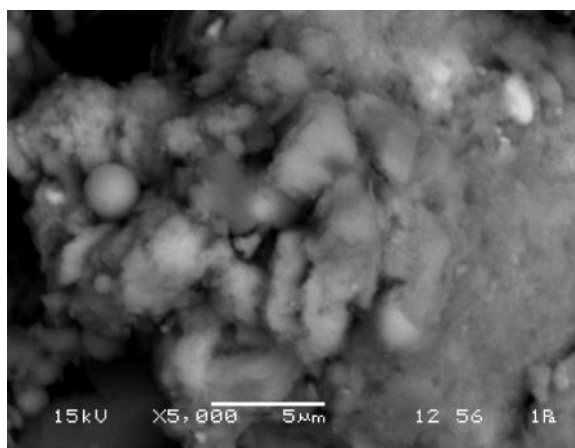


Figure 4.44 (e): SEM photograph of (25FA+75O/B) +9L



Figure 4.44 (c): SEM photograph of (20FA+80O/B) +6L

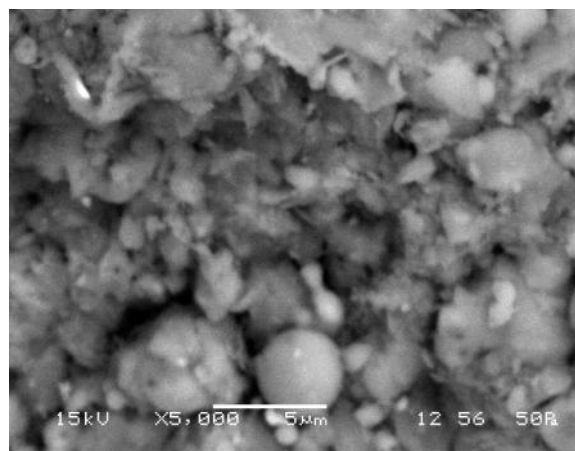


Figure 4.44 (f): SEM photograph of (30FA+70O/B) +2L

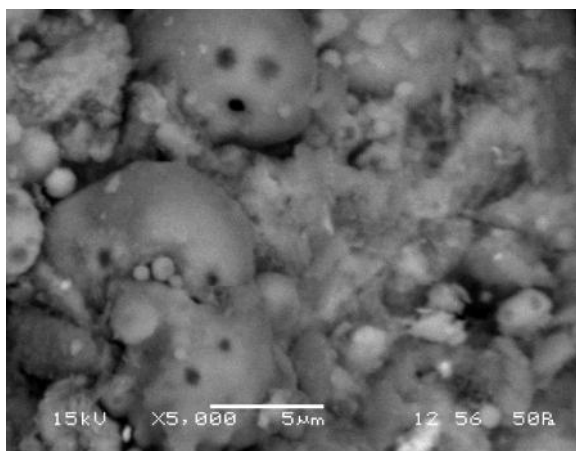


Figure 4.44 (g): SEM photograph of (30FA+70O/B) +3L

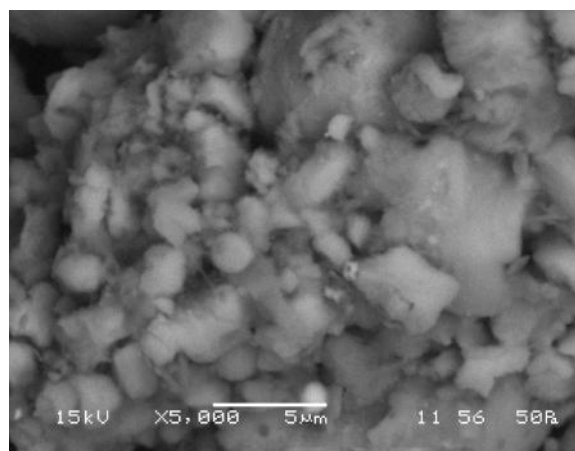


Figure 4.44 (j): SEM photograph of (40FA+60O/B) +9L

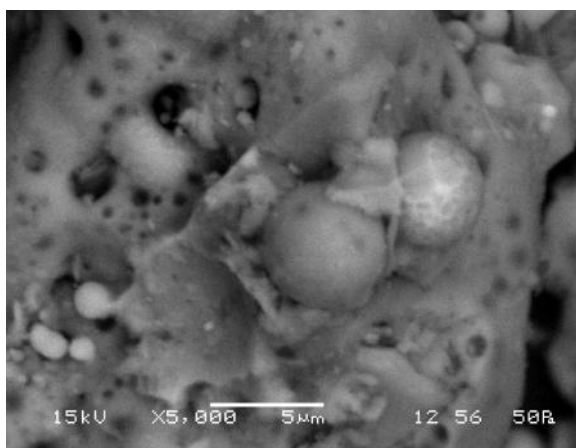


Figure 4.44 (h): SEM photograph of (35FA+65O/B) +2L

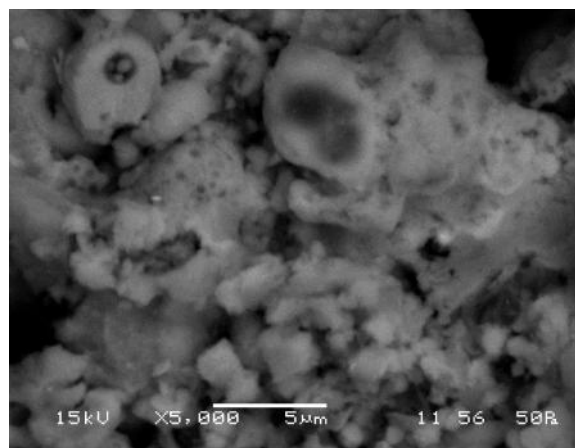


Figure 4.44 (k): SEM photograph of (45FA+55O/B) +9L

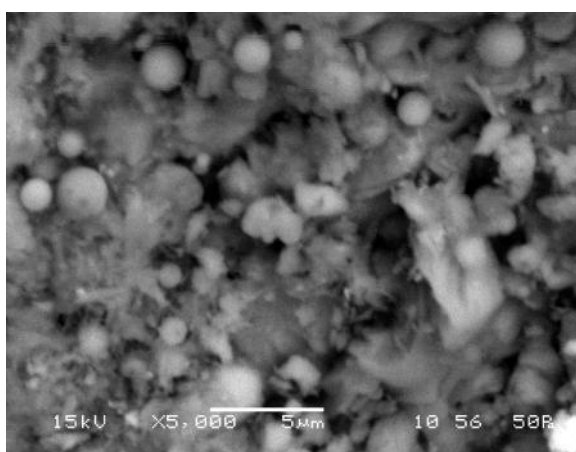


Figure 4.44 (i): SEM photograph of (35FA+65O/B) +6L

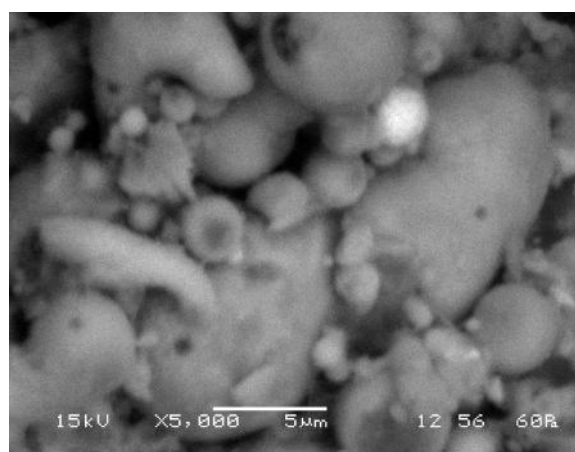


Figure 4.44 (l): SEM photograph of (50FA+50O/B) +9L

Figure 4.44: SEM photographs of fly ash composites at 28 days curing

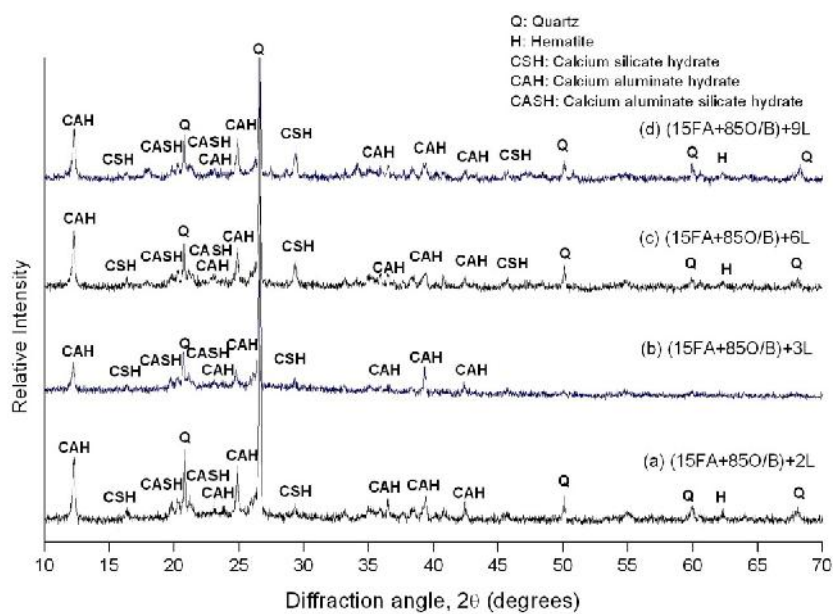


Figure 4.45 (a): XRD patterns of (15FA+85O/B) stabilised with 2, 3, 6 and 9% lime

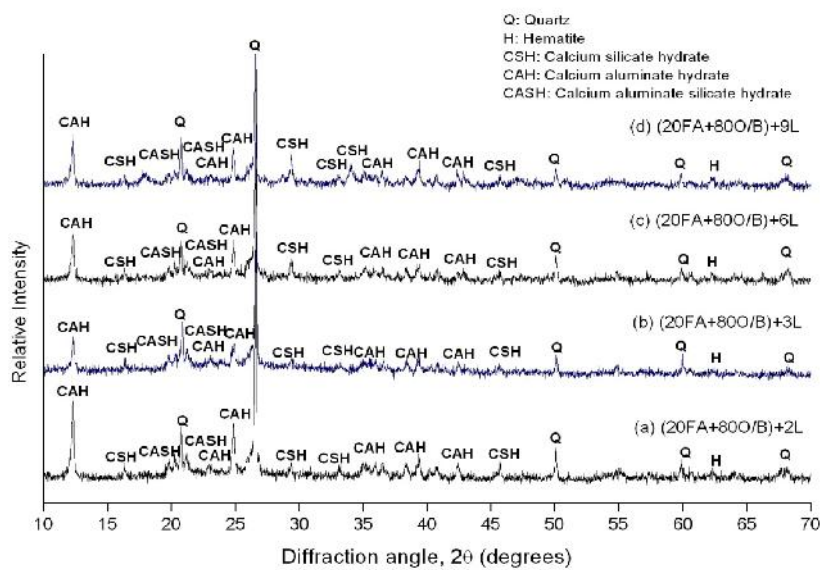


Figure 4.45 (b): XRD patterns of (20FA+80O/B) stabilised with 2, 3, 6 and 9% limes

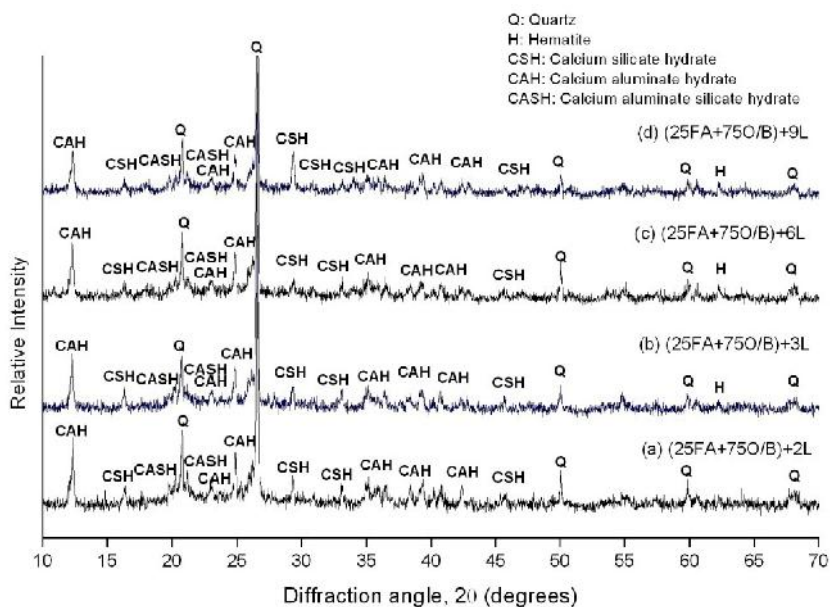


Figure 4.45 (c): XRD patterns of (25FA+75O/B) stabilised with 2, 3, 6 and 9% lime

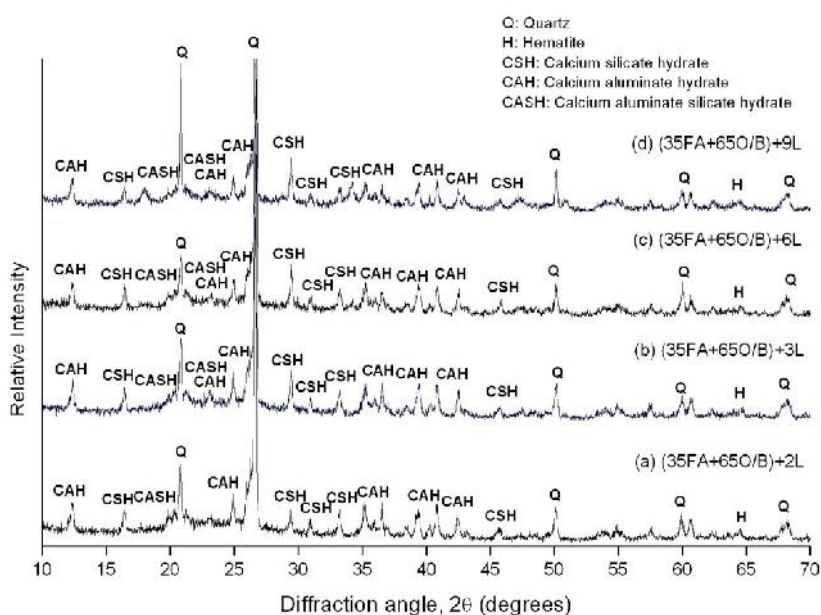


Figure 4.45 (d): XRD patterns of (35FA+65O/B) stabilised with 2, 3, 6 and 9% lime

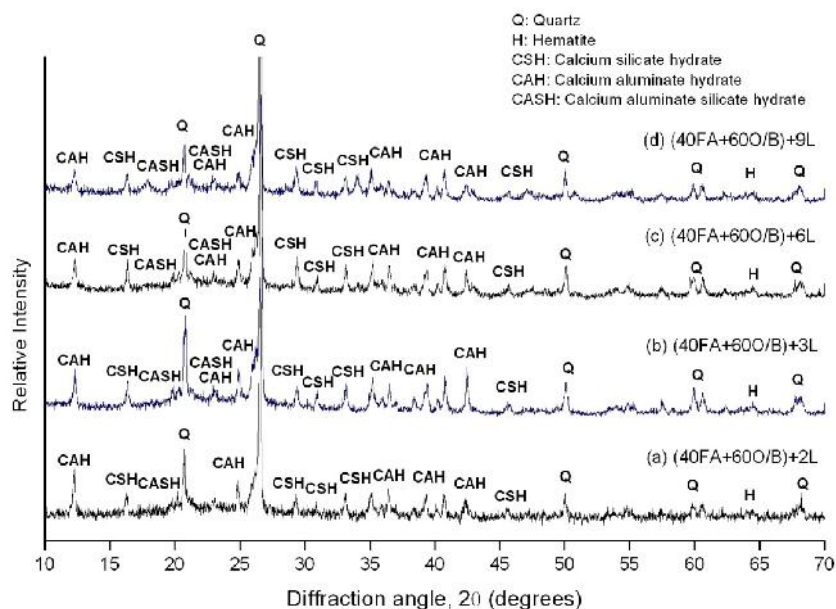


Figure 4.45 (e): XRD patterns of (40FA+60O/B) stabilised with 2, 3, 6 and 9% lime

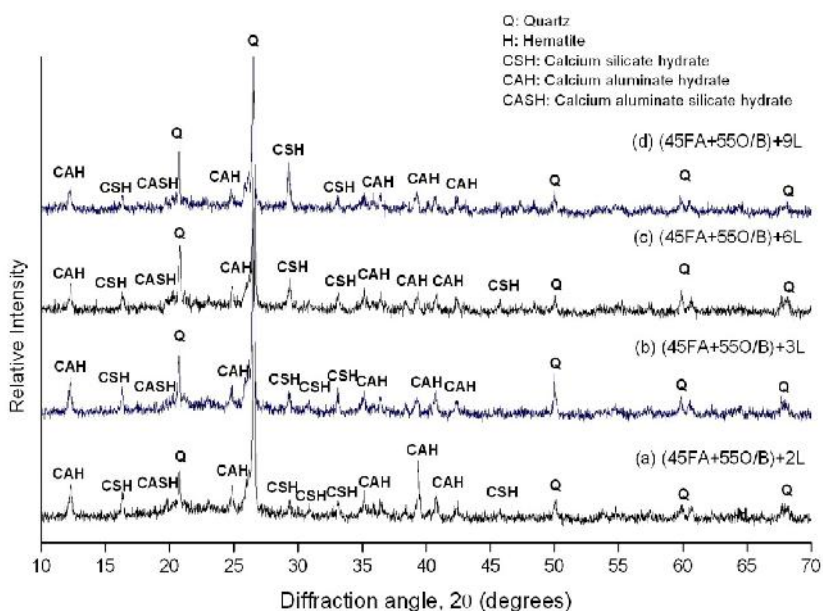


Figure 4.45 (f): XRD patterns of (45FA+55O/B) stabilised with 2, 3, 6 and 9% lime

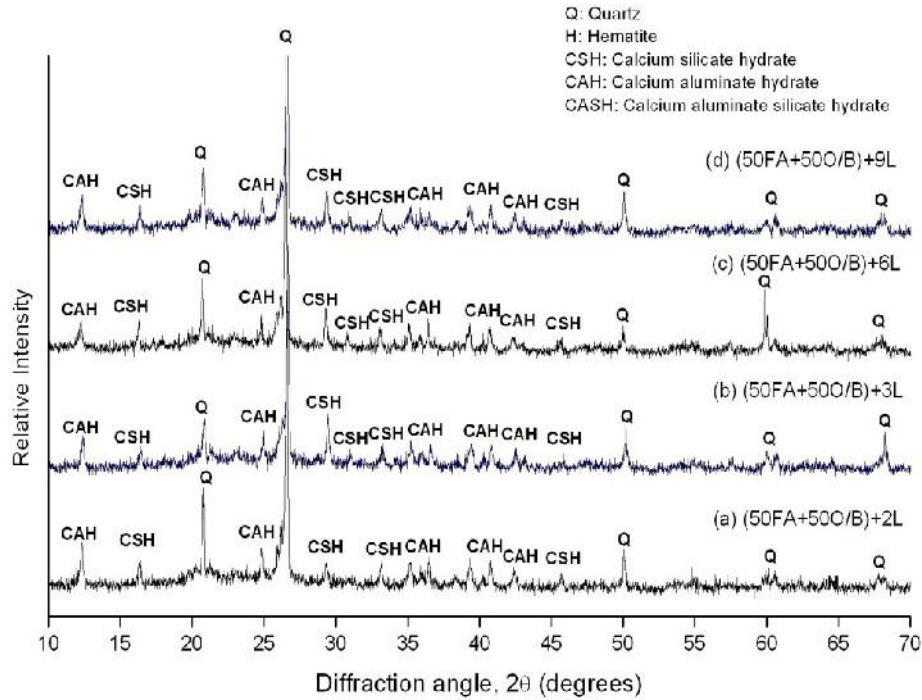


Figure 4.45 (g): XRD patterns of (50FA+50O/B) stabilised with 2, 3, 6 and 9% lime

Figure 4.45: XRD patterns of fly ash composites at 28 days curing

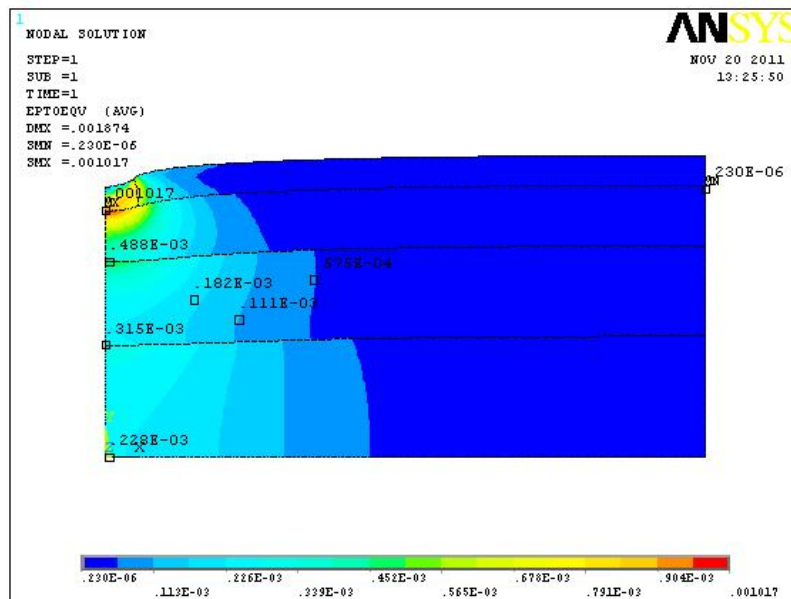


Figure 5.12 (a): Total strain at various layers of haul road pavement with ((15FA+85O/B)+9L) composite

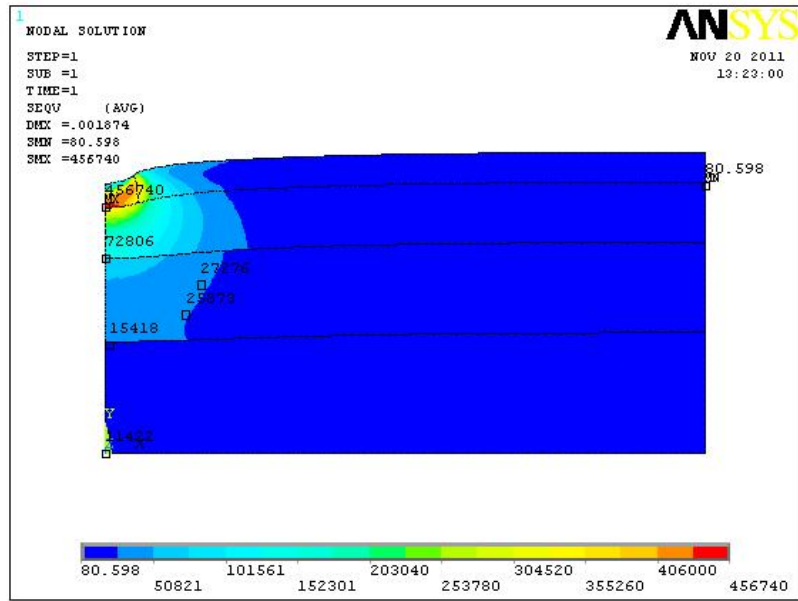


Figure 5.12 (b): Total stress at various layers of haul road pavement with ((15FA+85O/B)+9L) composite

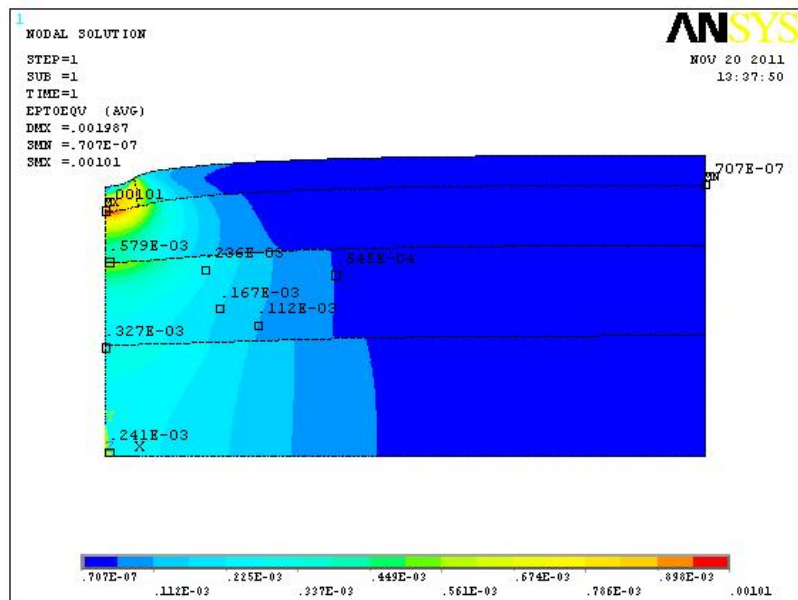


Figure 5.12 (c): Total strain at various layers of haul road pavement with ((20FA+80O/B)+3L) composite

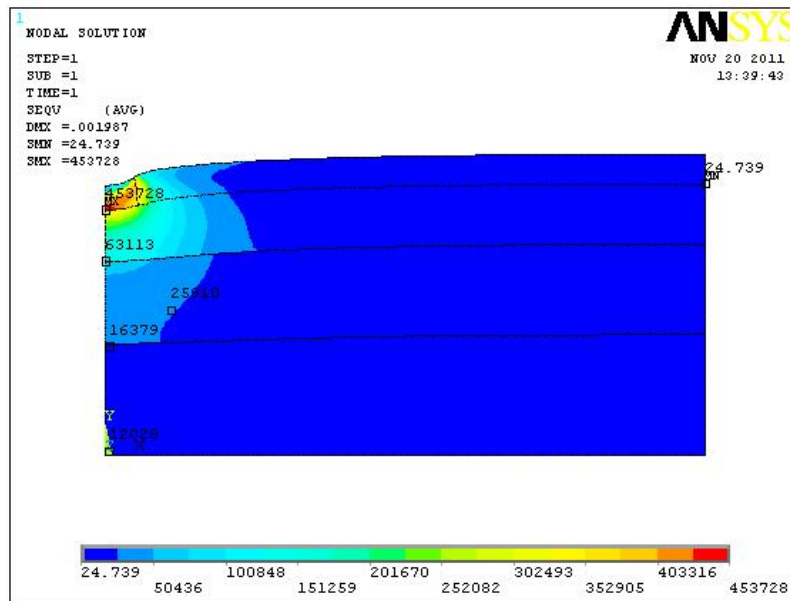


Figure 5.12 (d): Total stress at various layers of haul road pavement with ((20FA+80O/B)+3L) composite

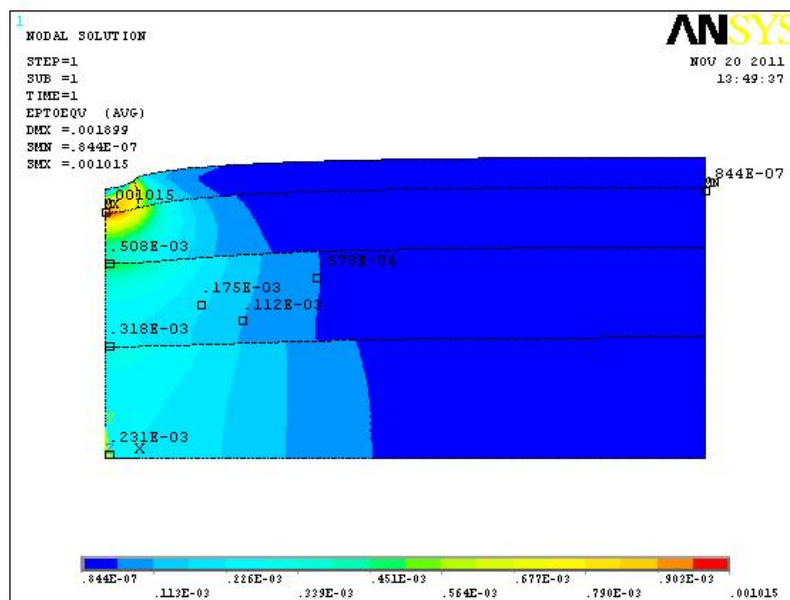


Figure 5.12 (e): Total strain at various layers of haul road pavement with ((20FA+80O/B)+9L) composite

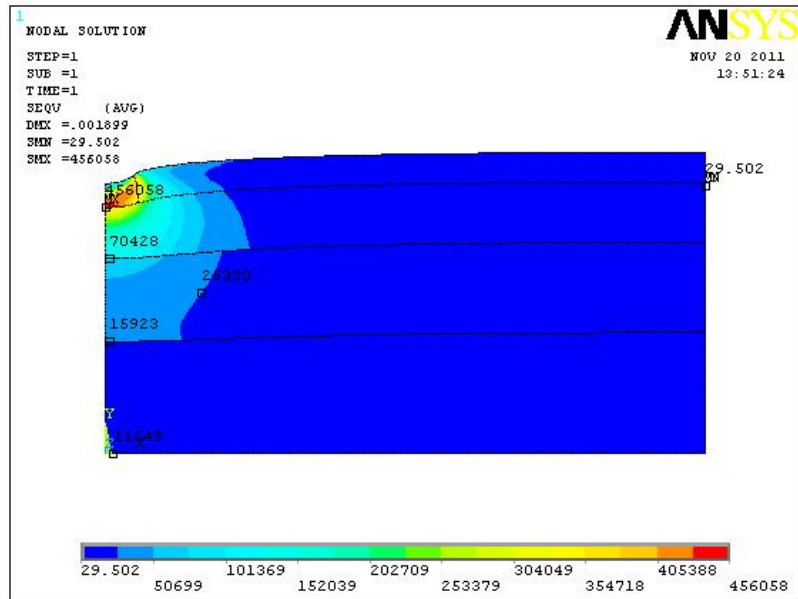


Figure 5.12 (f): Total stress at various layers of haul road pavement with ((20FA+80O/B)+9L) composite

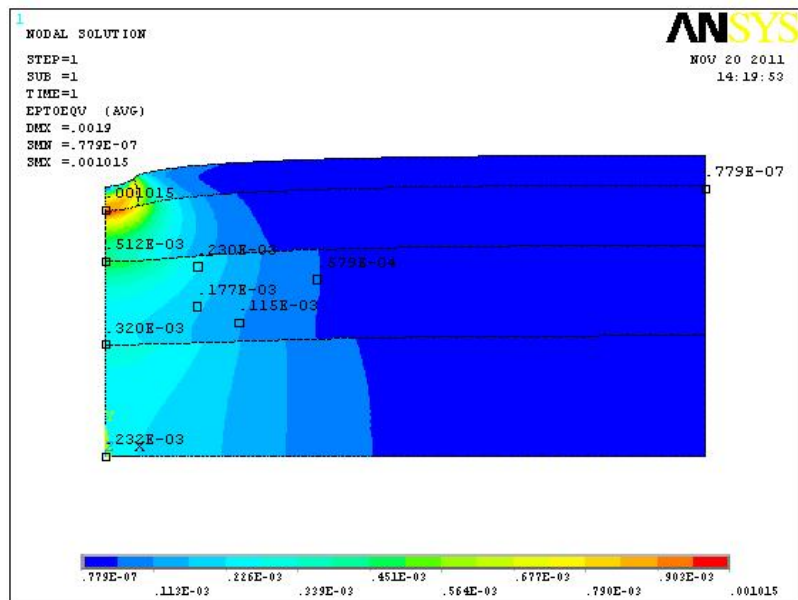


Figure 5.12 (g): Total strain at various layers of haul road pavement with ((25FA+75O/B)+9L) composite

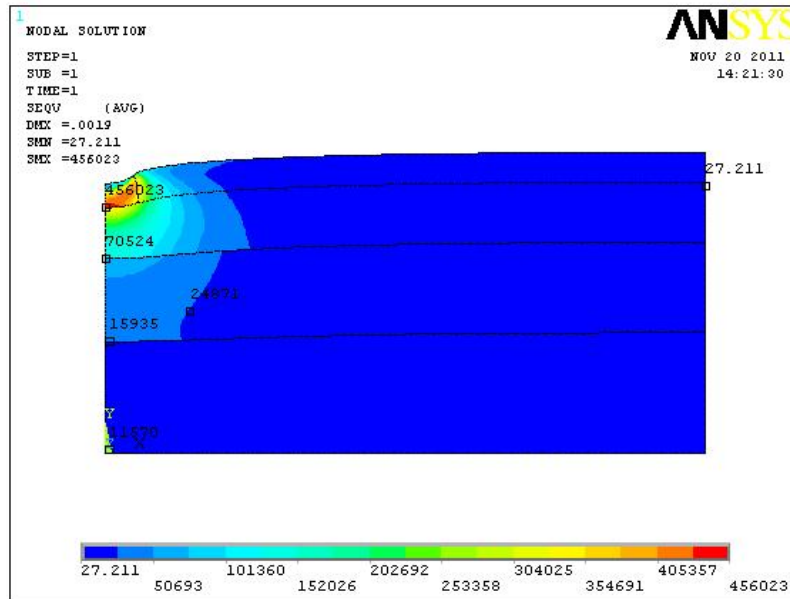


Figure 5.12 (h): Total stress at various layers of haul road pavement with ((25FA+75O/B)+9L) composite

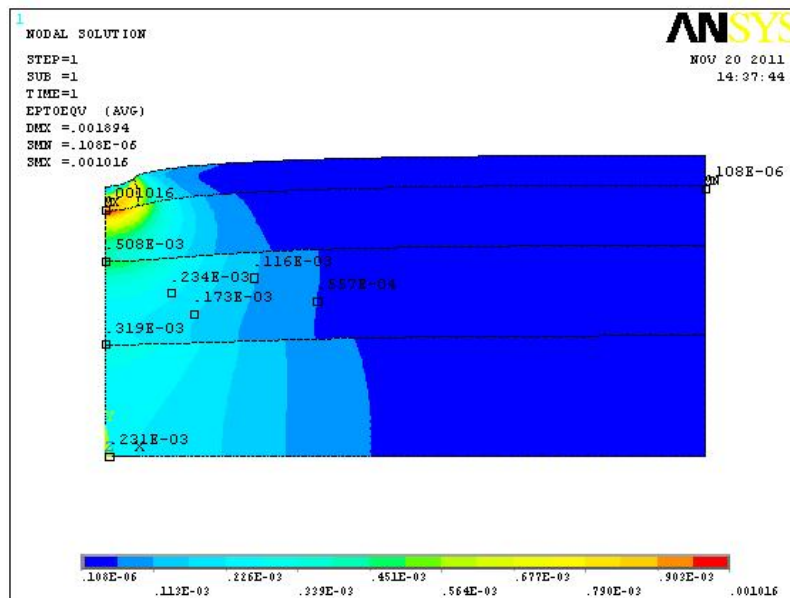


Figure 5.12 (i): Total strain at various layers of haul road pavement with ((30FA+70O/B)+6L) composite

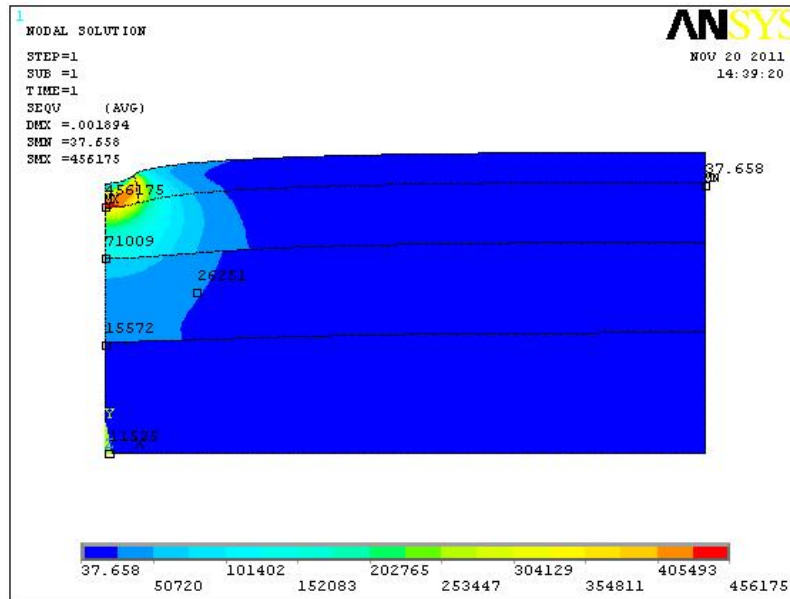


Figure 5.12 (j): Total stress at various layers of haul road pavement with ((30FA+70O/B)+6L) composite

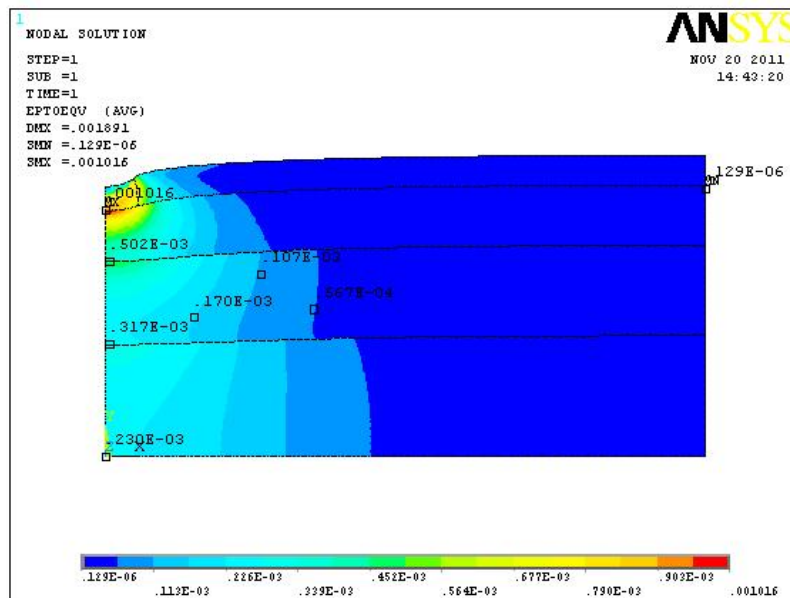


Figure 5.12 (k): Total strain at various layers of haul road pavement with ((30FA+70O/B)+9L) composite

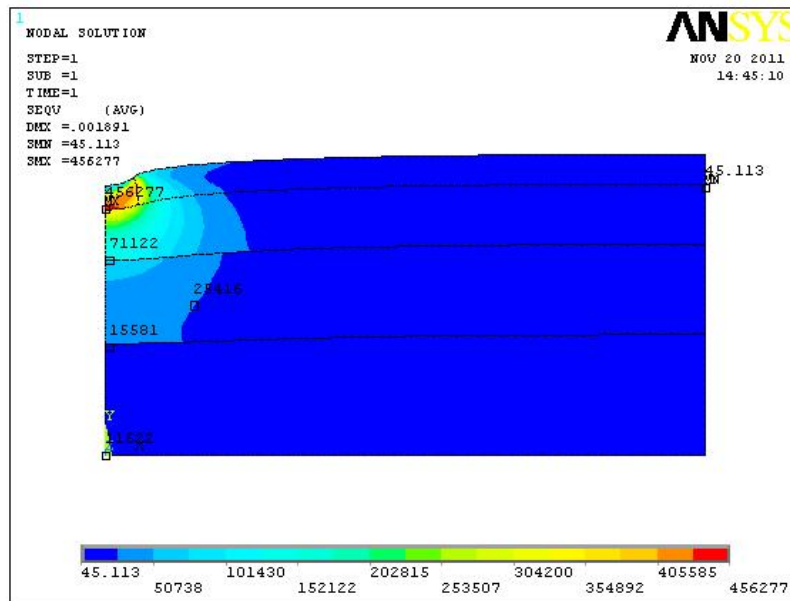


Figure 5.12 (l): Total stress at various layers of haul road pavement with ((30FA+70O/B)+9L) composite

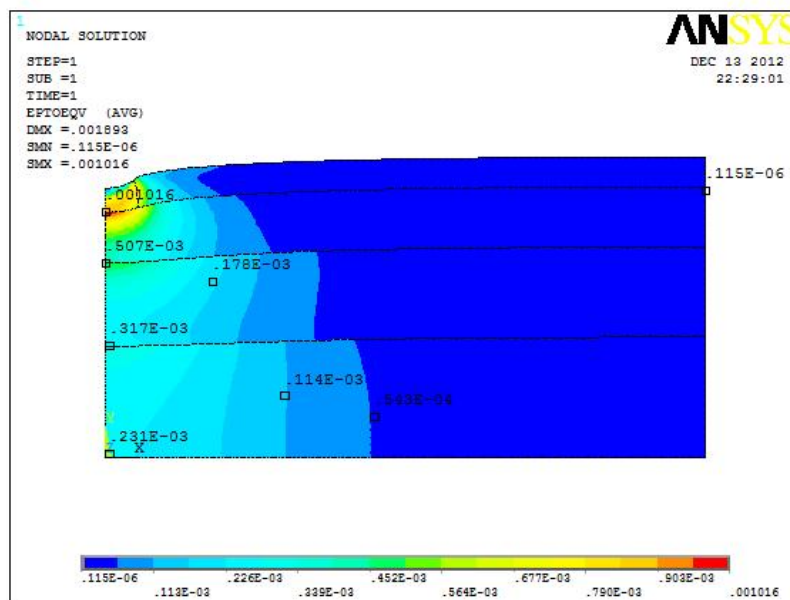


Figure 5.12 (m): Total strain at various layers of haul road pavement with ((35FA+65O/B)+9L) composite

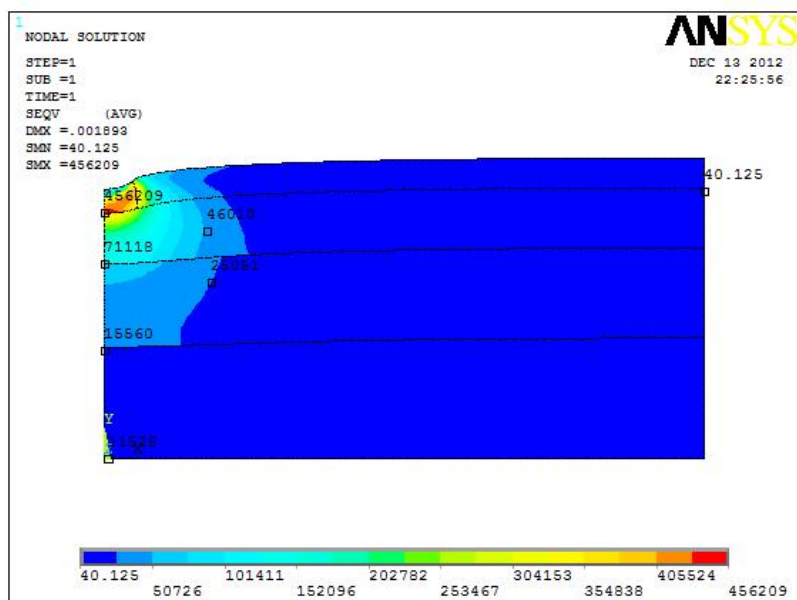


Figure 5.12 (n): Total stress at various layers of haul road pavement with ((35FA+65O/B)+9L) composite

Figure 5.12: Total strain and stress at various layers of haul road pavement with fly ash composites as subbase material

Calculation of fly ash for haul road

Any permanent haul road length = 5km

Haul road width = 20m

Subbase thickness = 1.5m

No. of surface coal mine = 200

Volume of the road pavement = $5\text{km} \times 20\text{m} \times 1.5\text{m}$

$$= 5000 \times 20 \times 1.5 \text{ m}^3$$

$$= 150000 \text{ m}^3$$

Density of the fly ash composite material = 1740 kg/ m^3

Quantity of material used = $1740 \text{ kg/ m}^3 \times 150000 \text{ m}^3$

$$= 261000000 \text{ kg}$$

$$= 0.261 \text{ MT}$$

Material used for 200 opencast mines = $0.261 \times 200 = 52.2 \text{ MT}$

Fly ash usage @ 30% of the material = $30\% \times 52.2 \text{ MT} = 16 \text{ MT}$

LIST OF PUBLICATIONS

Journals

1. **Behera, B.**, Mishra, M. K. and Mallick, S. R. (2010), "California Bearing Ratio behavior of mine overburden stabilized fly ash", *Journal of Indian Mineral Industry*, May 2010, pp. 133-135.
2. Mishra, M. K. and **Behera, B.** (2010), "Laboratory investigation on behaviour of surface coal mine overburden stabilized with fly ash and lime", *Journal of Mine Metal and Fuel*, May 2010, ISSN 0022-2755, pp. 129-133.
3. **Behera, B.** and Mishra, M. K. (2010), "Strength behaviour of Surface coal mine overburden-fly ash mixes stabilized with quick lime", *International Journal of Mining, Reclamation and Environment*, Vol. 26, Issue 1, pp.38-54.
4. **Behera, B.** and Mishra, M. K. (2011), "Effect of lime on the California Bearing Ratio behaviour of fly ash - mine overburden mixes", *Division of Civil and Environmental Special Journal Issue, WASET*, ISSN 2010-3778, vol. 75, pp. 161-166.
5. **Behera, B.** and Mishra, M. K. (2012), "California Bearing Ratio and Brazilian Tensile Strength of Mine Overburden-Fly Ash-Lime Mixtures for Mine Haul Road Construction" *International Journal of Geotechnical and Geological Engineering*, Vol. 30, Issue 2, pp. 449-459.
6. **Behera, B.** and Mishra, M. K. (2012), "Strength assessment and compositional analysis of lime stabilized fly ash and mine overburden mixes upon curing" *International Journal of Solid Waste Technology and Management*, Vol. 38, Issue 3, pp. 211-221.

Conferences

1. **Behera, B.**, Mishra, M. K. and Naik, H. K. (2008), "Critical Review of Fly Ash Utilization in Mines", *Conference on Emerging Trends in Mining and Allied Industries (ETMAI-2008)*, NIT Rourkela, Feb. 2-3, pp 277 – 283.
2. **Behera, B.** and Mishra, M. K. (2009), "Utilisation of fly ash composite material for surface coal mine haul road stabilization", *International Symposium on Rock Mechanics and Geo-Environment in Mining and Allied Industries (RGMA-09)*, IT BHU, Varanasi, Feb. 12-14, pp 327 – 333.
3. **Behera, B.** and Mishra, M. K. (2009), "Stabilization of Surface Coal Mine Overburden by Fly ash and lime", *National Conference on Advances in Environmental Engineering (AEE-09)*, NIT, Rourkela, Nov. 14-15, pp. 98-103.

-
4. **Behera, B.** and Mishra, M. K. (2010), “Mechanical properties of lime treated fly ash-overburden mixes in relation to their use in mine haul road construction”, *International Conference on Developments in Road Transportation (DRT-10)*, NIT Rourkela, Oct. 08-10, pp. 572-578.
 5. **Behera, B.** and Mishra, M. K. (2011), “Effect of lime on the California Bearing Ratio behaviour of fly ash - mine overburden mixes”, *International Conference on Environmental and Civil Engineering, World Academy of Science, Engineering and Technology (WASET)*, Bangkok, Thailand, Mar. 29-31, vol. 75, pp. 213-218.
 6. **Behera, B.** and Mishra, M. K. (2011), “The use of lime-stabilized fly ash-overburden mixtures as haul road construction materials” *International Conference on Technological Challenges and Management Issues for Sustainability of Mining Industries (TMSMI 2011)*, NIT Rourkela, Aug. 04-06, pp. 117-123.
 7. **Behera, B.** and Mishra, M. K. (2011), “Some aspects of lime treated fly ash and mine overburden composite samples” *34th International Conference of Safety in Mines Research Institutes*, New Delhi, Dec. 7-10, pp. 257-264.
 8. **Behera, B.** and Mishra, M. K. (2012), “Microstructure and leaching characteristics of fly ash-mine overburden-lime mixtures” *International Conference on Chemical, Civil and Environment Engineering*, Dubai, Mar. 24-25, pp. 256-260.

Curriculum Vitae

Name Banita Behera

Date of Birth 01-06-1983

Educational Qualification

2006 M.Sc. (Physics), NIT, Rourkela, India

2003 B.Sc. (Physics Hons.), Sambalpur University, Odisha, India

Experience 5 years, Research experience

Permanent Address C/O: Lokanath Behera
Q. No. – F/7, NIT Campus,
Rourkela – 769 008
Sundargarh, Odisha
Email: banita@nitrkl.ac.in,
banita25@gmail.com
Phone: 07204732598 (M)